Barts and The London
School of Medicine and Dentistry

Isolation and identification of putative oral cancer stem cells (OSCCs) and changes associated with tumour progression

Thesis submitted with regulations

for the degree of doctor of philosophy

by

Dr. Bilal Ilyas Fazil

Supervisors:

Prof. Ian. C. Mackenzie

Prof. Farida Fortune

March 2012

Department of Clinical and Diagnostic Oral Sciences

Barts & the London, Queen Mary School of Medicine and Dentistry

Abstract

Oral squamous cell carcinomas (OSCC) appear to contain a sub-population of cells endowed with indefinite self-renewal capacity, usually referred to as cancer stem cells (CSCs). These cells are clonogenic and are responsible, in all probability, for tumour initiation and propagation. Cancer cell lines consistently show morphological patterns similar to normal keratinocytes (holoclones, meroclones and paraclones) reflecting a hierarchical organization associated with stem, amplifying and differentiated cells. In-vitro studies of OSCC cell lines have revealed further phenotypic differences in colony formation between the stem and non-stem fractions and have identified cell surface proteins such as CD44, E-Cadherin, ß-catenin and Vimentin which are differentially expressed in association with stemness. Recent studies suggest tumour progression to be associated with Epithelial Mesenchymal Transition (EMT), a process occurring in SCCs which confers invasiveness and motility to CSCs and also suggests a strong involvement of external factors such as those present within the tumour-host microenvironment. Analysis of these properties may provide insight into mechanisms of stem cell fate determination and provide mechanisms for therapeutic targeting of CSCs.

Methods and Materials: Immunocytochemistry was used to analyze differential expression of cell surface and internal markers for their role in stemness and EMT, FACS was used to isolate and analyze sub-fractions of cells for clonal studies. Real time videos of cell lines were used to examine cell movement in colonies and cell acquisition of a fibroblastic phenotype. As a test of whether this process is actually EMT, cells were exposed to TGF-ß, a known inducer of EMT, to determine whether this enhanced the formation of the mesenchymal-looking cells at colony margins.

Results and Conclusions: Video images showed cells at the margins of holoclones acquiring a motile phenotype. Immunohistochemical analysis revealed that certain stem-cell-related cell surface molecules were expressed at higher levels in holoclones than paraclones and at different levels within holoclones. Expression of CD44 was stronger in the center than at the edge of holoclones suggesting that this molecule plays a role in maintaining a stem-like state. Some images indicated nuclear translocation of CD44 and ß-catenin at colony margins. TGF-ß increased the incidence of mesenchymal-like cells at the edges of colonies and seemed to scatter and mobilize these cells with loss of the normal colony architecture. Further, TNF-α alsogreatly enhanced this effect by working synergistically with TGF-β suggestingthe involvement of external factors such as inflammatory cytokines and other cells present within the tumour-host environment,collectivelycontributing tothe generation of EMT cells with stem potential.

Acknowledgements

I would first like to thank Prof. Ian Mackenzie for the invaluable help and support he offered during the course of this project. I enjoyed working with him immensely and greatly admire and respect his seemingly endless patience in painstakingly teaching me everything regarding the project and waiting till I had gotten the hang of it. I thank him for pushing me on when I think I needed it the most and for always being there to talk to, and most of all, for being a friend. Dr. Alan Cruchley,I enjoyed teaching oral pathology with you, the things you taught me helped me get to where I am today. You were always there with the right advice, the right joke, also the right barb, and for the kindness, support and understanding you showed towards the end, I have no words. Steve, I enjoy our little chats throughout the day, even though you still haven't got the hang of riling me up where cricket is concerned and I will miss you. Usually, they are better pick-me-ups than coffee as your candour and honest judgment are much appreciated, being a rare commodity in this day and age. A special thanks to Dr. Eleni Haji Pavli for finding time in her hectic schedule to talk and help and for being my friend throughout these years; you are truly the nicest person in this world. I would like to thank all members of my team by name. Adrian, you are the perfect gentleman and I thank you for all the help you gave. Luke, thanks for helping out with the time lapse and your rare good moods will be missed. Lisa, you were always there with something to say with a smile. Helena, although you're relatively new, I still enjoyed working with you. I honestly have no words to say to my best friend in the building, Ryan...you're like my brother from another mother, thank you for everything and I am privileged to have a friend like you. Bianca, I have to say they send us to all these computer courses for office and word, but none of them could hold a candle to what you're capable of doing with it. Mandy, thanks for scanner privileges and help with scale bars, and I will thank you by pulling your wisdom teeth out next month at work. Last but not least, I would like to thank Prof. Fortune for her role in my project and for being there with the right advice and pep talks and encouragement. It was always a dream of mine to study at a prestigious research institute such as this and to everybody mentioned here I thank them from the bottom of my heart for making it a realization. Finally I would like to thank my wife, Hina, for standing by me through the difficult times, for putting up with my countless nocturnal absences to the lab, the non-weekends spent working and for taking care of me through the never ending british colds. For all the encouragement, emotional and financial support they offered, and the sacrifices they made to ensure that I complete the course, I dedicate this dissertation to my parents, my sister and my wife without whom it would not have been possible. I will always be grateful to you for this.

Table of contents

List of figures

List of tables

Abbreviations

BSA	Bovine serum albumin
cDNA	Complementary DNA
dH_2O	Distilled water
DMBA	7,12-dimethylbenz[a]anthracene
DMEM	Dulbecco's modified Eagle's medium
DMSO	Dimethyl sulfoxide
DNA	Deoxyribonucleic acid
EBV	Epstein-Barr virus
ECM	Extracellular matrix
EDTA	ethylenediaminetetraacetic acid
EGF	Epidermal growth factor
EGFR	epidermal growth factor receptor
FACS	fluorescence activate cell sorting
GAPDH	glyceraldehyde-3-phosphate dehydrogenase
HIF-1	Hypoxia-inducible factor-1
HPV	human papillomavirus
KGM	Keratinocyte growth medium
mRNA	Messenger RNA
NCBI	National Center for Biotechnology Information
NCI/NCII	Non canonical function of telomerase (type I and II)
nm	nanometer
PBS	Phosphate buffered saline
PCR	polymerase chain reaction
polyHEMA	polyhydroxyethylmethacrylate
qPCR	quantitative PCR
RNA	Ribonucleic acid
RNase	Ribonuclease
SD	Standard deviation
SCC	squamous cell carcinoma
TNF-α	Tumour necrosis factor
TBE	Tris/Borate/EDTA buffer
TGF-β	Transforming growth factor-Beta
UV	Ultraviolet
CRUK	Cancer Research United Kingdom
CEBP-α	Ccaat-enhancer-binding-proteins
PSCA	Prostatic Stem Cell Antigen
ESA	Epithelium Specific Antigen (EpCAM)
DKK3	Dickkopf-related protein 3
OSCC	Oral squamous cell carcinoma
HNSCC	Head and Neck squamous cell carcinoma
HSCs	Hematopoietic stem cells
CSC	Cancer stem cell
IL-1	Interleukin One
KGF	Keratinocyte growth factor
AML	Acute myeloid leukemia
EMT	Epithelial to mesenchymal Transition
MET	Mesenchymal to epithelial transition
MSCS	Mobile cancer stem cell
CAFs	Cancer associated fibroblasts

IGFBP3	Insulin like growth factor binding protein 3
ErbB3	Receptor tyrosine protein kinase
DEPC	Diethylpyrocarbonate
ATP	Adenosine tri phosphate
TNE	Tris-NaCl-EDTA buffer
EDTA	Ethylenediaminetetraacetic acid
BMI-1	Polycomb ring finger oncogene
STAT3	Signal transducer and activator of transcription 3
FSC	Forward Scatter
SSC	Side scatter
DAPI	4',6-diamidino-2-phenylindole
PE	phycoerythrin
APC	Allophycocyanin
NOD-SCID	Non obese diabetic/severe combined

-

Chapter 1: Introduction and literature review

1.1 Cancer

The word cancer is used to describe a particular class of diseases in which cells making up tissues and organs display uncontrolled growth and invasion into surrounding stroma.It often culminates in metastasis where the cancerous cells spread through the bloodstream or the lymphatic system to colonize secondary sites as new tumours. As early as 370 BC, Hippocrates described several types of cancers, referring to them with the Greek word '*carcinos'* (The history of cancer, 2009). Carcinos was later translated into the Latin word '*cancer'* also meaning crab. The oldest references to surgical treatment for cancers are from Egypt and date back to 1600BC. With development of the microscope in the 1800s it was recognized that the body is made up of tissues that, in turn are made up of millions of cells. Genetic patterns were later recognized to contribute to cancer initiation and the accidental discovery of the effects of radiation on bone marrow was instrumental in the development of marrow transplants for leukaemia.Benign tumours resemble the tissue of origin and grow locally but do not invade into surrounding tissue and are usually walled off by a capsule of connective tissue. They can arise in most organs and may generate all the cells concerned within the organ or just some components within it, patterns apparent with tumour formation in organs with tubular structures like the breast and kidneys. Benign tumours may grow to press on surrounding structures such as nervous tissue or, if they are in secretory tissues such as the pituitary, may cause symptoms due to excessive production of hormones. Malignant tumours lack a fibrous capsule, invade into the surrounding tissues or even manage to gain access to the bloodstream and lymphatic systems to travel to distant sites which they colonize as new tumours. Cancers are also classified on the basis of the type of cell that the tumour resembles which, as discussed later, is usually also assumed to act as the cell of origin of the tumour. The causes of cancer appear to relate to both environmental and genetic influences which lead to failure of regulation of tissue growth (Mehanna et al, 2010). This process is normally very tightly controlled in all cells, but especially so in those which are responsible for the lifetime renewal of organs (discussed later in the chapter). Growth is usually under the command of tumour suppressor genes and oncogenes. Oncogenes are of a class of genes that promote cell

Engraving with two views of a dutch woman who had a tumor removed from her neck in 1689

growth and reproduction, whereas tumour suppressor genes usually inhibit cell division and survival. Mutations in these genes have been linked to aberrations in cell proliferation in many organ systems. The transformation of a normal cell to a cancer cell appears akin to a chain reaction where an initial event causes errors, which are progressively compounded into cumulative errors allowing the cell to escape normal growth limits. Cancers also evolve as they grow becoming progressively more aggressive through clonal evolution, the process usually responsible for the progressive change of cancers into more invasive subtypes (Hanahan, 2000, 2011).

1.2 Head and Neck Cancer and Oral cancer

The term head and neck cancer encompasses a group of biologically similar cancers that commonly originate and occur in the upper aerodigestive tract. Their location can be the nasal cavity, lip, oral cavity, the larynx, pharynx and even the paranasal sinuses (Cancer, 2009; ISBN: 14392-6386-8). Almost ninety percent of these tumours are squamous cell carcinomas (HNSCC) and originate from the epithelia of these regions. HNSCC commonly spread to the lymphatics of the neck and this may be the first and sometimes the only manifestation of the disease. Smoking and alcohol are amongst the major risk factors for HNSCCs (Murata et al, 1996) and account for about 75% of cases discovered. Viral infections such as Epstein Barr virus (EBV) and human papilloma virus (HPV) have been strongly correlated with HNSCCs and genetic tendencies are also recognized as significant risk factors for oral cancer (Hirsch et al, 2010). Oral cancers are the 10^{th} most common cancers occurring worldwide and the seventh most common cause of cancer induced deaths in the world (Mehanna et al, 2010).

Oral SCCs, a subtype of HNSCC, are usually highly aggressive and arise as primary lesions from within oral epithelium, most commonly of the tongue, but also of the floor of the mouth, cheek, lips and the palate (Rogers et al, 2010). When precursor lesions for these tumours exist they are referred to as leukoplakias (adherent white patches on the mucous membranes) and erythroplakias (red patch or lesion). The latter are less common but more highly correlated with future transformation into malignancy (Bouquot, 1995). The progression pathways for OSCCs are well established and premalignant lesions present themselves histologically as squamous dysplasia, usually graded as mild, moderate or severe (Anneroth et al, 1986), previously also termed carcinoma in situ, based on structural differences and cellular atypia. This grading is dependent on the thickness of the epithelium affected and if the full thickness of the epithelium is altered it is considered severe dysplasia, moderate if the middle third or prickle layer is

affected and mild if only the lower layers are involved. Tumours invading through the basement membrane are described as invasive squamous carcinomas. These gradings, although usually reflective of the severity of the lesion, can be misleading as they cannot consistently predict malignant potential (Hunt, 2011).

Histologically, lesions are associated with hyperplastic (excessive cell proliferation) or dysplastic (abnormal cell maturation) cellular changes or a combination of both (Jon and Albrecht, 2003). Dysplastic lesions are characterized by loss of the organization and maturation patterns typical of squamous epithelia and dysplastic cells show aberrant features ranging from nuclear enlargement, irregularities in the nuclear membrane and hyperchromatism. Squamous carcinomas typically show some degree of keratinization and, when it is marked, the tumour is termed well differentiated whereas those tumours showing little evidence of keratin formation are considered poorly differentiated. Histological evaluation distinguishes between different variants of SCCs such as verrucous carcinoma, papillary SCC, basaloid SCC, spindle cell, acantholytic and undifferentiated carcinoma. HNSCCs can present with many symptoms depending on where they originate. Laryngeal cancers cause hoarseness of the voice while pharyngeal cancers present with dysphagia and sore throat. Many patients only have a painless lymph node. One of the common presentations of tongue carcinomas at the time of diagnosis is the presence of a non-healing ulcer on the lateral aspect of the tongue (Mehanna et al, 2010). Other signs and symptoms are listed in the figure below.

Any of the following lasting for more than three weeks	Signs
Symptoms	Red or white patch in the mouth
Sore throat	Oral ulceration, swelling, or loose tooth
Hoarseness	Lateral neck mass
Stridor	Rapidly growing thyroid mass
Difficulty in swallowing	Cranial nerve palsy
Lump in neck	Orbital mass
Unilateral ear pain	Unilateral ear effusion

Figure 1.0: Signs and symptoms commonly associated with head and neck cancers (adapted from Mehanna et al, 2010)

Worldwide almost 500,000 new cases of head and neck cancer are diagnosed annually (Pisani et al, 2002). Patients with malignant cancers of the oral cavity and oropharynx have a 5-year survival rate of 56% which has not reduced over the last few years (Joshua et al, 2010). These

tumours have poor prognosis as most patients present with advanced stage disease many of whom are diagnosed incidentally by dental practitioners by which time the disease has spread to the regional neck lymph nodes (Lee and Moon, 2011). The percentage of oral and oropharyngeal cancers diagnosed early stands at 64% and 16% respectively. Males are affected more than females and this ratio varies from 2:1 to 15:1 depending on the epidemiological area examined (Mehanna et al, 2010).

The treatment of early stage head and neck cancers centres on surgery, to produce healthy margins, or radiotherapy.The choice between the two depends on preservation of function. Although radiotherapy is the preferred method in tongue carcinomas allowing the preservation of speech and swallowing, recent advances like the carbon dioxide laser have reduced morbidity by increasing organ preservation compared to open surgery (Mehanna et al, 2010). In advanced head and neck malignancies, single modality treatment alone has proved ineffectual and studies have proved that surgery coupled with radiotherapy or chemotherapy provides a better chance of a cure. Although advancements in molecular science have made different and new chemotherapeutic agents available, most of them are still associated with high morbidity owing to adverse side effects.

1.3 Stem Cells

Adult tissues maintain their structure and function through cell division patterns that are associated with cyclical renewal or tissue repair (Mackenzie et al, 2006). Cell loss is delicately balanced by cell renewal and normal epithelial function requires cell loss to be balanced through an appropriate number of cells entering the differentiation pathway.

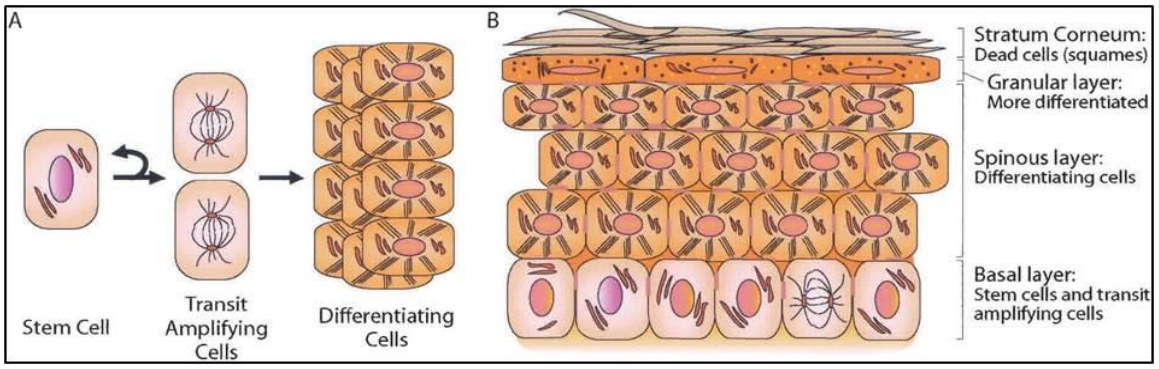

Figure 1.1: Figure showing hierarchy of cells present within the epidermis. A stem cell is shown which divides relatively infrequently to produce proliferative transient cells which lack extensive self-renewal capacity. These in turn divide to form the differentiated cells for tissue function and leave the basal layer. (Adapted from Alonso and Fuchs, 2003)

The maintenance of this delicate balance ensures effective homeostasis and overall control of this process depends on relatively small populations of cells within a tissue that possess the ability both to self-renew and to give rise to a cellular hierarchy within tissues (Lavker et al, 2000). They are known as **somaticstem cells**. When stem cells divide, they typically give rise to a cell that retains stem cell properties, thus ensuring that there is a continuous supply of these long-lived cells, together with a cell committed to differentiation, providing cells for tissue function and ensuring that cell loss balances cell turnover. Stem cells are often slow cycling *in vivo* (Mackenzie et al, 2006) and divide relatively infrequently as compared to other cells. Earlier views stating the equal potential of all proliferatively active cells in tissues are incompatible with the results of later studies which make it clear that cells within a tissue are heterogeneous with regard to their proliferative capacities (Tudor et al, 2004). A slow cell cycle may make stem cells less prone to the adverse effects of mutations which are most likely to occur at the time of division. Understanding stem cell and progenitor cell behaviour and its relationship to pathways involved in homeostasis is one of the main foci of current stem cell research. For the majority of adult tissues the mechanisms by which stem cells maintain a balance between proliferation and differentiation remain unclear.

An asymmetry model is the basis of the hypothesis that tissue homeostasis is maintained by stem cells which divide to give rise to a daughter stem cell and a committed cell which eventually differentiates. With the *invariant asymmetry/division asymmetry* model cell loss is balanced by the asymmetry of division at the single cell level, where slow cycling stem cells give rise to daughter stem cells and cells that continue to differentiate (Potten and Loeffler, 1990; Klein et al, 2011). This has been welldocumented in Drosophila (Knoblich, 2008). It is

thought that this type of division takes place either through polarization of stem cells prior to division or owing to external signals from the microenvironment (Voog and Jones, 2010). An alternate mechanism, called the *population asymmetry* model, proposes that there is a pool of stem cells that divides to produce either two stem cells, two differentiating cells, or one of each and it is by the overall balance within these probabilities that homeostasis is achieved (Jones, 2010). Earlier studies on intestinal epithelium and murine oesophageal cells are also in line with the idea of population asymmetry (Cheng and LeBlond, 1974; Marques-Pereira, and LeBlond, 1965).

Figure 1.2: Tissue self-renewal models. In (A) a stem cell divides to produce a stem (green) and a differentiating (red) cell. In (B) half the stem cells divide to self-renew while the other half differentiates (Jones, 2010).

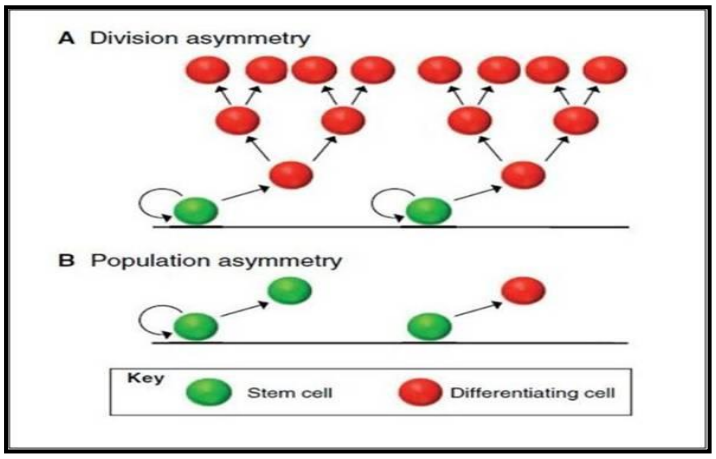

Stem cells are thought to reside in restrictive environments called '*niches*' (Alison et al, 2002; Burkert et al, 2006) that are involved in generating signals that collectively control stem cell fate (Watt and Hogan, 2000). These dynamic microenvironments within tissues balance stem cell activity, maintaining homeostasis during normal physiological development and in disease. Schofield (1978) proposed the existence of a niche, or specialized location, for hematopoietic stem cells (HSCs) and showed that hemopoeitic cells from the spleen are more proliferatively active than cells isolated from within bone marrow and suggested that this was because the cells in the spleen were not associated with niches. This was the first suggestion of a stem cell niche as a physiological microenvironment consisting of specialized cells that physically anchor the stem cell and provide factors necessary to maintain its 'stemness' and prevent maturation of these cells. Stem cell interactions with the niche microenvironment may actually control many facets of stem cell behaviour, including self-renewal and clonogenicity (Sneddon et al, 2007). Niches have been identified for mammalian stem cells in the neural, epidermal, and hematopoietic systems (Li and Xie,2005;Weissman et al, 2001; Palmer et al, 2000). The figure below shows the various niches isolated and the determinant organisms and assays used in eliciting this information.

M. musculus	blood	hematopoietic stem cell	single cell transplant	osteoblasts, osteoclasts, vascular, perivascular cells	Wnt, N, ANG1, OPN, CXCL12	reviewed in Weissman et al. (2001); Wagers (2005); Garrett and Emerson (2009)
M. musculus	muscle	muscle stem cell	lineage analysis, single cell transplant	basement membrane, myofiber	N, Wnt, CXCL12	(Conboy and Rando, 2002)
M. musculus	intestine	intestinal stem cell	lineage analysis, in vitro culture	vascular, fibroblasts, Paneth cells	Wnt, BMP, N	Barker et al. (2007)
M. musculus	hair follicle	hair follicle stem cell	lineage analysis	vascular, fibroblasts, dermis	Wnt, BMP	reviewed in Blanpain and Fuchs (2009)
M. musculus	epidermis	epidermal stem cell	lineage analysis, in vitro culture	basement membrane, dermis	N, Wnt, SHH	Clayton et al., (2007); Nowak et al. (2008)
M. musculus	sebaceous gland	sebaceous gland stem cell	lineage analysis	basement membrane, dermis	?	Horsley et al. (2006)
M. musculus	testis	spermatogonial stem cell	lineage analysis, stem/progenitor transplant	vascular, interstitial cells, Sertoli cells	BMP,GDNF, FGF	Yoshida et al. (2007)
M. musculus	neural	neural stem cell	lineage analysis, in vitro culture	vascular, ependymal cells, astrocytes	Wnt, SHH, FGF, VEGF, N	Palmer et al. (2000)

Figure 1.3: Proposed stem cell niches in different tissues and assays used for their identification (Voog, Jones,2010).

Studies of hematopoietic systems *in vitro* have shown the survival of progenitor cells to be dependent on factors produced by other cells (Watt and Hogan, 2000; Quesenberry and Becker, 1998). Secreted factors such as TGF-β have been shown to be important in the maintenance of neural crest stem cells through both paracrine and autocrine mechanisms (Shah, et al, 1996; Watt and Hogan, 2000). Interaction between epidermal stem cells and extracellular matrix through integrins and similar adhesion proteins are thought to be crucial for maintaining a stem-like state (Zhu and Watt, 1999).

1.3.1 Classification of Stem cells

The criteria used to define a stem cell vary quite widely but, stem cells are usually classified on the basis of their origin as embryonic, germinal or somatic.

Embryonic stem (ES) cells are derived from the inner cell mass of the blastocyst and during normal development give rise to all the tissues of the body. They hold great potential for regenerative medicine but they require very sensitive culture conditions. ES cell research is considered unethical by some people as they believe that human embryos have full developmental potential and destroying them to harvest cells is morally unjustifiable. In some places ES cell research is considered illegal (Alison et al, 2002). S**omatic stem cells** are cells present in adult tissues that are responsible for the maintenance of these tissues throughout the life of the organism, whereas**germinal stem cells** are responsible for gamete production.

Stem cells can also be classified largely on the basis of potency. Cells derived from the early blastocyst are said to be **totipotent** as they can give rise to all the tissues of the body and also

the placenta; hence they are the most versatile and the least committed. These cells, on further division, give rise to **pluripotent** cells of the three germ layers of the body, namely the ectoderm, the mesoderm and the endoderm (Smith, 2001). Subsequently, these cells, whilst still capable of long-term self-renewal, become committed to certain lineages, are responsible for the maintenance of specific tissues, and can be termed **multipotent**. Multipotent cells are more committed than pluripotent cells and give rise to lineage restricted progenitor cells which in turn can generate specific tissue systems. For example, in the hemopoeitic system hemopoeitic stem cells (HSCs) give rise to relatively undifferentiated progenitor cells that divide in turn to generate the various haematopoietic lineages (Priddle, et al, 2006). Although immature epithelial cells can be stimulated experimentally to form morphologically and phenotypically distinct types of cells, they are normally lineage specific (Mackenzie et al, 1983).

Forced lineage specification studies carried out by Weintraub et al (1989) demonstrated that fibroblasts could be converted to skeletal muscle cells by the forced expression of a transcription factor MyoD. Since then fibroblasts have been shown to convert into neurons, cardiac cells and blood-cell progenitors (Chambers et al, 2011). In the early 1960s Gurdon and colleagues found that a nucleus from a differentiated frog cell, when transplanted into an enucleated germ cell could give rise to a new frog, indicating that a differentiated cell retains the same genetic information as an early embryonic cell (Hochedlinger and Stadtfeld, 2010). The potential applications of this were unveiled with the cloning of Dolly the sheep in 1996 from a differentiated cell. These applications gave rise to the induced Pluripotent Stem Cell (iPSC) technology, when it was shown that transcription factor based programming of cells could also yield cells with stem like capabilities (Takahashi and Yamanaka, 2006) and this has now revolutionized the field of regenerative medicine.

1.4 Proliferative patterns of normal stem cells

As described, stem cells in the hematopoietic system divide relatively infrequently to give rise to a hierarchical pattern in which immature progenitor cells eventually differentiate to form all the cells derived from the bone marrow (Morrison et al, 1995; Reya et al, 2003). Stratified squamous epithelia have also been shown to follow a similar pattern of division where undifferentiated cells in the basal layer divide to form transient amplifying cells that divide to give differentiated cells which move up through the epithelium to be shed.

1.5.1 Asymmetric Division

Although asymmetric division patterns have been established for many tissues, it is still uncertain how and when asymmetric cell fate is determined; i.e., at the time of division or by events taking place after the cell has divided. However, either pattern provides a means for the balanced homeostatic turnover required for a tissue to function normally in a steady state. Typically, three cell compartments are present in a tissue, a stem cell compartment, a transient amplifying compartment and a differentiated one. It has been estimated that for the epidermis, a stem cell has to divide only once to generate a stem daughter and 8 differentiated cells (Potten, 1997; Tudor et al, 2004). Watt et al (2000), demonstrated that asymmetric divisions define the architecture of human oesophageal epithelium. In developing mammalian skin, cells in the basal layer were shown to undergo two types of divisions (Lechler and Fuchs, 2005). The first type of division was seen frequently in early embryonic skin (up to day 12) and took place with the mitotic spindles of cells aligned parallel to the basement membrane where cells divided laterally to form a single layer of cells (Figure 1.4a). A few cells, however, showed a second pattern where the mitotic spindles were arranged at right angles to the basement membrane (Figure 1.4b). The mechanisms by which mammalian skin undergoes stratification are still poorly understood but it was proposed that the cells dividing at right angles to the basement membrane resulted in the production of a cell which lost contact with the basal layer thus inducing its exit from this layer and commitment to differentiation. (Lechler and Fuchs, 2005). The figure below shows the two types of divisions discussed.

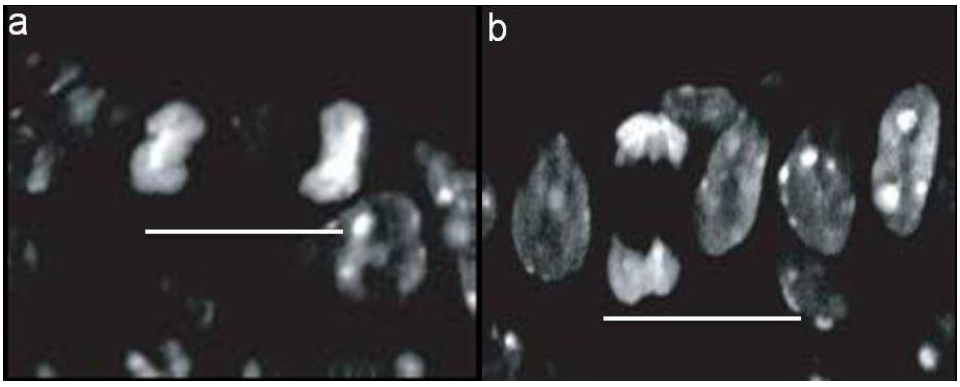

Figure 1.4:The parallel (a) and perpendicular (b) orientation of the mitotic spindles during cell division. The white line is representative of the basement membrane (Adapted from Lechler and Fuchs, 2003).

Later in development, once stratification began, most of the spindles were oriented at ninety degrees to the basement membrane (Figure 1.4b). Thus it was inferred that most of the late

divisions occurring in the basal layer were asymmetrical, giving rise to a stem cell compartment and a transient amplifying compartment. The cells leaving the basal layer migrate towards the surface showing expression of differentiation markers such as keratins and involucrinsuggesting again, that loss of contact of basal cells with the basement membrane initiates a differentiation stimulus (Seery et al, 2000).

1.5.2 Symmetric division (1)

It is also possible for a stem cell to divide to produce 2 cells, both of which enter the differentiation pathway. This pattern, which leads to depletion of the stem cell population, could result from a depleted number of niches available to support stem cell survival e.g. after irradiation therapy (Costea et al, 2006) or from a change in the signalling pathways associated with stem cell maintenance. Inducing such a division pattern could also be of potential value in the removal of cancer stem cells. Gupta and co-workers demonstrated this through the use of a screening process and identified small molecule inhibitors that induce differentiation of CSCs in breast cancer cell lines(2009).

1.5.3 Symmetric division (2)

In an third pattern of division, a stem cell can divide to give rise to two stem cells, a pattern expected when stem cells have been lost through wounding and new stem cells need to be generated. Time lapse video of cancer cells suggest that this sort of division occurs *in-vitro* in cultures of cell lines derived from tumour tissue (Mackenzie lab, 2006). It is thought that murine cells in culture divide symmetrically, as suggested by the continuously expanding central zone of cells in murine cultures (Tudor et al, 2006), a pattern described in more detail in section 1.5. As described below, colonies formed by oral cancer cell lines show a similar pattern in which cells around the edges of colonies look and behave differently from cells within the center.

1.5.4 De-Differentiation

Once a transient amplifying cell has been formed, it is expected to continue down the differentiation pathway. However, Potten and Grant (1998) suggested that if stem cell survival is disturbed (i.e. the self-renewing cell dies or is lost) then a transient amplifying cell may stop differentiating and revert back to a stem cell state. Barrandon and Green (1980) showed that if paraclones, representing late amplifying cells, are transfected with a viral oncogene, they can revert back to a stem cell state with full restoration of growth potential. This suggests that the transition from stem to amplifying to differentiated cells may not be irreversible although the mechanism by which this happens still remains unclear. Stem cell divisions and their various outcomes are illustrated in Figure 1.5, which has been adapted from Costea et al, 2006.

Figure 1.5: Hierarchical stem cell concept in human oral mucosa. Stem cells (red) with a low proliferative rate but high self-renewal capacity, undergo a symmetric division to generate two new stem cells (left), an asymmetric division (centre) to produce a new stem cell and a more differentiated transit amplifying cell (pink), or a symmetric division to give two cells committed to differentiation (right). TA cells differentiate into specialized cells that maintain the tissue (blue round cells), and finally desquamate from the epithelial surface (blue flattened cells) (Costea et al, 2006).

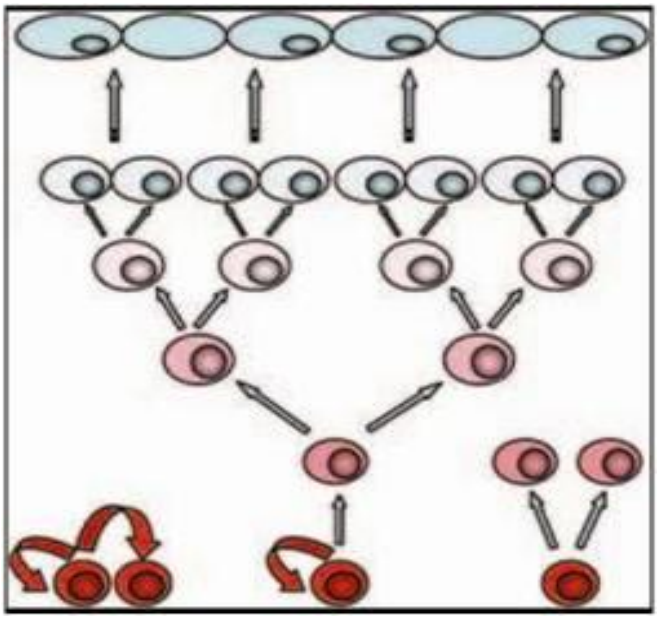

1.5 *In vitro* behaviour of Epithelial Stem cells

Hemopoeitic stem cells (HSCs), known to be responsible for the generation of all cell types in the blood in mice and humans, have been positively identified and successfully isolated (Weissman et al, 2001). As this system is the most widely studied of all adult tissues, and hence the best characterized, information generated from it has been used as a basic conceptual guideline for other systems studied, particularly the adult epidermis (Mackenzie, 2006). The existence of epithelial stem cells was proposed as early as 1970 by Mackenzie when small proliferative units were discovered in mouse epidermis. It was also hypothesized that cells at

the center of this unit had the ability to remain quiescent. Localization of slowly-cycling cells in murine epithelia was examined through a process called ‘label retention’. The epithelium was labelled with titrated thymidine, which is taken up by DNA during the S-phase of cell division and the tissues were sampled a month or later (Bickenbach, 1981). This method relied on the concept that stem cells, being slow cycling, would be the only cells retaining the label at the end of the month, while, the cycling cells, would have diluted the label through cell division (Mackenzie and Bickenbach, 1985).

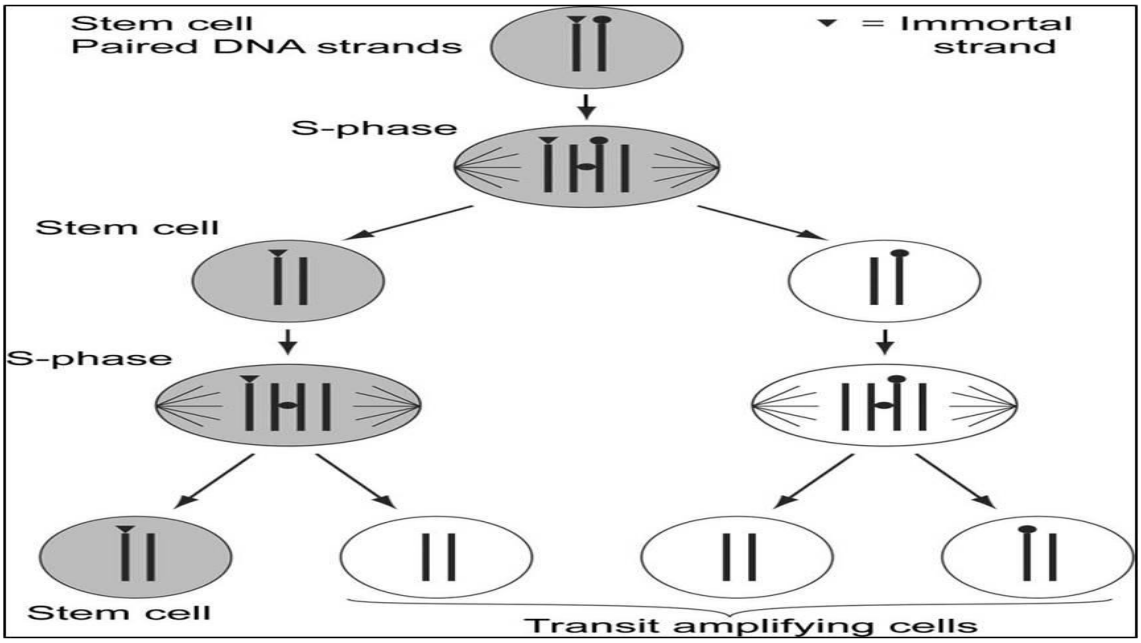

Figure 1.6: The ‘immortal strand’ hypothesis; a possible way for stem cells to maintain the integrity of their genome. (Adapted from Burkert et al, 2007)

This interpretation is complicated somewhat by the ‘immortal strand hypothesis’, in which Cairns (1975) gives another potential mechanism for label retention. As depicted in the figure above, he suggested that stem cells have evolved protective mechanisms to help conserve the integrity of the genome. A cell is most prone to carcinogenic mutations generated through copying errors at the time of cell division and one way to protect against this would be to segregate newly synthesized, potentially error prone strands from pre-existing parent strands. In this way, a distinct set of strands (immortal strands) would be retained at every division,with a pre-existing DNA strand in each chromosome selected as the strand destined to remain with the stem cell. The newly synthesized strand incorporates label and this is given off to the daughter cell, destined for differentiation and loss from tissue. The original strand (unlabelled) will be kept by the stem cell and theoretically preserved indefinitely. This also means that

potentially there would be two types of labelled stem cells formed. The first type would lose the label by the time it has divided twice as the younger strand would have been segregated to the differentiating daughter. However, in conditions where stem cells are being actively recruited at times of injury it would become possible to label the immortal strand at the time when the new stem cell is created. This cell, according to the hypothesis should reduce the label at the first division and then remain labelled indefinitely. This was demonstrated by Potten and co-workers in 1978 where labelled cells were shown to halve the label at the first division and then maintain what was left for up to four weeks (Cairns et al, 2006). Experiments carried out on this phenomenon have largely been inconclusive as results indicate that DNA segregation is largely random. Nevertheless people have also shown that a small number of cells may selectively segregate their DNA strands. Experiments performed by Potten's group on small intestinal crypt cells demonstrated the presence of both types of cells, those which lost the label after about two divisions and those which retained the label for up to four weeks. In each case, cells either retaining or losing the label were demonstrated close to regions where stem cells were thought to reside that is support for Cairns hypothesis has been found in experiments carried out by Potten's group (Potten et al, 2002). Clevers demonstrated asymmetric division in Drosophila and showed that disruption of this balance led to cells acquiring cancer like states (2005). A small subset of breast cancer cells were shown to possess slower cell cycle kinetics in culture where these cells retained their label longer than the bulk of the population, a larger proportion of which were also shown to be positive for proliferation markers suggesting that these cells had a slower cell cycle (Fillmore and Kuperwasser, 2008).

The presence of stem cells has since been demonstrated in most epithelial tissues that have been carefully studied, for example, the skin (Janes, 2002), the liver (Cantz et al, 2007), pancreas (Bonner-Weir, 2002) andbreast (Stingl, 2009). The majority of cells with high clonogenic potential in the skin are present in the bulge region of the hair follicle (Alonso et al, 2006) and label retaining cells (LRCs), isolated from the bulge region are not only slow cycling but can be cultured extensively over many passages, one of the properties of stem cells. Other studies have also shown that interfollicular epidermal stem cells retain the ability to be reprogrammed and have the potential to give rise to multiple lineages (Liangand Bickhenbach, 2002). This concept is a main focus of biomedicine, where research has made it possible to generate new skin *in vitro* for grafting onto burns victims (Alonso and Fuchs, 2002).

Further information about human stem cells has been obtained from both *in-vitro* studies and from those involving NOD/SCID mice where the property of clonogenicity has largely been

used to assess stem-potential. As already mentioned, epithelial tissues contain cells with a range of growth potentials, i.e. the cell population is heterogeneous. *In vitro* this was first shown by Barrandon and Green in 1987, who plated human keratinocytes isolated from normal human epithelia, at clonal density, and found that three types of colony patterns were consistently generated. Some cells gave rise to round, tightly packed colonies of relatively small cells with a high nuclear to cytoplasmic ratio. These were termed **holoclones** (Figure 1.7a) and, as they contained cells which could be extensively replated to generate similar colony patterns, they were thought to contain stem cells. These cells could also regenerate a functional epithelium when transplanted onto mice (Fuchs and Blanpain, 2009). Other cells generated colonies consisting of loosely packed cells with an irregular outline, which were less capable of extensive growth and were termed **meroclones** (Figure 1.7b). The proliferative behaviour of these cells suggested an intermediate stage between stem and committed cells corresponding to transient amplifying cells. Some cells generated only small, abortive colonies which were not capable of much growth, corresponding to late transient amplifying cells, and were termed **paraclones** (Figure 1.7c). Such colony morphologies can be repeatedly generated in culture under a wide variety of culture conditions thus supporting the hierarchical concept of heterogeneity of epithelial cell behaviour while suggesting that the mechanisms by which these colony patterns are generated reside autonomously within the cells. (Tudor et al, 2004).

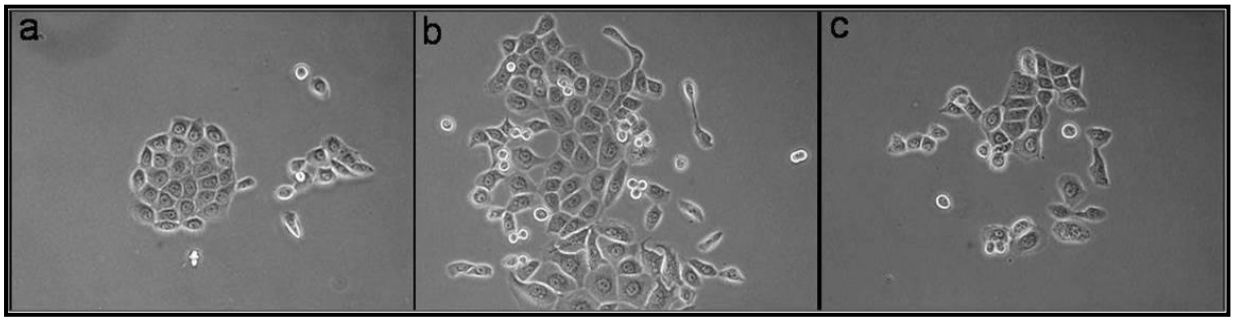

Figure 1.7: Cellular heterogeneity of oral keratinocytes when cultured. Holoclones are formed from small tightly packed cells (a). Meroclones are made up larger, loosely arranged cells (b). Paraclones contain large irregular shaped cells and show little growth(c).

Studies involving murine keratinocytes reveal similar patterns of cell behaviour although the morphology of the colonies formed differs from human keratinocytes (Tudor et al, 2007). Murine keratinocytes plated at clonal density form three distinct types of colonies, termed Type 1, Type 2 and Type 3 colonies, as shown in the figure below.

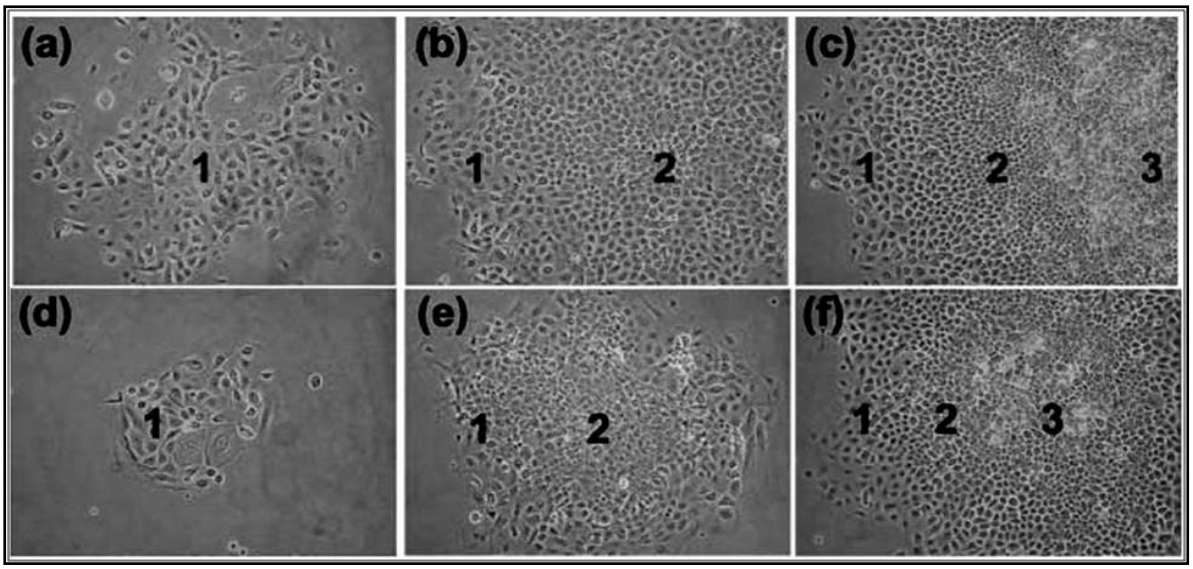

Figure 1.8: Different colony morphologies generated by murine skin keratinocytes. Panels (a-c) show type 1, type 2 and type 3 colonies. The central zone (3) (c) is thought to contain the stem cells as cells in this zone are highly clonogenic and can also give rise to the other zones. Zones marked 2 and 3 contain early and late transient amplifying cells respectively. Panels (d-e) show similar patterns obtained when cells from murine tongue were cultured (Adapted from Tudor et al, 2007).

Type 1 colonies contain loosely packed and scattered cells that cannot be maintained in subsequent passages (panel a). Type 2 colonies consist of type 1 cells at the periphery with an additional inner zone of smaller more closely packed type 2 cells (panel b). Type 3 colonies (panel c) are similar to Type 2 colonies but contain a central zone of even smaller and more tightly packed Type 3 cells. Replating cells from type 2 colonies generated both type 1 and 2 morphologies but only the central cells from type 3 colonies were able to be passaged for longer periods of time and reconstitute all three colony morphologies. It was hypothesized that these cells have stem cell capabilities whereas type 2 and 1 colonies represented committed transient amplifying and differentiated cells respectively (Tudor et al, 2007).

Generally, however, human and murine keratinocytes lack the ability to grow indefinitely in culture and after repeated passages all cells eventually give rise to paraclones or Type 1 colonies, reflecting the depletion of stem cells. It is therefore interesting that epithelial cells that are expanded *in vitro* and then reintroduced into *in vivo* conditions (human and murine) (Compton, 1998; De Luca, 1990) are able to support a functional epithelium indefinitely. One can infer from this that although some aspects of the generation of hierarchical colony patterns are epithelium-autonomous, the *in vivo* maintenance of stem cells is also dependant on

interactions between epithelium and connective tissue (Mackenzie, 1994). Work done by Maas-Szabowski and co-workers on compound cultures has reinforced this observation by showing that fibroblasts release keratinocyte growth factor (KGF) in response to interleukin-1 (IL-1) produced by epithelial cells (Maas-Szabowski N et al, 1996).

1.6 Stem cells, cancer and cancer stem cells (CSCs)

A solid tumour is like an organ that has developed in an aberrant way but still contains a heterogeneous mixture of cells and tissues (Wei et al, 2006). Malignant tumours and their metastases remain one of the leading causes of death in developed countries. Hanahan and Weinberg (2011) have described certain traits which a cell must have in order to become a cancer cell, suggesting that tumourigenesis is a multistep process where each step represents a progressive change resulting from genetic alterations which eventually lead to the transformation of a normal cell into its malignant derivative. They list six essential alterations dictating malignant change:

- Self sufficiency of growth signals
- Insensitivity to anti-growth signals
- Invasion of apoptosis or programmed cell death
- Limitless replicative potential
- Sustained Angiogenesis
- Invasion and metastasis

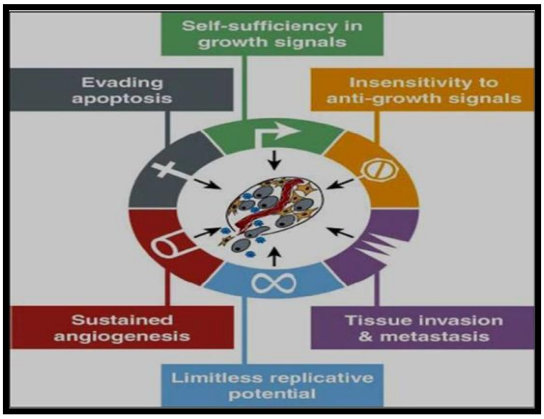

Figure 1.9: Sequelae of events required for carcinogenesis (Hanahan and Weinberg, 2009). Most cancers share all these characteristics with each of these acquired changes representing a breach in the normal anti-cancer protective mechanisms which cells have evolved. Self sufficiency of growth signals allows a cell to divide without being dependant on external signals which maintain a normal steady state. Anti-growth signals work by keeping cells either quiescent in a non-proliferative state or by forcing them into differentiation allowing cells to remain quiescent when they fail. Programmed cell death ensures that cell death balances cell turnover through mechanisms hardwired within cells, disruption of which allows cells to survive for prolonged time periods. Limitless replicative potential, a hallmark of normal stem cells, when

acquired by cancer cells allows them to multiply and eventually replace normal cells through a process of clonal expansion (Mackenzie, 2006). Angiogenesis is the process by which cells within tissues generate blood vessels to satisfy the demand for oxygen and nutrients and is very tightly regulated in normal tissues. Dysregulation of this process ensures a constant supply of nutrients for the cancer cells to survive indefinitely. Finally, the ability of cells to invade surrounding tissues provides a means for them to escape the primary tumour mass and colonize distant sites where nutrients and space to divide are available.

It is now generally accepted that, like normal epithelium and most other tissues, the growth of cancers, including oral cancers, is driven by a small population of self-renewing stem cells within the bulk of the tumour that allows the malignancy to be capable of extensive growth. This was first suggested as early as 1979 by Minden and co-workers and was demonstrated by Griffin and Lowenberg (1986) whose work with hematologic malignancies showed that only a small population of leukemic cells was clonogenic in culture. More conclusively, Bonnet and Dick (1997), by transplantation of acute myeloid leukemia (AML) cells into immunodeficient mice, showed that only cells with a CD34+/CD38- phenotype were able to form tumours. Since then CSCs have been identified in breast cancers (Al Hajj et al, 2003) where cells with CD24-/CD44+/ESA+ phenotype were shown to be related to tumour initiation when transplanted into mice. A study involving neuroblastomas identified cells expressing higher levels of CD133 as malignant progenitors (Jeanette et al, 2004). More recently malignant stem cells have been shown to exist in lung cancers (Kim et al, 2005), oral squamous cell carcinomas (Prince et al, 2007) and a range of other cancers. The finding that cancers are heterogeneous in both their cellular content and tumourigenic potential has led to 'the cancer stem cell' hypothesis (Clarke et al, 2006; Reya et al, 2001) which states that only a few subsets of cells within tumours have stem cell capabilities and that these are responsible for the long term growth and survival of cancers.

Experiments carried out by Locke and co-workers (2005), using cell lines derived primarily from oral cancers, have shown that stem cell patterns are also retained in OSCC cell lines. They showed that the in-vitro colony patterns of holoclones, meroclones and paraclones displayed by malignant cell lines are similar to those of normal keratinocytes. Further, one can predict not only the growth potential of these cells but also their surface molecular expression by the colony morphologies they give rise to. Malignant holoclones were comprised of small, rapidly adherent and highly clonogenic cells (Figure 1.10a) which show high surface expression of molecules such as CD44, β-integrin and β-Catenin, which are also highly expressed by normal

epithelial stem cells (Cotsarelis et al, 1999; Tudor et al, 2004). Correspondingly, paraclones expressed markers of differentiation, showed lower levels of expression of putative stem cell markers, and formed loose irregular colonies of flattened and less rapidly adherent cells which showed little growth potential. Meroclones had intermediate features with ovoid cells that were found to survive five or six passages. It was concluded that paraclones and meroclones represent populations of late and early transient amplifying cells respectively.

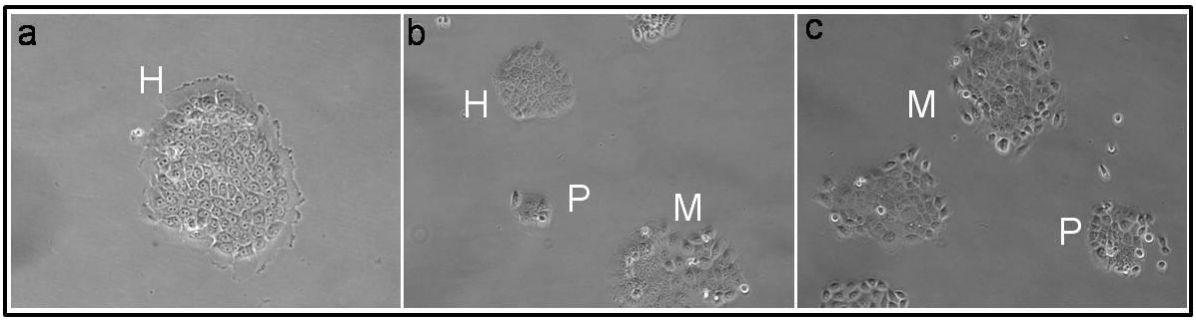

Figure 1.10: Ca1 cells plated at clonal density generate holoclones (H), meroclones (M) and paraclones (P).

Tumour cells cannot be easily studied *in vivo* and standard *in vitro* cultures fail to generate conditions present *in vivo* including cell to cell interaction patterns of normal epithelia. Although organotypic cultures do not fully correspond to *in vivo* conditions (Parenteau et al, 1992), they do provide a more normal environment with regard to cellular interactions and normal epithelial growth patterns seem to occur. The use of organotypic cultures with malignant oral cell lines has indicated a small population of cells with regenerative capabilities (Mackenzie, 2004).

Tumour cell populations, grown on a collagen matrix populated with fibroblasts form a stratified structure similar to that formed by normal keratinocytes. However, examination of a range of cell lines indicated that they all failed to form a well-organized epithelium and none generated a cornified layer. When tumour cells were incorporated into cultures of normal keratinocytes, they tended to remain in the basal layer and failed to differentiate normally (Mackenzie, 2004). With time, some tumour cells expanded to form clusters or islands of tumour cells growing at the expense of the surrounding normal epithelium (Mackenzie, 2004). The growth patterns of these clusters suggested a clonal origin and, as the number of clusters formed was less than the number of tumour cells initially seeded, that only a sub-fraction of cells was clonogenic.

1.7 The origin of the cancer stem cell

1.8.1 Malignant Transformation of normal stem cells

Maintenance of tissues by a small population of stem cells retained in the tissues throughout life suggests that they are likely to be the functional targets of carcinogens and acquire the deleterious mutations leading to cancer (Wei et al, 2006). Other epithelial cells, having a finite, and relatively short, life span, are unlikely to be retained in the tissue long enough to accumulate all the mutations necessary for carcinogenesis. However, there is some evidence that transient amplifying cells may be affected by such mutations and the in-vitro growth potential of human keratinocyte paraclones can be restored by transfection with viral oncogenes (Barrandon et al, 1989).

From review of the literature, it seems most likely cancer stem cells arise as a result of the accumulation of mutations in a normal stem cell which already possesses the properties of self-renewal and clonogenicity. As cancer stem cells lack pluripotency, it is likely that these cells are formed from adult stem cells (Biddle and Mackenzie, 2012). It seems reasonable to assume that mutations occur in genes controlling the genetic and epigenetic pathways linked to self-renewal mechanisms. Disruptions in this pathway could result in the maturation arrest of normal stem cells, thus reducing the normal proportion of asymmetric divisions and eventually leading to an increase in the number of altered stem cells. The two stage model of mouse skin carcinogenesis supports this observation as the interval between tumour initiation with dimethylbenzanthracene (DMBA) and the application of tumour promotion factors, such as phorbol esters, can be delayed with little reduction in tumour yield (Pardal et al, 2003), an observation strongly suggesting tumour origin from a long lived cell.

1.8.2 Epithelial Mesenchymal Transition

Epithelial Mesenchymal Transition (EMT) is a biologic process that allows epithelial cells to assume mesenchymal traits such as increased motility, invasiveness, resistance to apoptosis and survival in anchorage independent conditions (Thiery et al, 2009). Epithelial cells are arranged in a polarized pattern and maintain tight junctions with each other and with the substratum. They are separated from the surrounding stroma by a basement membrane that controls apico-basal polarity, distribution of adhesion molecules such as cadherins, and prevent changes in cell shape by controlling the cellular cytoskeleton (Gjorevski et al, 2011). All these ensure that epithelial cells are kept tightly in check and unable to migrate from their immediate environment (Mani et al, 2009).Many adult tissues are formed either by conversion of epithelial cells into mesenchymal cells or by the reverse process of mesenchymal to epithelial transition (MET) (Chaffer et al, 2006). EMT programs are activated in three biological settings and have been classified as Type 1, Type2 and Type3.

Type 1 EMT encompasses all EMTs occurring during gastrulation and early embryogenesis where epithelial cells generate mesenchymal cells which have the potential to undergo a MET to form secondary epithelia and initiate organogenesis. (Thiery, 2006; Sleeman, 2011; Kalluri, 2009).

Type 2 EMTs are activated during wound healing and tissue regeneration. They differ from Type 1 in that they are physiologically activated under inflammatory stress and stop once healing and repair is complete. Such EMTs are induced in response to growth factors and inflammatory cytokines produced as a consequence of the injury. Prolonged activation of these programs can result in fibrosis, for example renal fibrosis, where fibroblasts accumulating within the lesion are derived from epithelial cells undergoing EMT (Kalluri et al, 2003).

Type 3 EMTs refer to aberrant EMT programmes that are activated in cancer cells and produce changes favouring the uncontrolled growth that allows them to acquire invasive traits.As discussed later in this section, this enhances their metastatic potential and also allows them to acquire stem like states (Mani et al, 2009).

1.8 Epithelial Mesenchymal Transition and Cancer

The role of EMT in tumour progression is not completely understood (Tarin et al., 2005) but it has been proposed that EMT is a cyclic process that occurs initially at the primary tumour site to induce transformation and invasion. Later, as a reverse process, "mesenchymal–epithelial–transition" (MET), occurs to re-establish secondary tumours with epithelial properties similar to the primary tumour (Thiery, 2002). As discussed earlier, EMT is related to CSC behaviour and has been shown to play a role in the progression of many tumours. Cancer cells appear able to take control of existing EMT cellular machinery transforming themselves into invasive mesenchymal-like cells which have the ability to metastasize (Chaffer et al, 2006).

Mani and co-workers (2008) have suggested that EMT may contribute to the generation of stem-like properties of cancer cells. Induction of EMT in mammary epithelial cells enabled them to acquire mesenchymal traits, to express higher levels of stem cell markers and, additionally, an increased tendency to form spheres in culture, another property of self-renewing stem cells. Consequently, EMT cancer cells with stem cell characteristics have the ability to invade the adjacent stroma and to escape to distant sites and colonize new tumours.

In addition to acquisition of invasive abilities, metastasizing cancer cells need to complete a series of steps, referred to as the invasion-metastasis cascade (Mani et al, 2009). These are:

a) **Invasion**: Epithelial cells undergo EMT to become mesenchymal-like and breach the basement membrane.
b) **Intravasation**: The transformed cell moves into a blood vessel or into lymphatics, as is usually the case for HNSCCs.
c) **Extravasation**: On reaching a distant organ the cells leave the blood vessel and extravasate into the surrounding tissue to establish micro-metastases.
d) **Colonization**: This final step involves the growth of the micrometastases to form a macroscopic tumour.

The figure below is a schematic representation of steps discussed above.

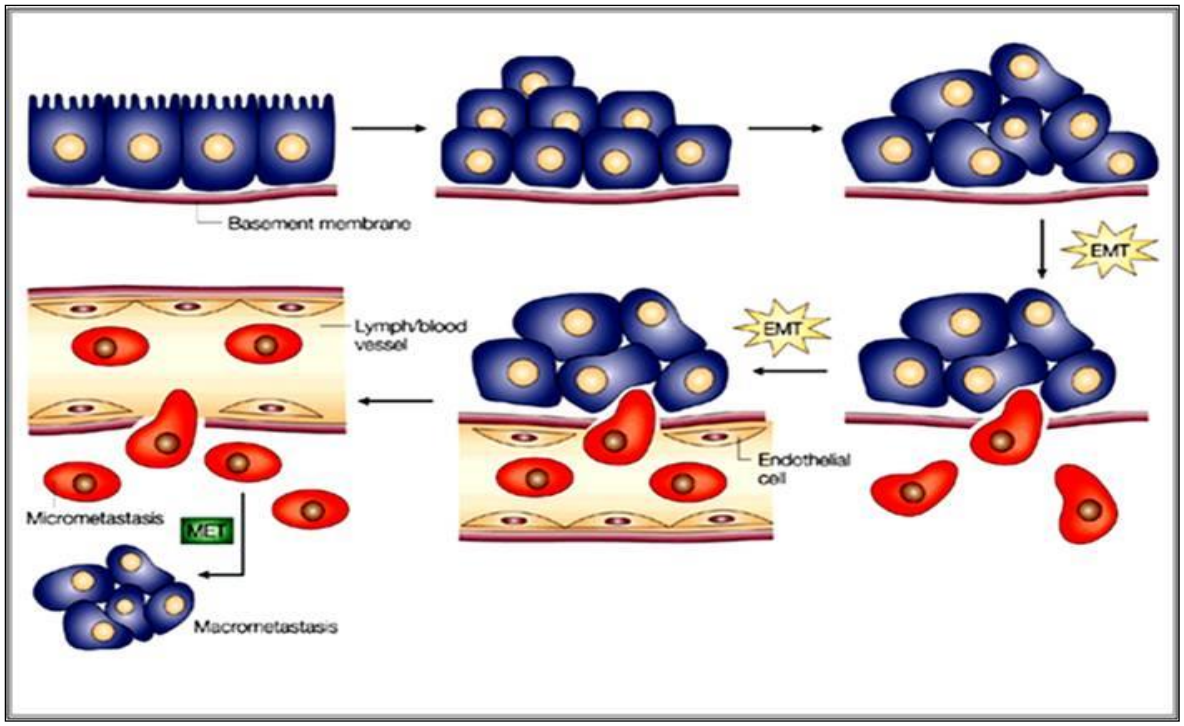

Figure 1.11: Schematic representation of tumour metastasis (Thiery, 2002).

As secondary tumours typically reconstitute the epithelial differentiation patterns present in the primary tumour, it appears that EMT, by a reverse process of mesenchymal to epithelial transition (MET) is necessary during secondary tumour formation (Chaffer et al, 2006). The implications of EMT in cancer have led to the mobile cancer stem cell model (MCSC). This model is important as it integrates both current cancer stem cell and EMT concepts. Tumour cells within the bulk of the tumour are relatively stationary and cannot disseminate but tumour cells at the tumour/host interface would be the ones most likely to undergo EMT in order to escape the primary tumour and these are termed migrating stem cells (MSCs). Understanding the biology of a tumour cell which can combine the traits of stemness and mobility is important in understanding malignant progression (Brabletz et al, 2005). This paradigm has led to studies of the tumour/host interface, also known as the "invasive front". It has also been shown that the tumour microenvironment contains inflammatory cells which produce cytokines such as epidermal growth factor (EGF), and transforming growth factor-β (TGF-β) and these have been shown to induce EMT (Eger, et al, 2004).Experimental studies into the pathways and signalling regulators of EMT have implicated the aberrant activation of the WNT programme which has been shown to be important in the development of stem cells and in the initiation of the EMT programme (Brabletz et al, 2005; Grunert et al, 2003). In colorectal cancer, the presence of cells expressing high levels of nuclear β-catenin at the tumour host interface is strongly

correlated with poor prognosis (Bankfalvi et al, 2002).

1.9Stem cell markers.

Currently, there is an absence of reliable markers for stem cells in various types of solid cancers but the expectation is that they may exist and that molecules expressed by normal stem cells will also be found in their malignant counterparts. If reliable markers for tumour stem cells can be found they are expected to provide target-oriented approaches that might be effective in tumour eradication and in prevention of recurrence and spread. In leukemias, rare cells with the CD34+/CD38- molecular phenotype are able to initiate tumours in mice(Bonnet et al, 1997).Breast cells enriched for CD24-/CD44+ form tumours in mice and also regenerate cellular heterogeneity *in vivo* and *in vitro*. (Al-Hajj et al, 2003). Functionally adequate markers have now similarly been identified for lung and brain cancers and, recently, for oral carcinomas (Prince et al, 2007). The figure below lists some of the known markers for normal and malignant stemcells.

Tissue/disease	Normal tissue stem cells*	Cancer stem cells†
Brain/medulloblastoma	$CD133^+$ $nestin^+$ $GFAP^+$ $A2B5^+$ Musashi1 SSEA-1	$CD133^+$
Breast	$\alpha6^+CK19^+ESA^+MUC1^-CALLA^-$	$ESA^+CD44^+CD24^{-/low}$
Haematopoietic/CML	$CD34^+CD38^-$ $CD133^+$ $ALDH^+$ SP	$CD34^+CD38^-$
Gastrointestinal	Musashi1 Hes-1 Nuclear β-catenin	SP—found at low frequency (0.3–2%) in 15/16 cell lines

Figure 1.12: Proposed markers for normal and malignant stem cells (Burkert. J et al, 2006).

Several cell surface molecules have been associated with stemness and tumourigenicity. In brain tumours, cells enriched for CD133 and Nestin (Uchida et al, 2000; Jeanette et al, 2004) were shown to form tumours in mice. Only CD133 positive cells were reported to form neurospheres, a hallmark for neuronal stem cells (Al-Hajj and Clarke, 2004). Interestingly CD133 has also been reported as a marker for lung cancers when it was found that CD133 positive cells were able to asymmetrically segregate their DNA strands. It was also found that this subpopulation was able to repopulate the entire tumour population under *in vivo* and *in vitro* (Pine et al, 2010).

A small population of cells within tumours cell lines has also been shown to possess the ability to efflux Hoechst dye and are termed the side population (SP).These cells were also shown to have stem cell characteristics of high self-renewal and clonogenicity (Ho et al, 2007). This ability was later attributed to these cells expressing high levels of ABC transporter proteins. They were first described by Goodall and co-workers (1996) in the bone marrow as cells expressing high levels of hematopoietic stem cell markers but since then they have been characterized in human cancers of many origins including leukemias, neuroblastomas, gliomas, lung and breast cancers (Ho. et al, 1996; Goodall et al, 2004). Further, SP cells have been shown to be resistant to standard chemotherapy and radiotherapy regimes (Moserle et al, 2009), this having been first demonstrated by Hirshmann-Jax and colleagues who showed that neuroblastomas were resistant to the drug mitoxantrone (2004). Experimental data from breast and brain models suggest that SP cells within many tumours may be resistant to radiation and this was shown to be connected to the aberrant activation of the Wnt/β-catenin pathway (Chen et al, 2007). However, concerning HNSCC, breast and prostate cancers, CD44 is one of the most extensively studied stem cell markers (Al-Hajj et al, 2002; Wang et al, 2006; Prince et al, 2008, Harper et al, 2007).

The designation CD44 encompasses a group of multifunctional, mostly cell surface, proteins existing as about nine or more isoforms. Different isoforms are generated by complex splicing of mRNA transcripts of the CD44 gene, and undergo post-transcriptional modification, leading to potentially complex functions (Bankfalvi et al, 2002). The smallest of these isoforms is the standard form of CD44 (CD44s) which is the most common member of this family (Mack and Gires, 2008) and is present on most vertebrate cells (Marhaba, 2003). CD44 is one of the main cell surface receptors for hyaluronic acid present within the extracellular matrix and probably plays a major role in cell adhesion (Gunthert et al, 2005). However, CD44 also possesses a range of signalling functions that include control of lymphocyte activation and homing (Gunthert et al, 1998), cell migration (Estess et al, 1999) and metastasis (Oliveira and Odell, 1997; Herrlich et al, 1993; Zoller, 2011). Deranged patterns of CD44 expression have been reported in bladder cancers (Matsumura et al, 1995), lymphomas (Koopman et al, 1993) and breast cancers (Ponta et al, 1995). In the 1990s it was recognized that CD44 isoforms, particularly CD44v6 might play a major role in tumour invasion and metastasis (Gunthert et al, 1991) through studies on a rat model. CD44 variants 4-7 were shown to play a vital role in the metastasis of pancreatic cancers in a rat model and it is interesting to note that blocking the function of v6 inhibited lymph node and lung metastases (Gunthert. et al, 1998). Since then

numerous reports have been published which implicate CD44 and its exons in the behaviour of many human tumours (Rousseau, 2010). In colorectal cancers CD44s, v3, v6 and v8-10 were shown to correlate with poor prognosis whereas in breast and ovarian cancers, CD44v3, CD44v6 and CD44v7/8 were related to more invasive disease (Kainz et al, 1995; Gotte et al, 2006).

Cells positive for CD44 in oral cancers have been shown to be more clonogenic than the rest of the cell population and are also able to instigate tumour formation in immune deficient (NOD/SCID) mice. (Prince et al, 2007). This was better demonstrated by Biddle et al (2011) who showed that transplantation of CD44 high cells rather than CD44 positive cells into the tongue of mice correlated with tumour yield and further showed that selection of $CD44^{high}$ cells with those expressing low levels of ESA (epithelium specific antigen, EpCAM) also resulted in lymph node infiltration. Harper et al (2007) demonstrated the clonogenicity of $CD44^{high}$ cells obtained from fresh cell lines generated from HNSCC tumour biopsies. Recently HNSCCs derived from Fanconi anaemia patients were also shown to have a subpopulation of clonogenic cells expressing high levels of CD44 (Gammon et al, 2011). These cells were also more resistant to apoptosis and spent an extended time in the G2 phase of the cell cycle which has been associated with DNA repair (Harper et al, 2011). Normal oral epithelia also express CD44 with basal cells generally staining stronger than the other layers (Oliviera and Odell, 1997). The expression patterns of CD44 and its variant v6 were evaluated by Mack and Gires (2008), who found the CD44s form to be abundantly expressed in all the normal and cancerous tissues examined. They also found no differential expression of v6 between normal and cancerous sectionsand question the validity of CD44 as a stem cell marker. Their findings are somewhat in contrast to those by Prince (2007) who stated that only a minority of cells (<10%) represented the $CD44^{positive}$, and hence the tumour initiating population

Based on the information present in the literature which implicates CD44 in initiation and progression of OSCC and other tumours, it would be a logical target for the development of therapy aimed at successful HNSCC treatment. Phase I clinical trials against v6 were developed and looked promising as they successfully blocked major aspects of tumourigenesis *in vitro*, but resulted in the death of a patient owing to adverse side effects on skin and have largely been abandoned. The efficacy of these peptides is currently being tested in xenograft models using breast and oesophagus cancer cells (Orian-Rousseau, 2010).Aldehyde Dehydrogenase (ALDH) is one of the recently implicated markers for head and neck cancers and ALDH positive cells were found to form tumours with greater efficiency in mice as compared to

ALDH low cells (Prince et al, 2010). High ALDH activity has also been used to characterize murine hemopoeitic stem cells (Armstrong et al, 2004), CNS stem cells (Pearce et al, 2005) and colonic cancers (Huang et al, 2009). Biddle and co-workers have shown that bi-potent stem like cells within oral cancer cell lines also express high ALDH1 activity (2011).

Signalling pathways, stem cells and cancer

Pathway	Stem cell	Cancer
WNT	Haematopoietic stem cells[31,32] Intestinal epithelial stem cells[47] Keratinocyte stem cells[30,85] Cerebellar granule-cell progenitors[86*] CNS stem cells[43]	Lymphoblastic leukaemia[60,61] Colorectal cancer[49] Pilomatricoma[45,46] Medulloblastoma[44] Gliomas?
SHH	Hair-follicle progenitors[87,88*] Cerebellar granule-cell progenitors[33*] CNS stem cells[35]	Basal-cell carcinoma[89–91] Medulloblastoma[34,92-94] Gliomas[95]
BMI1	Haematopoietic stem cells[13]	B-cell lymphomas[71] AML[14]
Notch	Haematopoietic stem cells[38] Mammary epithelial stem cells[96]	Lymphoblastic leukaemia[37] Breast cancer[97]
PTEN	Neural stem cells[41]	Gliomas[98]

In all cases it is unknown whether the cancers arise from the transformation of stem cells or other cells in their tissues of origin. *It is uncertain whether these WNT/SHH-responsive progenitor populations are multipotent stem cells or restricted progenitors. AML, acute myeloid leukaemia; CNS, central nervous system; PTEN, phosphatase and tensin homologue deleted from chromosome 10; SHH, Sonic hedgehog.

Figure 1.13: Known pathways of stem cell self-renewal and results of dysregulation(Pardal et al, 2003).

1.10 EMT pathways and the molecular mediators involved in this transition

Studies of pathways involved with 'stemness' have shown that the same pathways may be closely related to EMT. The Wnt pathway is one which is thought to activate some or all aspects of EMT and has also been shown to have a role in maintaining stem cell self-renewal (Wei et al, 2002) when its inhibition successfully blocked epidermal squamous cell carcinoma development. The loss of membranous E-Cadherin is crucial in the development of carcinomas from benign tumours (Hollier et al, 2009) and this cell adhesion protein is linked to EMT with its loss appearing to be a rate limiting step in this process. EMT is also characterized by a change in β-catenin location and this protein is also a central mediator of EMT. Brabletz et al (2009) have shown that where loss of E-cadherin characterizes EMT it is accompanied by dysregulation of β-catenin. There is evidence that accumulation of nuclear β-catenin increases

as E-cadherin is downregulated. In normal epithelial cells, membrane localized β-catenin exists in a junctional complex with E-cadherin but once this complex is inactivated, free β-catenin translocates to the nucleus where it activates target genes involved in oncogenesis and tumour progression (Kim, 2001). The integrity of the E-cadherin and β-catenin complex is thus vital for cell adhesion and disruptions of this adhesion complex are pivotal in the development of metastatic potential and the acquisition of invasive potential (Brabletz et al, 2009).

Transforming growth factor-β (TGF-β) is a member of a large family of cytokines that are involved in many processes, including growth, differentiation, migration, cell survival and adhesion. Its role as an inducer of EMT is also well documented. Excessive TGF-β signalling has been implicated in many pathological conditions such as fibrosis and cancer (Hill et al, 1999) and loss of TGF-β activity has been linked to compromised wound healing (Roberts and Sporn, 1993). This family of growth factors works through Type I and Type II receptor serine/threonine kinases, activation of which causes the two receptors to come together to form a complex. These signal the nucleus through the SMAD family of proteins that are categorized into three functional classes as receptor activated, co-mediator and inhibitory SMADS. Once activated, receptor and co-mediator SMAD proteins form complexes in the nucleus that are directly involved in the transcription of target genes. The inhibitory SMADs negatively regulate TGF-β signalling by competing for receptor sites and preventing phosphorylation of Type I and Type II receptors (Shi and Massague, 2003). TGF-β super family members have also been shown to activate the MAP-kinase pathways which control morphogenesis and growth, although the mechanisms underlying this are poorly understood (Massague and Chen, 2000).

TGF-β was first described as an EMT inducer for normal mammary epithelial cells by Duband (1994) but human alveolar epithelial cells have also been shown to undergo EMT under the influence of TGF-β (Zhang et al, 2005). Murine epithelial cells change morphology and acquire EMT characteristics when stimulated by low doses of TGF-β (Thiery, 2002). Similarly human keratinocytes show an E-Cadherin response to TGF-β (Zavadil et al, 2004). Other studies show that TGF-β may also be able to cause alterations in cell morphology directly through receptor activation without nuclear regulation (Perrez-Plasencia et al, 2007; Ozdamar et al, 2005). A large body of evidence strongly linking TGF-β mediated EMT to tumour progression, and particularly invasiveness, has now accumulated (Border and Noble, 1994). In breast cancer, colon cancer and squamous cell carcinomas, treatment with exogenous TGF-β leads to

increased invasiveness and metastasis (Massague, 2008; Bates and Mercurio, 2005; Cano et al, 2009).

1.11 Patterns of local invasion of HNSCC: the invasive margin.

At the time of starting the work for this thesis the questions thought to be of particular interest were a) how the apparently immortal CSC fraction of tumour cell lines was maintained in a self-renewing state and b) how changes occurred in a fraction of cells that resulted in them losing self-renewal and becoming identified as founders of meroclones and paraclones. The initial idea was that cells at the margins of holoclones were in less tight contact with other epithelial cells and might be subject to lesser levels of paracrine factors maintaining their "stemness". This concept was supported by the lesser staining of peripheral cells for markers such as CD44, e-cadherin, and ESA that are found at high levels on clonogenic cells. The figure below shows a colony of the CA1 cell line viewed in phase contrast microscopy and by fluorescence to show the pattern of staining for CD44.

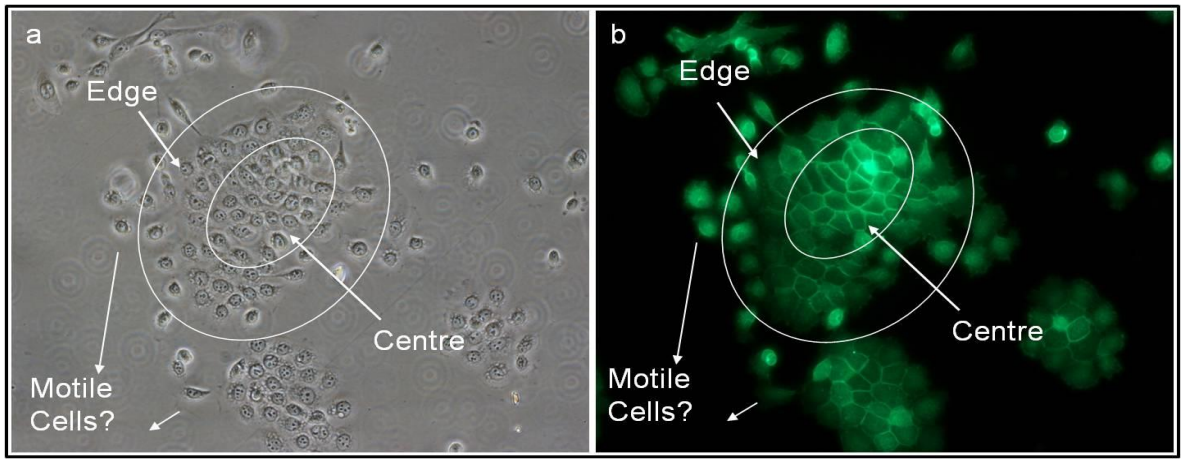

Figure 1.14: Culture of CA1 cells stained with anti-CD44 antibody.

Cells in the centre of the colony show strong staining for CD44 but this is reduced in peripheral cells and in the scattered isolated cells. However, some of the motile cells at the edge stain strongly for CD44. Our initial approach was therefore to search for markers that indicated further differentiation-related differences between centre and edge cells.

During the progress of work for this thesis, one of our research group members made the observation that the EMT detectable in cancer cell lines arose as a result of changes in the stem cell fraction and was able to further characterize various events associated with this process (Biddle et al, 2011). Phase contrast microscopy indicated the presence of elongated fibroblast-like cells in cultures of all cell lines and time-lapse video indicated that these cells appear highly

motile and seemed to be generated from cells at the colony periphery. As discussed below, it appeared that this phenomenon was potentially related to the *in vivo* invasion of cancers, and the focus of the research of the thesis therefore shifted towards mechanisms of EMT.

Concerning cellular changes potentially associated with invasion of HNSCC into the adjacent tissues, there have been reports of a range of factors associated with local invasion and metastasis (Finger and Giaccia, 2010). These are the growth factors, proteins and enzymes produced by the tumour cells and the cells present in the adjacent stroma, or tumour microenvironment. In normal conditions the cellular microenvironment keeps malignant growth in check through induction of control mechanisms discussed earlier (Figure 1.9), but tumour cells can modulate this to enhance their own survival, adhesion and motility (Scheel et al, 2011). The tumour's environment is made up of endothelial cells, fibroblasts, perivascular cells and inflammatory cells supported by an extracellular matrix or basement membrane and these components are thought to play critical roles in various processes involved during tumour progression including inflammation and angiogenesis. Inflammatory cytokines have been implicated in HNSCC tumour progression where their prolonged activation promotes an environment favouring invasion and migration (Mariotti et al, 2009). Tumour cells are also able to secrete cytokines which attract inflammatory cells and tumour associated macrophages that have been shown to produce pro-angiogenic factors (Schoppmann et al, 2002). TGF-β is one of the major mediators of this process and has been shown to aid the spread of cancer cells to lymph nodes (Coussens and Werb, 2002; Finger and Giaccia 2010). The region of interface between the tumour and the stroma, (variously referred to as the tumour front, invasive front, or invasive margin) is an area of particular prognostic importance (Bankfalvi and Piffko, 2000;Bryne et al., 1998). It is thought that disturbances in mechanisms controlling proliferation, differentiation and epithelial mesenchymal interactions at the tumour-host interface govern malignant progression of carcinomas. The evidence also strongly suggests that fibroblasts in the vicinity of the tumour cells undergo activation becoming 'cancer associated fibroblasts' (CAFs) and promote the spread of tumours by creating an environment favouring inflammation (Cirri and Chiarugi, 2011) through the production of inflammatory cytokines (Gerber et al, 2009). They also induce EMT in cancer cells that allows them to become more migratory and invasive (Kalluri, 2009; Thiery et al, 2009). The role of CAFs in promoting tumour progression has been documented in prostate (Gianonni et al, 2010), colon (De Wever et al, 2004), and breast cancers (Orimo et al, 2009). An increasing body of evidence suggests that the most aggressive cells within cancers are present at this invasive front. The significance

of the invasive front has also been demonstrated in squamous carcinomas occurring in the larynx, uterine cervix and the breast (Bryne et al, 2005; Zhang et al, 2005; Bankfalvi and Piffko, 2000). Elucidation of events involved in the molecular interactions occurring at the invasive front appears to be the key to understanding malignant progression,but few have been characterized. The Ki-67 protein is a marker of proliferation and it has been proposed that increased proliferative activity is in direct relation to dysplastic severity (Kearsley et al, 1990; Papadimitrakopoulou et al, 2002). Another widely studied protein is p53 and the p53 tumour suppressor gene (or guardian of the genome) that mediates cell cycle arrest and apoptosis in cells after DNA damage, mutations in which have been reported in many cancers (Vogelstein et al, 2000). Histologically-detected changes of prognostic significance in this region include increased expression of CD44v5 and v6 isoforms (Herold-Mende et al, 1996; Piffko et al, 1996). Immunochemistry of OSCCs showed a reduction of membranous E-cadherin, β-catenin and desmosomal proteins (Bankfalvi and Piffko, 2000). A wide range of molecular changes has also been reported in the expression levels of proteins such as vimentin, e-cad, b-cat, MMP9, α-SMA, snail and laminin-5 (Marsh et al, 2011; Franz et al, 2009; Berndt et al, 2001; Berndt et al, 1997; Lewis et al, 2004;Kristensen et al, 1999; Liu et al, 2009; Sterz et al, 2010; Wang et al, 2009). It is of interest that changes in most of these molecules have also been reported to be associated with EMT (Brabletz et al, 2009). These observations indicated that while, as we had initially considered, some holoclone cells have patterns of programmed cell division that lead to generation of differentiating cells, others are at the same time undergoing a process similar to EMT.

In some respects, therefore, a holoclone colony can be likened to a tumour with the center of the colony representing the bulk of the tumour and the edge representing the invasive front. Considering such parallels between the *in vivo* and *in vitro* conditions, it was thought that the behaviour of cell colonies *in vitro* might form an interesting model for study of the events associated with tumour growth and invasion *in vivo*.

1.12 Hypotheses

It is now generally accepted that cancer growth is ultimately driven by a sub-population of highly-clonogenic, long lived stem cells which generate the cells present within the bulk of a tumour. Experimental studies have established that these cells differ from the rest of the tumour cells in terms of their cell surface markers and gene expression patterns. Concerning the behaviour of cells in cancer cell lines, it was hypothesized that:

a) The changes associated with transition from holoclone to paraclone cells can be identified using immunocytochemistry and FACS analysis for key markers.

b) In-situ hybridization using radioactively labelled mRNAs for putative stem cell markers may identify stem cells in sections of biopsies of oral cancers

c) cell lines growing *in vitro* can be used as a model to study EMT processes related to the invasion and spread of tumours

1.13 Aims

a) To identify and isolate enriched stem cell populations from oral cancer cell lines.

b) To identify key proteins that are differentially expressed in holoclones, meroclones and paraclones.

c) To identify and localize stem cells in wax-embedded sections of oral squamous cell carcinomas and normal adult and foetal skin.

d) To examine changes inOSCC cell lines induced to undergo EMT by external factors.

Chapter 2: Results

2.1 Analysis of the distribution of putative stem-cell-related molecules in wax-embedded sections of OSCC using in situ hybridization.

2.1.1 Introduction:

Holoclone colonies are thought to be largely composed of stem cells as these cells can be passaged over a long period of time and display robust colony formation when isolated and plated out again. Paraclone cells on the other hand, express little in the way of stem cell markers and show little growth, an indication of their being formed from late transient amplifying cells. Affymetrix analysis of OSCC cell lines (Locke et al, 2005) showed a number of molecules to be differentially expressed in holoclones compared to paraclones. These differentially regulated markers were deemed suitable as possible stem cell markers and selected for in-situ probe design. It was hypothesized that these markers might better serve as stem cell markers and could reveal stem cells or stem cell zones within wax-embedded sections of OSCC and might identify changes of cellular expression in colonies *invitro*.

Proposed markers included CEBP-α, DKK3, Pirin, Hurpin7, IGFB3, RDHL, PSCA, Erb-b3, Notch3 and Vimentin. B-Actin was selected as a control to demonstrate the presence of hybridisable mRNA in the tissue sections studied which included foetal skin, lung tissue, heart musculature, adult skin and two blocks of HNSCC.

2.1.2 Materials and Methods

In Situ Hybridization

a) Tissue Preparation and Handling

Blocks of formalin-fixed and paraffin embedded tissues were obtained from the archives of Prof. Gareth Thomas at the University College Hospital for which ethics approval had already been obtained and a range of these was selected to analyse the specificity of the probes designed on different tissues. A microtome was used to cut 4-5µ thick sections which were floated on DEPC-treated Milli-Q (Sigma, 5758) water collected on pre-coated glass slides (Shandon, 9991002), and left to dry overnight in a 40ºC oven protected from dust. Next, the sections were de-waxed in Xylene for 5 minutes followed by rehydration washes with 100%, 80%, 60% and 30% ethanol containing 0.1% DEPC. The slides were washed in PBS followed by permeabilization with Proteinase K (Gibco) (20ug/ml) for 5 minutes. Washes in PBS/0.2% Tween 20 (Sigma, UK) were followed by two washes in PBS followed by post fixation in 4%

paraformaldehyde for 10 minutes and further rinsing. The tissue on the slides was acetylated with 0.1M Triethanolamine (Sigma, 1502) and 1.25 ml of acetic acid (Sigma, 6404), washed with PBS/0.2% Tween 20 followed by dehydration with alcohol in increasing concentrations from 30% to 100%,containing 0.1% DEPC, after which they were air dried.

Specific localization of probe mRNA was accomplished by in situ hybridization using an antisense riboprobe synthesized with T7 RNA polymerase (Amersham, UK).

b) Production of Riboprobes Labelled with ^{35}S

The mastermix components used the *invitro* transcription procedure for generation of the riboprobes are listed in the table below.

Mastermix Component	Volume for 4 reactions	Final concentration
5 X Transcription Buffer	10µl	1X
Rnasin	4 µl	~1.5U/µl
DTT	2.8µl	11.2mM
ATP, GTP, CTP mix	8 µl	1mM each
35S-UTP	14µl	14µM and 5.6mM

Table 2.0 - Mastermix constituents for production of riboprobes

The constituents of individual reactions for the generation of probes are listed in the table below.

Ingredient	Full reaction	Half Reaction
Mastermix	9.7µl	4.85µl
Probe	2.4µl	1.2µl
Appropriate polymerase	0.4µl	0.2µl

Table 2.1 - The constituents of an individual reaction

Using separate Eppendorf tubes, the constituents for each probe were mixed well, spun down at maximum speed for 10 seconds, and left to incubate for 60 seconds at 37-40ºC. The template DNA was destroyed by adding 1µl DNAseI to each reaction tube, mixing the constituents well and spinning them down for a few seconds. The tubes were incubated at 37ºC for 15 minutes. The Chromaspin column was inverted several times to ensure proper mixing of the gel, the top and bottom cap were removed and the column placed in a micro-centrifuge tube and spun down at 700g for 3 minutes at 15ºC. The eluate and the first collection tube were discarded. 4µl RNAsin plus and 6µl 100mM DTT were added to a new collection tube. At the end of the incubation period, the bulk of the reaction mix in the Eppendorf tubes was added to the gel in

the column and the assembly spun down again. The eluate was collected and used for hybridization procedure or stored at -20ºC.

c) Hybridization and post hybridization washes

For the hybridization procedure, 50% dextran sulphate solution was heated to 80ºC in a water bath to reduce its viscosity. The total volume of the hybridization buffer was calculated based on the number of slides being processed ($1x10^6$cpm/section). The constituents of the hybridization buffer are listed below and were added in the following order:

Ingredient	Quantity/ml
10X salts mixed in Denhardt's solution	100µl
Formamide	500µl
rRNA	30µl
Dextran Sulphate	200µl
1M DTT	10µl
DEPC-treated Milli-Q water	16µl
Probe	144µl

Table 2.2 - The constituents of the hybridization buffer

The hybridization buffer was heated to 80ºC for 1 minute and then spun down to reduce aerosols. 15µl of the buffer was pippetted onto each section after which a cover-slip was lowered down onto the slide until the whole section was covered. The slides were stored in a humidified box lined with blotting paper soaked in 50% formamide (Biorad AG-501), the box was sealed with PVC tape, and left overnight at 55ºC.The slides were placed in a clean rack, immersed in 1000ml of 50% formamide buffer at 55ºC, and placed on a rocking incubator. The buffer was changed thrice over a period of 3 hours. The slides were washed in 1000ml TNEbuffer(Tris/HCl-Sigma T3253, EDTA-Sigma E5134) at least 9 times to wash out traces of formamide. The constituents of TNE buffer were as follows.

Ingredient	Quantity/ml
3M Nacl	176.2g
100nM Na_2HPO_4	14.2g
100mM Tris/HCl	100ml
50mM EDTA	250ml
Milli-q water	650ml

Table 2.3 -TNE buffer constituents

Slides were then incubated in 100µg/ml RNAse A (Sigma R-5503) in TNE buffer for 1 hour at 37ºC after which the slides were washed in 2x standard saline citrate buffer (Sigma S-6689) for 30 minutes at 65ºC to wash off unbound probe fragments. The slides then passed through

graded ethanol (30% to absolute) containing 0.3M ammonium acetate (Sigma A-1542) to ensure fixation of labelled hybrids. The slides were covered and left to dry overnight.

d) Autoradiography

This procedure was carried out in a darkroom using a 902 filter and a 15W bulb. A water bath containing 25ml Milli-Q (Sigma W-4582) water was heated to 45ºC. Ilford K5 solution was added to make up volume to 45ml and left for 5-10 minutes for emulsion to melt. The slides were dipped into the stirred emulsion, placed flat on a cool metal surface to dry for 1 hour, placed in a black plastic bag, sealed with tape and left at 4ºC for 7 days to expose emulsion to the radioactive probe.

e) Developing, Counterstaining and Examination of slides

The slides were immersed in pre-prepared D-19 developer (KODAK) for 4 minutes at 18ºC, followed by 1% acetic acid (Sigma A-6604) for 30 seconds, tap water for 30 seconds and 30% Sodium Thiosulphate (Sigma S-7026) for two changes of 4 minutes each. Giemsa counterstain (BDH, 35086) was used to discriminate epithelial structures and appendages.The sections were examined under conventional or reflected light and dark field conditions on an Olympus BH2 epi-illumination microscope and photographed using a camera that allowed individual autoradiographic silver grains to be seen as bright objects on a dark background. Pictures were saved on an Apple Mac (Apple Inc) and viewed using Adobe Photoshop CS2 (Adobe Systems).

f) Technical help

The experimental work was carried out at Cancer Research United Kingdom (CRUK), (London Research Institute, Cancer Research UK, Lincoln's Inn Fields Laboratories, 4 Lincoln's Inn Fields, London, WC2A 3LY, United Kingdom), in collaboration with Richard Poulsom’s lab that provided technical help.

2.1.3 Results

(I) Wax-embedded tissue sections

a) β-Actin: (Control tissues)

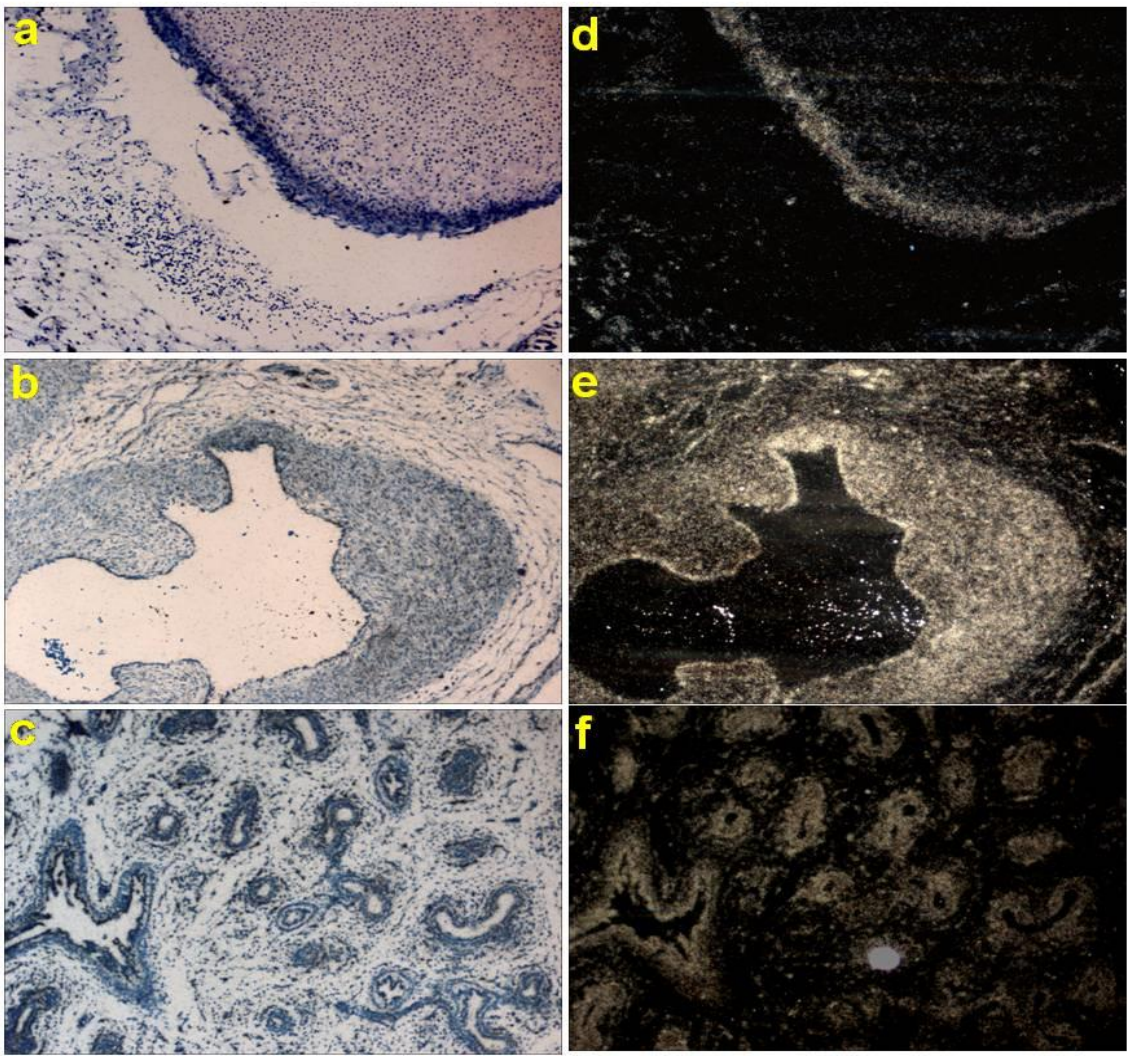

Figure 2.0: The expression of β-Actin mRNA in foetal skin (a, d), ventricular musculature (b, e) and alveolar epithelium (c, f). Panels a-c show brightfield views of histological sections of the tissues examined. Panels (d-f) show the same views photographed using epi-illumination to visualize the silver grains generated by the radioactive probe. β-actin is expressed strongly in foetal skin and is restricted mainly to the epithelium with only slight expression in the connective tissue (d). It is also strongly expressed in heart musculature (e), in lung alveolar epithelium and in endothelial cells (f).

b) B-Actin: (Adult skin and OSCC)

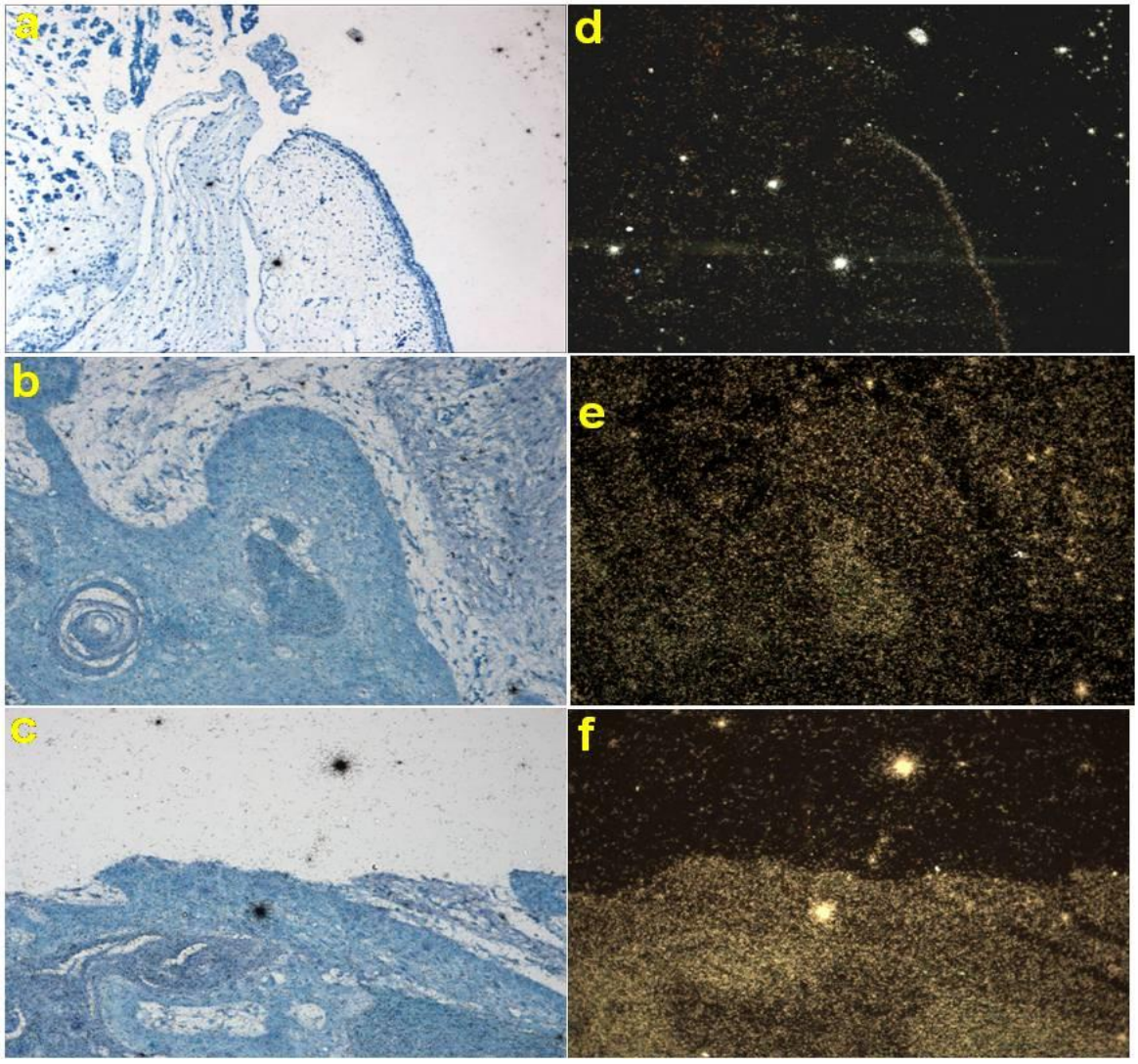

Figure 2.1: The expression of β-actin mRNA in adult skin and OSCC sections. Histological sections of adult skin (a) and OSCC blocks examined are shown (b, c). Panels (d-f) show the same views photographed using epi-illumination to visualize the expression of β-Actin mRNA in adult skin (d) and OSCC sections (e, f). Strong expression of β-actin is evident in adult skin, restricted mainly to the epithelium with only weak expression in connective tissues. β-Actin expression was present in both epithelium and connective tissue of the cancer sections examined (e, f).

c) CEBP-α: (Control tissues)

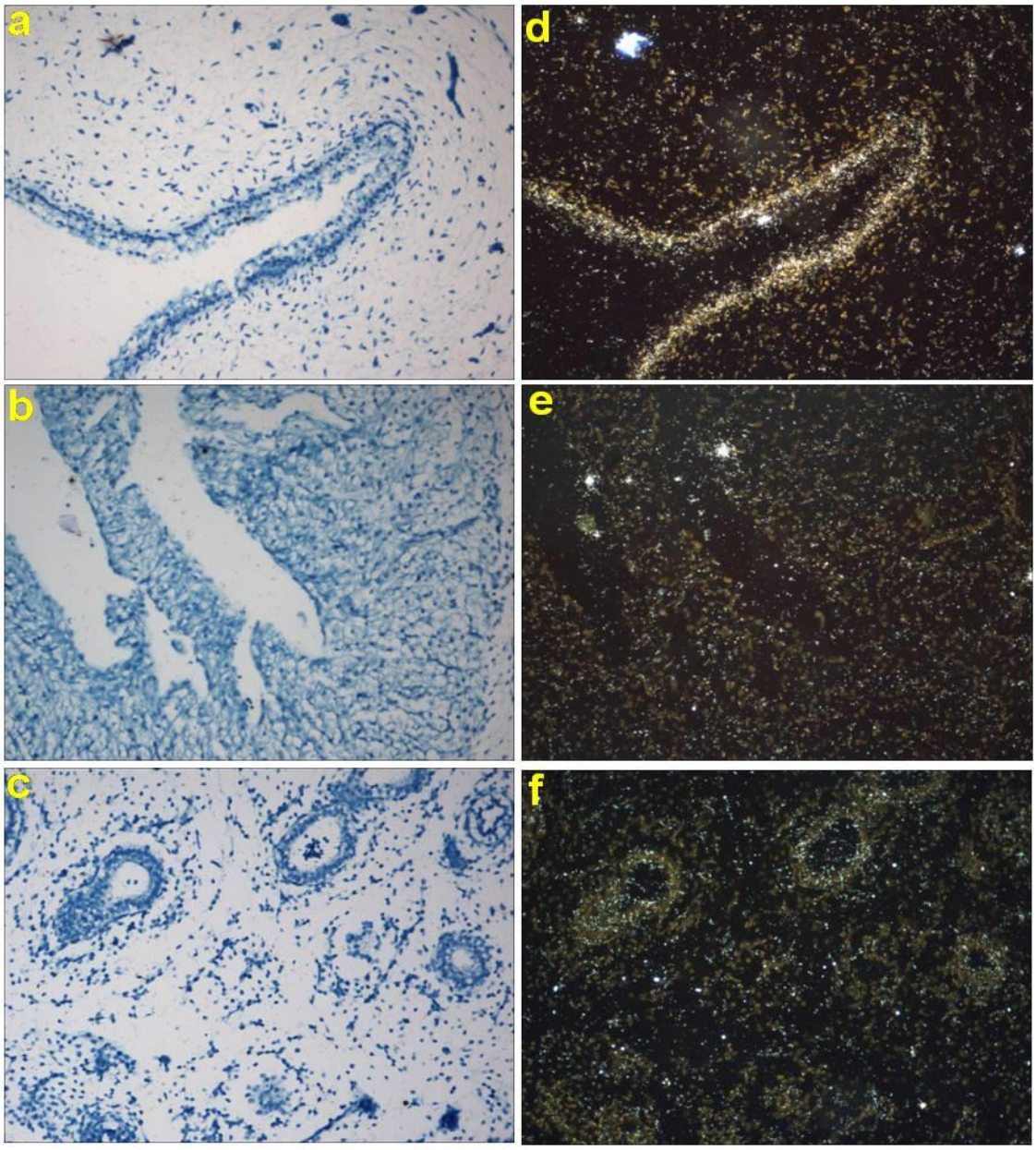

Figure 2.2: The expression of CEBP-α mRNA in foetal skin (a), heart musculature (b) and alveolar tissue (c). CEBP-α mRNA is strongly expressed in foetal skin (d), localized mainly to the basal layers of the epithelium. Weak expression is seen in heart musculature (e) and moderate expression in alveolar epithelium (f).

d) CEBP-α (adult skin and OSCC)

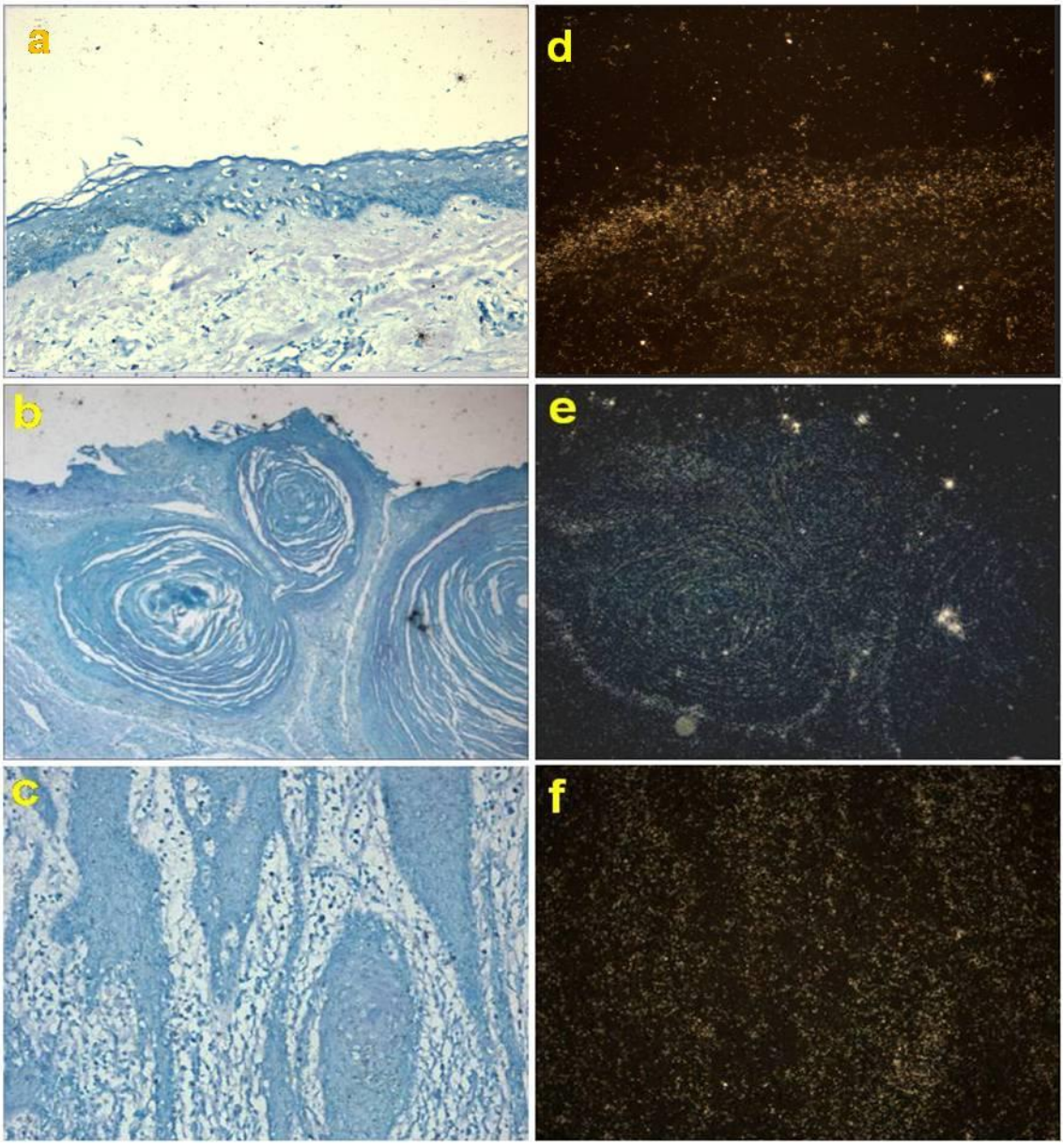

Figure 2.3: Expression of CEBP-α mRNA in adult skin (a), and OSCC sections (e, f). Moderate expression of CEBP-α was seen in adult skin mainly in the epithelium (d). Moderate expression in seen in OSCC sections examined (e, f) and was restricted to epithelial structures such as keratin pearls (e) and islands of epithelial tumour cells (f).

e) Vimentin: (Control Tissues)

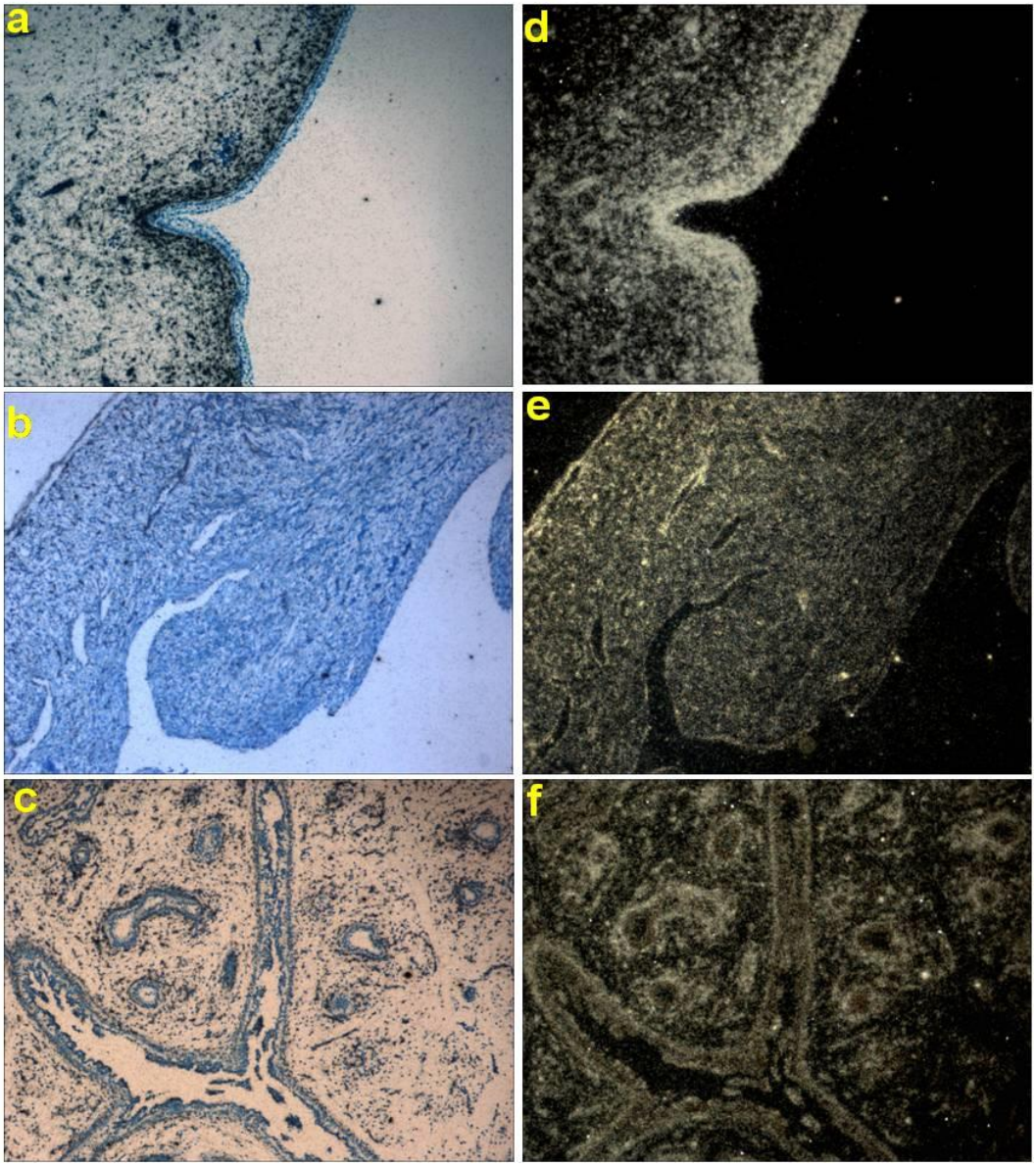

Figure 2.4: Expression of Vimentin mRNA in foetal skin (a), heart musculature (b) and lung tissue (f). Very strong expression of Vimentin is seen in foetal skin (d), localized mainly to the epithelium but with moderate to high expression seen in connective tissue. Heart tissue shows moderate expression throughout (e). Strong expression is evident in alveolar epithelia structures such as and blood vessel endothelium of lungs (f).

f) Vimentin (Adult skin and OSCC)

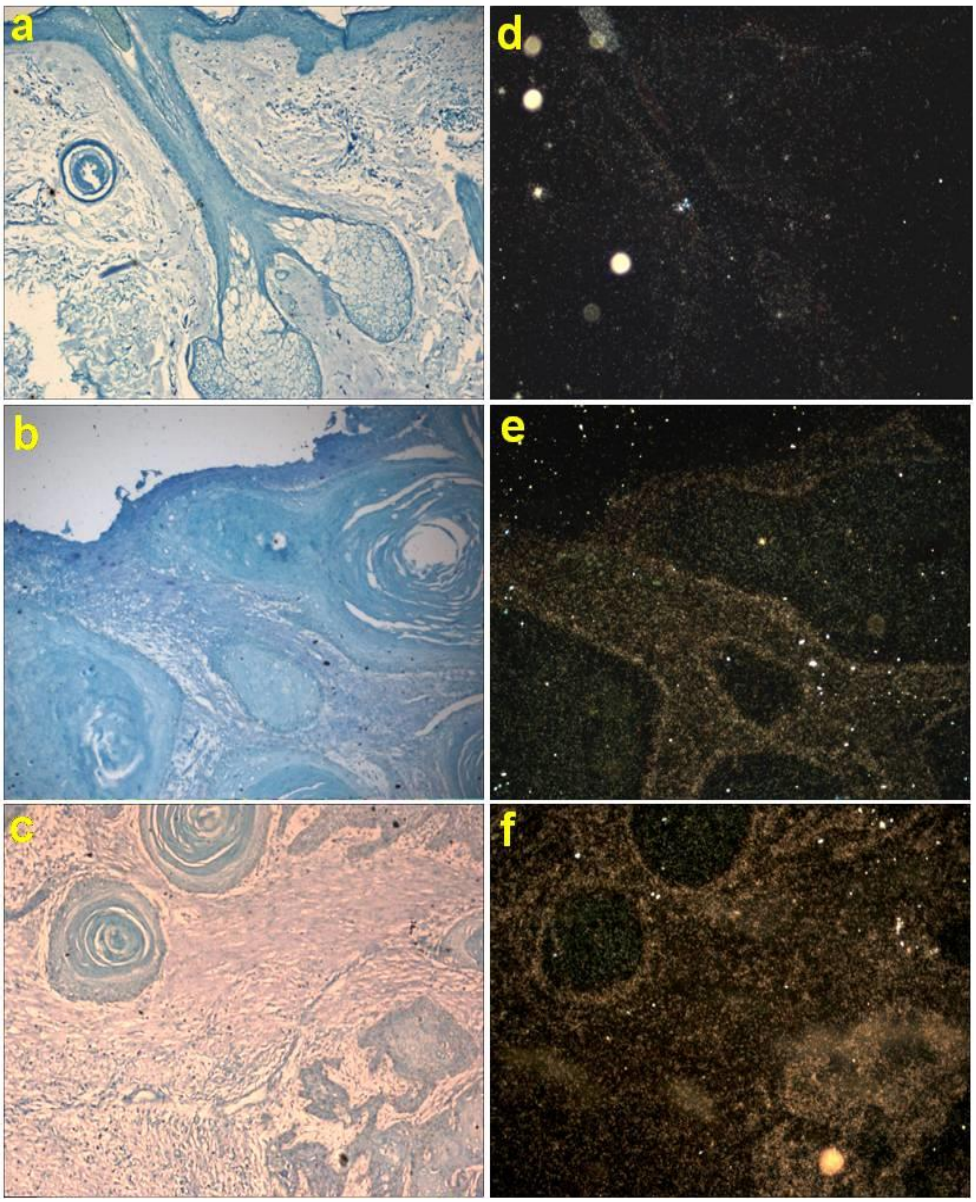

Figure 2.5: Expression of Vimentin mRNA in adult skin (a) and OSCC sections (b,c). Weak expression of vimentin is seen in adult skin in both epithelium and connective tissue (d). Both OSCC sections (e, f) show moderate to high levels of vimentin expressed in both connective tissue and epithelium with highest levels in the basal epithelium. The levels detected in OSCC sections are higher than those in adult skin.

g) Notch3: (Control tissues)

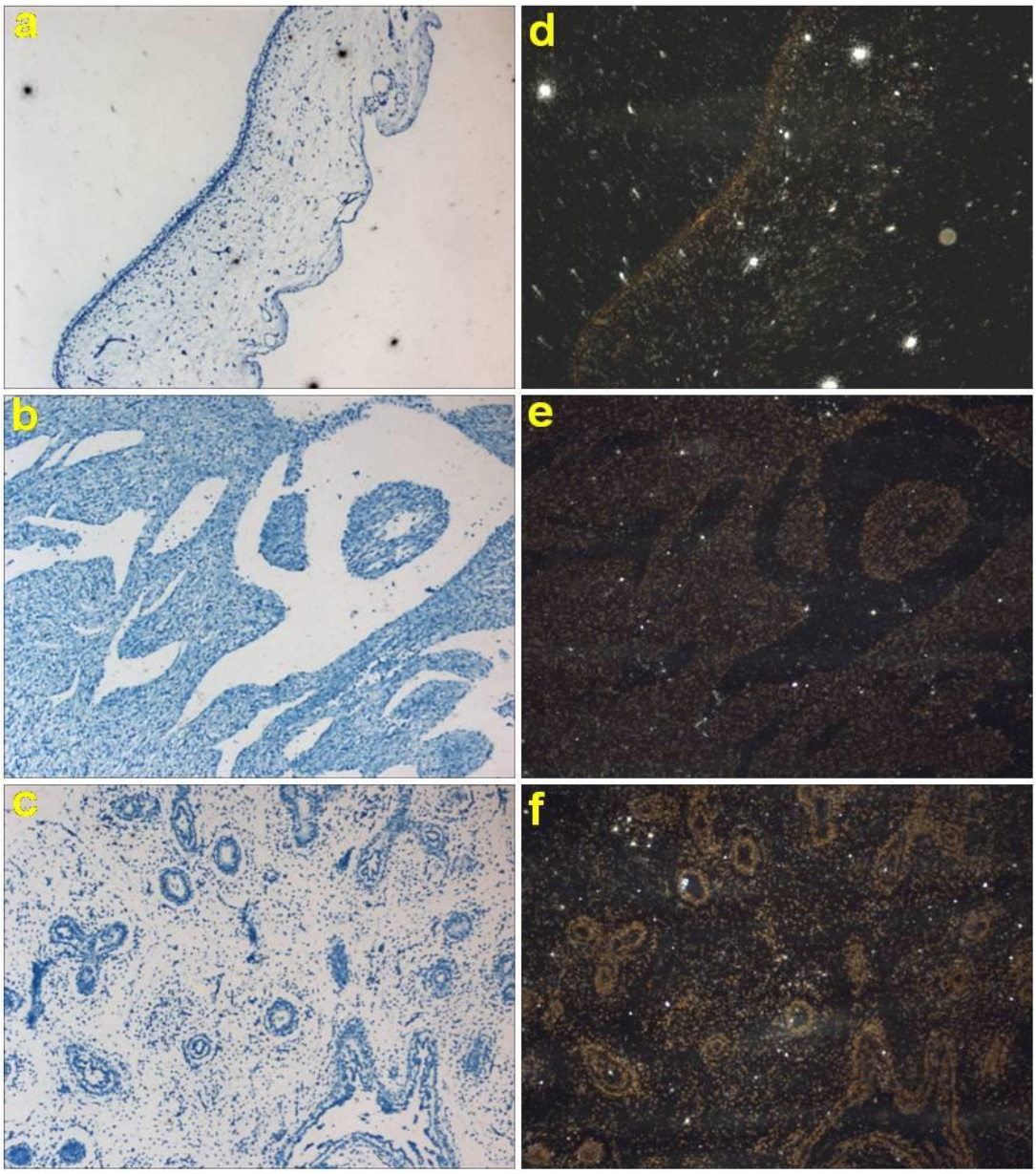

Figure 2.6: Expression of Notch3 in foetal skin (a), heart musculature (b) and lung tissue (c). Moderate expression of Notch3 is seen in foetal skin, localized mainly to the epithelium (d). Heart tissue shows very low expression throughout (e). Strong expression is restricted to the alveoli and blood vessel endothelium of the lungs (f).

h) Notch3 in adult skin and OSCC

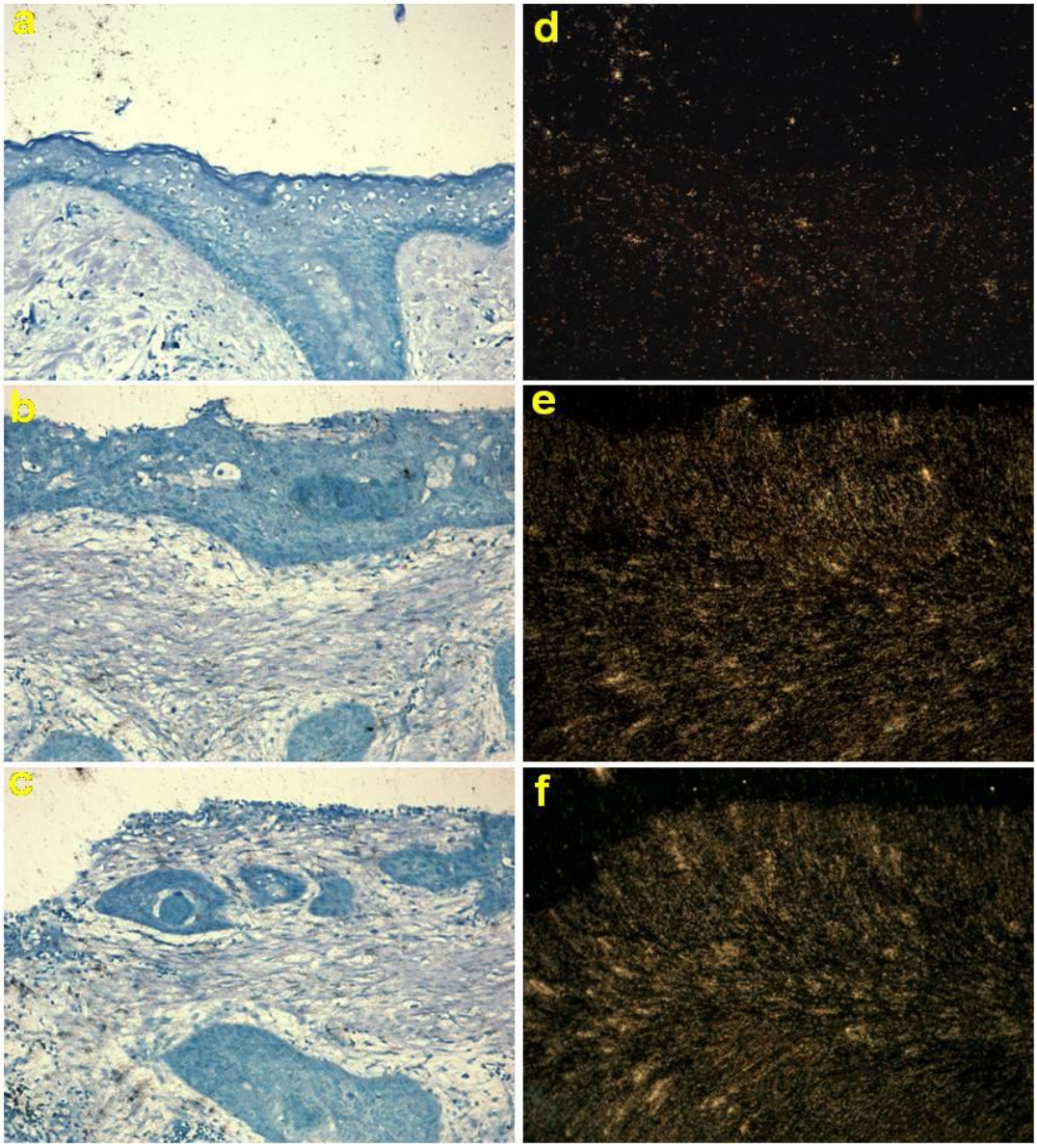

Figure 2.7: Expression of Notch3 mRNA in adult skin (a) and OSCC sections (b, c). Low expression of Notch3 is seen in adult skin (d) and is scattered throughout the epithelium and connective tissue. Strong expression of Notch3 was present in both epithelium and connective tissue of OSCC sections (e, f) in both superficial and deep layers of the tumours. The Notch3 levels detected in the cancers were higher than those in normal skin.

i) DKK3: (Control tissues)

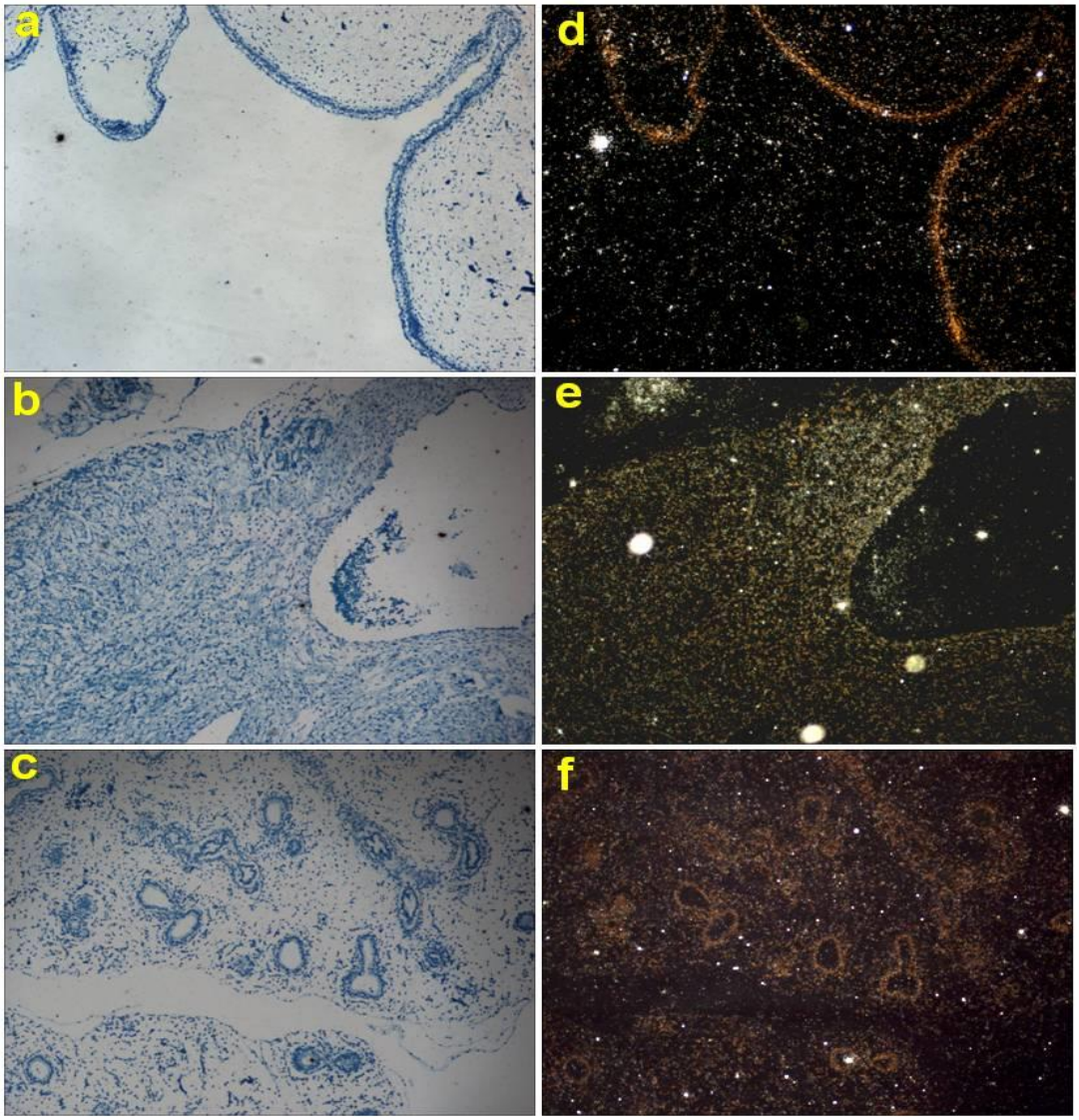

Figure2.8: Expression of DKK3 mRNA in foetal skin (a), heart musculature (b) and lung tissue (c). DKK3 mRNA is strongly expressed in the epithelium of foetal skin (d). Heart muscle shows moderate expression (e) whereas moderate poorly-localised expression is seen in lung tissue (f). The tumour sections probed for DKK3 were of questionable quality and were lost owing to technical failure.

j) PSCA (Control tissues)

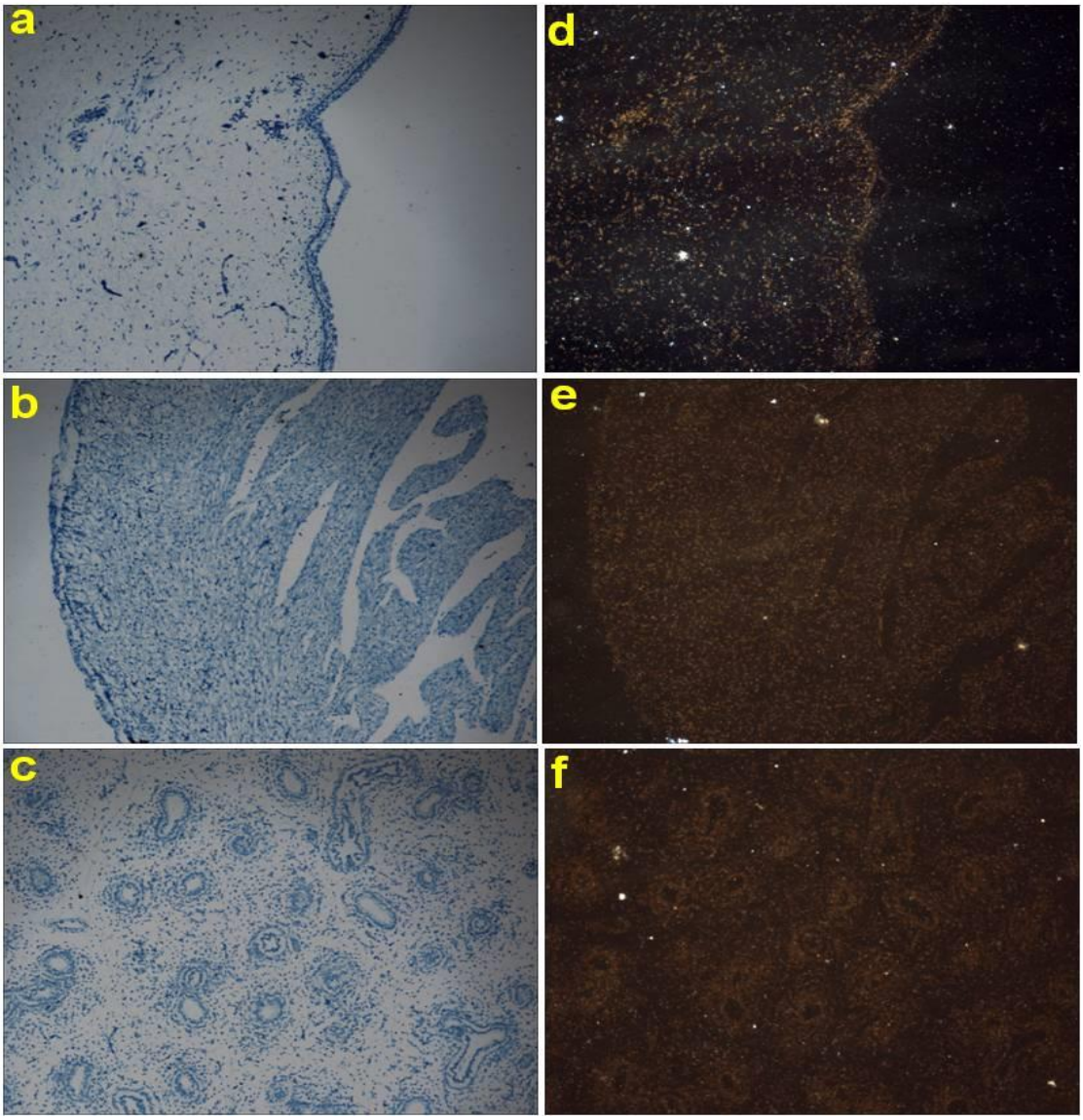

Figure 2.9: Expression of PSCA mRNA in foetal skin (a), heart musculature (b) and lung tissue (c). PSCA mRNA is moderately expressed in sections of foetal skin (d) and is present in both epithelium and connective tissue. However the quality of the slides is poor because of the background. Heart muscle (e) and lung tissue (f) show little or no expression and background staining remains a problem. The OSCC sections were again of questionable quality and lost to technical failure.

2.1.4 Discussion

Probes for in-situ hybridization were designed based on Affymetrix data obtained through experiments carried out with Locke and co-workers in 2005. Markers that showed differential expression in holoclones and paraclones were selected for in-situ probe design and it was hypothesized that the molecules selected might serve as stem cell markers and reveal stem cell zones in normal tissue sections and cancer blocks. Proposed markers included CEBP-α, DKK3, Pirin, Hurpin7, IGFB3, RDHL, PSCA, Erb-b3, Notch3 and Vimentin. B-Actin was selected as a control to confirm the presence of hybridizable mRNA in the tissue sections studied which included foetal skin, lung tissue, heart musculature, adult skin and cancer blocks 1 and 2.

β-actinwas used as a control as it is known to be stably expressed in many types of tissues (Ruan and Lai, 2007). Strong β-Actin expression was evident in both foetal and adult skin(2.1 a, c; 2.2 a, c)restricted mainly to the basal epithelium with a scanty signal detected in connective tissue. β-Actin was also detected in heart musculature and lung tissue (Figure 2.1b, e; c, f). Both cancer blocks showed a good signal from the β-Actin probe in epithelium and connective tissue(2.2 c-f). These control tissues indicated that both the probe and the vector functioned well to give a good signal in both the cancer blocks and the control tissues. Out of the nine probes examined, only CEBP-α (2.2, 2.3), Notch3 (2.6, 2.7) and Vimentin (2.4, 2.5)showed a good differential hybridization signal in cancer sections compared to normal adult skin. DKK3 showed some promise as a marker but the OSCC slides did not develop cleanly and were lost owing to technical reasons(2.8 a-f). Although the probes for these molecules showed a higher signal in cancer blocks, they failed to localize stem cell zones/hot spots as had been hoped at the beginning of the study. This was disappointing as, in addition to date from Locke et al (2005), altered expression of these molecules has previously been associated with cancer and stem cells (Dahl and Veeck, 2012; Blanpain and Fuchs, 2006).

Impaired function of CEBP-α contributes directly to the development of acute myeloid leukemia and decreasing CEBP-α function represents a promising target for novel therapeutic strategies in this disease (Mueller et al, 2006). CEBP-α mRNA was strongly expressed in the basal epithelium of foetal skin (Figure 2.2 a, c) whereas only weak expression was evident in adult skin (Figure 2.3 a, c). Both heart and lung tissue showed weak and diffuse hybridization of the probe (Figure 2.2 b-f). However both cancer blocks showed moderate to strong hybridization of the probe restricted to epithelial structures, namely basal epithelium and

keratin pearls (Figure 2.3 c-f). Although not localised to distinct zones, it was still evident that expression of this molecule was higher in the cancer blocks as opposed to adult skin.

Notch proteins have been shown to be key modulators and regulators of stem cell self-renewal in diverse populations (Molofsky et al, 2004) including hemopoeitic and neural stem cells. Conversely, Notch proteins have also been linked to promoting the differentiation of glial cells **a**nd are known to play a key role in maintaining the stem cell niche in the drosophila (Xiaoqing Song et al, 2007). Similar mechanisms might exist in oral cancer cell lines and enable stem cellpopulations to proliferate and remain undifferentiated.Very low levels of Notch3 mRNA were detected in adult and foetal skin (Fig 2.4 a, d; 2.5 a, d). Similarly, hardly any signal was detected in lung and heart tissue (Fig 2.4 b-f). Interestingly, a very strong signal was detected in sections of both blocks of SCCs (Fig 2.5 b-f) and Notch3 levels appear high in cancer as compared to normal skin.

Vimentin was strongly expressed in foetal skin and lung tissue (2.4 d, e), being localized to basal and alveolar epithelia respectively. Probe hybridization was seen in most of the muscle architecture of the heart (2.4c, f). Moderate to high expression was seen in SCC blocks (2.5 e, f), which was interesting as a low signal was detected in normal adult skin (2.4 c),where the probe hybridized mainly to epithelium More studies of this probe would be worthwhile as this protein has been linked to the metastatic spread of epithelial tumours through epithelial mesenchymal transition (EMT), characterized by, among other events, up regulation of vimentin (Eastham et al, 2007) and it could play a crucial role in controlling the invasive properties of malignant stem cells. Furthermore EMT cells have been shown to be associated with stem cell properties and are able to reconstitute tumours *in vivo* in mice (Weinberg et al, 2008). As discussed later, collaborative work done in the Mackenzie lab (Biddle et al, 2011) has shown that Vimentin mRNA is highly expressed in $CD44^{high}$ cells, the potential stem cell fraction in oral cancer cell lines and that this fraction also generates tumours when transplanted into mice.

DKK3 is one of a family of soluble dickkopf (DKK) proteins that act as Wnt regulator proteins and there is evidence that increased expression of DKK3 in gastrointestinal stem cells promotes non-canonical Wnt signalling which could have a crucial role in maintaining the undifferentiated state of these cells (Marsh et al, 2008). DKK3 was expressed at moderate levels in both adult and foetal skin (Figure 5a, 5d) where it localized strongly to the basal epithelium, although expression was stronger in foetal skin. Moderate expression was evident

throughout heart musculature) but little or no DKK3 mRNA was detected in lung Most of the OSCC sections had to be discarded owing to technical failure.

The rest of the probes examined, namely Hurpin, Pirin, RDHL and Erb-b3, were similarly selected on the basis of their differential expression in holoclones and paraclones (Locke et al, 2005) and suggestions in the literature of their potential differential expression in stem cells. However these probes (only PSCA is shown, 2.9) failed to elicit any interesting patterns of probe localization. Thus, although it was hoped that patterns of stem cell localization within oral mucosa and oral tumours might be revealed with these probes, the observed distribution of label did not provide such information. Vimentin and CEBP-α showed good differential expression patterns in the wax-embedded sections and were selected for further examination of OSCC lines alongwith BMI1 and Lgr5. In the intestinal epithelium, cells expressing Lgr5 were shown to possess stem cell properties and are responsible for its maintenance, and it is also known that dysregulation of Lgr5 signalling leads to colon cancer (van der Flier and Clevers, 2009). Bmi-1is a memberof the polycomb family that represses the transcription of its target genes via epigeneticmechanisms (Hanson et al, 1999) and, Lessard and Sauvageau (2003), showed in a mouse model of leukemia that Bmi-1 is also needed for the self-renewal of the leukemia initiating cell (LIC). It is now known to regulate stem cell potential in a range of cancers (Al-Hajj and Clarke, 2004). OSCC lines showed localization of the probe in all the cells examined and was seen in the nucleus as well as the cytoplasm and showed very poor specificity. It was hoped that this study would help localize and identify stem cells in OSCC lines but differential expression patterns were not observed, and slides were also lost to technical failure.

2.2: Identification and isolation of stem/stem-like cells in OSCC cell lines

2.2.1 Introduction

Studies were undertaken to confirm that malignant HNSCC cell lines, grown under similar culture conditions, consistently generate hierarchical colony morphology patterns corresponding to stem, early and late transient amplifying cells. The expression of putative stem cell markers within holoclones, meroclones and paraclones was examined to find out if they could be used to identify and isolate stem cells within our cell lines. 3 markers of potential interest were selected, as suggested by the literature and previous work of the Mackenzie laboratory (Locke et al, 2005), and immunocytochemistry was used to analyse their expression. The first marker studied was CD44 as the literature indicates it to be one of the pivotal stem markers in head and neck squamous cell carcinomas (HNSCC) (Prince et al, 2007)and breast (Al-Hajj et al, 2003) and prostate cancers (Zhang et al, 2012). The next marker studied was β-catenin which has not only been linked to stem cell survival/renewal but has also been implicated in the process of epithelial mesenchymal transition (Smalhofer et al, 2009). The third marker studied was E-cadherin as it is closely associated with β-catenin and normally forms a catenin/cadherin complex within the cell. Disruptions in this complex are strongly linked to stem cell survival, EMT and poor prognosis (Smalhofer et al, 2009).

Aims:

- To study the growth patterns and morphology of different cell lines.
- To identify stem cells in cell lines
- To study the expression patterns of known stem cell markers in these cell lines
- To investigate differences in the expression patterns of these markers within the hierarchy of cells that is present in these cell lines

2.2.2 Materials and methods

2.2.2.1 Cell Culture

All of the cell lines examined werederived from head and neck squamous cell carcinomas (HNSCC). The CA1 cell line was previously derived in our laboratoryfrom a biopsy of OSCC of the floor of the mouth (Mackenzie, 2004). Other lines examined were UK1 (Mackenzie lab), H357 (derived by S. Prime from sporadic OSCC), Fanconi (Zeeburg et al, 2005) and 5PT (derived by T. Carey, University of Michigan). Unless otherwise stated cells from all lines were grown in RM+ medium. This is a basal medium (DMEM-F12) supplemented with 10% FBS, 2ng/ml epidermal growth factor (GIBCO), 0.4ug/ml hydrocortisone (Sigma), 5ug/ml insulin (Sigma), 20ug/ml transferring (Sigma), 100 U/ml Penicillin, 100ug/ml streptomycin and 20ug/ml glutamine (PAA). These were obtained from CRUK central stores, collectively available as the RM+ supplement. Cells were maintained at 37ºC in an atmosphere of 5% CO_2 / 95% air and were usually cultured in 75cm² T-Flasks (Nunc).For experimental use, all cell lines were plated at clonal density, i.e. 1000-2000 cells per ml, adding 10 ml RM+ per T-75 T-flasks. Good patterns of morphologic variation between colonies were usually visible by day 5. For some studies, cells were also plated at clonal density in 6-well plates or onto 13mm sterile glass cover slips inside 6-well plates in 3ml DMEM/ RM+ medium per well.

2.2.2.2 Immunocytochemistry

a) Cells cultured in T-75 slide flasks

Cells were fixed as required in either 4% buffered (7.0-7.2) paraformaldehydefor 15 minutes at room temperature or a 1:1 solution of acetone-methanol for 15 minutes at 4ºC. The cells were then washed once with phosphate buffered saline (PBS) and a drill was used to cut out the flask base. Areas of colony growth were outlined by a hydrophobic pen (DakoCytomation™) and allowed to dry. The cells were rehydrated in PBS for 10 minutes. To visualise surface proteins, the cells were blocked using a 2% solution of BSA in PBS or DMEM-F12 (basal medium) for one hour. Alternatively, for nuclear or cytoplasmic proteins, cells were permeabilized and blocked at the same time using 0.2%TritonX/ 2%BSA (IgG free) (all from Sigma) in PBS for a period of one hour. Following blocking or permeabilization the cells were washed x3 with PBS at 10 minute intervals.The primary antibodies used are listed in table 2.2.1 below. All primary antibodies were made up in PBS or DMEM-F12 with 5%

goat serum (Sigma). Following incubation with primary antibodies in a humidified atmosphere, either overnight at 4ºC or for 1 hour at room temperature, cells were washed three times in PBS with 10% Tween20 for 30 minutes at 10 minute intervals. Cells were incubated with concentrations of secondary antibodies as listed in Table 2.1.2 below. DAPI (1:100) was used as a nuclear counter stain after which stained areas of the flasks were covered with Immumount-Anti Fade reagent (Thermo Scientific) and covered with glass cover slips. The flasks were visualized immediately or stored at 4ºC.The cells were examined with a NIKONmicroscope (Nikon Eclipse TE 2000-S with Super High Pressure Mercury Lamp Power Supply) using fluorescence and phase contrast modes.

Antibody	Company	Dilution	Source
CD44	BD Biosciences	1:100/1:250	Mouse monoclonal
β-Catenin	Sigma	1:100	Mouse monoclonal
ESA	Miltenyi Biotech	1:1200	Mouse Monoclonal
E-Cadherin	Santa Cruz	1:100	Mouse polyclonal
EGF-R	Zymed	1:100	Mouse Polyclonal

Table 2.4: Table listing primary antibodies and concentrations used.

Antibody	Company	Dilution	Source
Fitc conjugated Goat-anti-mouse	Alexafluor	1:500	Goat
Fitc conjugated Goat-anti-Rabbit	Alexafluor	1:500	Goat
Fitc conjugated Goat-anti-rabbit	DAKO	1:60	Goat

Table 2.5: Table listing secondary antibodies used for visualization

b) Cells cultured on cover slips

Coverslips were fixed in either 5mls of a 4% solution of paraformaldehyde/formaldehyde for 15 minutes at room temperature or a 1:1 solution of acetone-methanol for 15 minutes at 4ºC. A 6 by 6 cm glass slab was covered with tightly stretched parafilm to which evenly spaceddrops (18µl) of primary antibodies were applied. The primary antibodies used are listed in table 2.1.1 and were prepared as described in section 2.2.1. Cover slips bearing cells were removed from the 6-well plates and inverted onto the drops of primary antibody for 1 hour at room temperature. The cover slips were then transferred onto a 25 µl drop of PBS with 10% Tween20 for 5 minutes and this was repeated three times over a period of 10 minutes..Appropriate secondary antibodies were prepared in DMEM-F12 with 5% goat serum (Sigma) as described in section 2.2.1 and the cover slips were inverted onto them for a period of 1 hour at room temperature. After further washing, coverslips were counterstained with DAPI (1:100) for nuclear visualization and mounted onto plain glass slides using Immumount anti-fade.

2.2.3 Results:

A) Cellular heterogeneity within OSCC cell lines.

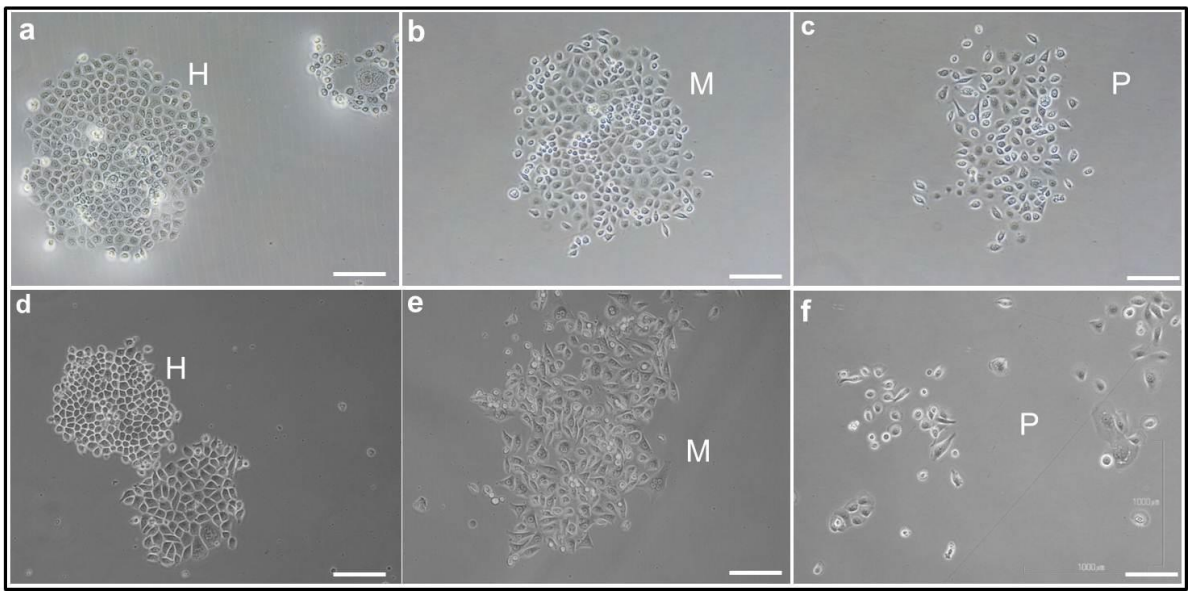

Figure 2.10: Colony formation by OSCC cell lines(Scale=50µm).

The figure above shows the colony morphology generated by CA1 (a-c) and H357 (d-f) cells after five days. Both cell lines give rise to round colonies (H) called holoclones (a, d)made of small tightly adherent cells. They also form meroclones (M) made up of looser cells that are larger in size (b, e). In addition to this all cell lines also form small abortive colonies (c, f) that show few rounds of division, termed paraclones (P).

B) The expression of CD44 in cell lines derived from OSCCs

I) CA1

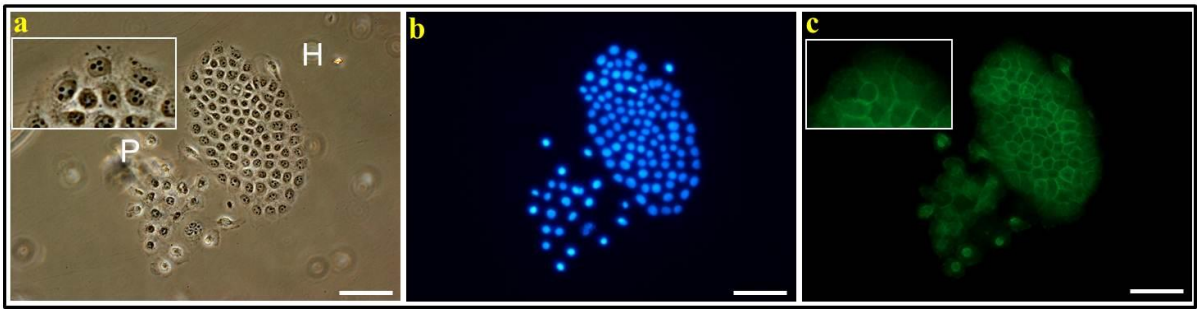

Figure 2.11: The expression of CD44 in the CA1 cell line (Scale=50µm). A culture of CA1 cells grown for 5 days showing a phase contrast image (a) of a holoclone colony (H) next to a paraclone (P), stained with DAPI (b) and anti-CD44 antibody (c).The holoclone consists of tightly packed cells with somewhat larger less tightly packed cells around the periphery. The staining for CD44 is restricted mainly to the cell surface region with little or no signal in the cytoplasm (c). CD44 expression also appears higher in the central cells of the holoclone than those at the periphery. Holoclones generally show higher levels of CD44 compared with paraclones.

II) H357

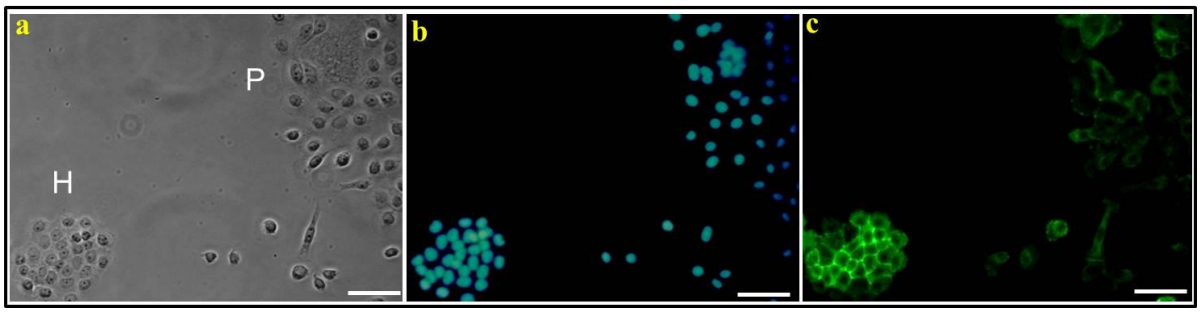

Figure 2.12: The expression of CD44 in H357 cells (Scale=50µm).A culture of H357 cells grown for 5 days showing a phase contrast image (a) and shows a holoclone (H) next to a paraclone (P) stained with DAPI nuclear stain (b) and anti-CD44 antibody (c). CD44 is strongly expressed at the surface of cells in holoclones compared to paraclones where low expression is seen. The central cells of the holoclone stain markedly strongly for CD44 than those at the periphery that show weak expression.

III) Fanconi 1131

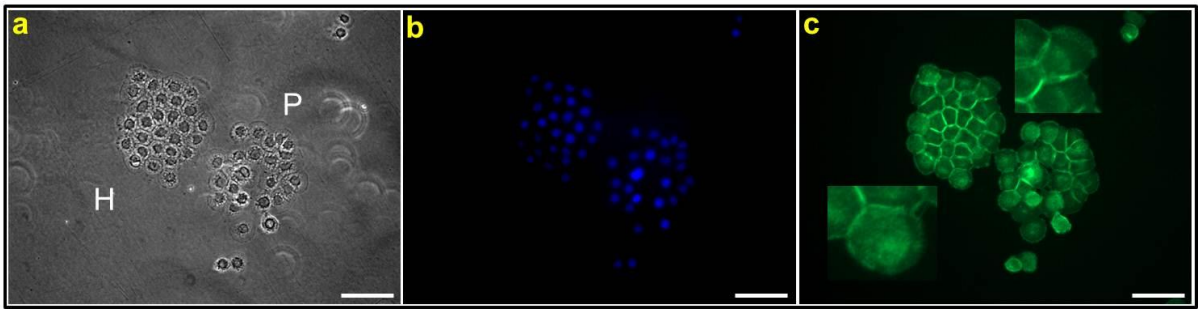

Figure 2.13: The expression of CD44 in Fanconi VU1131 cells (Scale=50µm).A phase contrast image of a culture of Fanconi cells grown for 5 days (a)showing a holoclone (H) next to a paraclone (P) stained with DAPI nuclear stain (b) and anti-CD44 antibody (c). CD44 is strongly expressed at the periphery of cells in holoclones compared to paraclones where only low levels are detected. The holoclone appears to be made of two cell types, those that stain markedly strongly for CD44 and are towards the center of the colony and those which express lower levels which are around the edge of the colony. The edge cells show evidence of nuclear translocation of CD44 (c; insets) which is slightly different from what was seen for CA1. The paraclone next to the holoclone shows weaker expression of CD44 in the peripheries and cytoplasm of these cells and there is more nuclear CD44 in almost all the cells (c).

C) The expression of β-catenin in cell lines derived from OSCCs.

I) CA1

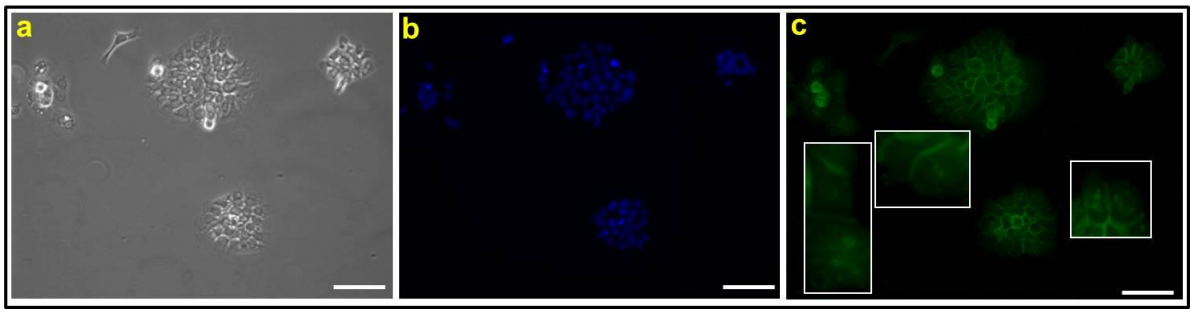

Figure 2.14: The expression of β-catenin in CA1 cells(Scale=50µm). A culture of CA1 cells showing a phase contrast image of holoclones and a paraclone (a) stained with DAPI nuclear stain (b) and anti-β-Catenin-FITC antibody (c). Ca1 cells form holoclones, meroclones and paraclones as discussed. Again holoclone cells tend to be tightly clustered with small cells forming the center of colonies and larger cells arranged around the edge (a). The expression of β-catenin is seen in the cell surface with little or no expression in the cytoplasm. Holoclones stain brighter than paraclones and meroclones and the cells forming the centres of colonies show higher expression than those at the edge. Cells at the edge also show nuclear expression of β-catenin as shown in the enlarged insets (c).

II) H357

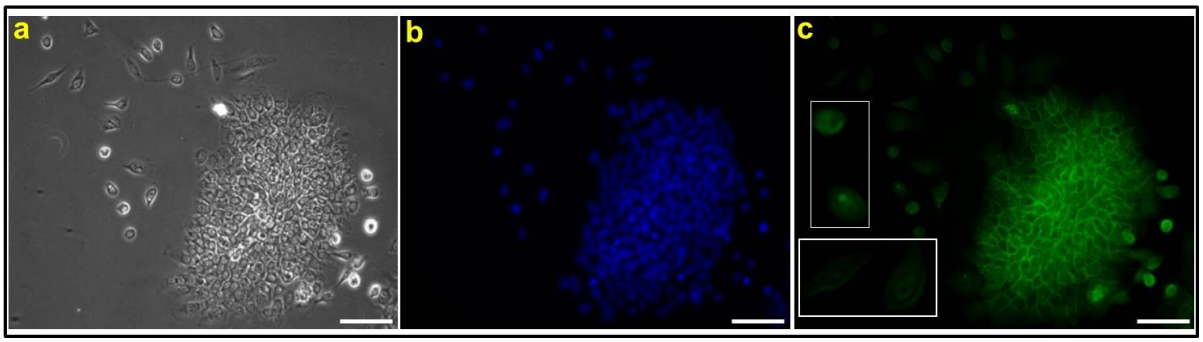

Figure 2.15: The expression of β-catenin in H357 cells (Scale=50µm). A phase contrast image of a holoclone formed from the culture of H357 cells (a) stained with DAPI nuclear stain and anti-β-catenin-FITC antibody (c). The cells in the center of the holoclone are tightly packed while those at the edge are loosely arranged and are slightly larger compared to the central cells. β-catenin expression is seen on the cell surface with little or no expression in the

cytoplasm and it appears to be higher in the central cells of the holoclone than those at the edge. Cells at the edge also show nuclear localization of the protein (insets; c) and reduced expression at the cell surface.

III) VU1131 Fanconi

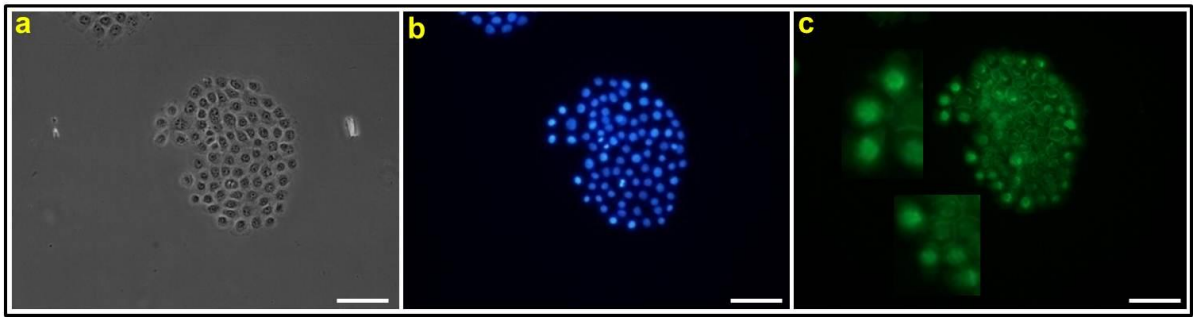

Figure 2.16: The expression of β-catenin in Fanconi VU1131 cells (Scale=50µm). A phase contrast image of a holoclone formed from culture of VU1131 cells (a), stained with DAPI nuclear stain (b) and anti-β-catenin-FITC antibody (c). As stated before, Fanconi cells tend to form predominantly holoclone like colonies and the formation of meroclones and paraclones is scarce. Central holoclone cells express β-catenin in primarily on the cell surface and weak expression is also seen in the nucleus. Cells at the edge however show the opposite with very strong levels expressed in the nucleus and very weak levels evident in the membrane. This can be clearly seen by examination of the magnified insets which show enlarged views of the edge cells (c).

D) The expression of E-cadherin in OSCC cell lines.

I) CA1

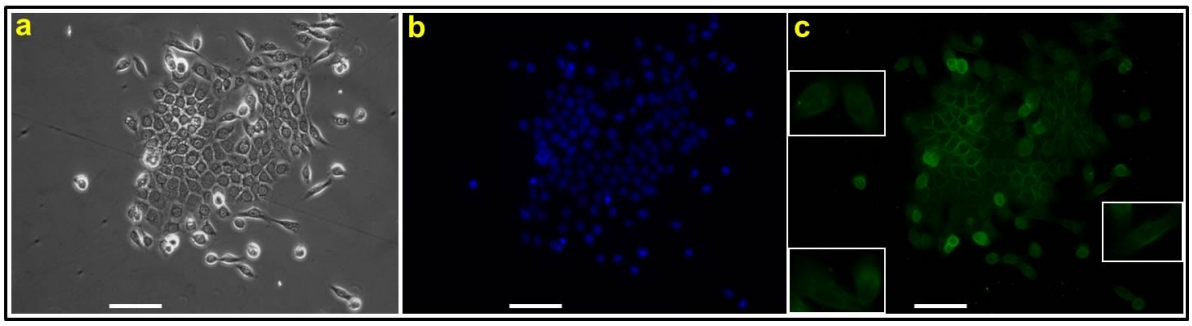

Figure 2.17: The expression of E-cadherin in CA1 cells (Scale=50µm). A phase contrast image of a holoclone colony formed from CA1 cells (a) stained with DAPI nuclear stain (b) and anti-E-cadherin antibody (c). E-cadherin is localized mainly to the cell surface and appears stronger within central cells as compared to the edge which show weaker expression of the protein mainly within the cytoplasm (c).

II) H357

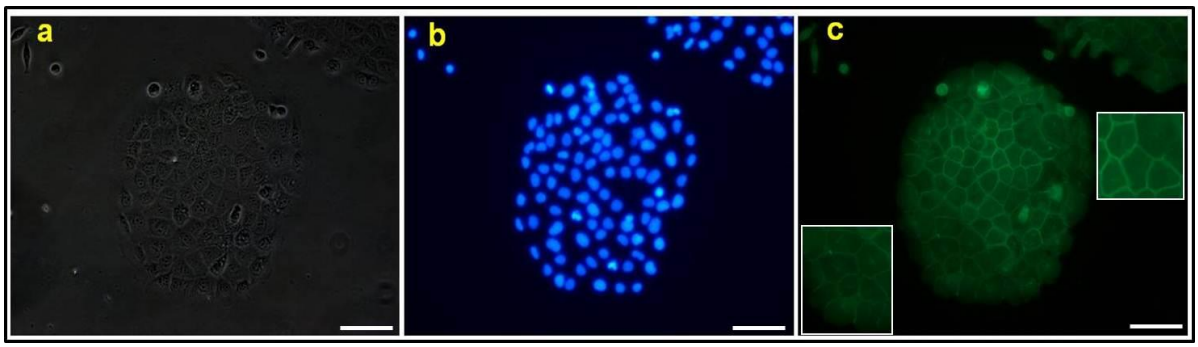

Figure 2.18: The expression of E-Cadherin in H357 cells (Scale=50µm).A phase contrast image of a holoclone colony formed from culture of H357 cells (a), stained with DAPI nuclear stain (b) and anti-E-cadherin-FITC antibody (c). E-cadherin expression is seen mainly at the cell surface and cells within the center of the holoclone show stronger expression as compared to those at the edge and on closer examination E-cadherin can be seen to be present in the nucleus (inset bottom right, c). The inset on the top right shows a magnified view of the center of the colony to emphasize the high central expression pattern of E-cadherin compared to the edge.

III) Fanconi 1131

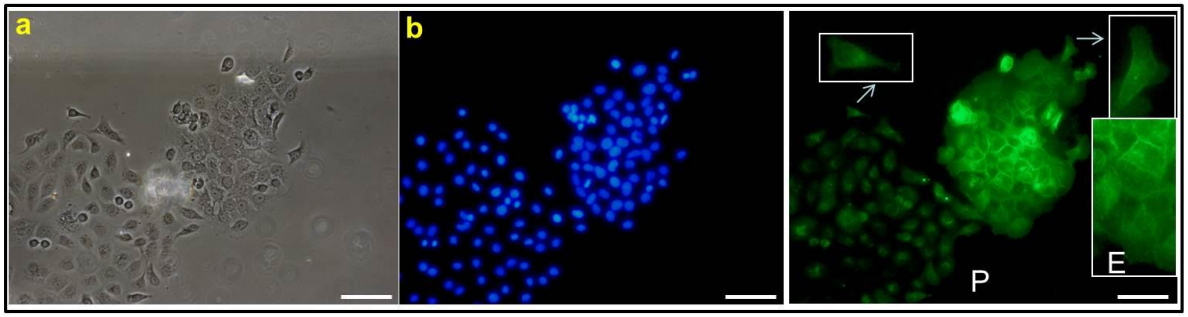

Figure 2.19: The expression of E-cadherin in Fanconi 1131 cells (scale=50µm).A phase contrast image of a holoclone (H) and paraclone (P) from a culture of Fanconi 1131 cells for 5 days (a), stained with DAPI nuclear stain (b) and anti-E-cadherin antibody (c). E-cadherin is localized mainly to the cell surface of holoclone cells and moderate staining is seen in the cytoplasm. The paraclone shows lower expression of E-cadherin and cells show low membrane expression and peri-nuclear accumulation of E-cadherin to the nucleus. The cells at the edge of the colony express lower levels of E-cadherin (c) than those in the center. The insets in (c) show magnified images of these cells showing cells with lowered E-cadherin in the membrane and expression shown around or in the nucleus.

E) Time-Lapse video analysis of OSCC cell lines.

To study the division of cells during colony formation they were cultured in an incubator with a microscope and a camera, and photographed at 15 minute intervals to create time-lapse videos. Videos were created of cells immediately after plating and also after cells had formed established colonies discussed later. (i) Early cultures

Note: To play files

1. use VLC media player (VideoLAN), the installation file for which has been provided in the SOFTWARE folder on the CD,

   or

2. To view in Windows media player, kindly install K-lite codec pack, also provided in the SOFTWARE folder on the CD.

(The files have been checked by Kaspersky Pure Antivirus [Kaspersky Labs™] and do not contain any malicious content)

2.2.4 Discussion

Each of the cell lines examined consistently showed the generation of three types of colony morphologies, classified as holoclones meroclones and paraclones after cells were plated at clonal densities, as previous work with these cell lines has shown that colonies formed under these conditions are usually clonal in origin. It also appeared that the cells forming holoclones are heterogeneous. The center of the holoclone is made up of tightly packed cobblestone shaped cells and slightly larger cells at the edge that are arranged loosely.

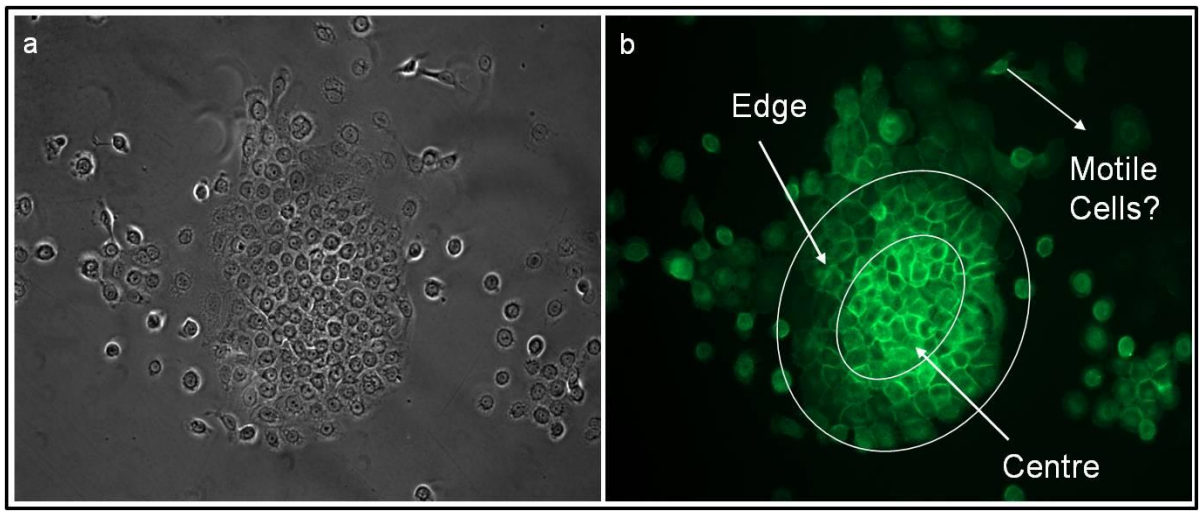

Figure 2.20: The centres and edges of holoclone colonies.

When stained for CD44, holoclones show the brightest staining, with meroclones being the next in intensity and the weakest signal being detected in paraclones. The CD44 in holoclones seems to be predominantly present in the cell surface in all the cell lines examined. However there is some variation in the VU1131 Fanconi line in that there seems to be some nuclear expression of CD44 in addition to the membrane staining consistently seen. This nuclear localization is present in mostly all the cells making up the meroclones and paraclones and only weak nuclear staining of CD44 can be detected within the central cells of the holoclone (Figure 2.13) but it seems to be more pronounced in the cells making up the edge. Also seen consistently was the pattern of strong CD44 expression in the central cells of the holoclones and weak expression in cells making up the edges of these colonies (Figure 2.20) which suggests that the cells are undergoing some change at the central/peripheral cell interface and led to the hypothesis that the cells in the center are different from those at the edge in that the central cells better represent the stem cell population.

E-cadherin was shown to be expressed at the protein level in all the cell lines examined. In holoclone colonies E-cadherin was shown to be present at the cell periphery with little or no expression in the cytoplasm. Interestingly the central cells of the holoclone were shown to express higher levels than those making up the edge of the colonies. The scattered fibroblast-like cells showed reduced expression in the membrane and very weak levels within cytoplasm. A few cells also showed nuclear accumulation of the protein.

β-Catenin was seen to be expressed in all three cell lines examined however the patterns observed differed. CA1 and H357 cells showed strong expression of the protein almost exclusively at the cell periphery with very little being present in the cytoplasm. Cells at the edge showed reduced levels. In the Fanconi 1131 cell line, β-catenin was expressed in the cell membrane and in the nucleus of all the cells in the colonies but nuclear accumulation was more marked in cells present at the edge.

A recent study carried out by Xieand co-workers(2008) showed that inhibition of the CD44 molecule by RNAi not only increased the susceptibility of hepatocellular carcinoma cells to apoptosis by anti-cancer drugs, but decreased tumourigenicity as well. This study supports the study of CD44 as a stem cell marker in oral cell lines as the same responses could help move us a step closer in targeting these troublesome cells therapeutically and specifically. Recent work done in the lab also suggests that down regulating CD44 in oral cell lines negatively affects clonogenicity. The fact that CD44 is lowered around the edge could mean that the cells at the edges of holoclone colonies are differentiating into more committed cells, but then what does the nuclear translocation of CD44 signify? A study on colon cancer cells has shown that CD44 can migrate to the nucleus where it binds to promoters of TWIST and other genes involved in invasion and metastasis (Su et al, 2011) and that cells with nuclear CD44 showed increased invasion, characteristics of EMT cells, and increased tumour initiation when transplanted into mice. Another study showed that nuclear translocation of CD44 is followed by the formation of a STAT3/CD44 complex that then binds to the cyclin D1 promoter, enhancing cell proliferation (Lee et al, 2009). These data suggest that the nuclear translocation of CD44 seen in OSCC lines in our lab could also be an indicator of cells acquiring invasive traits.

The loss of membranous E-Cadherin has been shown to be important in the formation of carcinomas from benign tumours (Hollier et al, 2009) and this cell adhesion protein has been linked to EMT with its loss appearing to be a rate limiting step in this process. EMT is also

characterized by a change in β-catenin location from the membrane to the nucleus as shown by Brabletz-Schmalhofer and co-workers (2009). They showed that loss of E-cadherin characterizedepithelial mesenchymal transition (EMT) and this was usually accompanied by dysregulation of β-catenin. Accumulation of nuclear β-catenin increases as E-cadherin is downregulated. In normal epithelial cells, membrane localized β-catenin exists in a junctional complex with E-cadherin but once this complex is inactivated, free β-catenin translocates to the nucleus where it activates target genes involved in oncogenesis and tumour progression (Joo et al, 2001; Hay, et al 2002). Another study carried compared the expression of E-cadherin and β-catenin in normal and cancerous breast tissues and how this correlated with changes in CD44 expression (Bankfalvi, 1999). This comparative study showed that reductions in E-cadherin and β-catenin were routinely seen in cancerous tissue, correlated strongly with nodal metastasis, and also resulted in poor survival when accompanied with a downregulation in CD44v6. The integrity of the E-Cadherin and β-Catenin complex is vital for cell adhesion and disruptions of this adhesion complex are pivotal in the development of metastatic potential and the acquisition of invasive potential (Brabletz et al, 2009). The results above collectively suggest that there is some change going on at the edge center interface of holoclones as indicated by the loss of cell surface CD44 and E-cadherin and the reduced expression of β-catenin and its translocation to the nucleus. This could mean that the cells are either differentiating or undergoing some other change similar to EMT.On video it can be seen that when holoclones form, 2 types of cells exist, the ones forming the central zone and the other the colony periphery. The central cells appear relatively stationary and adhere tightly to other cells and have characteristic cobblestone morphology. These cells are also seen to divide to maintain the central region of the holoclone. Cells at the edge of colonies are spindle-shaped in appearance and appear to want to break away from the colony. There are also spindle-shaped cells lying outside the edges of the colonies that are highly motile and make contact with other cells. Further, these spindle cells appear to be generated from the colony itself. The links for the movies are below.

These observations led into the next part of this study whichrevolves around Fluorescence Activated Cell Sorting (FACS) and analysis of subpopulations of cells within different cell lines. This involves the detection of CD44 at the protein level in cells present in suspension form. This was done to investigate whether it was possible to (a) isolate $CD44^{high}$ and $CD44^{low}$ cells and (b) whether this difference could be used to predict stem like potential of these cells and was it reflected in the colony morphology and count generated as a result.

2.3 Detection of CD44 at protein level using Fluorescent Activated Cell Sorting (FACS)

2.3.1 Introduction:

The patterns of expression of CD44revealed by immunocytochemistry indicated that although most cells show some staining for CD44 there is a wide range of levels of CD44 expression. Prince and co-workers (2007) have suggested that CD44 positive cells, when isolated by FACS, are more tumorigenic when transplanted into NODSCID mice. Harper and co-workers (2007) had previously associated CD44 expression with clonogenicity in OSCC cells. Further studies were undertaken to see whether cells which stained brightly for CD44 ($CD44^{high/+}$) were different from those which did not ($CD44^{low/-}$). The questions asked were (a) whether it was possible to separate the $CD44^{high/+}$ cells from $CD44^{low/-}$ cells and (b) which of these 2 cell types, when isolated and cultured, showed the most clonogenicity. The FACS used to carry out these investigations, relies on a machine to analyze single cellsin suspension using a laser system that also enables isolationof cells with different expression levels of the proteins of interest. Cells were identified as a total population (a) preliminarily on the basis of forward and side scatter (FSC-A, SSC-A) using 2-dimentional histograms, where forward scatter is a measure of cell size and side scatter that of cell complexity and granularity and were gated (b) to exclude cell clumps and subcellular debris giving rise to the parent population (p1). Dead cells (black) were excluded and viable cells (red) were selected by staining cells with DAPI and gating those that were negative (c). The figure below explains this procedure and this was done for each of the cell lines examined.

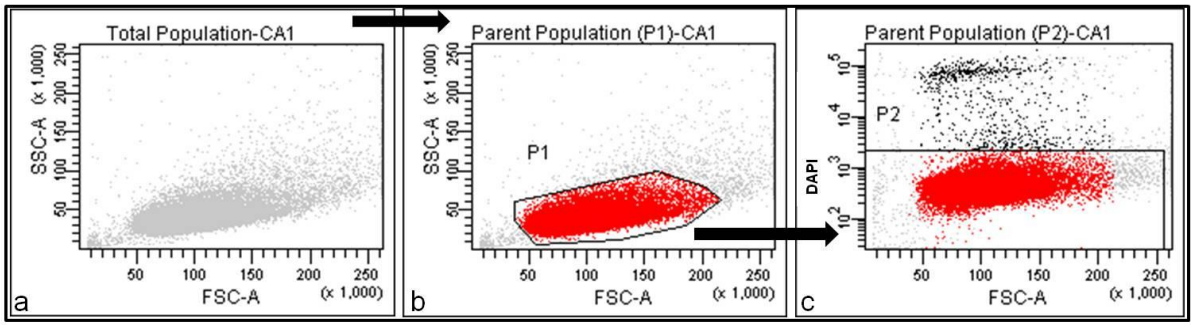

Figure 2.21: Selection of suitable cells from within the total population

The cell lines chosen were stained with mouse PE-conjugated FACS anti-CD44 antibodies with the cells first analyzed, and then sorted into and collected as two populations one $CD44^{high}$ and the other $CD44^{low}$. These two populations were plated at clonal density and the numbers of colonies formed by each sorted fraction counted.

2.3.2 Materials and methods

FACS:

Cells from OSCC lines were seeded at clonal density (2000 cells/ml) in RM+ medium in T75 cell culture flasks and grown for 5 days. 24 hours before harvesting the cells, the medium was changed to basal DMEM/F12 medium as it was thought that it improved the specificity of the staining due to the lack of EGF and other additives, normally present in the RM+ medium. The cells were washed once with PBS and detached using Accutase (PAA) or Trypsin-EDTA (1%) for 5-10 minutes. The Accutase or trypsin was neutralized with an equal amount of DMEM-F12 with serum and the cells were transferred to a sterile Falcon tube and spun down at 1500rpm at 4ºC. The medium was aspirated and the pellet resuspended in sterile PBS containing 1% FBS, again spun down, the supernatant aspirated, and the cells resuspended in 300 µl PBS containing 1% FBS. 5µl of either PhycoErythrin (PE)-conjugated or FITC-conjugated anti-CD44 antibody was added and cells were left on ice in the dark for 15-20 minutes. Unstained control cells were used to calculate autofluorescence. After 20 minutes 1ml of PBS+1% FBS was added, the Eppendorf centrifuged at 4°C, 1500 rpm for 5 minutes, and the pellet washed with PBS, again spun down and resuspended in 1 ml PBS+1%FBS and transferred to a sterile FACS tube. Samples were analyzed and sorted using the BD FACSARIA cell sorter with cells from selected gates collected and plated at clonal densities.

Before sorting, cells were counted and samples were normalized for similar cell numbers and an equal quantity of antibody was used so as to give equal levels of cells stained. Three repeats were plated for each of the samples collected and were used for colony counts.

Statistical analysis was performed using Microsoft Excel and unless otherwise stated all data is based on at least three experimental repeats and are reported as mean (average) ± standard deviation (SD). The student's t-test was used to analyze statistical significance between the studied samples. The table below shows the values used to assess significance, denoted '*' on the graphs. Data that was not statistically significant was left unlabelled.

P value	Wording	Summary
>0.05	Not significant	ns
0.01 to 0.05	Significant	*
0.001 to 0.01	Very significant	**
< 0.001	Extremely significant	***

Figure 2.22: Statistical significance of samples.

2.3.3Results

A) CA1 cell line:

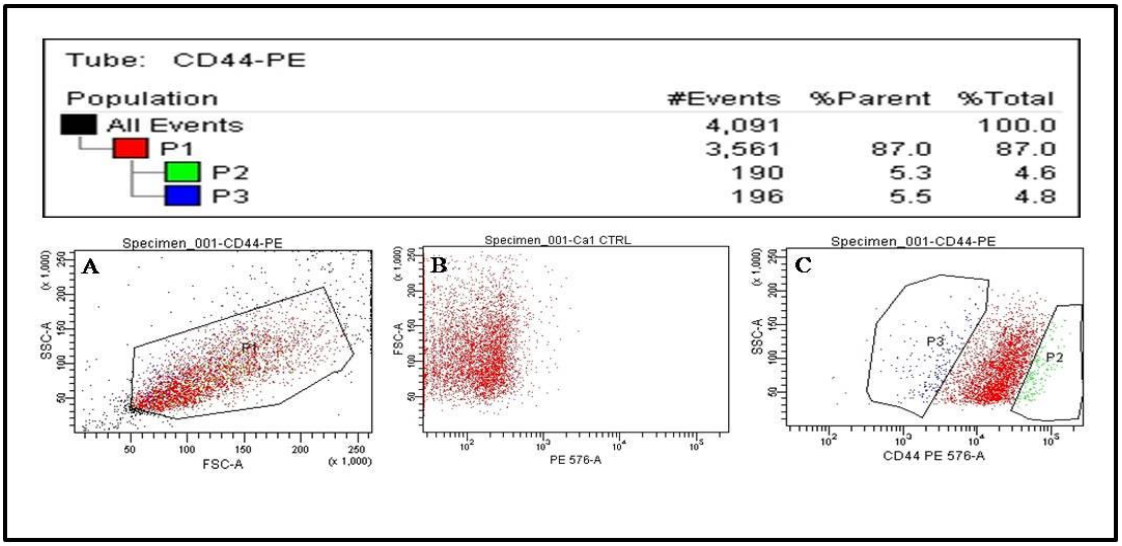

Figure 2.23: Flowcytometric analysis of CA1 cells. Representative FACS plots obtained for CA1 cells. Doublets were excluded using a forward vs. side scatter profile (A) and suitable cells were gated (P1). Unstained control cells were analyzed (B) and compared with cells stained by the PhycoErythrin-conjugated anti-CD44 antibody (C). 5-6% of the cells expressing the highest levels of CD44 (P2) were collected as representing $CD44^{high}$ cells and 5-6% of cells showing the lowest CD44 expression were collected as representing $CD44^{low}$ cells. Following collection, cells were cultured for 5 days and the colonies formed were counted.

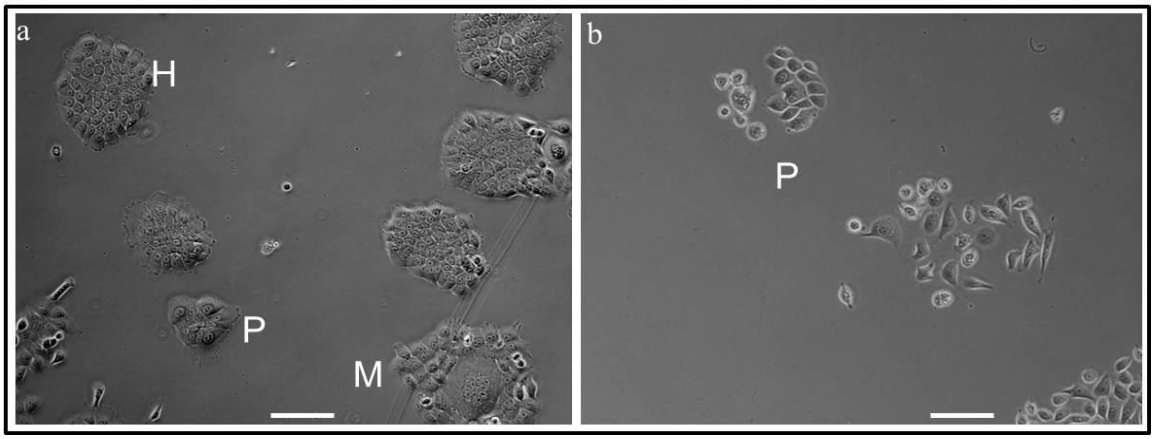

Figure 2.24: Growth of $CD44^{high}$ (a) cells vs. $CD44^{low}$ (b) CA1 cells. Cultures of $CD44^{high}$ (a) and $CD44^{low}$ (b) CA1 cells shown in phase contrast. Compared to $CD44^{low}$ cells, $CD44^{high}$ cells show robust colony formation, forming more holoclones, consisting of tightly packed small cells (H) and meroclones, made from larger but cohesive cells (M). $CD44^{low}$ cells show

poor clonogenicity mainly forming paraclones that show little growth and consist of larger more scattered and irregularly shaped cells (Scale=100µm).

CA1	**Average Holo**	SEM	**Average Mero**	SEM	**Average Para**	SEM
CD44^{high}	20.89	2.34	15.78	1.35	14.56	2.50
CD44^{low}	6.33	0.88	12.11	2.78	23.22	2.87

Table 2.6: Colony counts for the CA1 cell line for CD44^{high} vs. CD44^{low} cells.

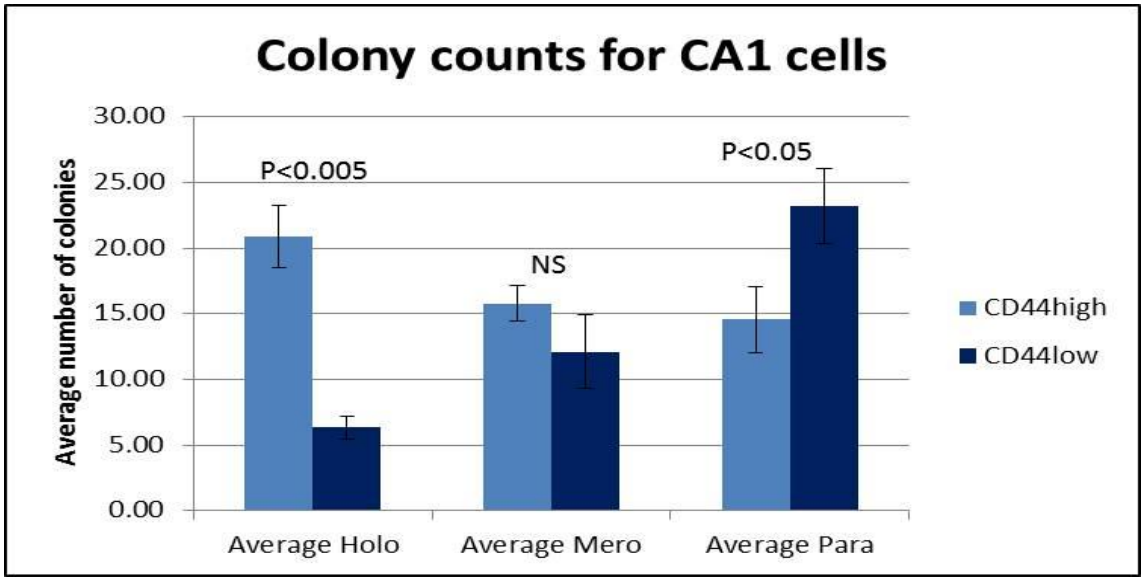

Figure 2.25: Comparison of colony counts obtained for CD44^{high} vs. CD44^{low}CA1 cells. The figure above shows the number of holoclones, meroclones and paraclones counted when the two sorted populations were plated out at clonal density and allowed to grow for five days. CD44^{high} cells formed significantly more holoclones (17.67) and meroclones (19.33) per 1000 cells as opposed to CD44^{low} cells. CD44^{low} cells formed the highest number of paraclones (20.33) per 1000 cells and this was significant. They formed the least number of holoclones (4.67). The total number of colonies formed by CD44^{high} cells was also higher (48) than those by CD44^{low} cells (37).

B) H357

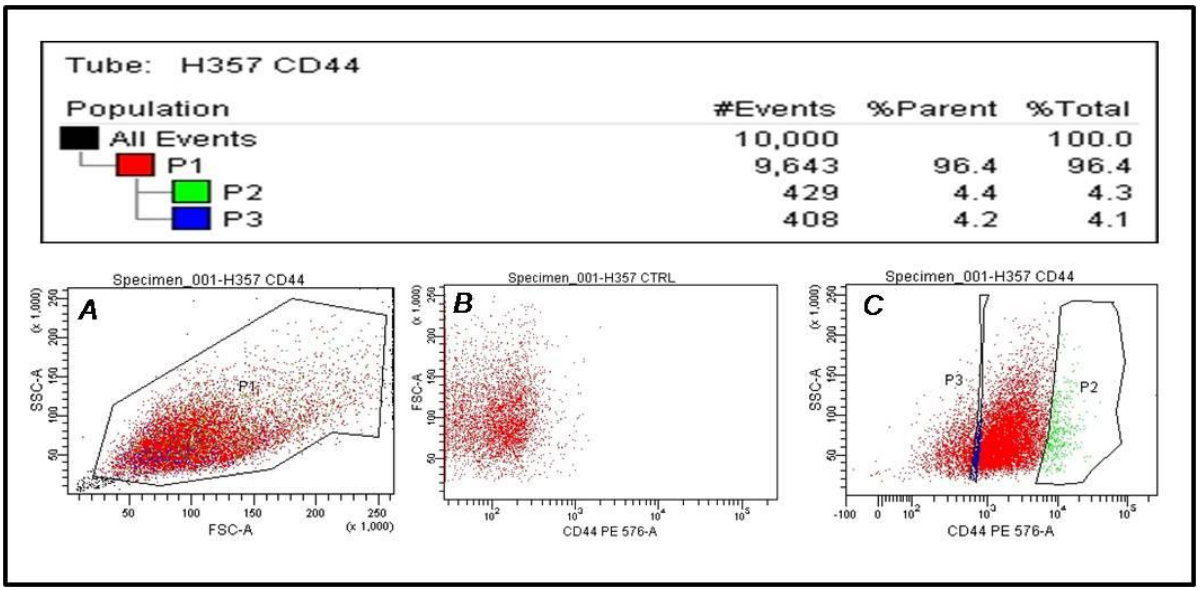

Figure 2.26: Flowcytometric analysis of H357 cells. Representative FACS plots obtained for H357 cells. Doublets were excluded using a forward vs. side scatter profile (A) and suitable cells were gated. Cells were analysed as control without adding antibody to the sample (B) and after the addition of PhycoErythrin-conjugated anti-CD44 antibody (C). 4.4% of the cells expressing the highest levels of CD44 were collected as $CD44^{high}$ cells and 4.2% of cells showing the lowest or no expression were collected as $CD44^{low}$ cells. For this cell line the gate for $CD44^{low}$ cells was positioned further forward to ensure exclusion of cells expressing only background levels of fluorescence. Following collection, cells were cultured for 5 days and the colonies formed were counted.

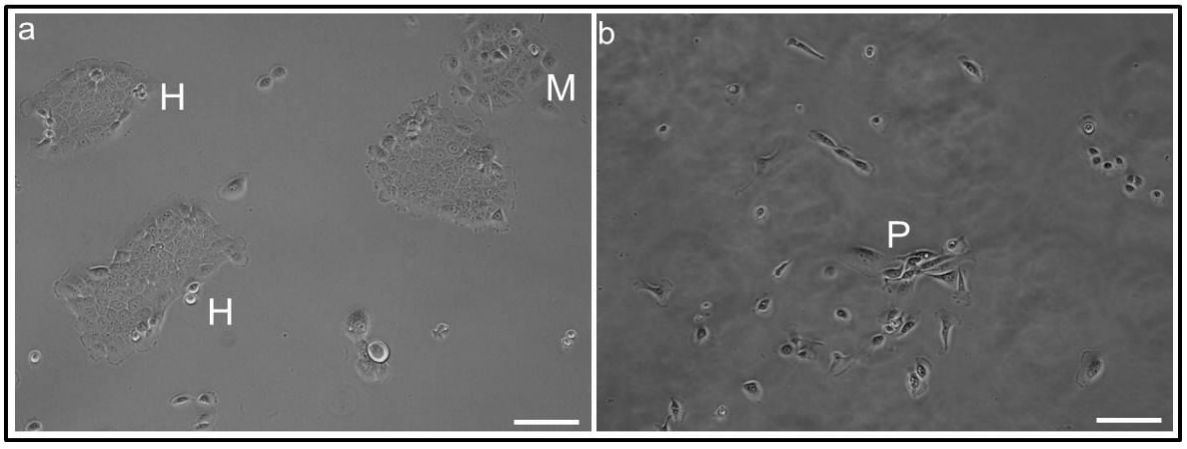

Figure 2.27: Growth of $CD44^{high}$ cells vs. $CD44^{low}$ H357 cells. Cultures of $CD44^{high}$ (a) and $CD44^{low}$ (b) H357 cells shown in phase contrast. $CD44^{high}$ cells show higher colony forming

efficiency and form more holoclones (H) and meroclones (M) thanCD44^{low} cells (a). CD44^{low} cells show poor colony forming efficiency and mainly form paraclones (P) that show little growth and form small abortive colonies.(Scale=100µm)

H357	**Average Holo**	SEM	**Average Mero**	SEM	**Average Para**	SEM
CD44^{high}	**28.67**	2.96	**17.11**	1.64	**15.33**	1.15
CD44^{low}	**8.67**	0.67	**11.33**	2.03	**23.33**	1.86

Table 2.7: Colony counts for the H357 cell line

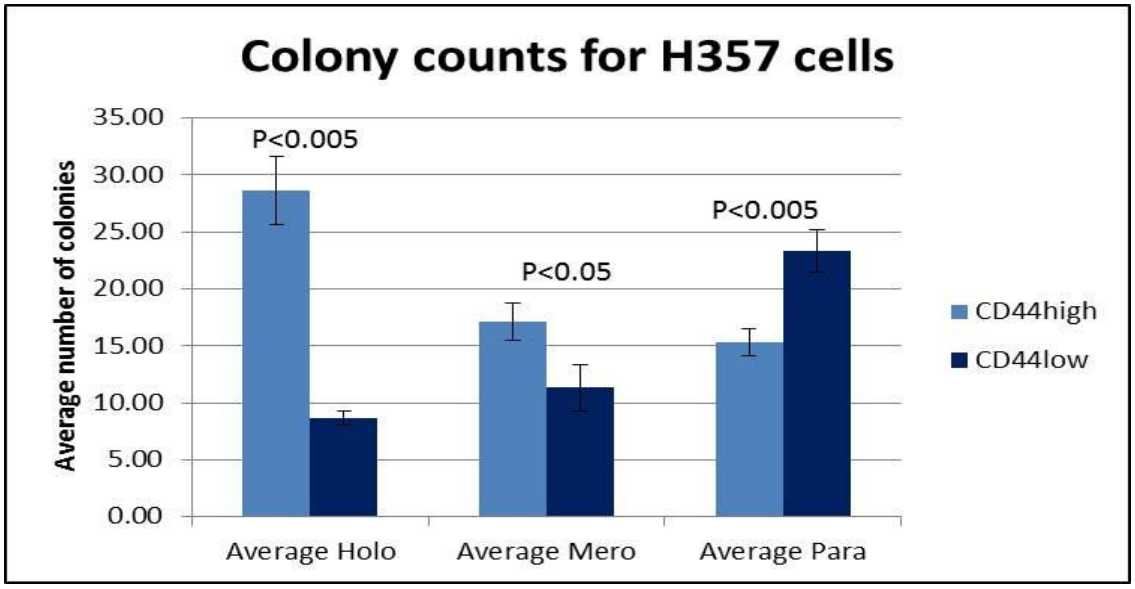

Figure 2.28: Comparison of colony counts obtained for CD44^{high} vs. CD44^{low} H357 cells. The figure above shows the number of holoclones, meroclones and paraclones formed when equal numbers of cells from the two sorted population were plated at clonal density and cultured for five days. CD44^{high} cells formed significantly more holoclones (28.67) and meroclones (17.11) per 1000 cells as opposed to CD44^{low} cells (8.67, 11.33). CD44^{low} cells formed the highest number of paraclones (23.33) per 1000 cells and the least number of holoclones (8.67). The total number of colonies formed by CD44^{high} cells was also higher (48) than CD44^{low} cells (37).

2.3.4 Discussion

The potential role of CD44 as a stem cell marker in oral cancer cell lines was examined as it had been proposed as a marker for oral cancer stem cells by Prince (2007) who showed that $CD44^{positive}$ cells, but not other cells from the oral cancer samples were able to produce tumours when injected subcutaneously into nude mice at low numbers. As stated previously, work done in the Mackenzie Lab showed that the cells at the edge of a holoclone stain less strongly for CD44 than those in the center. Thus, the brighter cells at the center perhaps better represent the stem cell population and this differential pattern could be exploited using the cell sorter method to enrich reliably for stem cells. Cells were sorted on the basis of CD44 expression and the 4-6% of the highest and lowest expressing cells wereselected as $CD44^{high}$ or $CD44^{low}$. When plated out at clonal density, the $CD44^{high}$ population consistently produced more holoclones and meroclones and also formed a higher total number of colonies in comparison to the $CD44^{low}$ cells. This trend was also demonstrated in each of the three cell lines examined namely H357, Ca1 and UK1.It has been previously demonstrated that holoclones are composed of cells capable of extensive division, display self-renewal and restore cellular heterogeneity in the epidermis and in OSCC cell lines (Tudor et al, 2004; Potten et al, 1981). Although these observations encourage the acceptance of CD44 as a stem cell marker, it is still worthwhile to note that the overall number of clonogenic cells remains low as out of 2000 cells plated only 48-60 colonies were counted on average for the $CD44^{high}$ population, which is less than 10% of the total cells plated. It could also be argued that the colony number is low owing to the fact that cells die during the sorting process as they are stressed. Laser capture sections of cells, taken from the centres and edges of holoclones, analyzed through qPCR for stem cell markers showed the central cells had high expression of stem cell signature genes (Biddle et al, 2001). Similar experiments performed on cultured murine keratinocytes showed that cells isolated from the centres of type 3 murine colonies showed high expression of stem cell genes compared to type 2 and type 1 cells (Tudor et al, 2007). These observations also suggest that $CD44^{high}$ cells within the center of holoclones are more clonogenic than the cells present at the edge, it also points out the fact that CD44 is not the only molecule related to clonogenicity and possibly interacts and functions synergistically with other molecules. Based on this, it was hypothesized that other markers, in combination with CD44 might play a role in better enriching for a stem cell population. CD24 is a small cell membrane protein comprising 27 amino acids and is a ligand for P-selectin (Aigner et al, 1998). The interesting fact about this protein is that it is usually not present in human adult tissues but has been found to be upregulated in human

carcinomas such as small cell carcinoma (Aigner et al, 1998). $CD44^{high}CD24^{low}$ cells have been used to prospectively identify breast cancer stem cells in humans and injections of low numbers of these cells into mice gave rise to tumours (Al-hajj et al, 2005). This has been further reinforced by work published in a more recent paper (Mani, 2008). Thus experiments were undertaken to check the role of CD24 in OSCC and whether it could provide a better way to enrich for stem-like cells when used in combination with CD44.

2.4 Detection of CD44 and CD24 at protein level using Fluorescent Activated Cell Sorting (FACS)

2.4.1 Introduction:

The initial FACS experiments demonstrated that CD44+ cells were different from CD44- cells, in being more clonogenic, i.e. formed more holoclones per number of cells seeded whereas CD44- cells formed more paraclones and meroclones. It was also demonstrated that CD44+ cells formed more colonies per number of cells seeded. Al-Hajj and Clarke (2003) had demonstrated that the combination of CD44 and CD24 and lineage markers could be used to sort out a population of stem-like cells from breast cancers that had a $CD44^{high}CD24^{low}$ phenotype. To check whether CD24 plays a role in stemness in OSCC, it was used in combination with CD44 to see if this could better enrich for stem-like cells in oral cancer lines. The protocol followed for cell selection was the same as discussed in section 2.2.2.1, shown in figure 2.21.

2.4.2 Materials and Methods

FACS was used to carry out these investigations and the principle has been discussed in the previous section. The cell lines used for this part of the study were CA1 and 5PTand were chosen to show that the trends seen were consistent over a range of OSCC lines. Cells from these lines were stained with FITC-conjugated anti-CD24 and PE-conjugated anti-CD44 antibodies and the cells were first analyzed and then sorted into four quadrants. These were Q1 (44+24-), Q2 (44+24+), Q3 (44-24-) and Q4 (44-24+) respectively. Cells were sorted into separate tubes and then seeded for cell culture at 1000 cells /flask in T25 culture flasks and cultured for 5 days. The type and number of colonies were counted under a microscope in 9 (1cmX1cm) squares drawn on the bottom of each flask at 4X magnification. The following section deals with the results obtained. The gates were adjusted to include at least 5% of each population in order to have sufficient cells that recovered after the sorting process. Colonies were counted immediately after plating (p0) and, after the first passage (p1).

2.4.3 Results

A) CA1

1) FACS Analysis

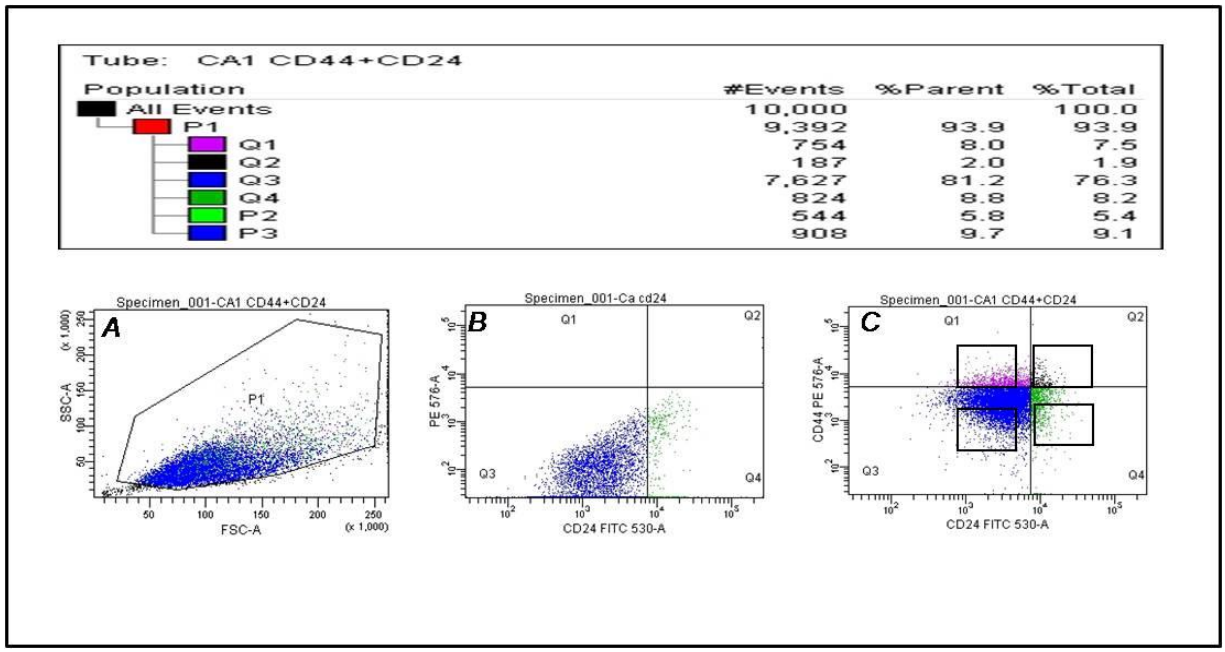

Figure 2.29: Flowcytometric analyses of CA1 cells stained with CD44 (PE) and CD24 (FITC) antibodies. Representative Facsplots obtained for CA1 cells, stained with anti-CD44 (PE) and anti-CD24 (FITC) antibodies. Doublets were excluded using a forward vs. side scatter profile (A) and suitable cells were gated. Control cells were analyzed without adding any antibody to the sample (B) and after the addition of PhycoErythrin-conjugated anti-CD44 and FITC-conjugated anti-CD24 antibody (C). As explained before, to improve the efficiency of the sort, the gates were positioned to include at least 5% of the total population studied with cells selected on either expression of the highest or the lowest levels. They were collected as $CD44^{high}CD24^{low}$ (Q1), $CD44^{high}CD24^{high}$(Q2), $CD44^{low}CD24^{low}$ (Q3) and $CD44^{low}CD24^{low}$ (Q4).

2) Cell morphology

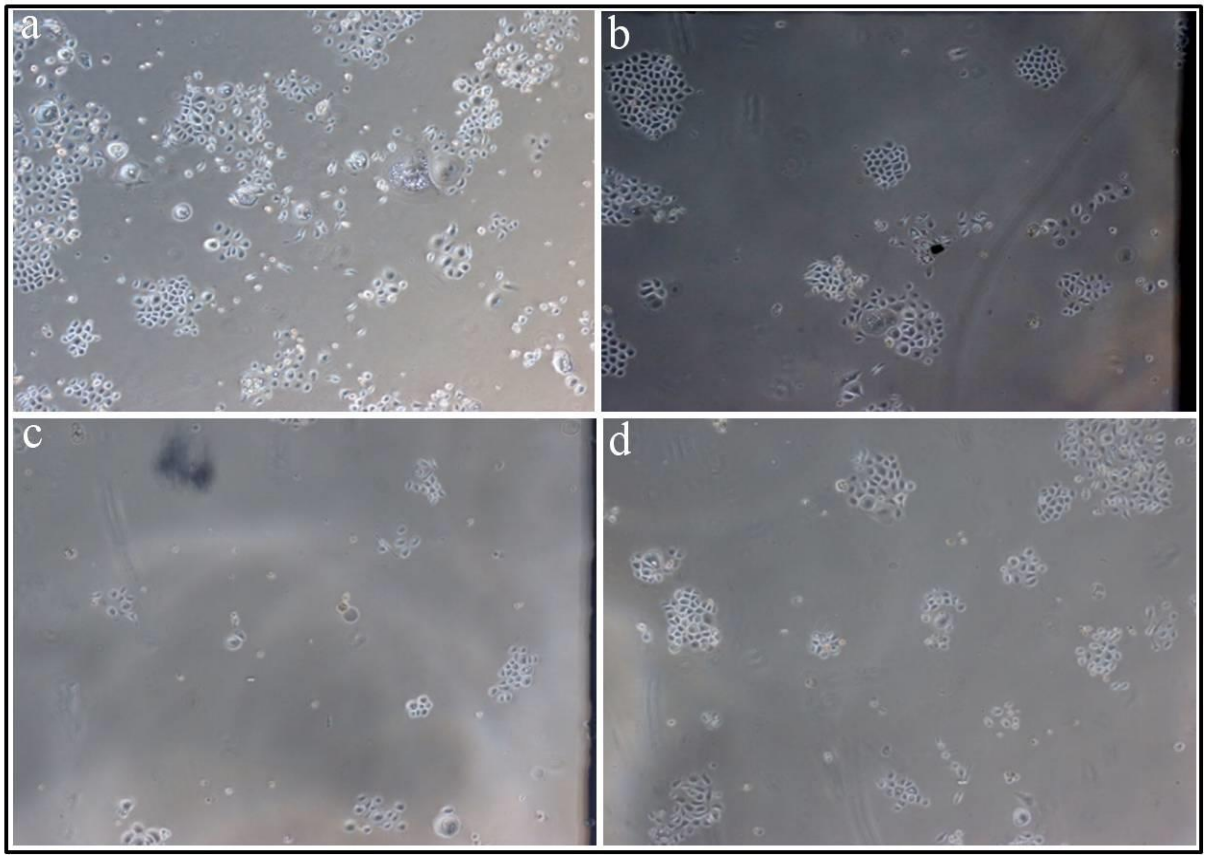

Figure 2.30: Culture of sorted CA1 cells. Phase contrast images of $CD44^{high}CD24^{low}$ (a), $CD44^{high}CD24^{high}$ (b), $CD44^{low}CD24^{low}$ (c) and $CD44^{low}CD24^{high}$ (d).$CD44^{high}CD24^{low}$ cells show good growth although they mostly formmeroclones and a few holoclones. $CD44^{high}CD24^{high}$cells form mostly holoclones but with a few dispersed paraclones. $CD44^{low}CD24^{low}$ cells show very poor growth and formed mostly small abortive paraclone colonies (c). $CD44^{low}CD24^{high}$ cells form mostly meroclone-like colonies (b).

3. Colony forming efficiency of sorted CA1 cells when plated at clonal density:

Cells were plated for culture immediately after sorting (p0) and colonies were counted. Following, they were detached from the dish and plated again for colony counts to see if the trend seen could be repeated after the first passage (p1).

(i) Cells plated immediately after sorting (p0):

This section shows the type and number of colonies formed by plating the different cell populations collected immediately after sorting, also termed Passage 0 (P0).

Quadrant	Average Holo	SEM	Average Mero	SEM	Average Para	SEM
Q1(44+24-)	**31.50**	4.82	**82.70**	7.13	**46.33**	6.43
Q2(44+24+)	**79.27**	3.41	**49.73**	6.14	**39.63**	4.05
Q3(44-24-)	**15.10**	2.35	**43.80**	7.23	**86.23**	7.60
Q4(44-24+)	**30.83**	1.26	**51.73**	8.40	**42.03**	3.08

Table 2.8: Colony counts for sorted CA1 cells (p0)

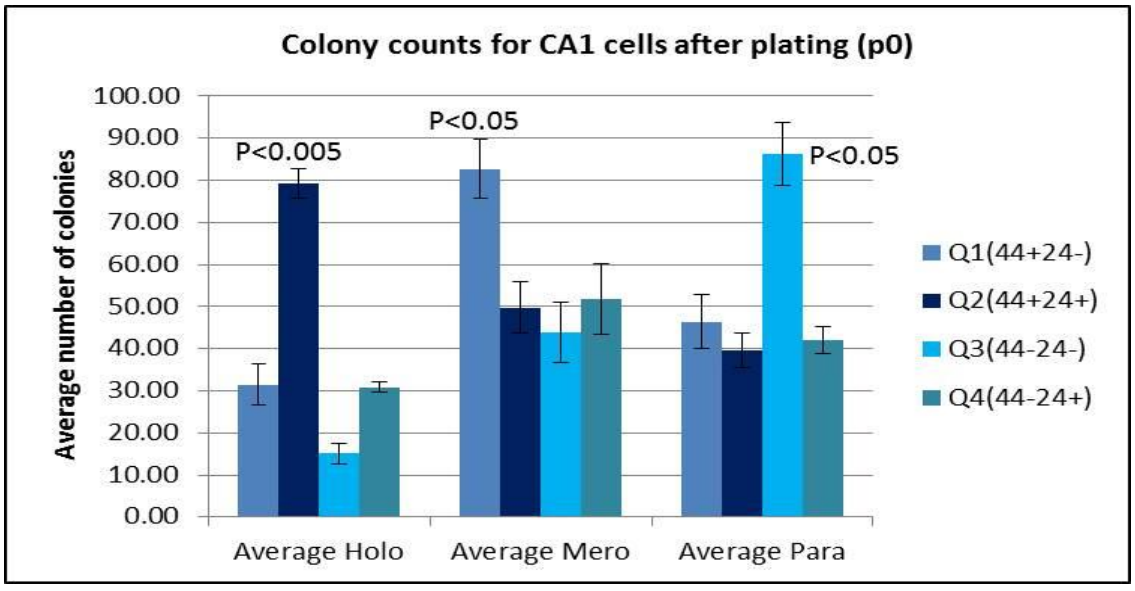

Figure2.31: Colony forming efficiencies of sorted populations of CA1 cells immediately after plating (p0).Q2 ($44^{+}24^{+}$) double positive cells formed a significantly higher proportion of holoclones as opposed to the other populations (table 2.8). Q1 ($44^{+}24^{-}$) cells formed the most number of meroclones and the next highest number of holoclones. Q3 (44-24-) cells formed the highest number of paraclones and meroclones and the least number of holoclones. Q4 showed more holoclones and meroclones than Q3 but fewer paraclones.

(ii) Cells plated after first passage (p1):

Following colony counts, cells were detached and replated at clonal density for further counts, also termed Passage 1 (p1).

Quadrant	Average Holo	SEM	Average Mero	SEM	Average Para	SEM
Q1(44+24-)	19.50	2.12	30.30	1.70	42.25	1.77
Q2(44+24+)	40.00	3.54	24.15	6.86	31.55	4.17
Q3(44-24-)	12.50	2.83	23.15	1.91	51.20	8.77
Q4(44-24+)	16.05	2.76	31.95	2.05	36.63	1.59

Table 2.9: Colony forming efficiency of sorted CA1 populations at first passage (p1)

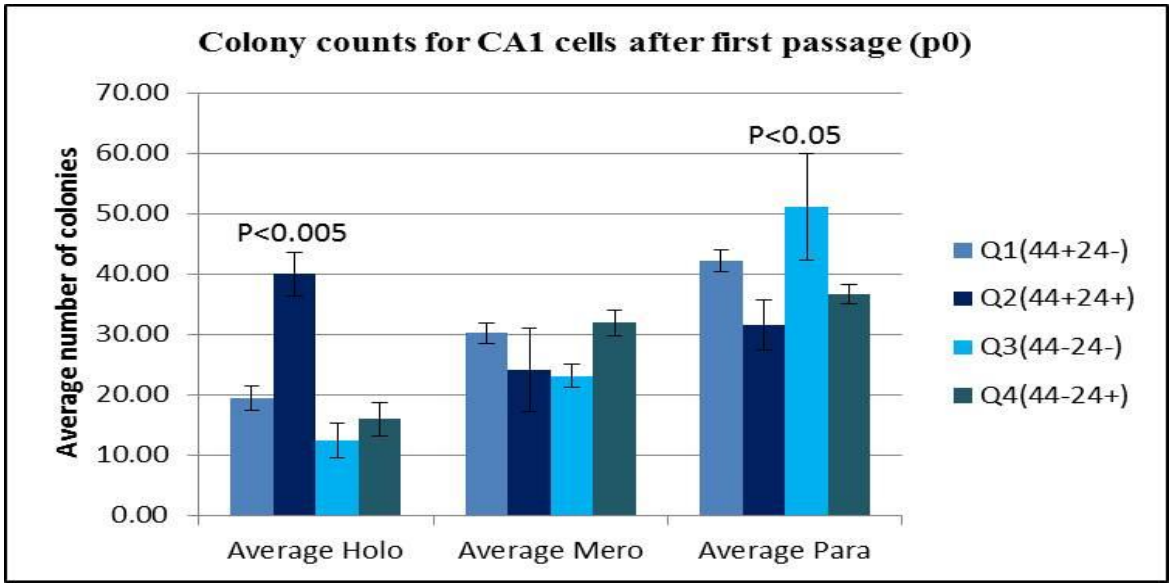

Figure 2.32: Colony forming efficiency of sorted CA1 cells after first passage

This graph shows the numbers of the different types of colonies counted for each quadrant examined after the cells had been passaged once. The cells obtained from quadrant Q2 ($CD44^{high}CD24^{high)}$ still show a significantly higher number of holoclones than the other quadrants. Q3 still shows the highest number of paraclones counted. The overall numbers of each type of colony formed is also less than immediately after plating.

4) Average total number of colonies formed immediately after sorting (p0) and at first passage (p1)

Quadrant	CA1(p0)	SEM	CA1(p1)	SEM
Q1(44+24-)	170.0	2.8	93.5	6.4
Q2(44+24+)	175.5	13.4	106.0	5.6
Q3(44-24-)	139.0	2.8	84.0	1.3
Q4(44-24+)	136.5	16.3	84.0	7.1

Table 2.10: Average total number of colonies formed by the sorted populations immediately after sorting (p0) and after first passage (p1).

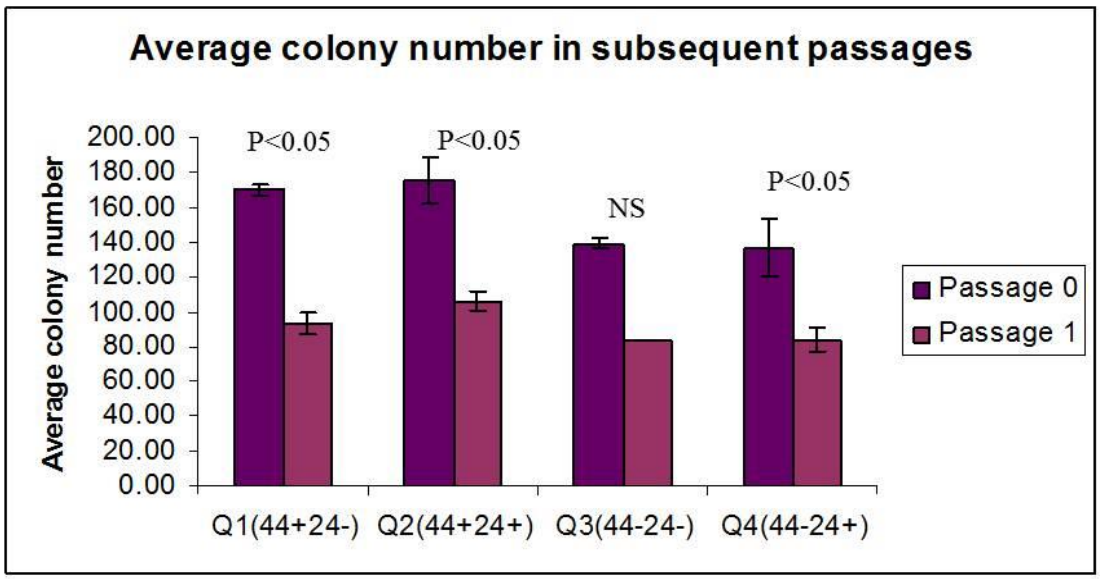

Figure 2.33: The average total number of colonies formed immediately after plating (p0) and after the first passage (p1). The overall number of colonies formed by all the four sorted populations after the first passage was also significantly less (Q1-93.5, Q2-106, Q3-84 and Q4-84) as compared to the numbers formed immediately after plating (170, 175, 139, 136), and are listed in the order $CD44^{high}CD24^{low}$ (Q1), $CD44^{high}CD24^{high}$ (Q2), $CD44^{low}CD24^{low}$ (Q3) and $CD44^{low}CD24^{high}$ (Q4).

Quadrant	% Holoclone	%Meroclone	%Paraclone	Total Colonies
Q1(44+24-)	19.7	50.3	30.0	170.0
Q2(44+24+)	45.1	29.9	25.7	175.5
Q3(44-24-)	12.6	29.8	57.5	139.1
Q4(44-24+)	22.7	43.9	33.3	136.5

Table 2.11: Colony forming efficiencies of sorted cells immediately after plating

Quadrant	%Holoclone	%Meroclone	%Paraclone	Total Colonies
Q1(44+24-)	22.5	33.7	43.8	93.5
Q2(44+24+)	40.9	27.4	32.5	106.0
Q3(44-24-)	17.3	29.2	53.5	84.0
Q4(44-24+)	21.4	36.3	42.3	84.0

Table 2.12: Colony forming efficiencies of sorted cells after first passage

The tables above show the percentages of holoclones, meroclones and paraclones formed for each of the sorted quadrants immediately after plating (table 3.3f) and after the first passage (table 3.3g). The extreme right hand column shows the total numbers of colonies counted for each set of experimental runs.$CD44^{high}CD24^{high}$ cells (Q2) consistently formed the highest percentage of holoclones, immediately after plating (45%) and also after the first passage (40.09%). The percentage of paraclones formed by these cells also increased after the first passage (25.07%, 32.55%). They also gave rise to the most number of colonies compared to all the other quadrants (175.5, 106). However the number of colony forming cells seemed to decrease after the first passage for all the 4 quadrants examined. The average number of paraclones increased after the cells were passaged. Meroclones formed by $CD44^{high}CD24^{low}$decreased significantly after the first passage (p0=50.29; p1=33.69) and they showed a significant increase in the percentage of paraclones formed. The highest percentages of paraclones were counted for $CD44^{low}CD24^{low}$ cells and this remained the case immediately after plating and after the first passage.

B) 5 PT cell line

1) FACS Analysis

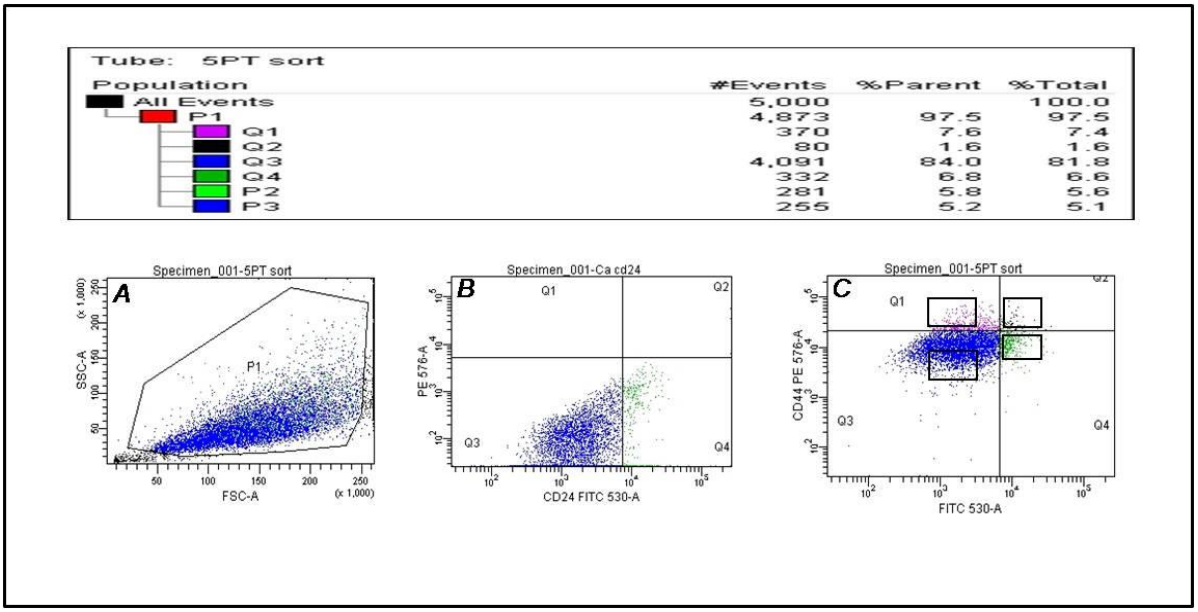

Figure 2.34: Flowcytometric analyses of 5PT cells stained with anti-CD44 (PE, y-axis)) and anti-CD24 (FITC, x-axis) antibodies. Representative Facsplots obtained when CA1 cells were stained with anti-CD44 (PE) and anti-CD24 (FITC) antibodies. Doublets were excluded using a forward vs. side scatter profile (A) and suitable cells were gated. Control cells were analyzed without adding any antibody to the sample (B) and after the addition of PhycoErythrin (PE)-conjugated anti-CD44 and FITC-conjugated anti-CD24 antibody (C). As explained, to improve the efficiency of the sort, the gates were positioned to include at least 5% of the total population studied with cells selected on either expression of the highest or the lowest levels. They were collected as $CD44^{high}CD24^{low}$ (Q1), $CD44^{high}CD24^{high}$(Q2), $CD44^{low}CD24^{low}$ (Q3) and $CD44^{low}CD24^{low}$ (Q4).

2) Cell morphology:

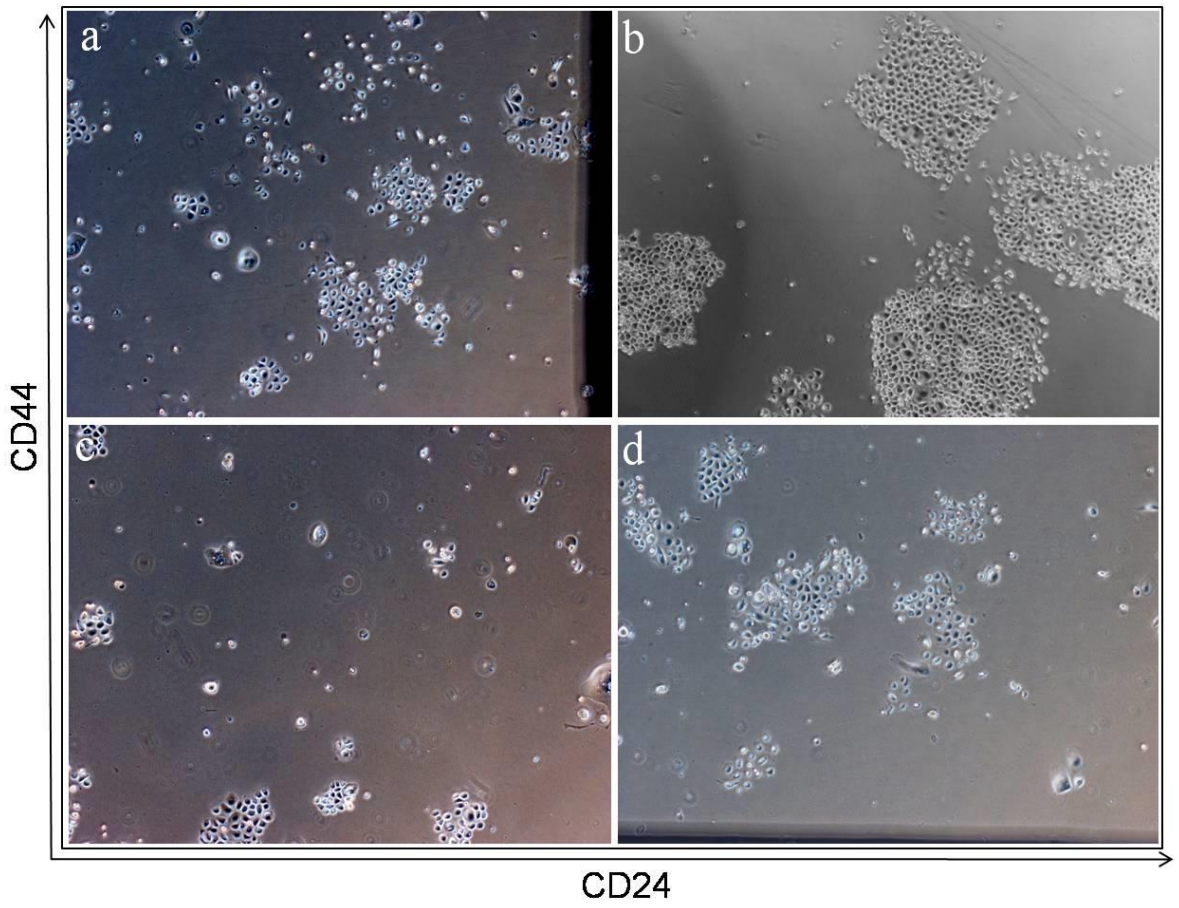

Figure 2.35: Culture of sorted 5PT cells. Phase contrast images of $CD44^{high}CD24^{low}$ (a), $CD44^{high}CD24^{high}$ (b), $CD44^{low}CD24^{low}$ (c) and $CD44^{low}CD24^{high}$ (d). $CD44^{high}CD24^{low}$ cells showgood growth although they mostly formed meroclones and few holoclones. Panel (b) shows the colonies generated by $CD44^{high}CD24^{high}$ cells that form mostly holoclones with a few scattered paraclones. $CD44^{low}CD24^{low}$ cells showed very poor growth and formed mostly small abortive colonies (c). $CD44^{low}CD24^{high}$ cells form few holoclones, forming mostly paraclones and meroclones (d).

3) Colony forming efficiency of sorted 5PT cells when plated at clonal density:

Cells were plated for culture immediately after sorting (p0) and colonies were counted. Following, they were detached from the dish and plated again for colony counts to see if the trend seen could be repeated after the first passage (p1).

(i) Cells plated immediately after sorting (p0):

This section shows the type and number of colonies formed by plating the different cell populations collected immediately after sorting, also termed Passage 0 (P0).

Quadrant	Average Holo	SEM	Average Mero	SEM	Average Para	SEM
Q1(44+24-)	**24.50**	2.12	**65.75**	4.60	**39.00**	0.71
Q2(44+24+)	**63.60**	5.80	**36.00**	2.12	**33.00**	3.54
Q3(44-24-)	**16.75**	5.30	**38.25**	15.91	**82.50**	10.61
Q4(44-24+)	**14.50**	0.71	**30.00**	1.41	**60.25**	6.36

Table 2.13: Number of colonies of each type formed by sorted cell populations immediately after plating.

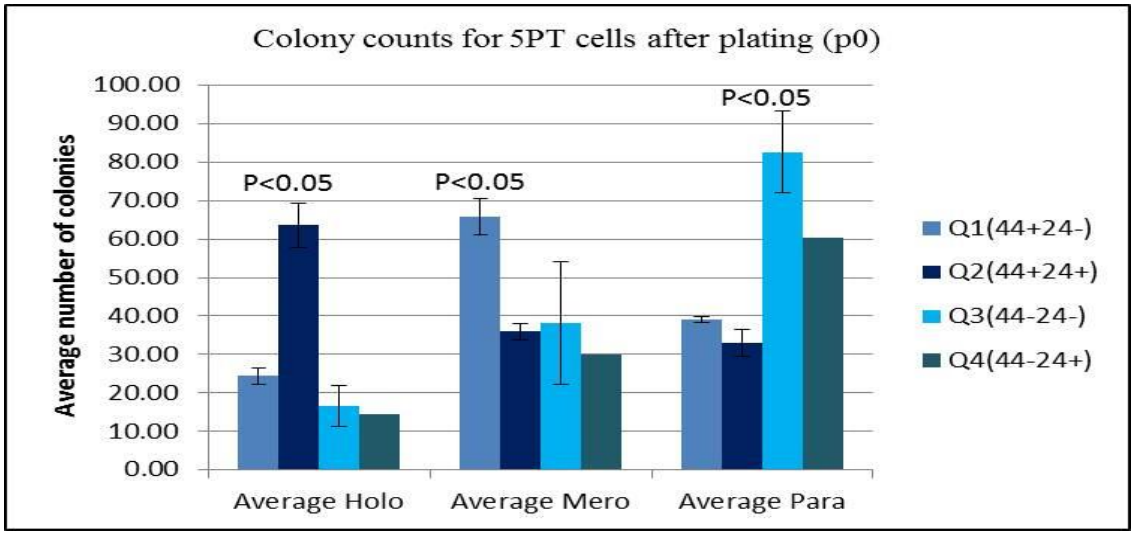

Figure 2.36: Colony forming efficiencies of sorted populations of 5PT cells (p0). $CD44^{high}CD24^{high}$ cells (Q2) again formed a significantly higher proportion of holoclones as opposed to the other populations (table 3.3h). $CD44^{high}CD24^{low}$ cells (Q1) were formed the most number of meroclones and the second highest number of holoclones. $CD44^{low}CD24^{low}$ cells (Q3) formed mostly paraclones and the second highest number of meroclones. They also formed low numbers of holoclones. $CD44^{low}CD24^{high}$cells (Q4) formed the least number of holoclones and meroclones and the second highest number of paraclones.

(ii) Cells plated after first passage (P1):

Quadrant	Average Holo	SEM	Average Mero	SEM	Average Para	SEM
Q1(44+24-)	**14.75**	3.182	**34.2**	2.2627	**39.575**	1.461
Q2(44+24+)	**38.2**	2.2914	**28.5**	2.1213	**27.5**	3.5427
Q3(44-24-)	**10**	2.8284	**29.225**	6.7529	**50.3**	3.8184
Q4(44-24+)	**14.75**	2.4749	**31.5**	3.6078	**32.5**	3.5263

Table 2.14: Colonies formed by sorted cells after the first passage (P1).

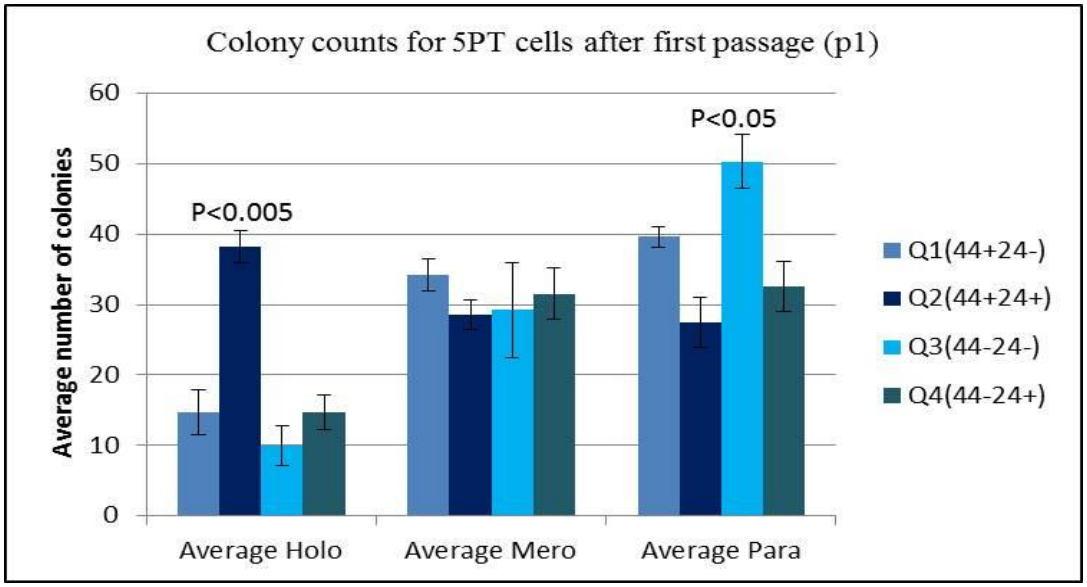

Figure 2.37: The type and number of colonies formed by sorted 5PT cell populations after the first passage (P1). The numbers of the types of colonies counted for each quadrant examined, after the cells had been passaged once are shown. The cells obtained from quadrant Q2 ($CD44^{high}CD24^{high}$) still show a significantly higher number of holoclones than the other quadrants. Q3 formed a high proportion of paraclones but the highest numbers of paraclones were counted for $CD44^{low}CD24^{high}$ cells. The overall numbers of each type of colony formed were also less compared to those formed immediately after plating.

4) Average total number of colonies formed immediately after sorting (p0) and at first passage (p1).

Quadrant	**5PT(po)**	SD	**5PT(p1)**	SD
Q1(44+24-)	134.5	9.2	95.0	1.4
Q2(44+24+)	123.5	9.2	90.5	0.7
Q3(44-24-)	157.5	10.6	87.0	12.7
Q4(44-24+)	107.0	4.2	110.0	7.1

Table 2.15: Average total number of colonies formed by the sorted populations immediately after sorting (p0) and after first passage (p1).

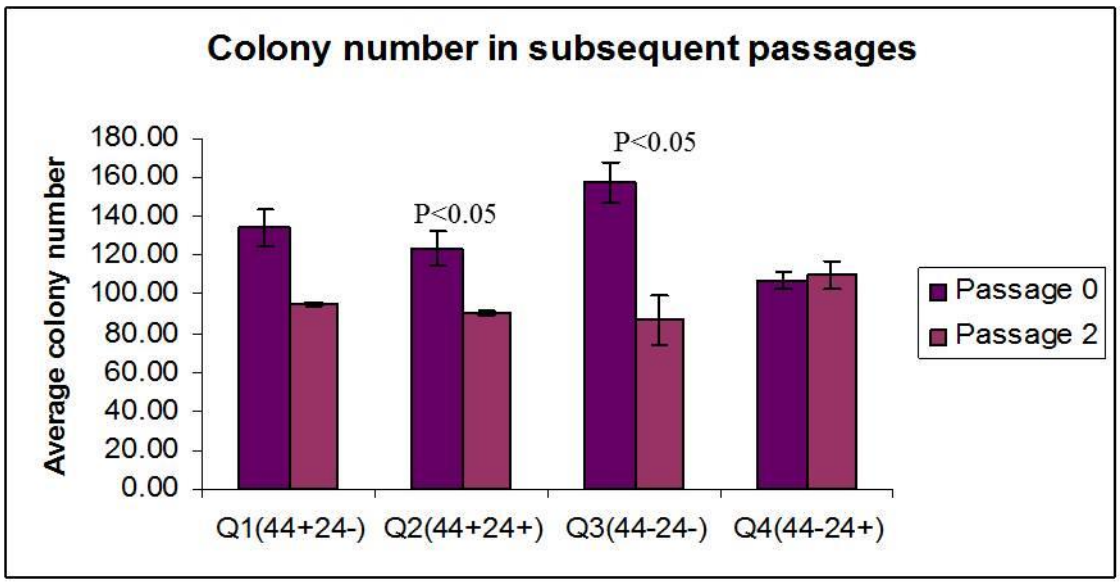

Figure 2.38: The average total number of colonies formed immediately after plating (p0) and after the first passage (p1). The total number of colonies formed after the first passage was lower for three of the sorted populations (Q1, Q2, and Q3), however this was only significant for Q3 cells (Q1-95,134; Q2-90.5, 123; and Q3-87, 157). Q4-cells showed a slight increase in the colony number but this was insignificant (110).

Quadrant	%Holoclone	%Meroclone	%Paraclone	Total Colonies
Q1(44+24-)	19.3	51.3	29.4	134.5
Q2(44+24+)	48.2	27.9	23.8	123.5
Q3(44-24-)	13.1	31.4	55.6	157.5
Q4(44-24+)	14.2	28.9	57.1	107.0

Table 2.16: Colony forming efficiencies of sorted cells immediately after plating

Quadrant	%Holoclone	%Meroclone	%Paraclone	Total Colonies
Q1(44+24-)	16.8	39.5	43.6	95.0
Q2(44+24+)	40.3	28.3	31.4	90.5
Q3(44-24-)	11.4	29.3	59.2	87.0
Q4(44-24+)	12.2	28.6	59.1	110.0

Table 2.17: Colony forming efficiencies of sorted cells after first passage.

The tables above show the percentages of holoclones, meroclones and paraclones formed for each of the sorted quadrants immediately after plating and after the first passage. The extreme right hand column shows the total numbers of colonies counted for each set of experimental runs.$CD44^{high}CD24^{high}$ cells (Q2) consistently formed the highest percentage of holoclones, immediately after plating (48.2%) and also after the first passage (40.3%). The percentage of paraclones formed by these cells also increased after the first passage (23.89%, 31.49%). The number of colony forming cells seemed to decrease after the first passage for all the 4 quadrants examined. The average number of paraclones increased after the cells were passaged and this was seen in all four quadrants examined. Meroclones formed by $CD44^{high}CD24^{low}$again decreased after the first passage (p0=51.3; p1=39.47) and they showed an increase in the percentage of paraclones formed (29.37, 43.68). The highest percentages of paraclones were counted for $CD44^{low}CD24^{low}$and $CD44^{low}CD24^{high}$cells and this remained the case immediately after plating and after the first passage.

2.4.4 Discussion

The 5PT cell line, generated from oral carcinoma by Tom Carey (Michigan Lab) was added to the study as cells from this line give rise to good colony morphologies and we wanted to demonstrate that the trends seen were consistent over a range of cell lines from different cancers. Cells were separated into quadrants and sorted into four distinct populations namely, **CD44**^{high}**CD24**^{low} (Q1), **CD44**^{high}**CD24**^{high} (Q2) **CD44**l^{ow}**CD24**^{low} (Q3) and **CD44**^{low}**CD24**^{high} (Q4) and plated out at clonal density in T25 flasks.**CD44**^{high}**CD24**^{high} (Q2) cells from both cell lines formed significantly higher proportions of holoclones ($p<0.05$) compared to those formed by all other quadrants.The number of holoclones formed by these cells remained significantly higher when cells were plated immediately after sorting and also after the first passage. The total colony counts for Q2 were also higher than those obtained for Q1, Q3 and Q4 but this difference was not statistically significant ($p>0.05$). These resultswere consistent for the cell lines examined,suggesting that these proteins are similarlyexpressed in both cell lines. Q1 cells were seen to form the most number of meroclones in both cell lines, 91.5±4.95 for CA1 and 69±5.66 allowing us to deduce that CD44^{high}CD24^{low} cells probably enrich for transient amplifying cells. Q3 cells significantly formed the highest number of paraclones, i.e. 79±4.24 for CA1 and 87.5±3.54 for 5PT. They also formed the least amount of holoclones, 32.5±3.54 for CA1 and 26±5.66 for 5PT. The number of colonies generated by these cells were also more than the other populations, but this difference was not only insignificant ($p>0.05$), but it could also be argued that paraclones divide more frequently than holoclones which is why they give rise to a much larger colony number. Q4 showed more holoclones and meroclones than Q3 but less paraclones. These results suggest that the use of CD44 and CD24 together does give greater enrichment for stem cells as opposed to CD44 alone, and suggest that CD44 and CD24 are both expressed on stem cells in oral cell lines. Al Hajj and co-workers showed that CD44^{high}CD24^{low} cells were more clonogenic, reconstituted the entire tumour population when transplanted into mice, and were also more invasive than their CD44^{high}CD24^{high} counterpart (2003). Later it was shown that CD44^{high}CD24^{high} cells were also clonogenic, represent the epithelial component of the tumour, and gave rise to the invasive CD44^{high}CD24^{low} cells (Vonderhaar et al, 2009). The overall percentage of colony forming cells remainedbetween 8-10% for both cell lines immediately after sorting, but the number of holoclones formed by CD44^{high}CD24^{high} population of CA1 cells dropped to 42.5±4.95, and for the 5P% line to 36.5±2.32 after the first passage. Hence the percentage of clonogenic cells, taken as a measure of the number of stem cells remains very low, even after sorting for the marker combination. This also showed that

although $CD44^{high}CD24^{high}$ cells were clonogenic, the number of holoclones formed by them dropped as cells seem to revert to parental levels after enrichment.

The addition of further markers to the sorting process might help to sort a purer population of clonogenic cells. The sorting process itself stresses cells and some cells may lose clonogenicity because of this. It might also be feasible to let the cells recover overnight after the sorting process before harvesting them the next day to plate for colony counts. The purity of the isolates may even, after rigorous compensation controls,be influenced by instrument error with contamination by undesired cells from different quadrants.

These results demonstrate heterogeneous patterns of cell surface expression of markers, and that they are related to the heterogeneous behavioural properties of cell sub-populations present in cell lines.

2.5 Induction of EMT in cancer cell lines and the role of TGF-β and external factors that may influence the extent of this process

2.5.1 Introduction

Examining the appearance of cultures plated at clonal densities indicates that when holoclones form by cell division:

1. Cells remain tightly in contact with the surrounding cells.
2. As colonies grow, some cells around the edges show tendency to break away from the colony.
3. Thesecells appear more motile andhave a spindly morphology.

Additionally, staining holoclones with stem cell markers reveals a pattern where cells in the center stain strongly for markers such as CD44, β-Catenin and E-cadherin with cells at the edge showing weaker staining indicating their down regulation. Time lapse videos of cell lines show that when colonies form, cells making up the center of the colonies that are relatively stationary and maintain contact with neighbours whereasthose around the edge of the colony are more motile and show a spindle morphology when they leave. Thus, these spindly cells are generated from the colony itself and show scattering.If a holoclone colony is compared to a tumour then cells at the center represent the main bulk of the tumour. The cells at the edge of *in vitro*colonies, may*in vivo*be considered to represent the cells making up the tumour-host interface or "invasive front" of a tumour (Bankfalvi; Brabletz et al, 2005).In *in vitro* conditions there is an absence of connective tissue, but *in vivo* tumours are exposed to a multitude of growth factors and chemokines produced by both stromal and inflammatory cells in the extracellular environment. Reciprocally, tumour cells are able to influence stromal cells with tumour cells creating an environment that feeds back, as in wound healing, to promote EMT (Kalluri and Weinberg, 2009; Wu et al, 2009). Analysis of videos and staining patterns of *in vitro* cells suggest that the cells at the edge of holoclones are undergoing EMT. Cells present at the tumour-host interface have been shown to possess genes related to stemness and the latter have also been shown to possess EMT signature genes (Shinto et al, 2004). The lowering of markers such as β-catenin and E-cadherin has been linked to EMT within a range of cancers including lung and pancreas (Debies, et al, 2008; Shah, et al, 2007) and therefore it is interesting to see a similar pattern in OSCC cell lines. In many cell types, TGF-β is one of the potent

inducers and mediator of EMT (Zavadil and Bottinger, 2005). It was shown that TGF-β interferes with E-cadherin and β-catenin function in mammary epithelial cells, promoting motility and the acquisition of an EMT phenotype (Bakin et al, 2000). TGF-β has been linked to the progression of many cancers and in breast, it interacts with SMAD proteins that activate snail and slug, known repressors of E-cadherin and lead to increased invasiveness and metastatic potential (Massague, 2008). The effect of TGF-β on OSCC cell lines was therefore investigated to see whether treatment could induce the formation of the motile cells similar to those seen at the edges of colonies. The effect of TGF-β on the expression of EMT markers was also investigated using immunocytochemistry and FACS analysis.

Aims:

- To determine whether TGF-β induces EMT in oral cancer cell lines.
- To investigate whether EMT generates cells with the properties of stem cells.
- To assess the role of other extrinsic factors present in the tumour microenvironment that may contribute to this process.
- To study the effect of EMT on known stem cell markers and their expression patterns in cancer cell lines.

To investigate the changes associated with EMT, immunocytochemistry for CD44, ESA, E-cadherin and β-catenin was carried out on control and treated cells. Sphere assays were also performed as sphere-forming ability is a hallmark of EMT and has also been linked to stemness (Mani et al, 2008). FACS analysis was also used to study the effect of treatments on different subpopulations present within OSCC cell lines stained for both CD44 and ESA. After initial experiments demonstrated that TGF-β induced EMT, whether the effect of TGF-β was permanent or was removed upon withdrawing TGF-β treatment was also examined. The effects of long term treatment with TGF-β were also investigated to see how this affected relative numbers of cells within subpopulations in OSCC cell lines.

2.5.2 Materials and Methods (Part 1)

Cells were cultured as described before (2.2.2.1).

TGF-β (R&D systems; TGFB1001B) was dissolved in PBS containing 0.001% HCL and was used at a concentration of 20 ng/ml. The inhibitor of TGF-β, SB431542 (Sigma; S4317) was resuspended in 5% DMSO in distilled water and used at 5µg/ml.

Fibroblast conditioned medium (FIBSCM) was prepared by growing sub-confluent cultures of fibroblasts that had been isolated from tumours by growth in RM+ culture medium for 5-6 days. The medium was transferred to a 50ml falcon tube and spun down at 3000 revs/min to remove any cellular debris. After centrifugation, the supernatant was filtered into a clean tube through a 0.45um filter. This medium was then used to culture cells from CA1 and H357 cell lines for 5-6 days at the end of which they were photographed and compared to control cells and TGF-β treated cells. For immunocytochemistry protocols were followed as discussed before (2.2.1.2b). The procedure for selecting cells for FACS was the same as has been discussed (2.2.2.1, 2.2.2.2).For suspension cultures,0.75 cm^2 tissue culture wells were coated overnight with polyhema (Sigma, Exeter, UK,12 mg⁄ml in 95% ethanol) to prevent cell attachment. The cells were then plated at a density of 1000 cells⁄well in 500 µl RM+ medium with addition of 1% methylcellulose (Sigma) to prevent cell aggregation. The cells were incubated (37_C, 5% CO2) and monitored for sphere growth for time periods ranging from 1-2 weeks depending on the cell line studied. Following counting, spheres were reintroduced into adherent culture conditions and left for 24 hours. They were detached and again plated into suspension cultures and monitored for sphere growth.

2.5.3 Results (Part 1)

The effect of TGF-β and medium conditioned by the growth of tumour associated fibroblasts (FIBS CM) on OSCC cells.

1) Cell culture

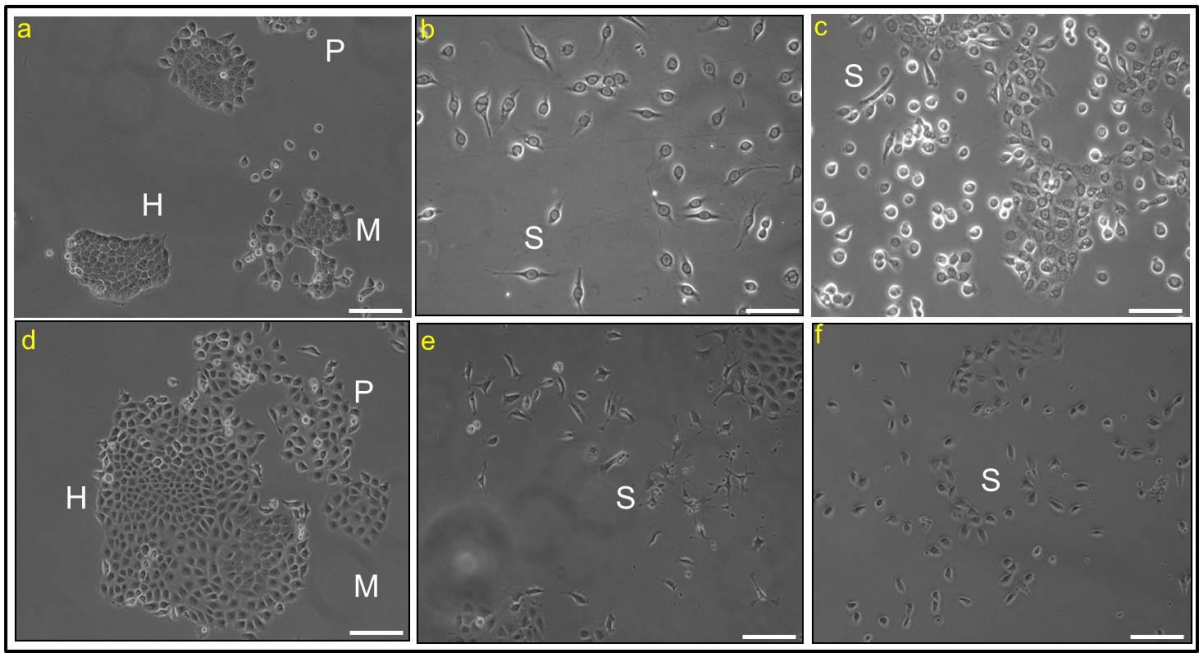

Figure 2.38: The effect of TGF-β and fibroblast conditioned medium (FIBSCM) on OSCC cells (Scale=50µm). Cultures of CA1 (a-c) and H357 (d-f) cells under control conditions (a, d), with TGF-β (b, e) and with conditioned medium from tumour-associated fibroblasts (c, f) shown in phase-contrast. Control cells show the normal colony morphology patterns by forming holoclones (H), meroclones (M) and paraclones (P). Treatment with TGF-β results in the formation of spindle-shaped cells that show scattering and were seen to be motile in time-lapse videos. Cells also lost the tendency to form colonies and developed elongated spindle-like morphologies. Treatment with conditioned medium from tumour associated fibroblasts also resulted in similar changes and a spindle-like morphology (S) was acquired by both cell lines (e, f).

2) Immunocytochemistry

Immunocytochemistry carried out on the CA1 and H357 cell lines for EMT and stem cell markers (CD44, ESA, β-catenin and E-cadherin).

I) CD44

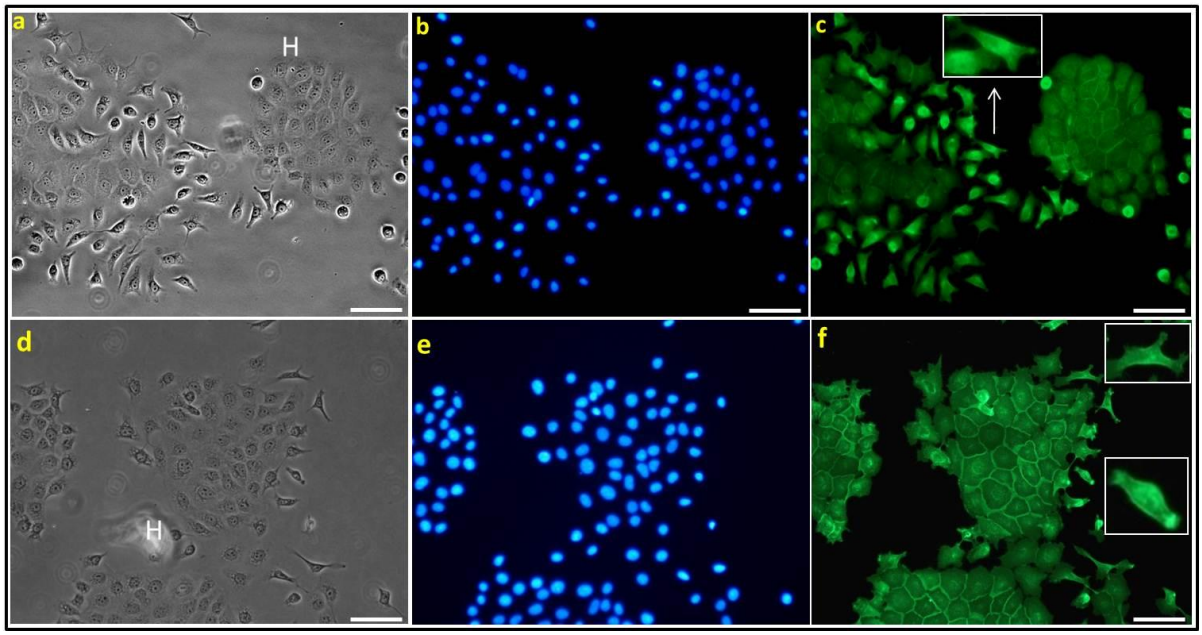

Figure 2.39: Expression of CD44 in OSCC cells under control conditions (Scale=50µm). Cultures of CA1 (a-c) and H357 (d-f) cells. Holoclones (H) formed by both lines are shown (a, d) in phase contrast, stained with DAPI nuclear stain (b, e) and with anti-CD44 FITC antibody (c, f) Cells showed good colony formation with a few scattered elongated cells present The patterns of CD44 expression were similar to those described earlier and strong expression of CD44 was seen at the cell surface and weak expression was seen in the cytoplasm. The elongated cells show strong expression of CD44 in the cytoplasm (c-inset), show peri-nuclear accumulation and in some cases nuclear localization of the protein.

TGF-β treated cells:

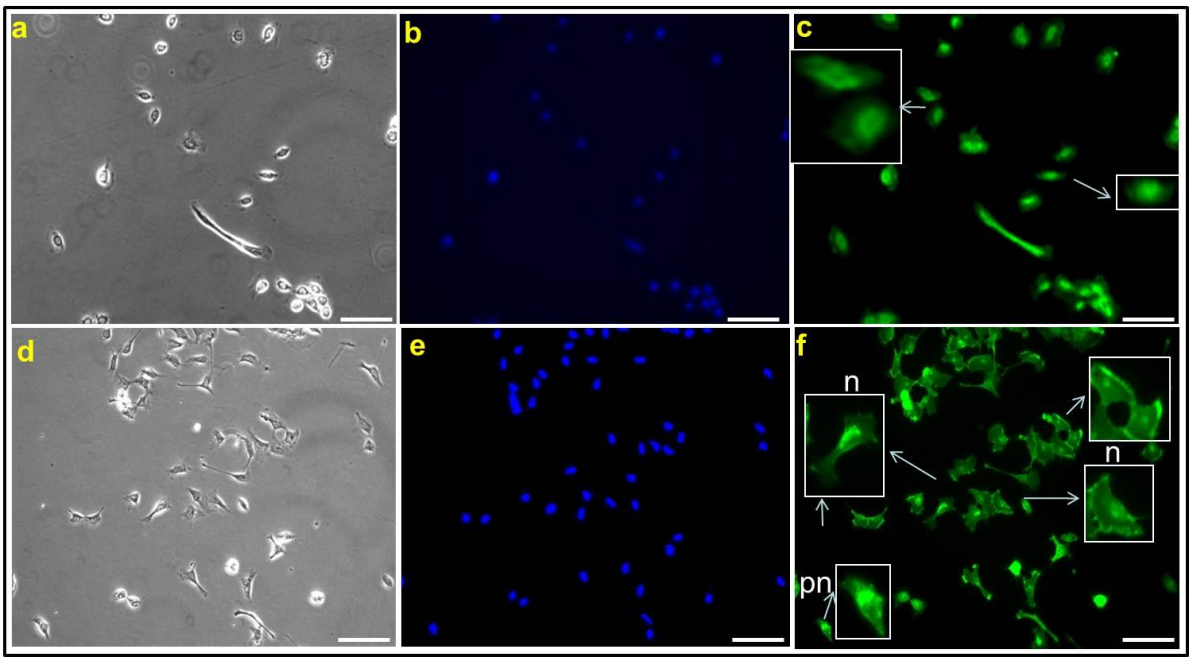

Figure 2.40: Expression of CD44 in OSCC cells treated with TGF-β (Scale=50µm). Cultures of CA1 (a-c) and H357 (d-f) cells treated with TGF-β and shown in phase contrast (a, d), stained with DAPI nuclear stain (b, e) and with anti-CD44 FITC antibody (d, f). Treated cells from both cell lines show a decreased tendency to form colonies, are scattered, and resemble fibroblasts. These cells also show strong localization of CD44 almost exclusively in the nucleus with very little being present in the cell peripheries. The nuclear localization is stronger in the CA1 cell line with all the cells showing nuclear expression of CD44 (insets-c) while H357 cells seem to show peri-nuclear (pn) accumulation and some show nuclear localization of the protein (n). A few H357 cells however show moderate expression at the cell surface (f- top right inset).

Conditioned medium from tumour associated fibroblasts

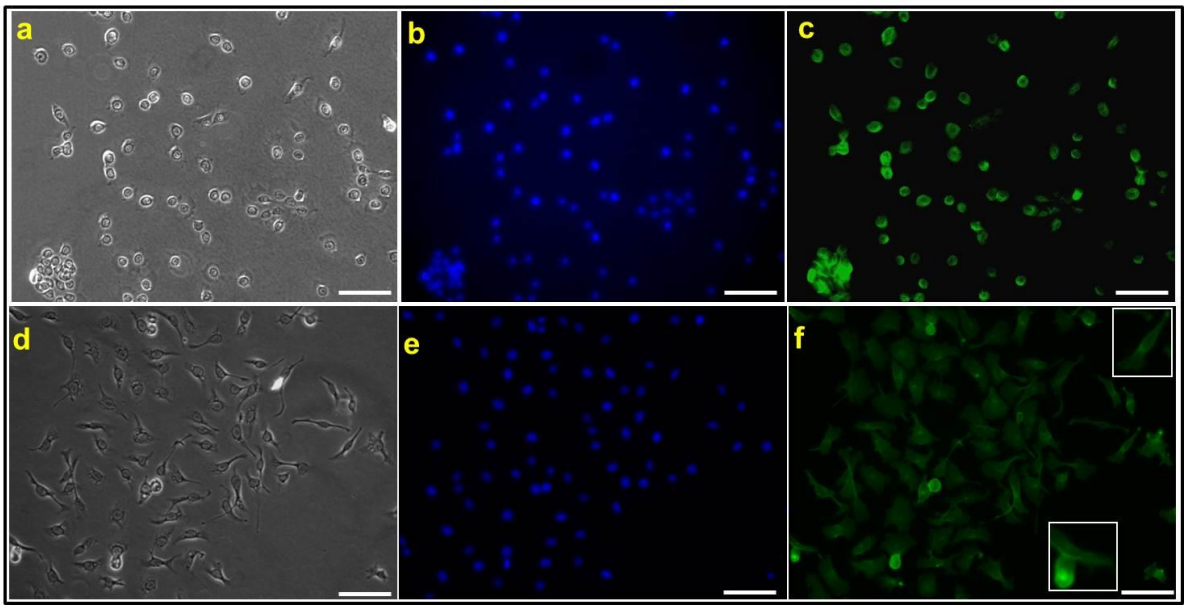

Figure 2.41: Expression of CD44 in OSCC cells after treatment with conditioned medium from tumour associated fibroblasts(Scale=50µm). Cultures of CA1 (a-c) and H357 (d-f) cells treated with medium conditioned by the growth of tumour associated fibroblasts and viewed in phase-contrast (a, d), stained with DAPI nuclear stain (b, e) and with anti-CD44-FITC antibody (c, f). Cells from each of the lines are scattered and display spindle-like morphology and dispersion on an individual level. CA1 cells show moderate to low expression at the cell surface whereas H357 cells generally show low expression at the cell surface with some cells showing peri-nuclear accumulation of CD44 (f- top right inset).

II) ESA

Control

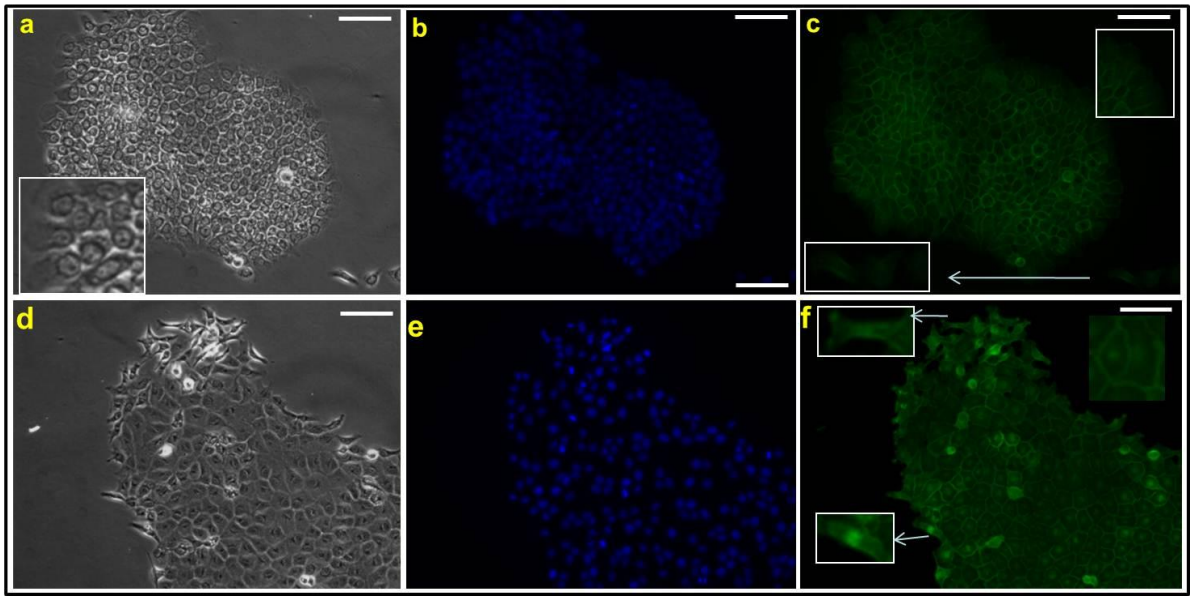

Figure 2.42: The expression of ESA in OSCC cells under control conditions(Scale=50µm). Cultures of CA1 (a-c) and H357 (d-f) cells cultured under control conditions and viewed in phase contrast (a, d), stained with DAPI nuclear stain (b, e) and with anti-ESA-FITC antibody (c, f). Cells from both cell lines form holoclones with spindle cells placed at the edge (d) or outside the colonies (a).Cells at the edges of the colonies show weaker expression of ESA than central cells that show strong expression at the cell surface. The spindle cells show weak expression at the surface with some cells showing nuclear localization of the protein (inset-f).

TGF-β treated cells:

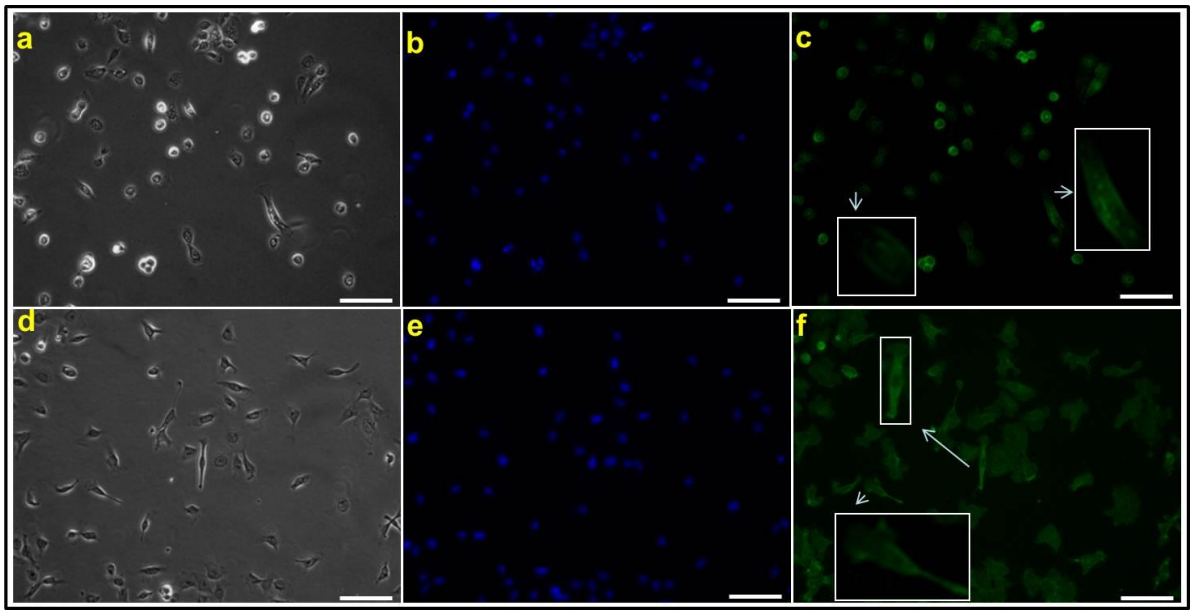

Figure 2.43: Expression of ESA in OSCC cells treated with TGF-β (Scale=50µm). Cultures of CA1 (a-c) and H357 (d-f) cells treated with TGF-β and shown in phase contrast (a, d), stained with DAPI nuclear stain (b, e) and with anti-ESA-FITC antibody (c, f). Treated cells from both cell lines appear elongated and show poor colony formation. Weak expression of ESA is seen in both cell lines and is present in the cytoplasm. Most of the treated cells also show no expression at the cell surface, the pattern seen typically in control cells. Overall the expression of ESA seen in treated cells seems lower than the controls.

Conditioned medium from tumour associated fibroblasts

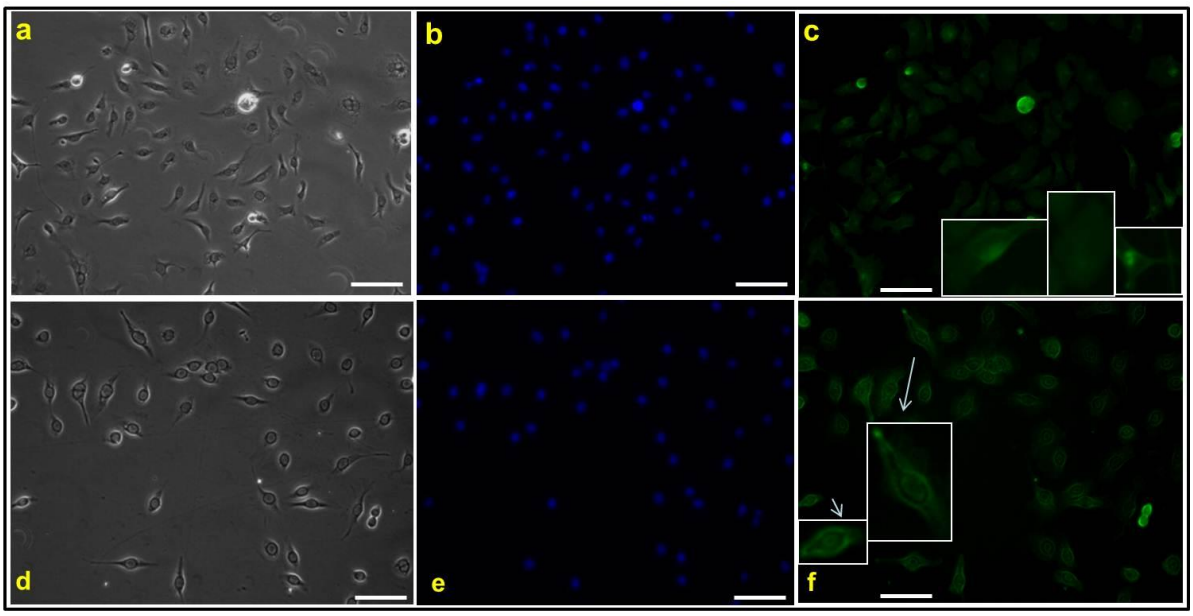

Figure 2.44: Expression of ESA in OSCC cells treated with conditioned medium from tumour associated fibroblasts (Scale=50µm). Cultures of CA1 (a-c) and H357 (d-f) cells treated with medium conditioned by the growth of tumour associated fibroblasts, viewed in phase contrast (a, c), stained with DAPI nuclear stain (b, e) and with anti-ESA-FITC antibody. Cultured cells show poor colony formation and an elongated spindle phenotype. Cells from both cells lines show very low expression of ESA at the cell surface and there are slight variations seen in patterns of expression in both cell lines. In CA1 cells, weak expression of ESA is seen in the nucleus of most cells, whereas H357 cells show peri-nuclear accumulation. Interestingly, cells that are about to divide show high surface expression of ESA.

III) β-Catenin

Control

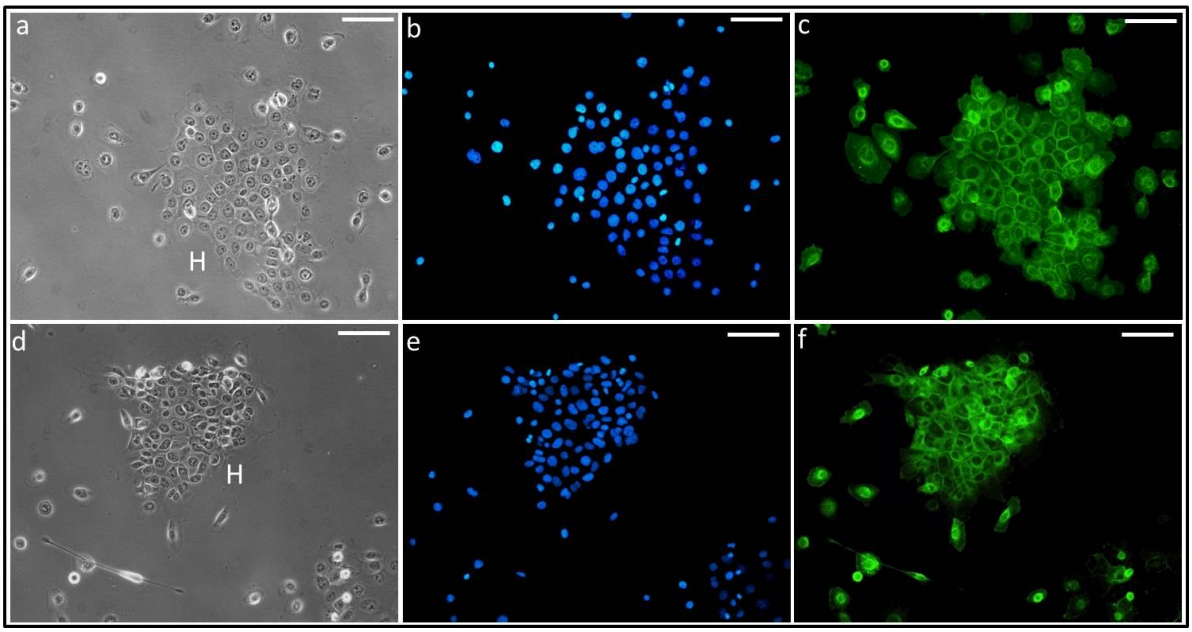

Figure 2.45: Expression of β-Catenin under control conditions in OSCC cells (Scale=50µm). Cultures of CA1 (a-c) and H357 (d-f) cells grown under control conditions. Both cell lines form holoclones (H), shown in phase contrast (a, d) with cells at the edge showing spindle-like morphologies and scattering. Cells stained with DAPI nuclear stain (b, e), and with anti-β-Catenin-FITC antibody (c, f) show strong surface expression of β-Catenin in central holoclone cells but none in the nucleus. Cells around the edge of the colony show strong nuclear localization of β-Catenin and reduced expression at the periphery.

TGF-β treated cells

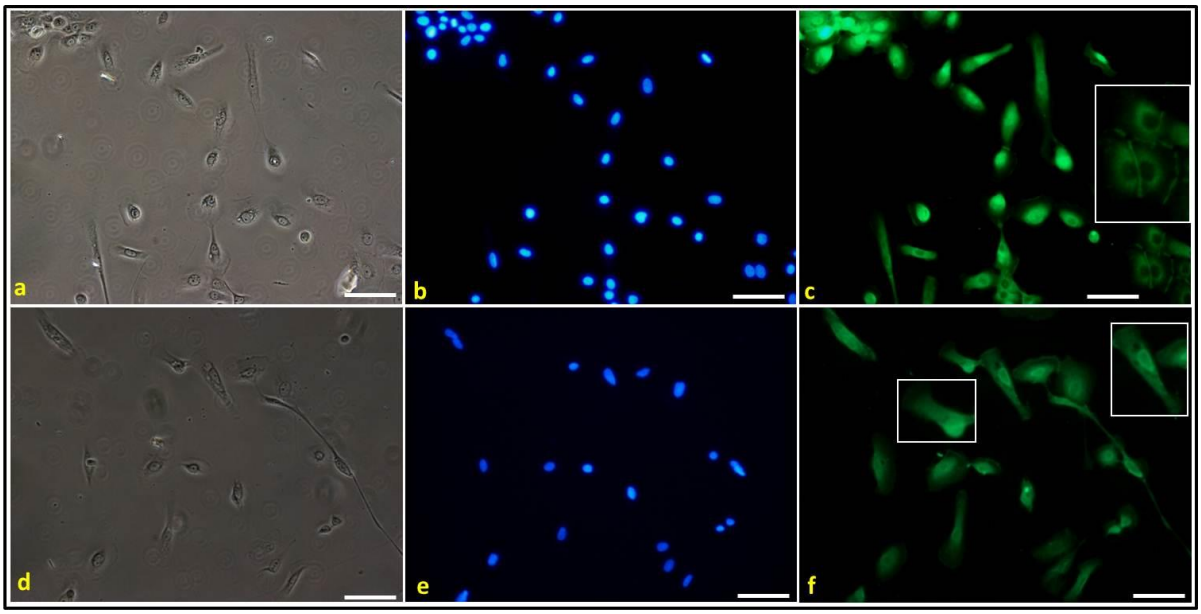

Figure 2.46: Expression of β-catenin in OSCC cells treated with TGF-β (Scale=50µm). Cultures of CA1 (a-c) and H357 (d-f) cells treated with TGF-β and shown in phase contrast (a, d), stained with DAPI nuclear stain (b, e), and with anti β-catenin FITC antibody. Cells from both cell lines acquire spindle-like morphology, showing a decreased tendency to form colonies (a, d) and show dispersal. The expression of β-catenin at the cell surface is reduced and almost all cells show strong nuclear localization of the protein. (c-inset). Some CA1 cells also show peri-nuclear accumulation with reduced surface expression.

Conditioned medium from tumour associated fibroblasts

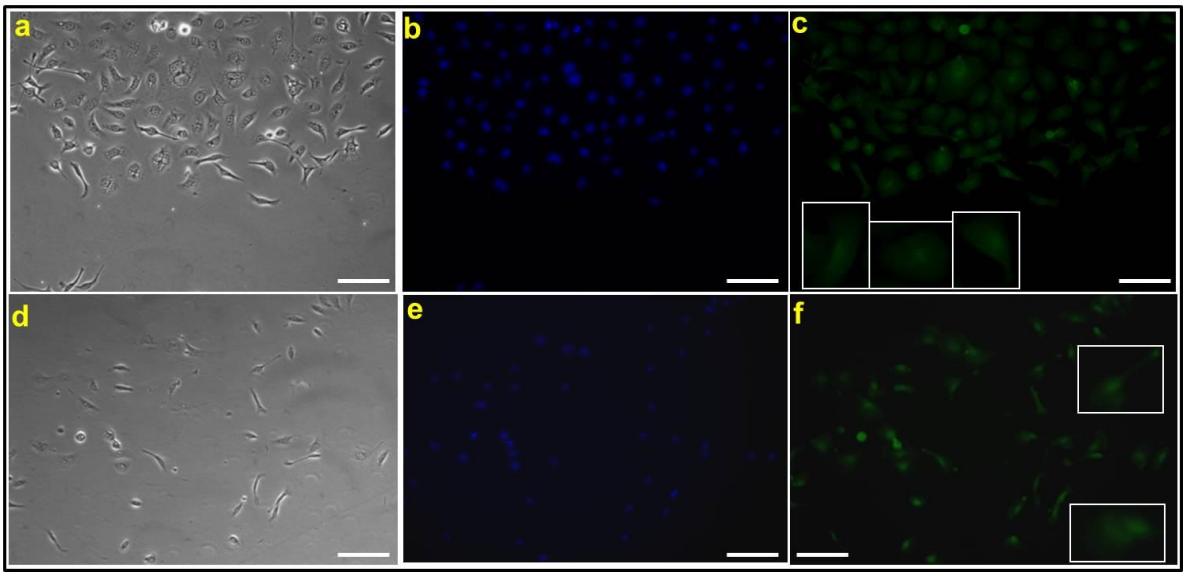

Figure 2.47: Expression of β-catenin in OSCC cells cultured with conditioned medium from tumour associated fibroblasts (Scale=50µm). Cultures of CA1 (a-c) and H357 (d-f) cells treated with medium conditioned by the growth of tumour associated fibroblasts shown in phase contrast (a, d), stained with DAPI nuclear stain (b, e) and anti-β-catenin-FITC antibody (c, f). Cultured cells show poor colony formation and acquire spindle morphology and appear scattered. Treated cells show no surface expression of β-catenin characteristic of control cells, but instead show weak-moderate expression in the cytoplasm and weak nuclear localization.

IV) E-Cadherin

Control cells

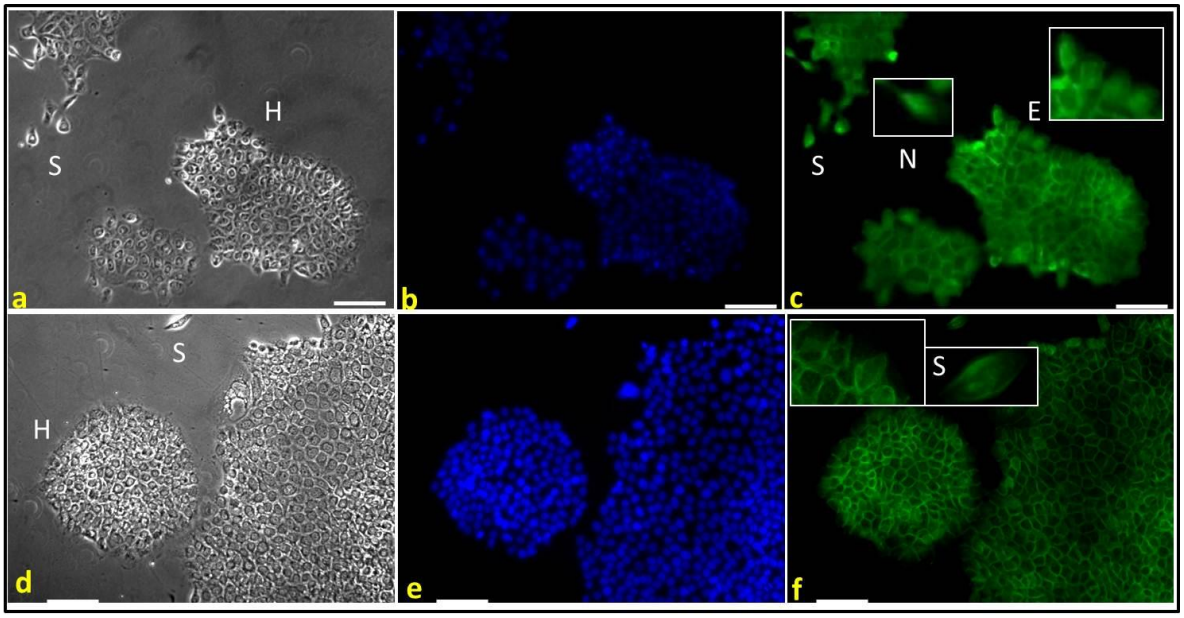

Figure 2.48: Expression of E-cadherin in OSCC cells cultured under control conditions (Scale=50µm). Cultures of Ca1 (a-c) and H357 (d-f) grown under control conditions and shown in phase contrast (a, d), stained with DAPI nuclear stain and with anti-E-cadherin-FITC antibody. Holoclones are shown with spindle cells (S) at the edge and outside the colony. Strong E-cadherin expression is seen at the cell surface of central holoclone cells than those at the edge (E). For CA1 cells, some cells at the edge (E) show nuclear accumulation of E-cadherin. Spindle cells lying outside the colony show weak expression at the cell surface and some CA1 cells show nuclear localization of the protein (N).

TGF-β treated cells

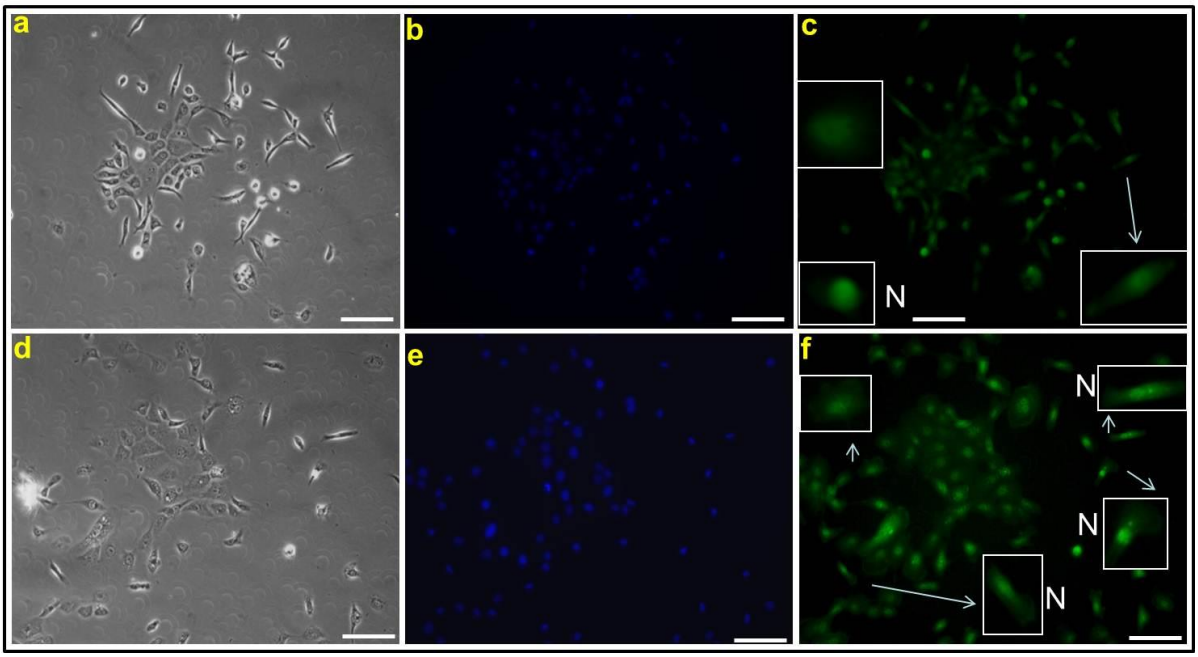

Figure 2.49: Expression of E-cadherin OSCC cells treated with TGF-β (Scale=50µm). Cultures of CA1 (a-c) and H357 (d-f) cells treated with TGF-β and shown in phase contrast (a, d), stained with DAPI nuclear stain (b, e) and with anti-E-cadherin FITC antibody (c, f). Treatment results in the formation of spindle cells and dispersal of cells. Strong nuclear localization (N) of E-cadherin is seen but none at the cell surface and this is more pronounced in H357 cells.

Conditioned medium from tumour associated fibroblasts

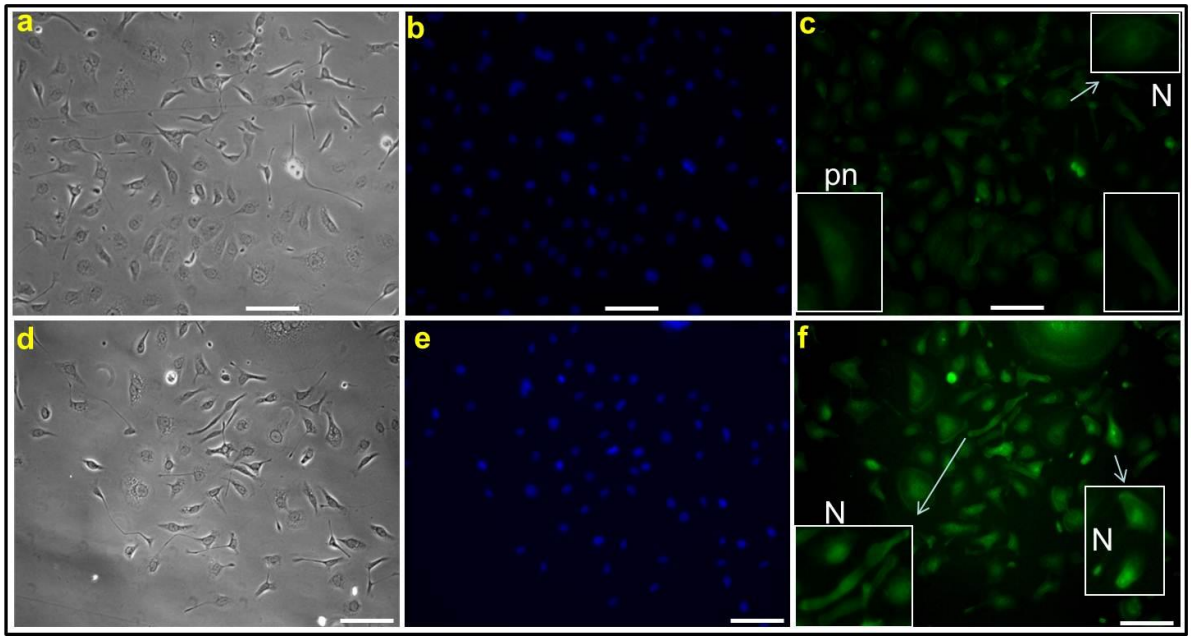

Figure 2.50: Expression of E-cadherin in OSCC cells cultured with conditioned medium from tumour associated fibroblasts (Scale=50µm). Cultures of CA1 (a-c) and H357 (d-f) cells treated with medium conditioned by the growth of cancer associated fibroblasts shown in phase contrast (a, d), stained with DAPI nuclear stain (b, e) and with anti-E-cadherin-FITC antibody (c, f). Treated cells acquire spindle morphology and show weak surface expression of E-cadherin. Nuclear localization (N) of E-cadherin is seen in the spindle cells and some of these show peri-nuclear (pn) accumulation.

3) FACS Analysis

FACS analysis of the CA1 and H357 cell lines was undertaken to assay for changes within subpopulations of cells in these cell lines. To determine the effect of treatment, the cell lines were stained with CD44 and ESA antibodies and three sub-populations were compared and analyzed, the $CD44^{high}ESA^{low}$ (a), the $CD44^{high}$(b) and the $ESA^{low/-}$ (c) populations. Staining of OSCC cells with CD44 and ESA antibodies and subsequent analysis through two dimensional facsplots consistently identified a population of cells that is $CD44^{high}ESA^{low}$ and stands to the left of the main population (Figure 2.50d). The co-expression pattern of high CD44 expression, a stem cell marker, with low expression of the epithelial marker ESA, suggested a possible relationship between EMT and cancer stem cells (Biddle and Mackenzie, 2012). When isolated and cultured, $CD44^{high}ESA^{low}$ cells form predominantly fibroblast-like cells whereas the $CD44^{high}ESA^{high}$ cells that form holoclones and represent the clonogenic population. $CD44^{high}ESA^{low}$ cells also formed more spheres than $CD44^{high}ESA^{high}$ cells, a further indication that they enrich for sphere forming EMT cells. qPCR analysis of $CD44^{high}ESA^{low}$ cells showed low message expression of E-cadherin and high expression of Vimentin and Twist, markers of EMT and both $CD44^{high}ESA^{high}$ and $CD44^{high}ESA^{low}$ cells can be passaged indefinitely, that is indicative of self-renewal ability (Biddle et al, 2011). The $CD44^{high}$ population was studied in this experiment to assess the effect of TGF-β on the stem cell population within OSCC lines. The size of the $ESA^{low/-}$ population was assayed as it was thought that a loss of epithelial markers would further strengthen the conclusion that cells were undergoing EMT.

Positioning of gates:

To set the gates for FACS analysis of different subpopulation within OSCC cell lines, cells without any added antibody were used to assess autofluorescence (Figure 2.50 a-c) Stained cells showed fluorescence several units higher on a log scale compared to a control sample that had no added antibody (d-f).

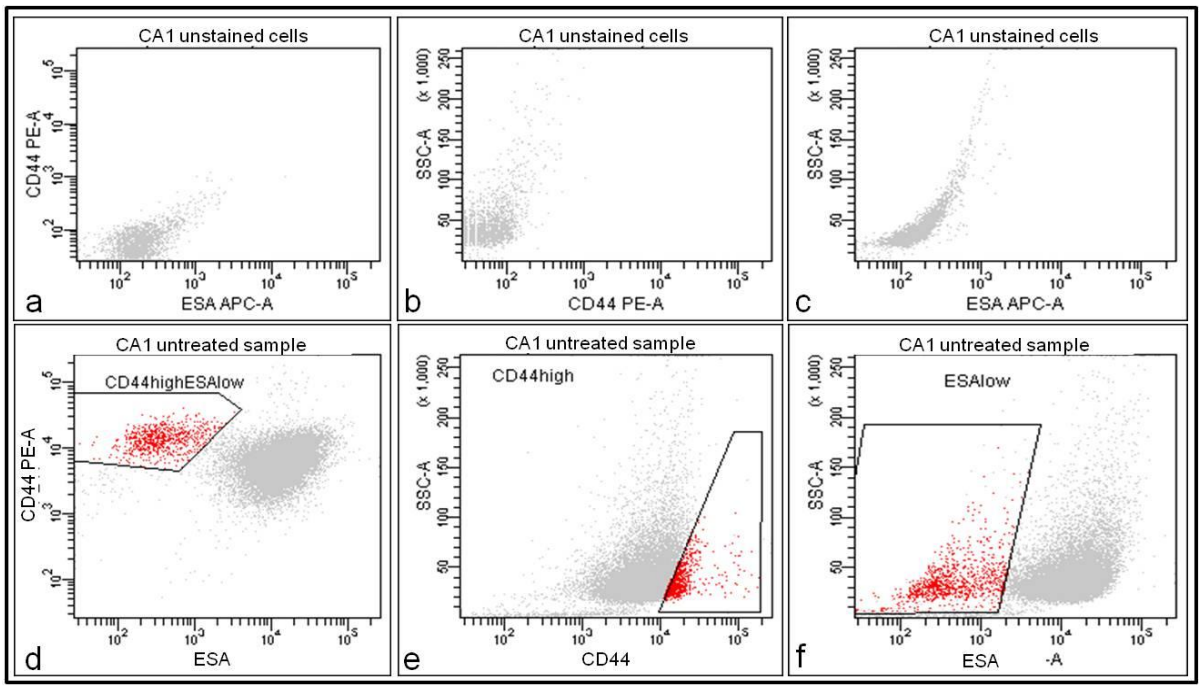

Figure 2.51: Characteristic FACS plots for CA1 cells. Analysis of CA1 cells for expression of CD44 and ESA and the positioning of the gates for the experiment. Panels (a-c) show the cells without any added antibody and corresponding cell populations with the antibodies added are shown above (d-f). Panel (d) shows the co-expression pattern of cells analyzed for CD44 and ESA and identifies a $CD44^{high}ESA^{low}$ population (red). The gates were drawn arbitrarily to include as much of this population without including cells from the main bulk of the total population. For each sample, the gates were kept in the same position when comparing control samples with treated ones. Panel (e) shows the expression pattern for CD44 that often shows an identifiably separate cluster of more highly expressing cells at the far right that assists in the positioning of the gate, but for some populations of stained cells clearly separated populations were not apparent and gates defining high expressing subpopulations were selected more arbitrarily according to the overall pattern of positive and negative staining. For both cell lines the 5% of cells expressing the highest levels of CD44 were selected and gated as $CD44^{high}$. Panel (f) shows the expression pattern for ESA and 5% of cells expressing the lowest levels were gated as $ESA^{low/-}$ (red).

I) CA1:

a) $CD44^{high}ESA^{low}$ cells

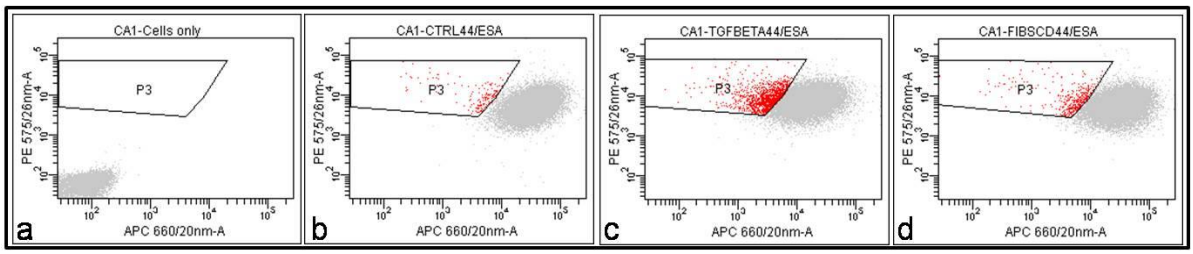

Figure 2.52: FACS analysis of CA1 cells stained with CD44 (y-axis) and ESA (x-axis) antibodies.FACS analysis of the $CD44^{high}ESA^{low}$ population (red) within the CA1 cell line Doublets were excluded using forward and side scatter and dead cells were excluded using DAPI as discussed (2.2.2.1). Panel (a) shows the cells without any added antibody. Panel (b) shows the $CD44^{high}ESA^{low}$ population in untreated control cells (gated). Panel (c) and Panel (d) show the changes of this population when cells were treated with TGF-β and conditioned fibroblast medium.

$CD44^{high}ESA^{low}$	1	2	3	Average	SEM
Control	0.93	1.50	2.62	**1.68**	0.86
TGF-Beta	6.33	7.23	7.57	**7.04**	0.64
Fibs CM	1.87	1.95	3.63	**2.48**	1.00

Table 2.18: Changes in the size of the $CD44^{high}ESA^{low}$ population within the CA1 cell line.

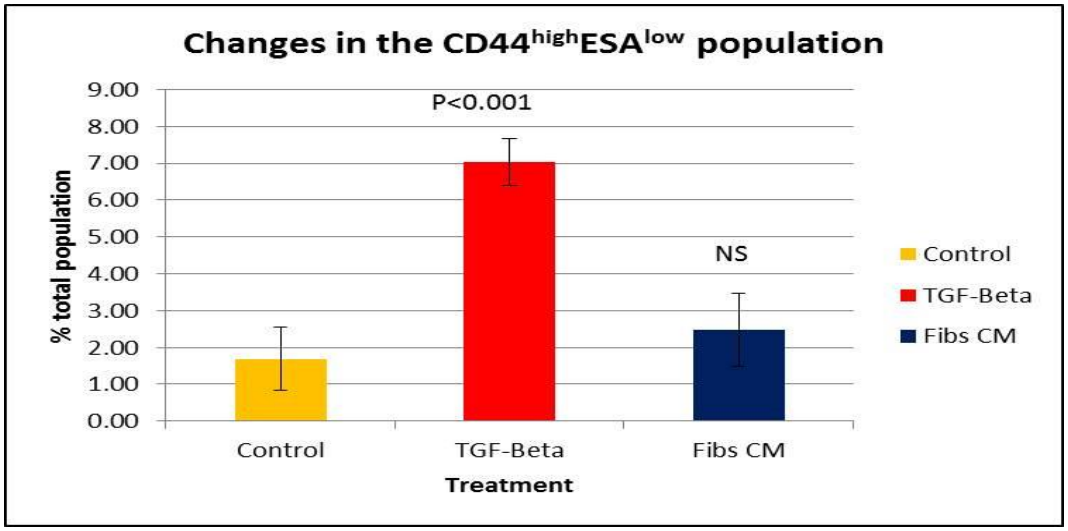

Figure 2.53: The percentage of $CD44^{high}ESA^{low}$ cells in controls and the response to treatment. Changes in the $CD44^{high}ESA^{low}$ population when controls were compared to

cellstreated with TGF- β and those treated with conditioned medium from fibroblasts. The size of

the gated $CD44^{high}ESA^{low}$ population is low in control cells (1.68±0.86%) and increases significantly when they are treated with TGF-β (7.04±0.64%). Treatment with FIBSCM also resulted in an increase in the number of these cells (2.48±1.00) but this was low compared to the increase seen for TGF-β.

b) $CD44^{high}$cells

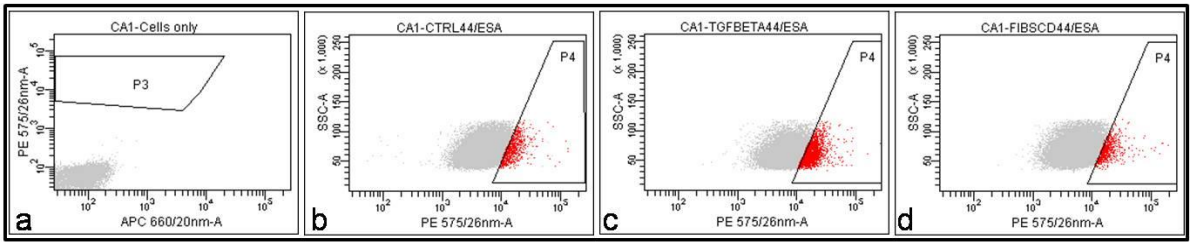

Figure 2.54: FACS analysis of cells stained with CD44 antibody.FACS analysis of the CA1 cells for expression of CD44. Cells were analyzed first without antibody to assess autofluorescence (a) and stained with anti-CD44-PE antibody (b-d). 5-6% of the cells expressing the highest levels of CD44 were selected as $CD44^{high}$ and gated (red) in the controls (b). This was then compared to the percentage of $CD44^{high}$ cells seen after treatment with TGF-β (c) or with FIBSCM (d). The percentage of CD44 ^{high} cells increased with both TGF-β and conditioned medium.

$CD44^{high}$	1	2	3	Average	SEM
Control	5.23	5.17	5.10	5.17	0.07
TGF-Beta	11.37	10.63	8.67	10.22	1.40
Fibs CM	7.89	6.97	7.50	7.45	0.46

Table 2.19: Changes in the $CD44^{high}$ population within the CA1 cell line.

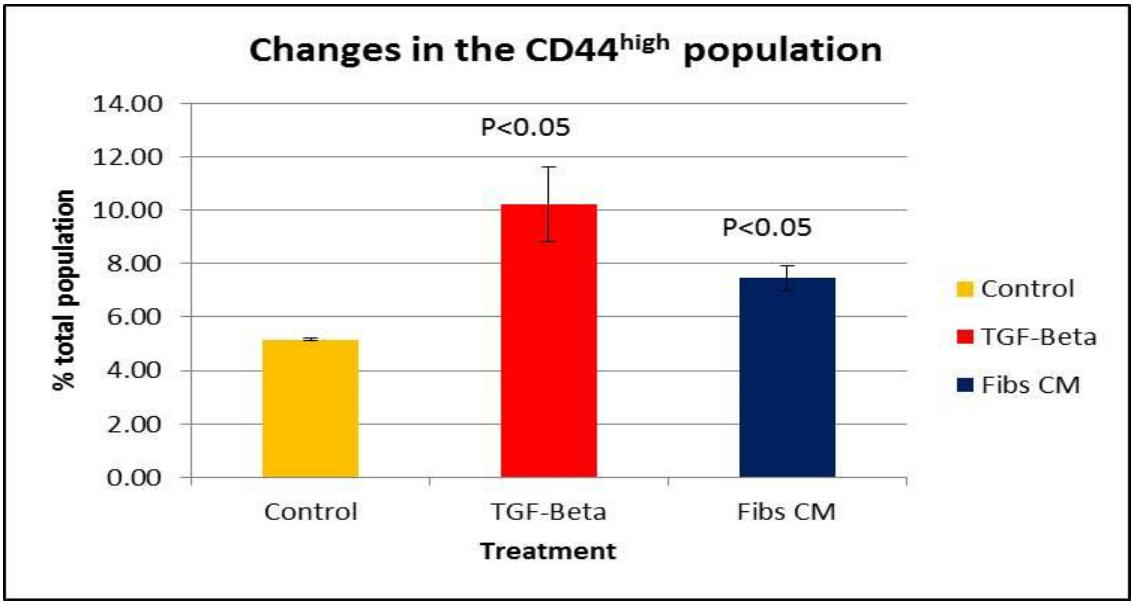

Figure 2.55: Changes in the CD44^{high} population with treatment. The change in the percentage of cells that express high levels of CD44. In control samples 5% of cells expressed were selected as CD44^{high}. When cells were treated with TGF-β this population increased highly significantly to 10.22±1.40%. Treatment with FIBSCM also resulted in a significant increase in CD44^{high} cells (7.45±0.46%).

c) ESA$^{low/-}$ cells

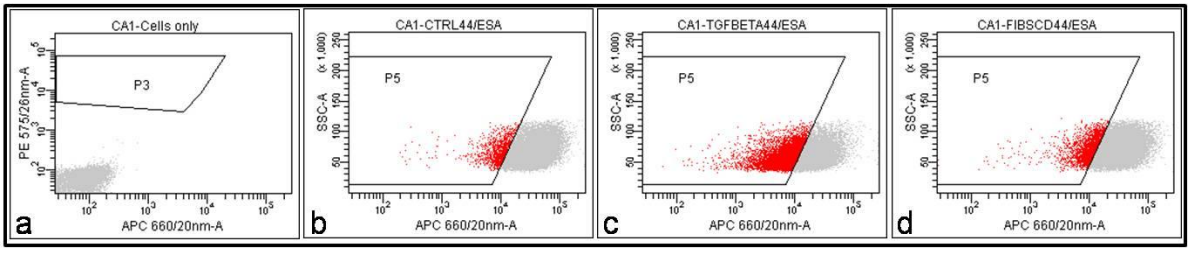

Figure 2.56: FACS analysis of cells stained with ESA (APC) antibody.FACS analysis of the CA1 cells for expression of ESA. Cells were analyzed first without antibody to assess autofluorescence. Cells were stained for anti-ESA antibody and 5-6% of the cells expressing the lowest levels of ESA were selected as ESA$^{low/-}$ and gated (red) in the controls (b). This was then compared to the percentage of ESA$^{low/-}$ cells seen with treatment with TGF-β (c) or with FIBSCM (d). The number of ESA$^{low/-}$ cells was seen to increase with both TGF-β and FIBSCM.

ESA^{low}	1	2	3	Average	SEM
Control	5.43	5.10	5.23	**5.26**	0.17
TGF-Beta	33.11	29.43	29.23	**30.59**	2.18
Fibs CM	8.52	10.03	8.52	**9.03**	0.87

Table 2.20: Changes in the ESA$^{low/-}$ population within the CA1 cell line.

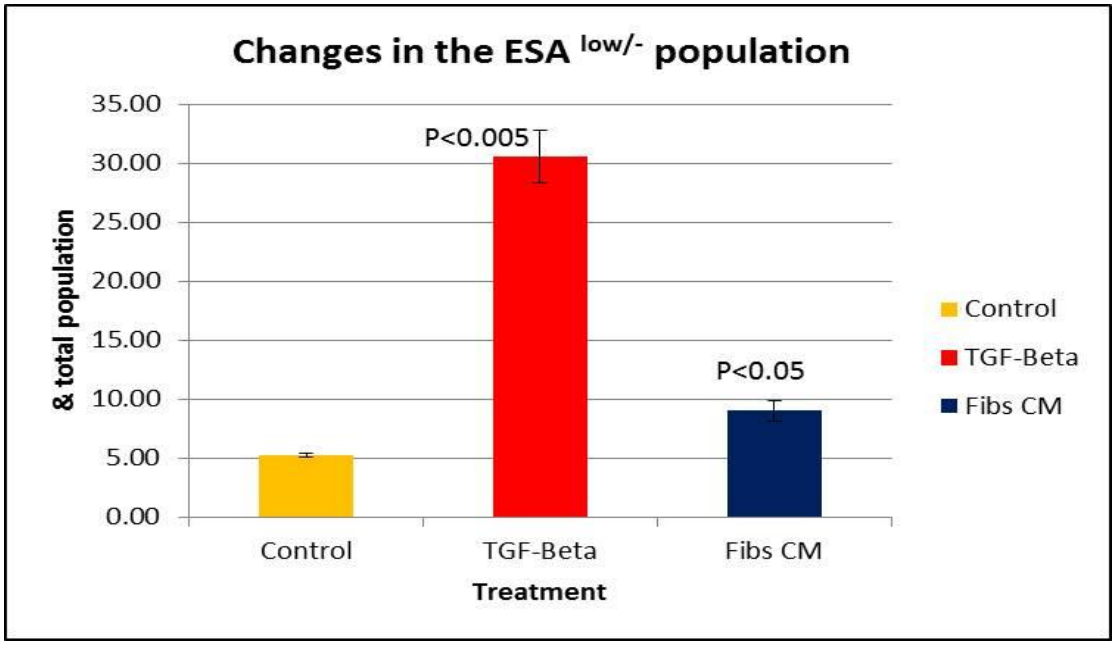

Figure 2.57: Changes in the ESA$^{low/-}$ population with treatment. The effect of treatment on ESA$^{low/-}$ cells. In control samples 5.43±0.15% of the cells expressed either low levels of ESA or no ESA at all (gated as ESA$^{low/-}$). This population increased to 33.11±3.02% with treatment with TGF-β which was highly significant ($p<0.005$). Conditioned medium from malignant fibroblasts also caused this population to significantly increase to 8.52±0.85%.

II) H357:

a) $CD44^{high}$ ESA^{low} cells

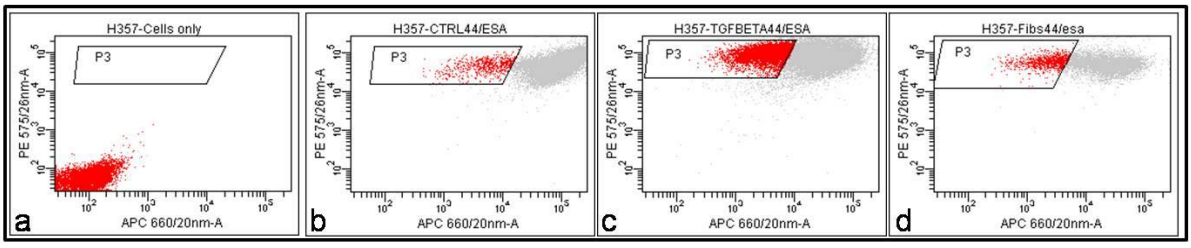

Figure 2.58: FACS analysis of H357 cells stained with CD44 (y-axis) and ESA (x-axis) antibodies.FACS analysis of the $CD44^{high}ESA^{low}$ population (red) within the H357 cell line and changes in the size of this population after treatment with TGF-β and FIBSCM. Panel (a) shows the cells without any added antibody. Panel (b) shows the $CD44^{high}ESA^{low}$ population in control cells (gated). Panel (c) and Panel (d) show the changes in the size of this population when cells were treated with TGF-β and conditioned fibroblast medium.

$CD44^{high}ESA^{low}$	1	2	3	Average	SEM
Control	3.67	4.00	4.07	**3.91**	0.21
TGF-Beta	32.57	30.81	26.90	**30.09**	2.90
Fibs CM	15.93	14.10	13.27	**14.43**	1.36

Table 2.21: Changes in the $CD44^{high}ESA^{low}$ population within the H357 cell line.

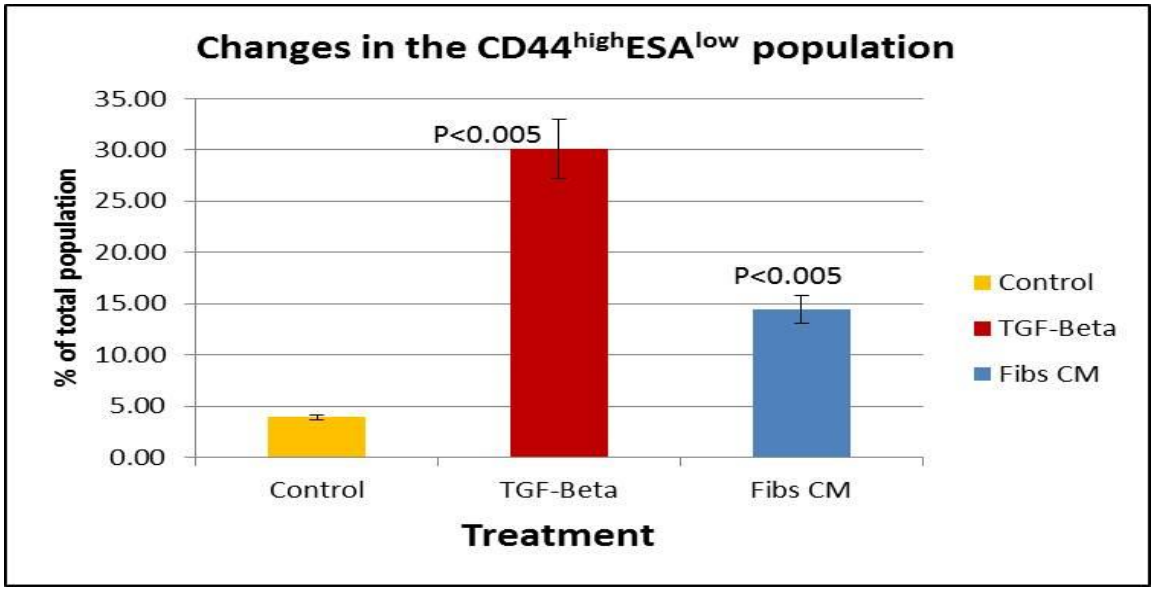

Figure 2.59: The percentage of CD44^{high}ESA^{low} cells in controls and the response to treatment. The changes in the size of the CD44^{high}ESA^{low} population when controls were compared to TGF-β treated cells and those treated with FIBSCM. The percentage of cells gated as the CD44^{high}ESA^{low} population is 3.91±0.21% for control cells. This increases significantly after treatment with TGF-β (30.09±2.9%). Treatment with FIBSCM also resulted in an increase in these cells (14.43±1.36) but was less than that seen for TGF-β. The response of this cell line to treatment was greater compared to the CA1 cell line.

b) CD44^{high}cells

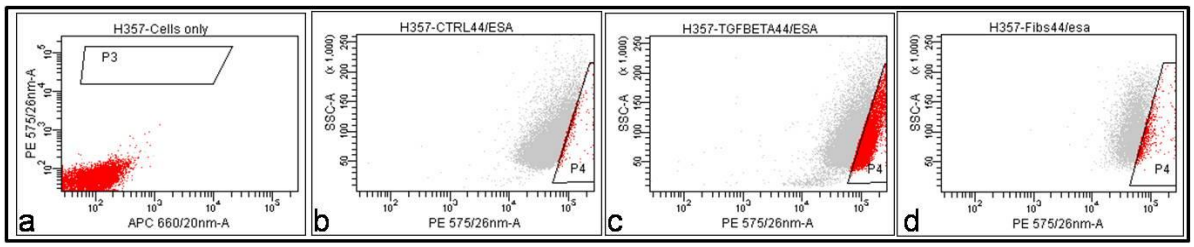

Figure 2.60: FACS analysis of H357 cells stained with CD44 antibody.FACS analysis of H357 cells for expression of CD44. Cells were analyzed first without antibody to assess autofluorescence (a), stained with anti-CD44-PE antibody (b-d). 5-6% of the cells expressing the highest levels of CD44 were selected as CD44^{high} and gated (red) in the controls (b). This was then compared to the percentage of CD44^{high} cells seen after treatment with TGF-β (c) or with FIBSCM (d). The percentage of CD44^{high} cells was seen to increase with both TGF-β and FIBSCM but this was more significant in the TGF-β treated cells.

CD44^{high}	1	2	3	Average	SEM
Control	5.47	5.13	5.23	**5.28**	0.17
TGF-Beta	32.90	24.73	28.23	**28.62**	4.10
Fibs CM	12.70	10.03	11.33	**11.36**	1.33

Table 2.22: Changes in the CD44^{high} population within the H357 cell line.

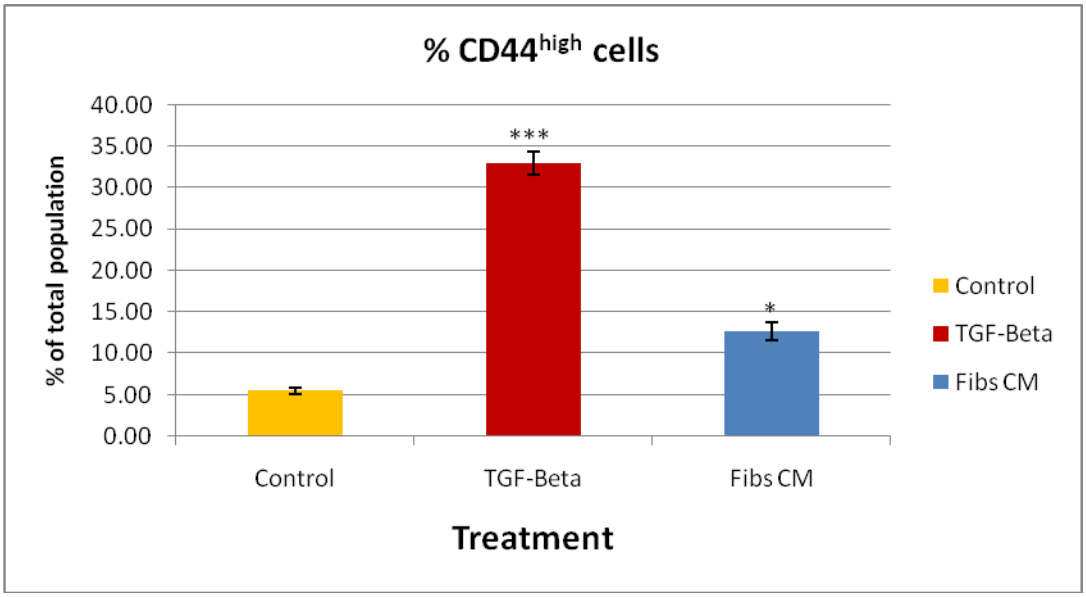

Figure 2.61: Changes in the CD44high population with treatment. The change in the percentage of cells expressing the highest levels of CD44. In control samples 5.28±0.17% of cells were gated as CD44^{high}. Treatment with TGF-β results in a (28.62±4.1) increase in the size of this population which was significant. Treatment with conditioned medium from fibroblasts also resulted in an increase in CD44^{high} cells (11.36±1.33%) but this was less than half the increase seen for TGF-β. The response of H357 cells was greater than CA1 cells.

c) ESA$^{low/-}$ cells

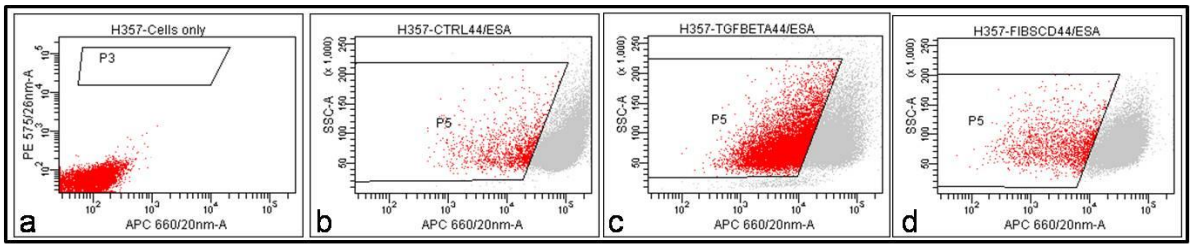

Figure 2.62: FACS analysis of cells stained with ESA (APC) antibody.FACS analysis of H357 cells for expression of ESA. Cells were analyzed first without antibody to assess autofluorescence (a). Cells were stained with anti-ESA (APC) antibody (b-d) and 5-6% of the cells expressing the lowest levels of ESA were selected as ESA$^{low/-}$ and gated (red) in the controls (b). This was compared to the percentage of ESA$^{low/-}$ cells seen after treatment with TGF-β (c) or FIBSCM (d). The percentage of ESA$^{low/-}$ cells increased with both TGF-β and FIBSCM but this was more significant in the TGF- β treated cells.

ESA$^{low/-}$	1	2	3	Average	SEM
Control	5.43	5.37	5.12	**5.31**	0.17
TGF-Beta	38.90	34.07	33.23	**35.40**	3.06
Fibs CM	15.50	11.17	11.67	**12.78**	2.37

Table 2.23: Changes in the ESA$^{low/-}$ population within the H357 cell line

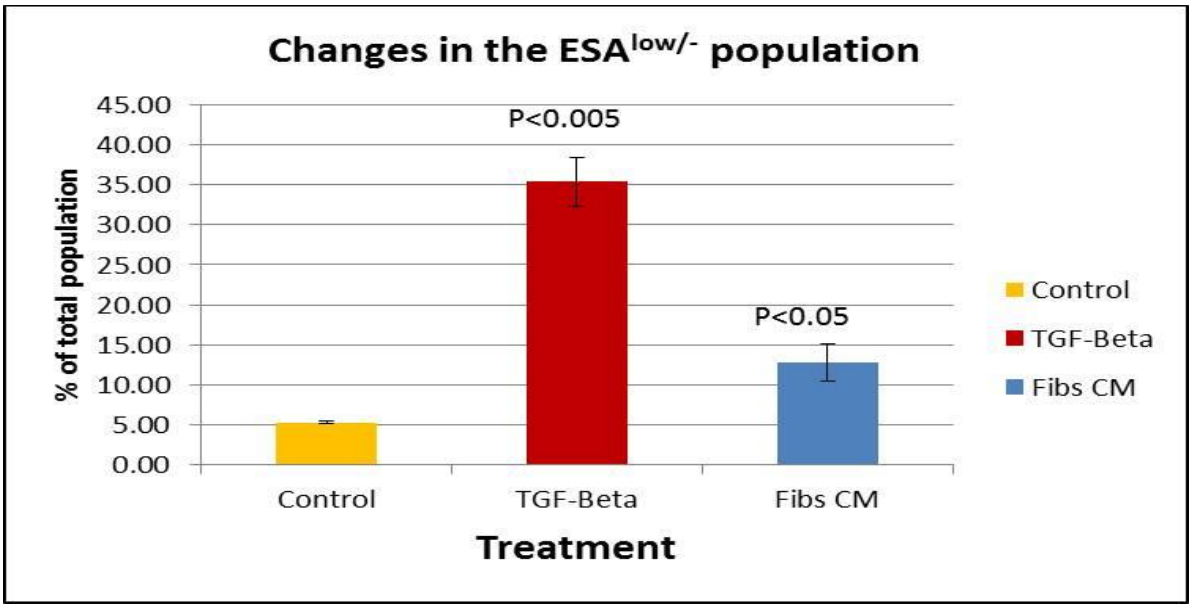

Figure 2.63: Changes in the ESAlow/- population with treatment. The effect of treatment on ESA$^{low/-}$ cells. In control samples 5.31±0.17% of the cells were gated as ESA$^{low/-}$. This population increased to 35.40±3.06% after treatment with TGF-β which was highly significant ($p<0.005$) and to 12.78±2.37% with FIBSCM. The response recorded overall for this cell line was also greater compared to that of CA1 cells.

4) Sphere Assays

This section shows the results when CA1 and H357 cells were cultured in non-adherent conditions as spheres. The design for the experimental setup has already been discussed (2.3.2). Sphere forming ability has been linked to both stemness and EMT (Biddle et al, 2011, Mani et al, 2008) and these experiments were designed to determine whether treatment with either TGF-β or conditioned medium from cancer associated fibroblasts (FIBSCM) affected sphere formation. The number of spheres formed by control cells were counted and compared to the number formed by cells that were treated with TGF-β and FIBSCM. After counts had been performed, the spheres were reintroduced into adherent conditions, left overnight, detached, and reintroduced into secondary sphere assays and monitored for sphere growth to assess for differences in sphere numbers.

a) CA1 cell line:

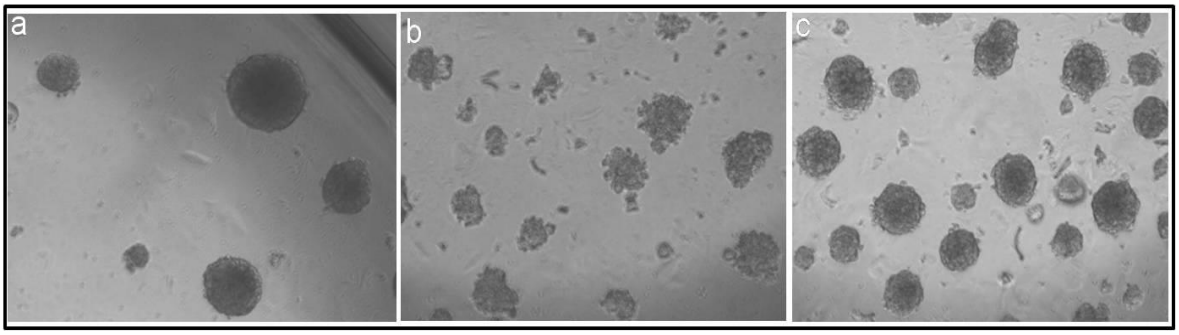

Figure 2.64: Sphere forming ability of Ca1 cells and the effect of treatment with TGF-β and FIBSCM. The formation of spheres by control CA1 cells (a), cells treated with TGF-β (b) and FIBSCM (c). Control cells form round compact spheres with clean edges that reach a larger size than those with either treatment. Treated cells form a larger number of spheres although they look to be less compact. Cells treated with conditioned medium from malignant fibroblasts form the most number of spheres.

CA1	I	II	III	IV	V	Average	SD	%
Controls	92.0	84.0	78.0	86.0	80.0	**84.0**	5.5	8.4
TGF-β	146.0	152.0	137.0	165.0	142.0	**148.4**	10.8	14.8
FibsCM	150.0	165.0	169.0	139.0	158.0	**156.2**	12.1	15.6

Table 2.24: The average number of spheres formed by CA1 cells with and without treatment.

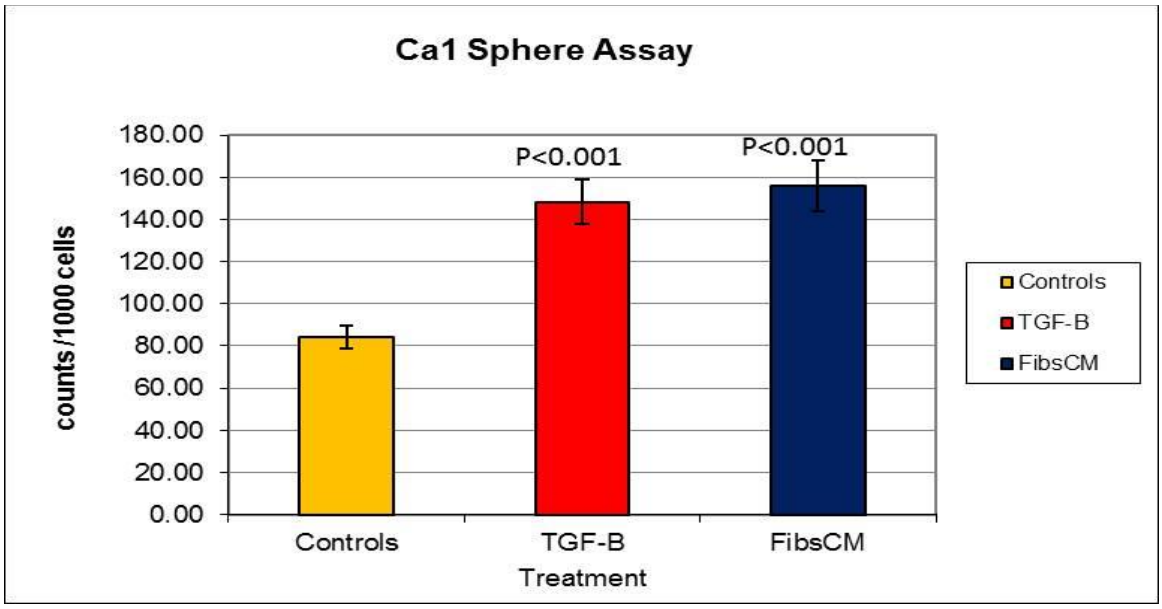

Figure 2.65 (i): The effect of treatment on sphere formation in CA1 cells. The number of spheres formed from CA1 cells per 1000 cells seeded and the effect of treatment with TGF-β or FIBSCM. Control cells formed on average 84 ±5.48 (8.4%) spheres per 1000 cells seeded. Cells treated with TGF-β formed 148.4±10.78 (14.8%) spheres while those treated with FIBSCM formed 156±12.03 (15.6%) spheres. Both treatments significantly increased sphere forming ability

CA1	I	II	III	IV	V	Average	SD	%
Controls	110.00	115.00	124.00	95.00	121.00	**113.00**	11.42	11.3
TGF-B	164.00	155.00	149.00	162.00	142.00	**154.40**	9.13	15.44
FibsCM	161.00	186.00	179.00	183.00	188.00	**179.40**	10.83	17.94

Table 2.25: The average number of spheres formed by CA1sphere-cells following introduction into adherent conditions.

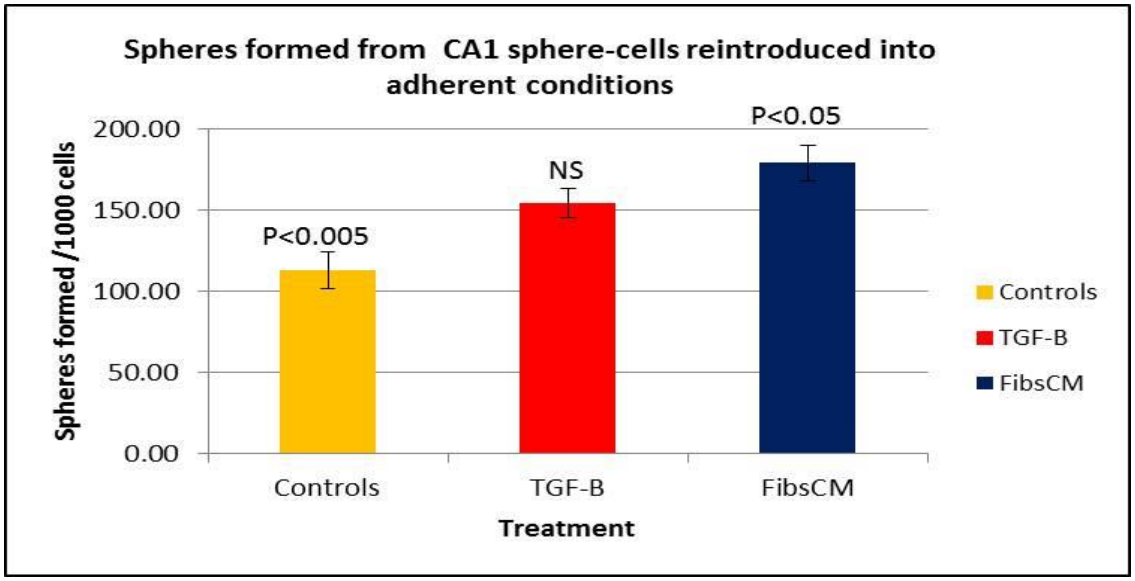

Figure 2.65 (ii): The effect of reintroduction into adherent conditions. The number of spheres formed by CA1 sphere cells reintroduced into adherent conditions for 24 hours and then seeded at 1000 cells per well. Control sphere-cells formed significantly more spheres on average than they had in the primary suspension cultures (113±11.42, 84±5.5). Sphere-cells treated with TGF-β (154.4±9.13) and conditioned fibroblast medium (179.4±10.83) formed more spheres than they did in primary cultures (148.4±10.8, 156.2±12.1) but the FIBSCM treated cells formed significantly higher numbers.

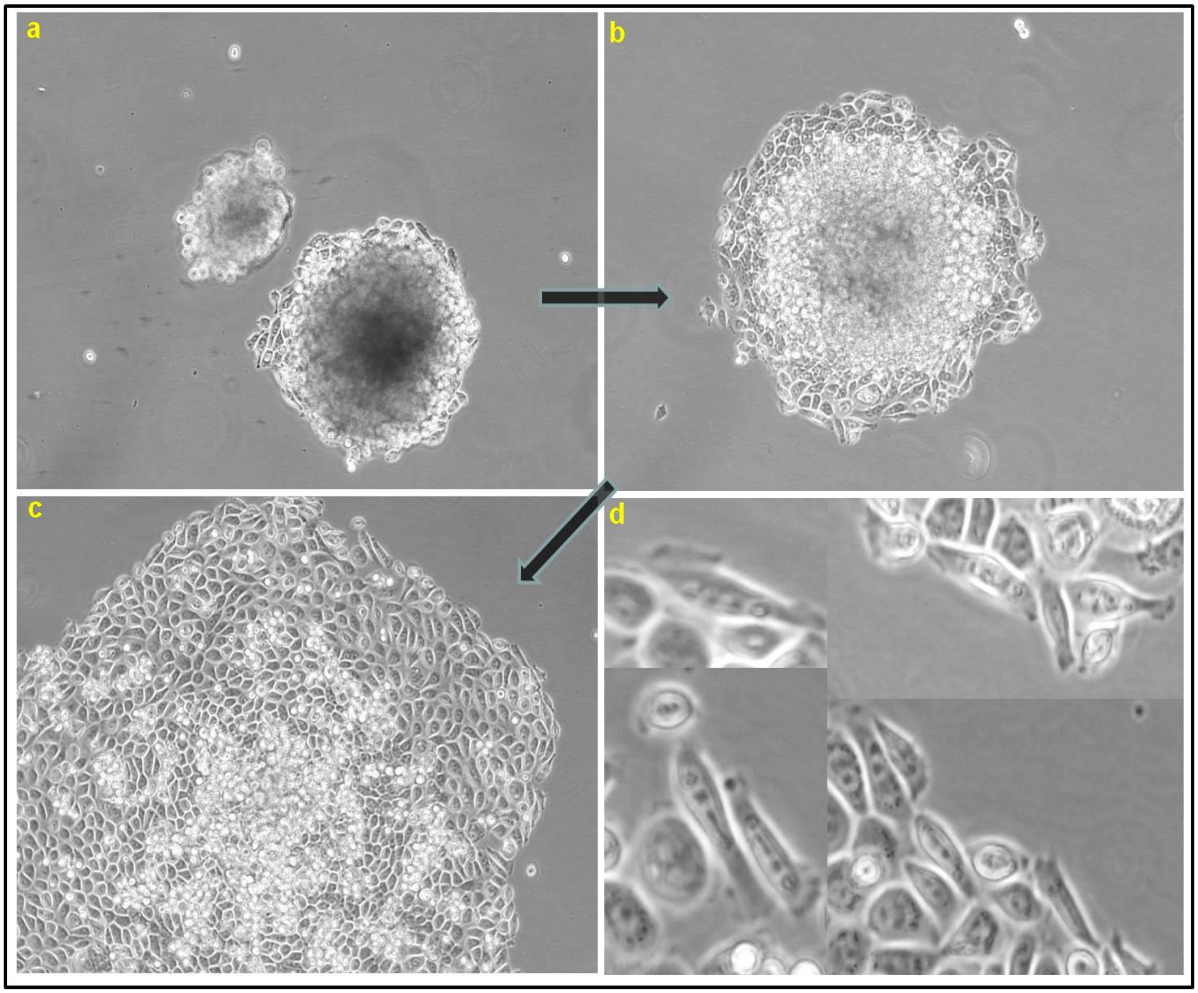

Figure 2.66: Re-introduction of CA1 spheres into adherent conditions. The morphology generated by CA1 spheres when reintroduced into adherent conditions. After about 4-6 hours cells have the appearance seen in (a). Left overnight, the cells start to spread out from the initial point of attachment (b). Within 48 hours the whole sphere flattens down to form an epithelial-like colony with elongated spindle shaped cells around the edges (c). Panel (d) shows magnified insets of cells at the edges of the colonies, forming both cobblestone shaped epithelial cells and elongated spindle-shaped cells at the edges.

B) H357 cell line:

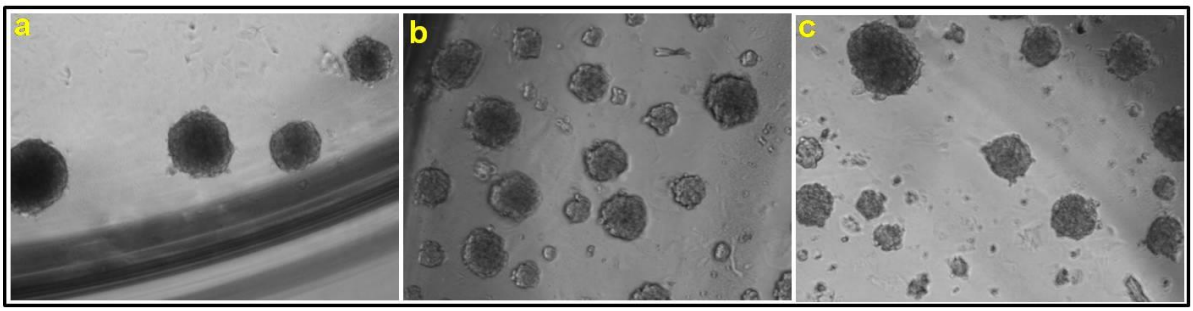

Figure 2.67: Sphere forming ability of H357 cells and the effect of treatment with TGF-β and FIBSCM. The formation of spheres by control H357 cells (a), cells treated with TGF-β (b) and conditioned medium from fibroblasts (c), shown in phase contrast. Control cells form round compact spheres with clean edges. TGF-β treated cells form a larger number of spheres but seem less compact. Cells treated with conditioned medium from tumour associated fibroblasts form the highest number of spheres which are of varying sizes.

H357	I	II	III	IV	V	Average	SD	%
Controls	146.00	132.00	119.00	126.00	88.00	**122.20**	21.55	12.22
TGF-β	271.00	325.00	267.00	195.00	195.00	**250.60**	55.68	25.06
FibsCM	336.00	321.00	360.00	420.00	348.00	**357.00**	38.07	35.7

Table 2.26: The average number of spheres formed by H357 cells with and without treatment.

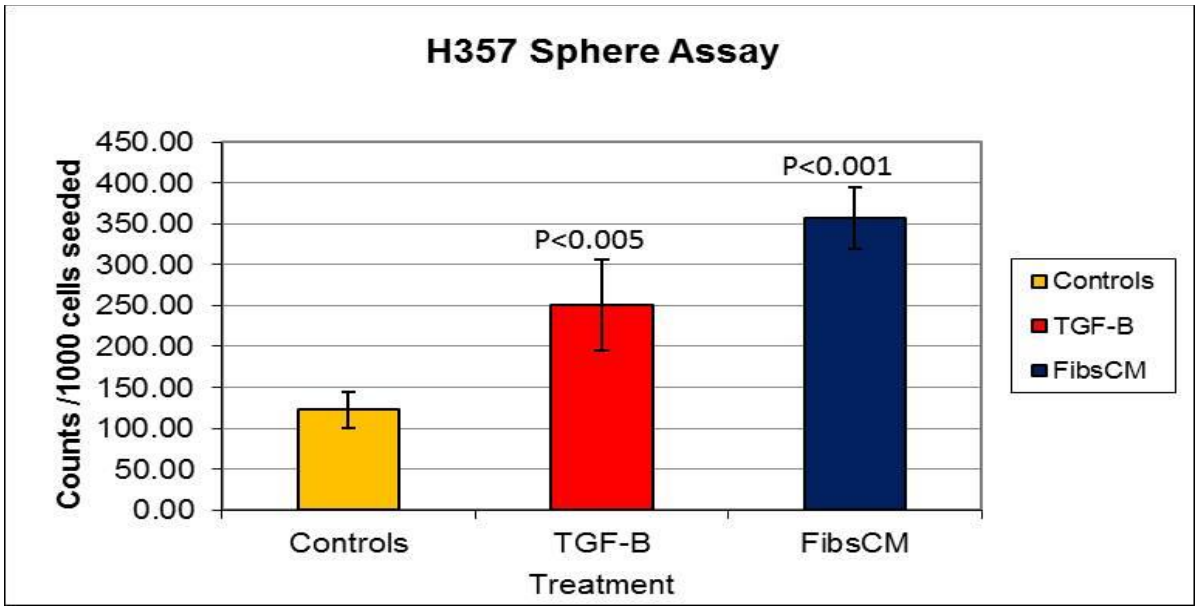

Figure 2.68 (i): The effect of treatment on sphere formation in H357 cells. The number of spheres formed by H357 cells per 1000 cells seeded and the effect of treatment with TGF-β or conditioned medium from tumour associated fibroblasts. Control cells formed on average 122 ±21.55 (12.2%) spheres per 1000 cells seeded. Cells treated with TGF-β formed 250±55.68 (25%) spheres while those treated with conditioned medium formed 357±38.07 (35.7%) spheres. Both treatments were seen to significantly increase sphere forming ability. Overall the H357 cell line formed a larger number of spheres under any of the conditions tested compared to the CA1 cell line.

H357	I	II	III	IV	V	Average	Stdev	%
Controls	286.00	345.00	291.00	332.00	248.00	**300.40**	38.82	30.04
TGF-B	325.00	401.00	420.00	365.00	380.00	**378.20**	36.31	37.82
FibsCM	300.00	331.00	340.00	260.00	355.00	**317.20**	37.77	31.72

Table 2.27: The average number of spheres formed by H357sphere-cells following introduction into adherent conditions.

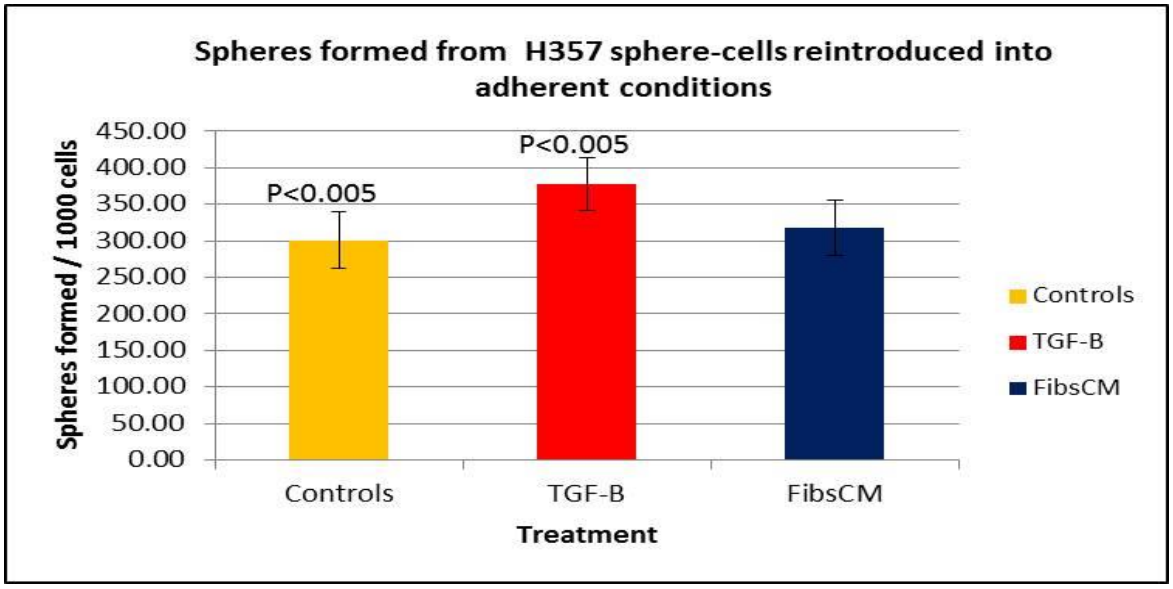

Figure 2.68 (ii): The effect of reintroduction into adherent conditions. The number of spheres formed by H357 sphere cells reintroduced into adherent conditions for 24 hours and then detached and seeded at 1000 cells per well. Control sphere-cells, and those treated with TGF-β formed significantly more spheres in secondary cultures (300.4±38.82, 378.2±36.31) than they had in primary suspension cultures (122.2±21.55, 250.6±55.68) The number of spheres formed by the FIBSCM were not significantly different when compared to the primary cultures.

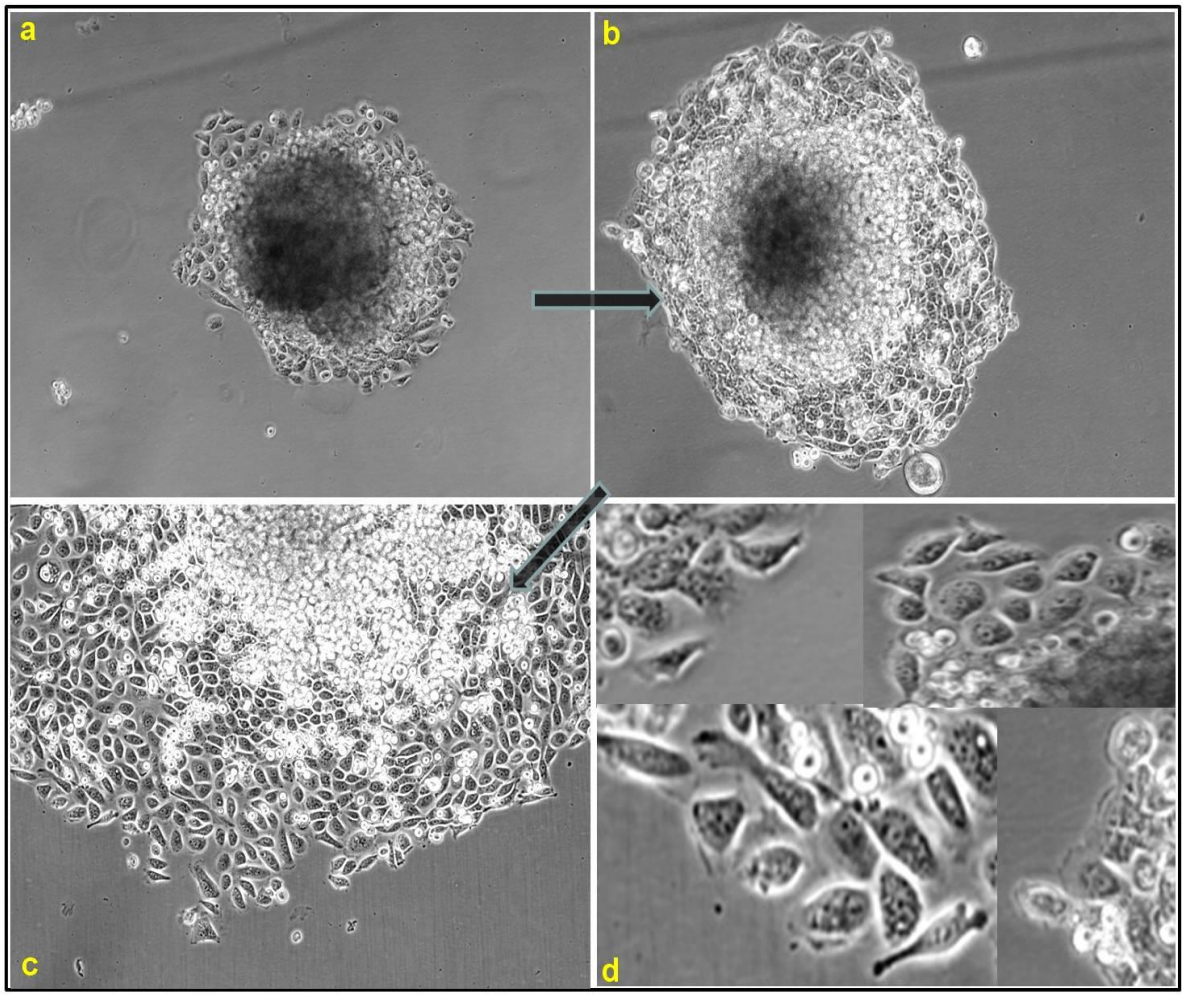

Figure 2.69: Re-introduction of H357 spheres into adherent conditions. The morphology generated when H357 spheres are reintroduced into adherent conditions. After about 4-6 hours cells resemble the appearance seen in (a). Left overnight, the cells spread out from the initial point of attachment (b). Within 48 hours the whole sphere flattens to form an epithelial colony with elongated spindle shaped cells around the edges (c). Panel (d) shows magnified insets of cells forming at the edges of the spheres and settling down to form both cobblestone shaped epithelial cells and elongated spindle cells at the edges.

5) Time Lapse Video of OSCC cells treated with TGF-β and FIBSCM:

Time lapse video analysis of OSCC cells grown under control conditions shows that, in both cell lines, when holoclones form, there appear to be two populations of cells present. The central cells within the holoclone show characteristic cobblestone morphology, are cohesive being in tight contact with neighbouring cells, and appear relatively stationary. The cells present at the edges of colonies show a spindle morphology and try to break away from the main colony, being motile. There are also cells lying outside the colonies that are elongated with spindle morphology and resemble fibroblasts. They also appear to be generated from the edges of colonies. Cells treated with TGF-β and FIBSCM show scattering on an individual level, do not form cohesive colonies, remaining instead, as a loose group of cells that show high motility, and make and break cell-cell contacts with other cells.

Note: To play files

1. use VLC media player (VideoLAN), the installation file for which has been provided in the SOFTWARE folder on the CD,

   or

2. To view in Windows media player, kindly install K-lite codec pack, also provided in the SOFTWARE folder on the CD.

(The files have been checked by Kaspersky Pure Antivirus [Kaspersky Labs™] and do not contain any malicious content)

2.5.4 Discussion:

The aim of this chapter was to ascertain whether EMT occurs in OSCC lines and whether this process could be influenced by TGF-β and other factors present in the tumour microenvironment such as cancer associated fibroblasts. Cells from CA1 and H357 cell lines were cultured under control conditions, with TGF-β and with conditioned medium from cancer associated fibroblasts (FIBSCM). Control cells formed characteristic colonies in the form of holoclones, meroclones, and paraclones as discussed. Populations of spindle shaped cells, resembling fibroblasts were seen at the edges of colonies or lying outside the colonies in both cell lines. Based on the results obtained in previous sections we hypothesized that the cells at the edges of holoclone colonies differed from those present in the center with regards to stem cell potential. The central cells were thought to represent clonogenic cells whereas those at the edge had probably begun some form of differentiation. We also hypothesized that some cells at the edge might be undergoing EMT to give rise to the spindle shaped cells seen routinely between colonies during cell culture. Cells treated with TGF-β tended not to form colonies but formed scattered cells that had elongated spindle morphology and looked similar to the cells formed at the edges of colonies. Time-lapse video showed that cells treated with TGF-β and FIBSCM show a high level of motility and scattering, and take on elongated spindle morphologies. The cells also showed decreased cohesiveness and did not form colonies as under control conditions (2.2.1.3 E). Thus both treatments enhanced the phenomenon occurring around the edges of colonies that resulted in the formation of elongated spindle cells just described.

Cells grown under control conditions showed good expression of ESA at the cell surface with central cells within colonies expressing higher levels of ESA than those at the edges. Elongated spindle cells at the edge also displayed loss of membranous ESA and some of these cells showed accumulation of ESA around the nucleus. Down-regulation of ESA and nuclear localization of its intracellular domain occurs in colon cancers with ESA interaction with members of the Wnt signalling pathway, specifically β-catenin (Maetzel et al, 2009). In the Ca1 cell line there was little evidence of nuclear localization of ESA under control conditions, while in the H357 cell line a majority of cells within colonies expressed nuclear as well as surface ESA. Treatment with both TGF-β and FIBSCM resulted in a lowering in cell surface ESA which occurs in EMT (Harrison, 2010). High expression of ESA has been linked to tumourigenicity and poor prognosis in breast cancer (Spizzo et al, 2004, 2011). Treated cells

also showed nuclear expression of ESA and this was associated with loss of the epithelial phenotype and the acquisition of a more mesenchymal, characterized by the elongated spindle cells. Further, Gires and colleagues (2009) showed that nuclear signalling by ESA increases tumourigenicity, promotes proliferation and invasion of pharyngeal and colon carcinoma cells and through interactions with members of the Wnt signalling pathway.

When examined for E-cadherin, in both cell lines the expression was seen at the surface of cells in the center of colonies and was lower in the cells around the edge. Treatment with TGF-β also resulted in loss of membranous E-cadherin. Strong expression of E-cadherin was seen in the nuclei of both types of treated cells but TGF-β caused a greater effect than the fibroblast conditioned medium. These findings suggest that cells are undergoing EMT in response to treatment, associated with possible disruptions in the Wnt signalling pathway or pathways involved in cell-cell adhesion (Franz et al, 2009). Nuclear E-cadherin has also been implicated in gain of invasiveness of many tumours such as pharyngeal, esophageal, renal and colorectal carcinomas and has been used as a prognostic marker in the diagnosis of these tumours (Salahshor, 2008; Chetty, 2008). The precise mechanism by which E-cadherin translocates to the nucleus is not well understood but it is thought that the catenin-cadherin pathway is involved. As discussed earlier, β-catenin was expressed at the surface of cells in the center of colonies (Fig 2.45-2.47), whereas edge cells show reduced membrane expression and often, translocation to the nucleus. This was also seen in the elongated spindle cells seen lying outside colonies. Treatment with both TGF-β and conditioned medium resulted in a loss of membranous β-catenin and translocation to the nucleus. This has previously been linked to poor prognosis and gain of invasiveness of many cancers and again seems to implicate that these cells have undergone EMT and have acquired a motile, mesenchymal phenotype (Schmalhofer et al, 2009; Kim et al, 2001).

The CA1 cell lines expressed strong cell surface CD44 within central colony cells with little evidence of nuclear accumulation. The motile cells differed in their CD44 expression patterns, with some staining brightly for CD44 in the cytoplasm, while others showed nuclear accumulation and moderate membrane expression. Nuclear CD44 has been linked to poor prognosis and the acquisition of stem cell potential (Lee et al, 2011). It also occurs in EMT and promotes tumour metastasis in colon cancer (Su et al, 2011). The staining patterns observed in our cell lines suggest that the cells around the colony edge acquire a mesenchymal phenotype by undergoing EMT. This is influenced by TGF-β as treatment exaggerates these expression

patterns and also by the fibroblast conditioned medium. This suggests that factors within the tumour host interface or the invasive front also plays a role in influencing this differentiation programme. The tumour-host environment, better referred to as the invasive front, is made up of tumour cells, fibroblasts, inflammatory cells and endothelial cells. TGF-β is known to be secreted by immune cells (Kalluri and Weinberg, 2009) and this is enhanced by tissue inflammation at the wounding site (Wu et al, 2009). The stromal tissue surrounding the tumour is known to play a vital role in promoting and maintaining tumour development through the involvement of cancer associated fibroblasts (Olumi et al, 1999) and recent work with TGF-β has also strengthened this observation (Kojima et al, 2010). Cancer cells are also known to secrete cytokines that promote inflammation and lead to the production of TGF-β (Finger and Giaccia, 2010; Franz et al, 2009) and it could be possible that fibroblasts present in the stromal environment, alongwith inflammatory cells release cytokines that promote the activation of the TGF-β pathways, resulting in oral cancer cells undergoing EMT.

FACS analysis using CD44 and ESA antibodies consistently identified a subpopulation of cells that was $CD44^{high}ESA^{low}$. This population also stood out from the main population of cells which generally stained high for both ESA and CD44 and represented the epithelial component of the cell lines. Analysis of CA1 cells showed that 2-3% of the total population were $CD44^{high}ESA^{low}$ whereas in H357 cells this number was much higher (4%-5%). Further, this population increased significantly with TGF-β treatment in both CA1 and H357 cell lines and shows a potential role for TGF-β in initiating EMT in these cells. Treatment with conditioned medium from malignant fibroblast also resulted in an increase in the size of this population, and suggests an alternate mechanism for EMT. TGF-β caused the proportion of $ESA^{low/-}$ cells to increase significantly (CA1 33.11±3.02%; H357) when compared to controls and this suggests that cells shed their epithelial phenotype in response to treatment. The number of cells expressing the highest levels of CD44 also increased with treatment with TGF-β and conditioned fibroblast medium. TGF-β may this play a role in influencing stem cell potential as $CD44^{high}$ cells have been shown to be clonogenic in oral and breast cancers (Al-Hajj et al, 2003; Prince et al, 2008). They have also been shown to more efficiently give rise to tumours *in vivo* (Biddle et al, 2011). CD44 is involved in contributing to the EMT process in breast cancers where CD44+CD24- cells were stem-like have characteristics of EMT cells (Mani et al, 2008). These cells reconstituted tumour heterogeneity in mice and also showed invasion and metastases to lymph nodes. Further Takahashi and co-workers (2010) demonstrated that CD44 is upregulated in response to TNF-α and interacts under the influence of TGF-β with SMAD

proteins to initiate EMT and increase the motility and invasiveness of these cells. Correspondingly the invasiveness and motility of breast cancer cells is reduced by antibodies targeting CD44 (Uchino et al, 2010). Interestingly CD44 also interacts with the Wnt pathway and induce nuclear translocation of β-catenin (Zoller, 2011). Conditioned medium from fibroblasts also caused an increase in the numbers of cells expressing high CD44 which was less marked than that caused by TGF-β but still suggests that factors in the tumour stroma interface can interact with CD44 and influence cancer stem cell behaviour and bring about EMT.

The ability of cells to survive in anchorage independent conditions has been used to enrich for tumour initiating cells. In 1992, Reynolds and Weis showed that neural cells formed spheres called "neurospheres" and that the cells making up the spheres were clonogenic and had self-renewal potential. They were further shown to reconstitute cellular heterogeneity and had the ability to divide into multiple lineages, a further defining hallmark for stem cells. When these cells were implanted back into the brain, they showed stem cell capabilities *in vivo*. Based on this model, breast cells were also shown to have the ability to form "mammospheres" containing cells that showed self-renewal and an ability to form multilineage colonies (Dontu and Wicha, 2005). Sphere forming capacity has been shown to be one of the hallmarks of EMT and recent evidence suggests that this process results in the generation of cells with stem cell properties (Mani et al, 2008; Morel et al, 2008). Our studies show that OSCC cell lines contain a population of cells which have the ability to form spheres (CA1=8.4%; H357=12%) under control conditions. Treatment with TGF-β caused a significant increase in the number of spheres formed and interestingly, treatment with fibroblast conditioned medium produced an even greater increase in the number of spheres formed. Interestingly, when control spheres were reintroduced into adherent conditions, cells from the spheres attached and spread out to form epithelial looking cells and formed large colonies resembling holoclones. These colonies had a prominent halo of spindly motile cells around the edge. Once these cells were again plated into a sphere assay, they formed more spheres per 1000 cells than they had before. This suggests that sphere formation enriches for cells that have clonogenic ability, that the epithelial populations in spheres and holoclones are interchangeable and that they are able to switch between the epithelial and mesenchymal phenotypes.

Part II

2.6 The effect of short-term treatment with TGF-β and its inhibitor

(SB431542) on subpopulations of cells within OSCC cell lines and their effects of these on the expression of vimentin.

2.6.1 Introduction

Further experiments were carried out with TGF-β to determine whether the effects of TGF-β were reversible or permanent by following cell changes after TGF-β was withdrawn. An inhibitor of TGF-β was applied to check the specificity of TGF-β treatment. Vimentin is a marker that is upregulated in EMT and is associated with the acquisition of invasive properties by pancreatic cancer cells (Krantz et al, 2010; Kong et al, 2011). To investigate the long term effects of TGF treatment, cells were also treated with TGF-β for 10 and 20 days. Various published reports describe agents that inhibit or augment the effect of TGF-β. One such agent is TNF-α, which as a fibroblast product, might be responsible for the effects of fibroblast conditioned medium. Therefore, the effects of TNF-α and NS-398 which acts through COX-II inhibition were investigated.

2.6.2 Materials and Methods

Cells were cultured as discussed (2.3.2). TGF-β (R&D systems; TGFB1001B) was dissolved in PBS containing 0.001% HCL and was used at a concentration of 20ng/ml. The inhibitor of TGF-β, SB431542 (Sigma; S4317) was resuspended in 5% DMSO in distilled water and used at 5µg/ml. TNF-α (R&D systems) was dissolved in distilled water and used at a concentration of 10ng/ml. The protocol followed for FACS was the same as has already been discussed (2.2.2.2, 2.2.3.2, Figure 2.50).

2.6.3 Results

1) CA1 cell line

A) Cell morphology

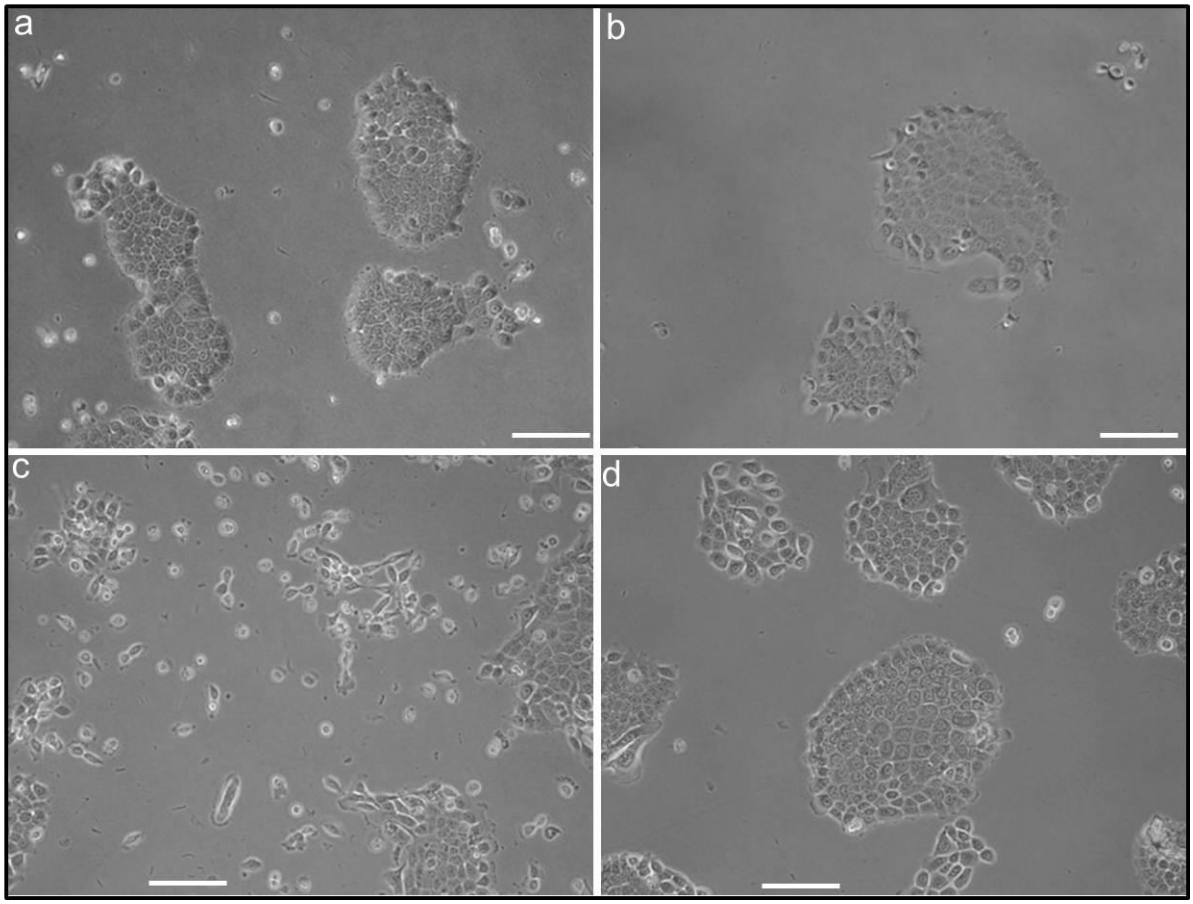

Figure 2.70: The effect of TGF-β and its inhibitor on CA1 cells. Culture of CA1 cells for 5 days under control conditions (a), with an inhibitor of TGF-β (SB431542) (b), TGF-β 20ng/ml (c) and with both TGF-β and SB431542 (d), shown in phase contrast. Control CA1 cells show good colony formation with holoclones and scattered motile cells. With the inhibitor, the colony formation seems unaffected but there is a decrease in the number of scattered cells (b). Cells treated with TGF-β, show a markedly decreased tendency to form colonies, appear scattered and acquire spindle morphology (c). When both TGF-β and the inhibitor are added, the cell morphologies generated are similar to those when the inhibitor is added alone (b) and cells form holoclones meroclones and paraclones and no spindle shaped cells (d).

B) FACS Analysis CA1 cells:

FACS analysis of the CA1 and H357 cell lines was used to assay for changes within subpopulations of treated cells. To examine the effects of treatments, cell lines were stained with CD44 and ESA antibodies and the $CD44^{high}ESA^{low}$, the $CD44^{high}$ and the ESA^{low} populations were analyzed.

a) $CD44^{high}$ ESA^{low} cells

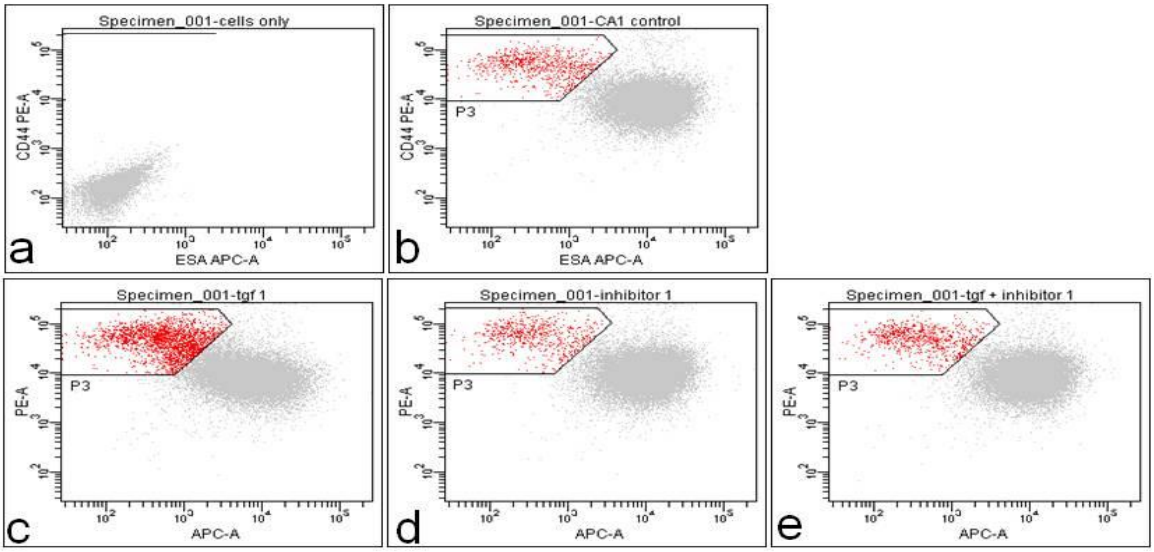

Figure 2.71: FACS analysis of CA1 cells stained with CD44 (y-axis) and ESA (x-axis) antibodies.FACS analysis of the $CD44^{high}$ ESA^{low} population (red) within the CA1 cell line and indicative changes of this population when control samples (b) were compared to cells treated with TGF-β (c), Sb431542 (d) and TGF+SB431542 (e). Doublets were excluded using forward and side scatter (2.2.2.2) and autofluorescence was determined using no antibody (a). The gated cells (red) represent the $CD44^{high}ESA^{low}$ cells corresponding to the EMT population. Treatment with TGF-β causes an increase in the number of **$CD44^{high}ESA^{low}$** cells (c). Cells treated with the inhibitor alone resembled the control samples (d). When the inhibitor was added together with the TGF-β (e), the percentage of cells within this population remained the same and the effect produced by TGF-β alone was not seen.

$44^{high}ESA^{low}$	1	2	3	Average	SEM
Control	3.13	3.19	3.42	**3.25**	0.15

TGF-Beta	9.20	9.17	9.33	**9.23**	0.09
Inhibitor	2.50	2.57	3.15	**2.74**	0.36
TGF+Inhibitor	2.00	2.61	3.00	**2.54**	0.50

Table 2.28: The effect of treatment on CD44^{high}ESA^{low} cells

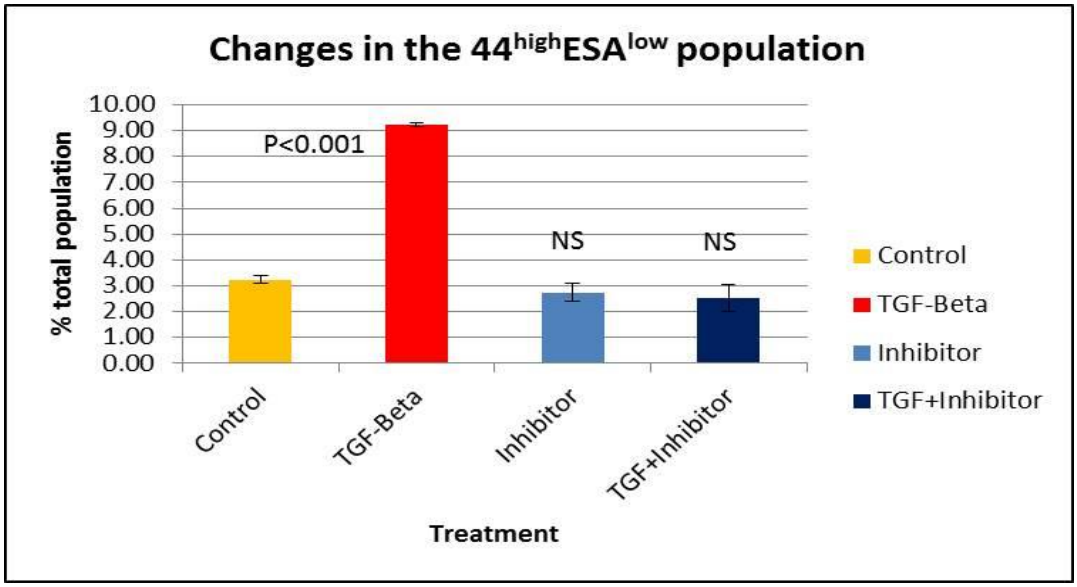

Figure 2.72: The effect of TGF-β and its inhibitor on the CD44^{high}ESA^{low} population within CA1 cells. The changes seen in the CD44^{high}ESA^{low} population when controls were compared to TGF-β treated cells, cells treated with inhibitor alone, and cells treated with both TGF-β and inhibitor. The percentage of cells gated as the CD44^{high}ESA^{low} population is low in control cells (3.25±0.15%) and this rises significantly (x3) when they are treated with TGF-β (9.23±0.09%). Treatment with inhibitor alone produces the same effect as when TGF-β and the inhibitor are added together (2.74±0.36%, 2.54±0.50%).

b) CD44^{high} cells

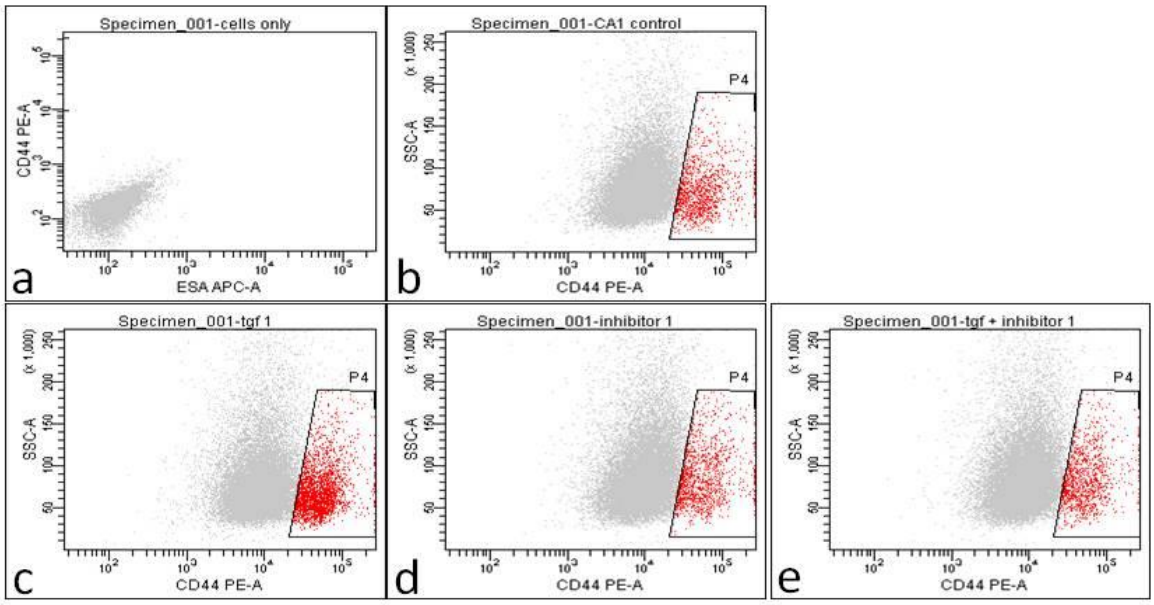

Figure 2.73: FACS analysis of CA1 cells stained with CD44 (x-axis) PE-antibody. FACS analysis of the $CD44^{high}$ population (red) within the CA1 cell line to examine changes of this population when control samples (b) were compared to cells treated with TGF-β (c), Sb431542 (d) and TGF+SB431542 (e). Doublets were excluded using forward and side scatter and autofluorescence was determined using no antibody (a). The gated cells (red) represent the $CD44^{high}$ cells, the putative stem population. Treatment with TGF-β causes an increase in the percentage **$CD44^{high}$**cells (c). Cells treated with the inhibitor resembled control samples (d). When the inhibitor was added together with the TGF-β, the percentage of gated cells remains the same and the effect produced by TGF-β alone was not seen (e). The increase in CD44 correlated with an increase in the $CD44^{high}ESA^{low}$ population.

44high	1	2	3	Average	SEM

Control	5.13	5.06	5.08	**5.09**	0.04
TGF-Beta	10.70	10.50	12.00	**11.07**	0.81
Inhibitor	5.40	5.33	5.15	**5.29**	0.13
TGF+Inhibitor	4.63	5.00	4.66	**4.76**	0.21

Table 2.29: The effect of treatment on the percentage of CD44^{high} cells

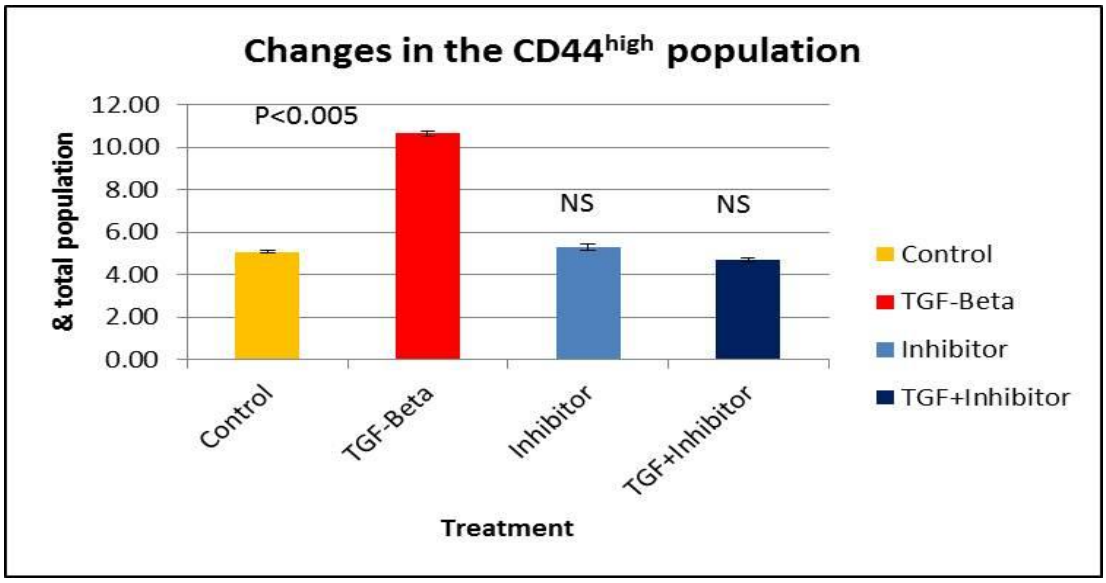

Figure 2.74: The effect of TGF-β and its inhibitor on the CD44^{high}population within CA1 cells. The changes in the CD44^{high} population when controls were compared to TGF-β treated cells, cells treated with inhibitor alone and cells treated with both TGF-β and inhibitor. The percentage of cells gated as the CD44^{high} population in control samples is 5.09±0.04% and increases significantly (x2) when they are treated with TGF-β (11.07±0.81%). Treatment with inhibitor alone produces the same effect as when TGF-β is added together with the inhibitor (5.29±0.13%, 4.76±0.21%).

c) ESA$^{low/-}$ cells

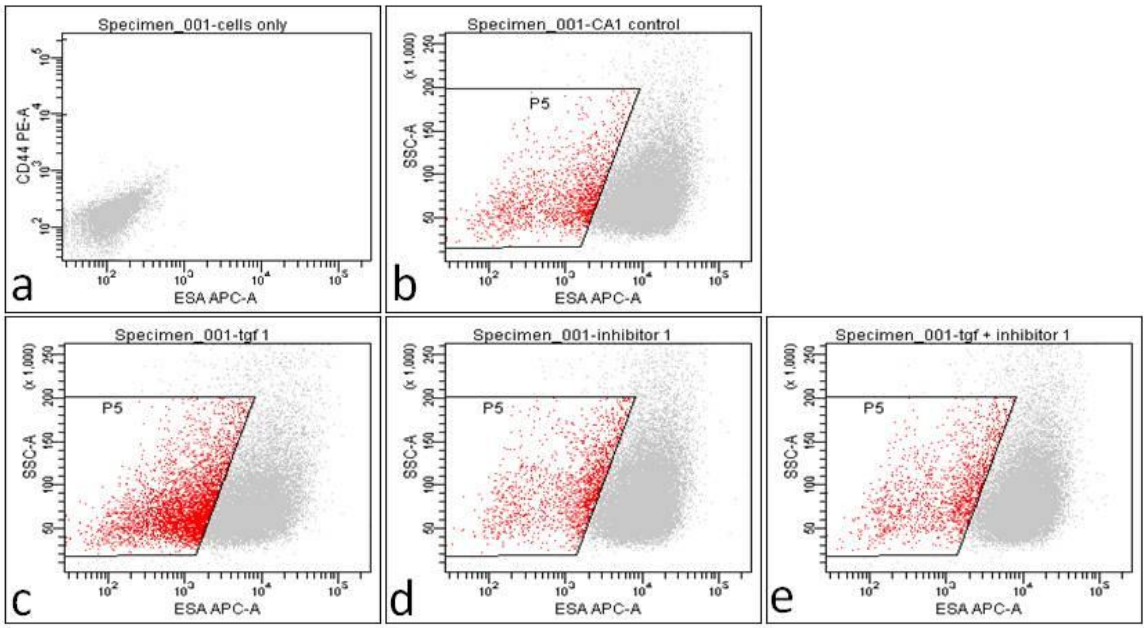

Figure 2.75: FACS analysis of CA1 cells stained with ESA (x-axis) PE-antibody. The y-axis denotes side scatter. FACS analysis of the ESA$^{low/-}$ population (red) within the CA1 cell line and changes of this population when control samples (b) were compared to cells treated with TGF-β (c), Sb431542 (d) and TGF-β+SB431542 (e). Autofluorescence was determined using no antibody (a). The gated cells (red) represent the ESA$^{low/-}$ population, representative of cells that are shedding the epithelial phenotype. Treatment with TGF-β causes an increase in the size of **ESA$^{low/-}$**population (c) and cells treated with the inhibitor alone resemble control samples (d). When TGF-β was added together with the inhibitor, the percentage of gated cells remained the same and the effect produced by TGF-β alone was not seen (e).

ESA$^{low/-}$	1	2	3	Average	SEM
Control	5.13	5.08	5.03	**5.08**	0.05
TGF-Beta	19.67	18.70	19.82	**19.40**	0.61
Inhibitor	5.63	5.80	5.10	**5.51**	0.37
TGF+Inhibitor	5.77	5.20	5.41	**5.46**	0.29

Table 2.30: The effect of treatment on the percentage of ESA^{low} cells

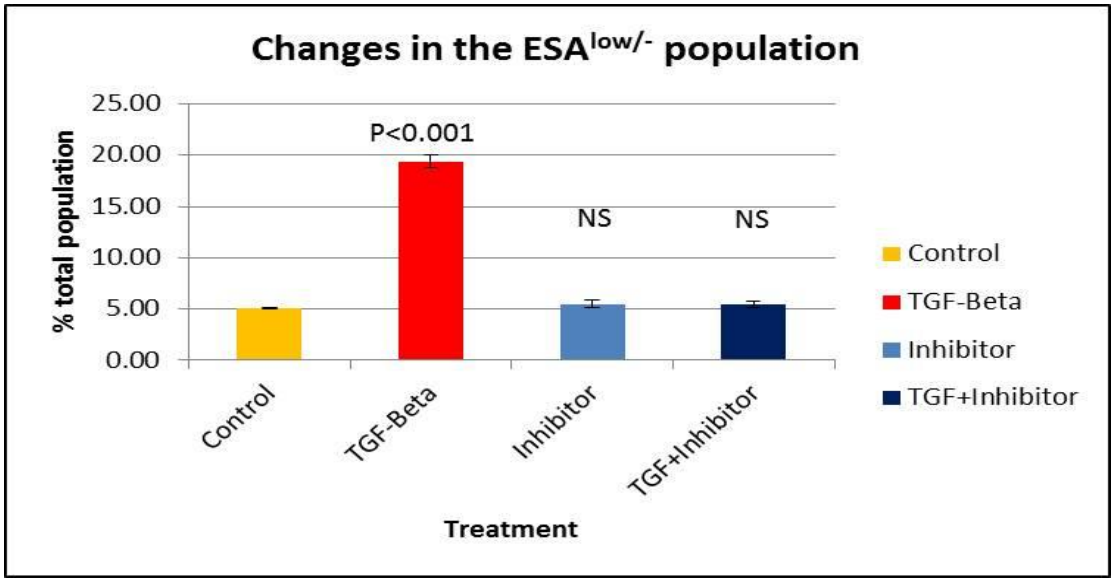

Figure 2.76: The effect of TGF-β and its inhibitor on the ESA$^{low/-}$ population within CA1 cells. The changes in the ESA$^{low/-}$ population when controls were compared to TGF-treated cells, cells treated with inhibitor alone, and cells treated with both TGF-β and inhibitor. The percentage of cells gated as the ESA$^{low/-}$ population in control samples was 5.08±0.05% and this increases significantly (x4) when they are treated with TGF-β (19.40±0.61%). Treatment with inhibitor alone produces the same effect as when TGF-β and the inhibitor are added together (5.51±0.37%, 5.46±0.29%).

2) H357 cell line

A) Cell morphology

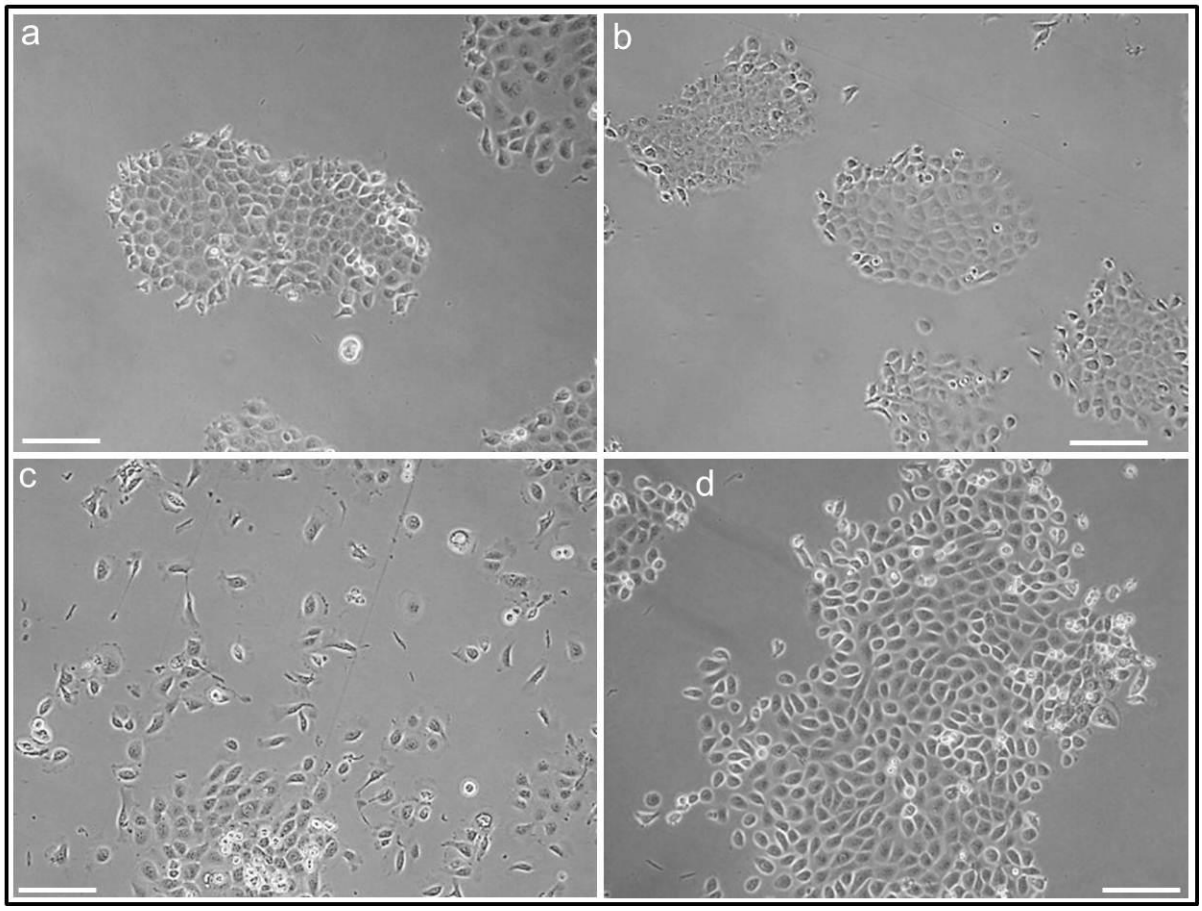

Figure 2.77: The effect of TGF-β and its inhibitor on H357 cells. Cultures of H357 cells for 5 days under control conditions (a), with inhibitor of TGF-β (SB431542) (b), TGF-β 20ng/ml (c) and with both TGF-β and SB431542 added (d), shown in phase contrast. Control CA1 cells show good colony formation with holoclones and scattered motile cells shown in (a). With the inhibitor, the colony formation seems unaffected but there is a decrease in the number of motile cells seen (b). Cells treated with TGF-β show a markedly decreased tendency to form colonies, appear scattered and take on a spindly morphology (c). The addition of TGF-β and the inhibitor together (d), results in the generation of colony morphologies similar to when the inhibitor is added alone (b) and cells form holoclones meroclones and paraclones and no spindle-shaped cells are seen (d).

B) FACS Analysis

a) $CD44^{high}$ ESA^{low} cells

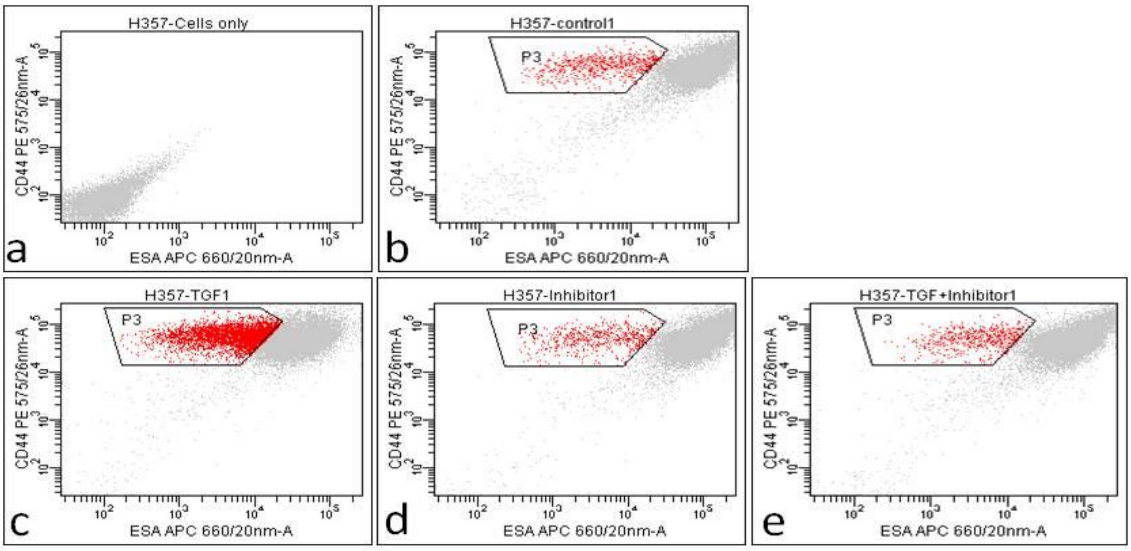

Figure 2.78: FACS analysis of H357 cells stained with CD44 (y-axis) and ESA (x-axis) antibodies.FACS analysis of the $CD44^{high}ESA^{low}$ population (red) within the H357 cell line and changes of this population when control samples (b) were compared to cells treated with TGF-β (c), Sb431542 (d) and TGF-β+SB431542 (e). Autofluorescence was determined using no antibody (a). The gated cells (red) represent the $CD44^{high}ESA^{low}$ cells, representative of EMT cells. Treatment with TGF-β causes an increase in the number of $CD44^{high}ESA^{low}$ cells and the population shifts towards the $CD44^{high}ESA^{low}$ quadrant. Cells treated with the inhibitor alone resembled the control samples (d). When the inhibitor was added together with the TGF-β, the percentage of cells gated as this population remains the same and the effect produced by TGF-β alone was not seen (e).

44highESAlow	1	2	3	Average	SEM
Control	4.30	4.88	4.82	4.67	0.32
TGF-Beta	25.80	26.13	29.25	27.06	1.90
Inhibitor	3.60	4.52	4.46	4.19	0.51
TGF+Inhibitor	3.33	4.52	4.23	4.03	0.62

Table 2.31: The effect of treatment on the percentage of $CD44^{high}$ ESA^{low} cells

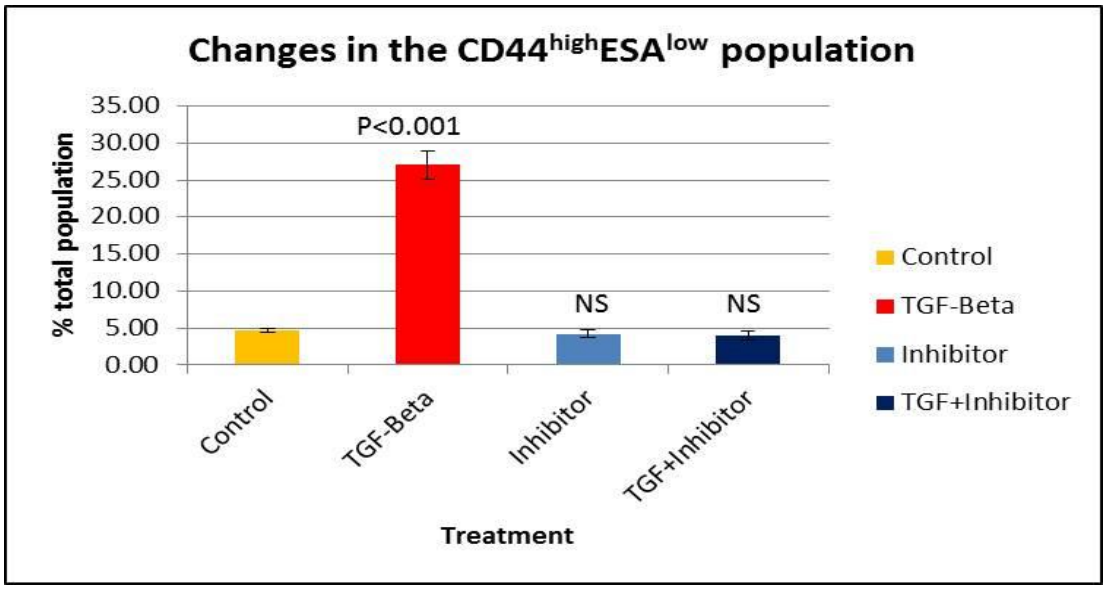

Figure 2.79: The effect of TGF-β and its inhibitor on the $CD44^{high}$ ESA^{low} population within H357 cells. The changes in the size of the $CD44^{high}ESA^{low}$ population of H357 cells when controls were compared to TGF-β treated cells, cells treated with inhibitor, and cells treated with both TGF-β and inhibitor. The percentage of cells gated as the $CD44^{high}ESA^{low}$ population in control cells is (4.67±0.32%) which is higher than the intrinsic proportion of these cells in the CA1 cell line. The size of this population increases significantly (x6) when they are treated with TGF-β (27.06±1.90%). Treatment with inhibitor alone produces the same effect as when TGF-β and the inhibitor are added together (4.19±0.51%, 4.03±0.62%). This cell line produces an overall greater response to TGF treatment than the CA1 cell line.

b) CD44^{high} cells

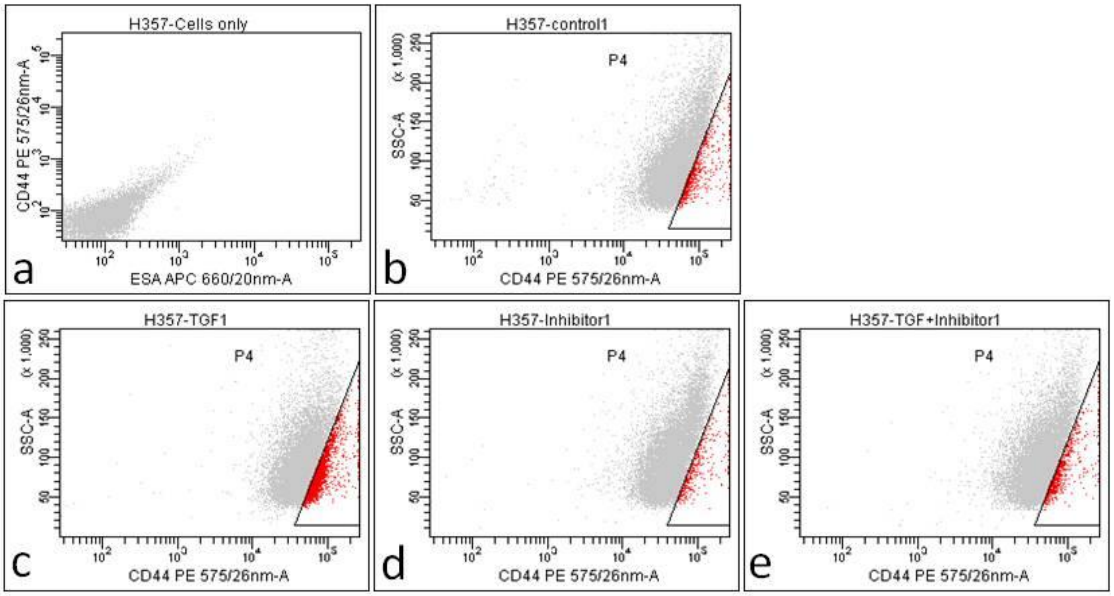

Figure 2.80: FACS analysis of H357 cells stained with CD44 (x-axis) PE-antibody. The y-axis denotes side scatter. FACS analysis of the CD44^{high} population (red) within the H357 cell line and changes in the size of this population when control samples (b) were compared to cells treated with TGF-β (c), Sb431542 (d) and TGF-β+SB431542 (e). Autofluorescence was determined using no antibody (a). The gated cells (red) represent the CD44^{high} cells which are the putative stem population. Treatment with TGF-β increases the number of CD44^{high}cells (c). Cells treated with the inhibitor alone resembled the control samples (d). When the inhibitor was added together with the TGF-β, the percentage of gated cells remains the same and the effect produced by TGF-β alone is not seen. The increase in CD44 correlated with an increase in the CD44^{high}ESA^{low} population.

44^{high}	1	2	3	Average	SEM
Control	5.20	5.18	5.09	**5.16**	0.06
TGF-Beta	19.76	19.89	19.94	**19.86**	0.09
Inhibitor	5.00	5.10	6.00	**5.37**	0.55
TGF+Inhibitor	5.17	5.21	4.92	**5.10**	0.16

Table 2.32: The effect of treatment on the percentage of $CD44^{high}$ cells

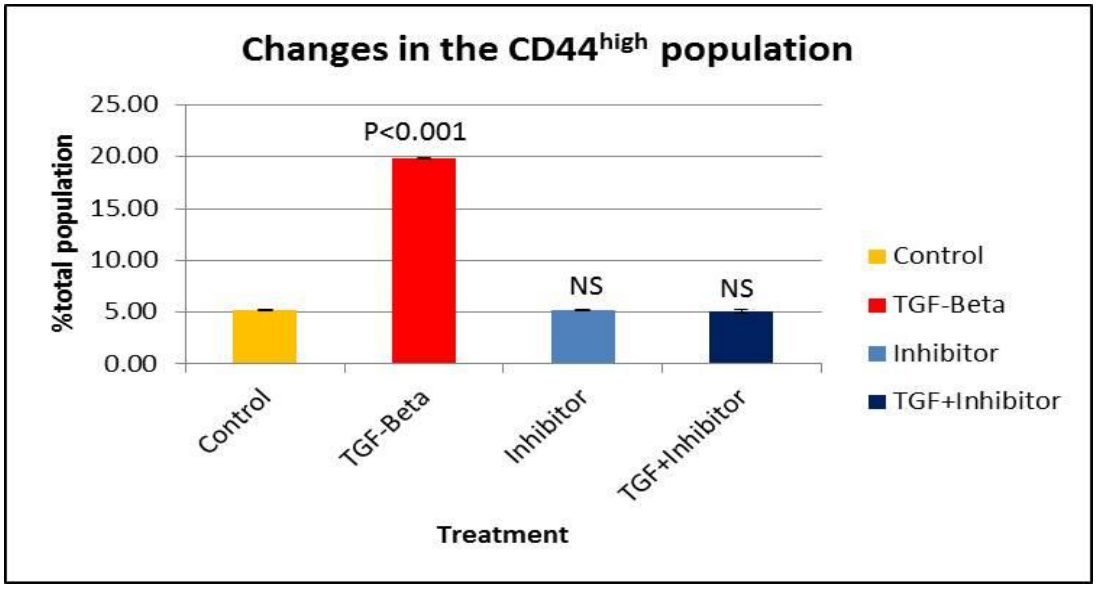

Figure 2.81: The effect of TGF-β and its inhibitor on the $CD44^{high}$population within H357 cells. The changes in the $CD44^{high}$ population when controls were compared to TGF-treated cells, cells treated with inhibitor alone, and cells treated with TGF-β together with inhibitor. The percentage of cells gated as the $CD44^{high}$ population in control samples is 5.16±0.06% and increases significantly (x4) when cells are treated with TGF-β (19.86±0.09%). Treatment with inhibitor alone produces the same effect as when TGF-β and the inhibitor are added together (5.37±0.55%, 5.10±0.16%).

c) ESA$^{low/-}$ cells

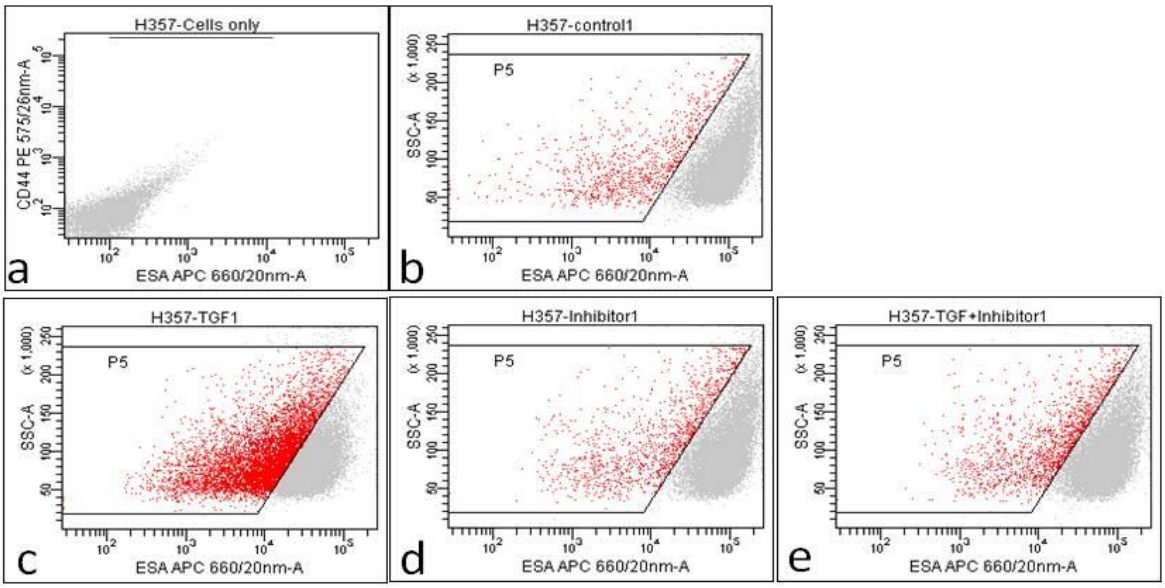

Figure 2.82: FACS analysis of H357 cells stained with ESA (x-axis) PE-antibody. The y-axis denotes side scatter. FACS analysis of the **ESA$^{low/-}$** population (red) within the H357 cell line and changes of this population when control samples (b) were compared to cells treated with TGF-β (c), Sb431542 (d) and TGF+SB431542 (e). Autofluorescence was determined using no antibody (a). The gated cells (red) represent the ESA$^{low/-}$ cells that represent putative EMT cells. Treatment with TGF-β causes an increase in the percentage **ESA$^{low/-}$**cells. Cells treated with the inhibitor alone also resembled the control samples. With the addition of inhibitor together with TGF-β, the percentage of cells within this population remains the same as controls and the effect produced by TGF-β alone was not seen.

ESA$^{low/-}$	1	2	3	Average	SEM
Control	5.23	5.60	5.13	5.32	0.25
TGF-Beta	34.83	36.05	31.05	33.98	2.61
Inhibitor	6.53	5.75	5.21	5.83	0.66
TGF+Inhibitor	8.63	8.66	8.56	8.62	0.05

Table 2.33: The effect of treatment on the percentage of ESA$^{low/-}$ cells.

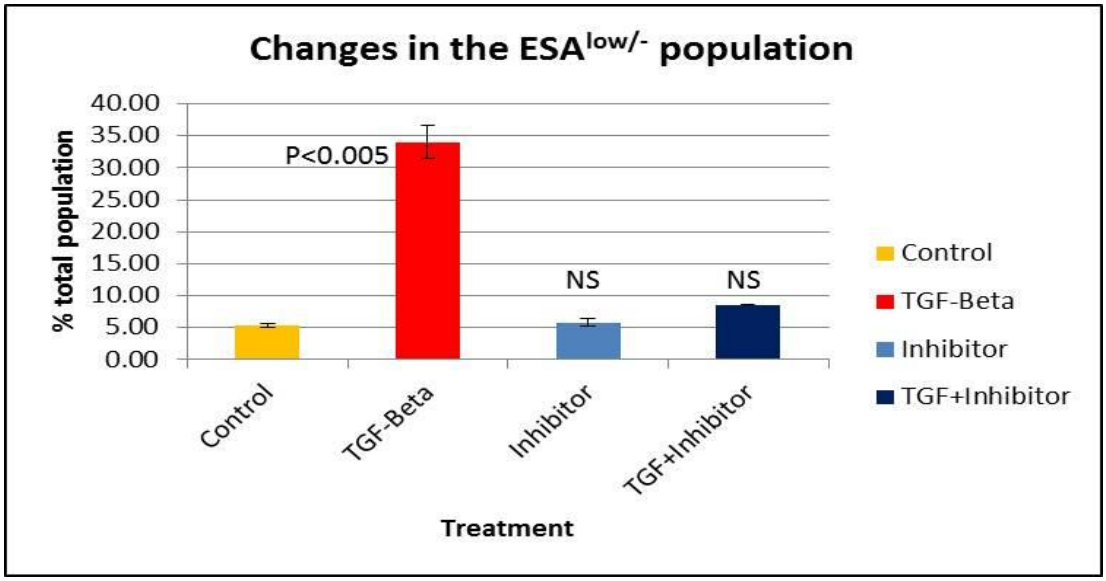

Figure 2.83: The effect of TGF-β and its inhibitor on the size of the ESA^{low} population within H357 cells. The changes in the ESA$^{low/-}$ population when controls were compared to TGF-treated cells, cells treated with inhibitor alone, and cells treated with both TGF-β and inhibitor. The percentage of cells gated as the ESA$^{low/-}$ population in control samples was 5.32±0.25% and rises significantly (x7) when they are treated with TGF-β (33.98±2.61%). Treatment with inhibitor alone causes no effect (5.83±0.66%).When TGF-β is added together with the inhibitor, a slight increase in this population is observed (8.62±0.05%) but this was not statistically significant.

C) Immunocytochemistry

Cells were further studied using immunocytochemistry to detect vimentin as an assay of the effect of TGF-β on the expression of this protein that acts as an EMT marker and has been associated with acquisition of invasive and motile potential.

1) Vimentin

a) Control cells

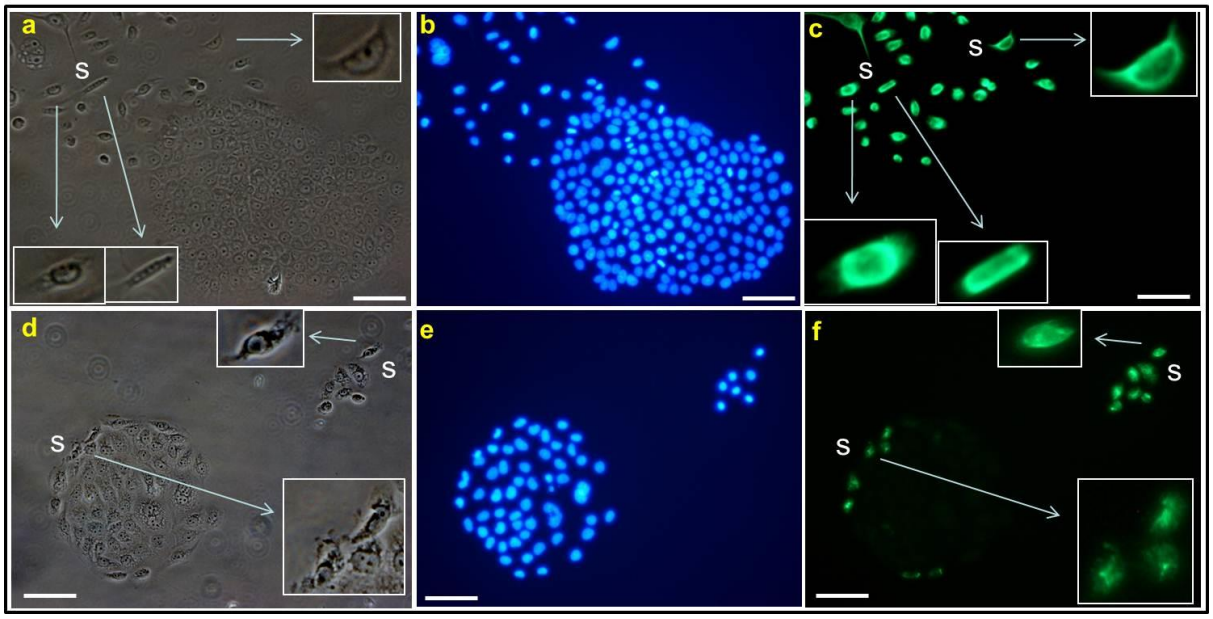

Figure 2.84: Expression of Vimentin in OSCC cells cultured under control conditions. Cultures of CA1 (a-c) and H357 (d-f) cells cultured under control conditions and shown in phase contrast (a, c), stained with DAPI nuclear stain (b, e) and anti-vimentin FITC antibody (c, f). CA1 and H357 cells form colonies with spindle cells lying outside and at the edges (a). The cells within the colony show no expression of vimentin while the spindle-shaped cells (S) show very high expression restricted mainly to the cytoplasm. H357 cells within colonies also remain largely negative for vimentin with the exception of elongated spindle-shaped cells (S) at the colony periphery that show strong cytoplasmic expression.

b) Cells treated with TGF-β

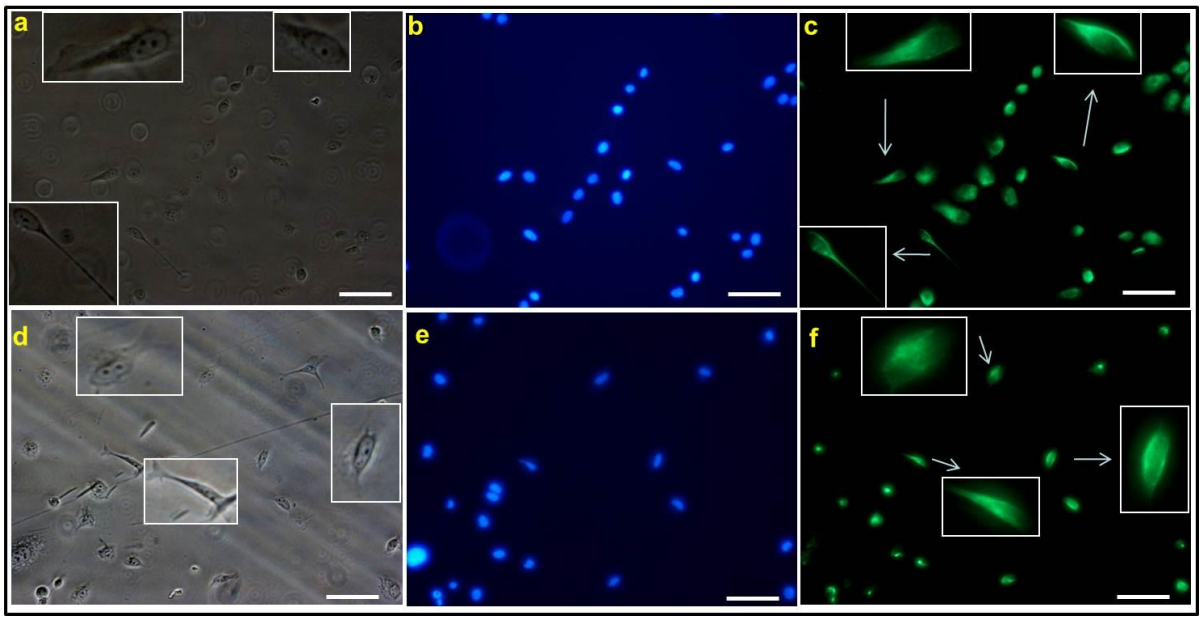

Figure 2.85: Expression of Vimentin in OSCC cells treated with TGF-β. Cultures of CA1 (a-c), and H357 (d-f) cells treated with TGF-β (a, c) shown in phase contrast, stained with DAPI nuclear stain (b, e) and anti-Vimentin-FITC antibody (c, f). Treated cells show elongated spindle morphology, resemble fibroblasts, remain scattered and in both cell lines, express high levels of cytoplasmic vimentin.

c) Cells treated with TGF added together with inhibitor.

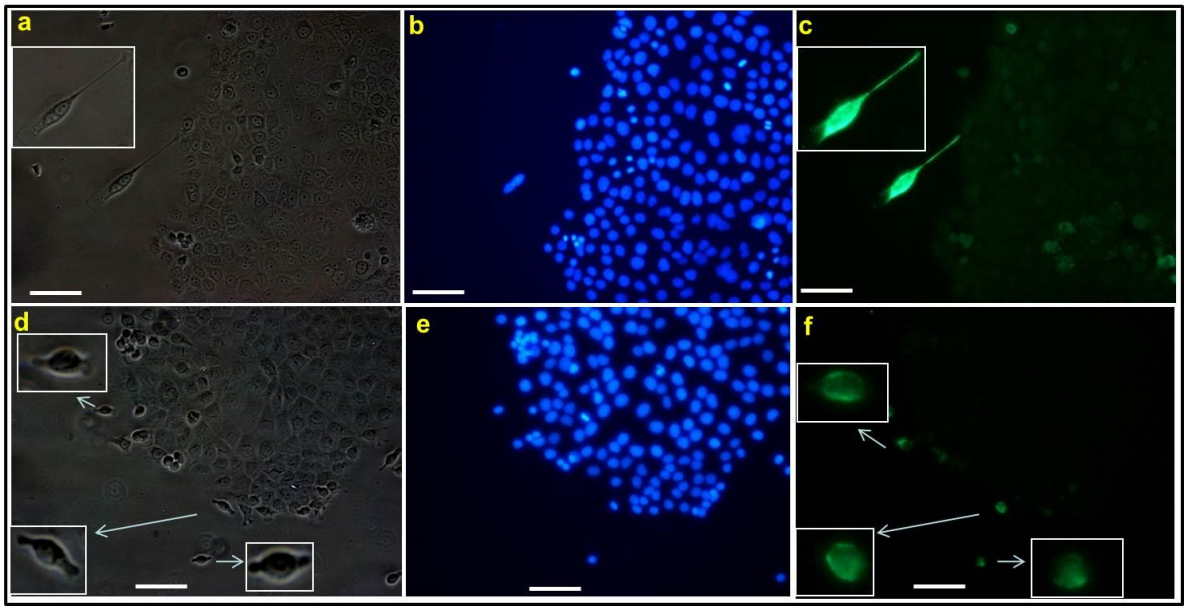

Figure 2.86: Expression of Vimentin in OSCC cells cultured with SB431542 and TGF-β. Cultures of CA1 (a-c) and H357 (d-f) cells grown with SB431542 and TGF-β added together (a, d) shown in phase contrast, stained with DAPI (b, e) and anti-vimentin FITC antibody (c, f). Cells resemble those grown under control conditions with normal colony morphology. CA1 cells making up the colony express very low Vimentin with the exception of one spindle cell (inset), lying outside the colony that expresses a very high level (c). H357 cells are shown with spindle cells at the colony edge that show moderate expression of Vimentin within the cytoplasm with the bulk of the cells forming the colony remaining negative for the protein.

2.6.4 Discussion:

To examine the effects of TGF-β and its inhibitor on OSCC cell lines, the CA1 and H357 cell lines were subjected to short-term treatment (5 days) with TGF-β and its inhibitor, SB431542. Additionally the Fanconi OHSU cell line was also analyzed (not shown). Cells from both cell lines displayed an elongated spindle-like morphology and showed increased migratory capacity as seen on time lapse videos. Cells from both lines also showed a decreased propensity to form adherent colonies. Treatment with the inhibitor had no adverse effects on the growth of these cells and SB431542 was seen to effectively block TGF-β activity as when cells were grown with both the inhibitor and TGF-β added together, they resembled control cells. FACS analysis for CD44 and ESA showed an increase in the size of the $CD44^{high}ESA^{low}$ and $CD44^{high}$ populations with treatment in both cell lines but it was the H357 cell line that was found to be more susceptible to TGF-β as seen by the greater responses to treatment.

This investigation was undertaken primarily to see whether the intrinsic $CD44^{high}ESA^{low}$ cells detected under control conditions with FACS analysis could be reduced or eliminated by removal of TGF-β to begin with. The inhibitor blocked the EMT induced with TGF-β, however some motile elongated cells remained when both cell lines were grown with just the inhibitor. This suggests that the motile population seen in OSCC cell lines under control conditions is not dependant on TGF-β to complete this process and this was also seen in Fanconi cells. The same result was seen when the Fanconi OHSU cell line was examined. These observations suggest that multiple signalling pathways may work synergistically to bring about EMT in cancer cell lines. Soluble factors and cytokines such as TNF-α and EGF have been implicated in working synergistically with TGF-β to cause EMT characterized by the acquisition of spindle morphology and invasiveness in breast and ovarian cancer cells. (Asiedu et al, 2011; Zhihua et al, 2010).In both, these changes were further characterized by the downregulation of surface E-cadherin and an increase in the expression of mesenchymal markers such as Snail, Slug and Twist. It could also mean that the EGF (2.2.2.1) supplement present in the culture medium could be responsible for the EMT cells observed routinely in OSCC cultures.The role of EGF in the progression of many cancers has been well documented (Mendelson et al, 2000). It is also known that tumour cells are capable of producing endogenous cytokines such as TGF-β, TNF-α, and these feedback contextually with the surrounding microenvironment to augment and possibly maintain a mesenchymal state. Other cells in the tumour microenvironment include cancer associated fibroblasts and it has recently been shown that they produce

endogenous TGF-β that inturn induces and maintains feedback loops with tumour cells promoting a favourable environment for tumour invasion (Kojima et al, 2010). The role of cancer associating fibroblasts in tumour progression has been shown for many cancers including those of the colon and breast where they augmented and stimulated the growth of tumour cells in mouse models (De Wever et al, 2004; Orimo et al, 2005). They are also known to induce EMT in prostate cancer cells which also results in the generation of stem capabilities (Cirri and Chiarugi, 2011; Gianonni, 2010).

The expression of Vimentin was assessed in OSCC cell lines and was seen to be high in spindle-shaped lying outside colonies (CA1) or in some cells at the edge (H357). Other cells in the colonies showed no expression. Treated cells showed strong cytoplasmic expression of vimentin. These staining patterns support the suggestion that $CD44^{high}ESA^{low}$ cells have undergone EMT (Biddle et al, 2011) and this is supported by qPCR analysis of these cells that shows high expression of EMT signature genes such as vimentin, snail and Twist. This population was also seen to increase with treatment and treated cells show strong expression and spindle morphology. Up-regulation of Vimentin has been associated with EMT in cancers, including pancreatic cancer (Krantz et al, 2012) and bladder cancers (Shorning et al, 2011). Further, this increase in Vimentin has specifically been associated with areas of tumours showing poor differentiation and is thus linked to poor prognosis of pancreatic cancers (Javle et al, 2007). Vimentin has been used as a diagnostic marker in many cancers including those of the cervix, bladder and breast (Dal-Vecchio et al, 2011). In head and neck cancers increased vimentin expression has been correlated with increased metastatic risk (Nijkamp et al, 2011), drug resistance to the anti-cancer drug, gefitinib (Frederick et al, 2007) and loss of anchorage dependence by cells with the acquisition of a spindle morphology (Tomson et al, 1996).

2.7 The effect of long-term treatment with TGF-β and treatment withdrawl on OSCC cells

2.7.1 Introduction

Short term treatment caused an increase in the overall percentage of $CD44^{high}ESA^{low}$ cells. This switching of cells into the $CD44^{high}ESA^{low}$ phenotype was interesting as it implies that there are cells within the main bulk of the tumour that have the ability to switch into the EMT phenotype, but how longer term treatment would continue to expand this population was uncertain. It was also uncertain whether these cells were able to switch back into the epithelial phenotype. To investigate this, cell were treated with TGF-β for a further 10 and 20 days to determine the effect of long term treatment.

2.7.2 Materials and Methods

The methods are the same as have been discussed previously (2.5.2)

2.7.3 Results

I) Long-term treatment with TGF-β and its effect on OSCC lines

i) CA1 cell line

A) $CD44^{high}ESA^{low}$:

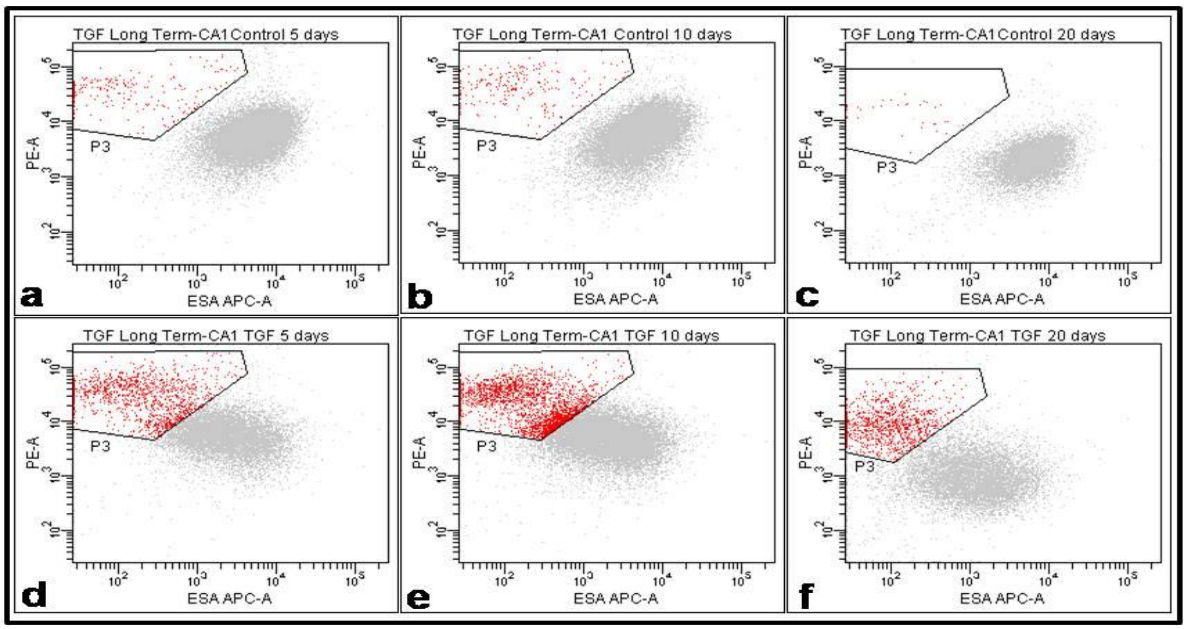

Figure 2.87: FACS analysis of CA1 cells stained with CD44 (y-axis) and ESA (x-axis) PE-antibody. FACS analysis of the $CD44^{high}$ ESA^{low} population (red) within the CA1 cell line and indicative changes in the size of this population when control samples (a-c) were compared to cells treated with TGF-β for 5 days (d), 10 days (e) and 20 days (f). The gated cells (red)

represent the $CD44^{high}ESA^{low}$ cells which are the hypothesized EMT population. Treatment with TGF-β for 5 days results in an increase in this population as seen before. Treatment with this for 10 and 20 days causes a progressive rise in the number of $CD44^{high}ESA^{low}$ cells.

Condition	I	II	III	% $CD44^{high}ESA^{low}$	SEM
5 days Control	1.23	1.53	1.41	**1.39**	0.15
10 days Control	1.47	1.50	1.56	**1.51**	0.05
20 days Control	0.53	0.76	0.70	**0.66**	0.12
5 days TGFβ	10.03	8.20	9.92	**9.38**	1.03
10 days TGFβ	13.00	12.66	12.89	**12.85**	0.17
20 days TGFβ	15.60	15.04	14.68	**15.11**	0.46

Table 2.34: The effect of long-term treatment with TGF-β on CA1 cells.

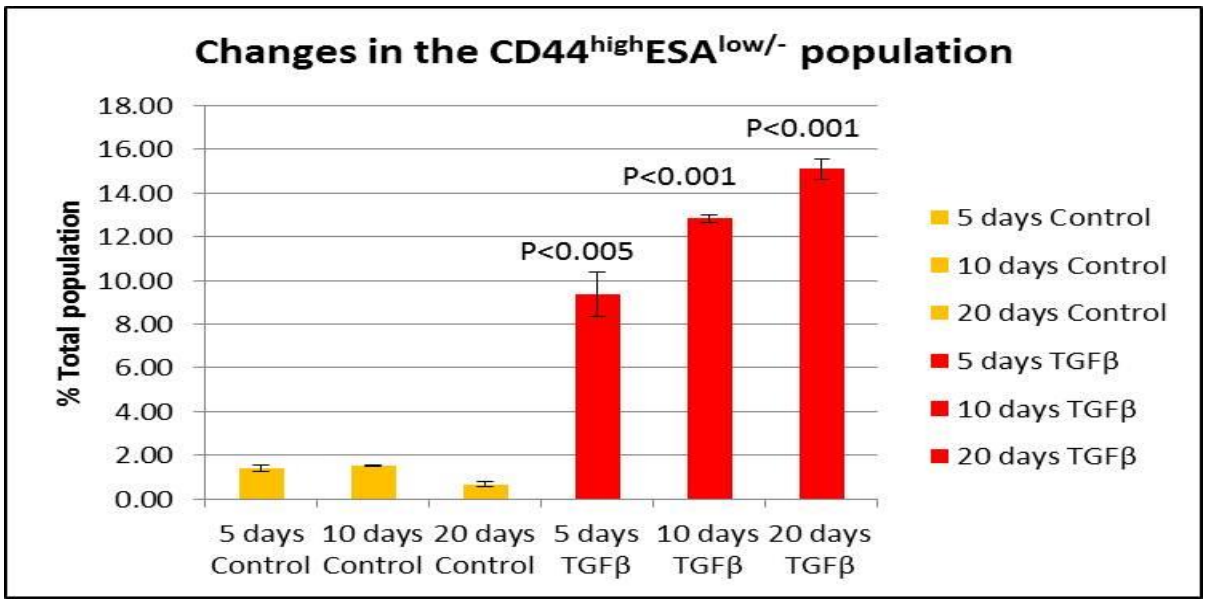

Figure 2.88: Long-term treatment with TGF-β and its effect on $CD44^{high}ESA^{low}$ cells. The changes in the $CD44^{high}ESA^{low}$ population when controls were compared with cells treated with TGF-β for 5, 10 and 20 days. The size of the $CD44^{high}ESA^{low}$ population gated in control cells is low (1.39±0.15%) and increases significantly when they are treated with TGF-β for 5 days (9.38±1.03%), 10 days (12.85±0.17%) and 20 days (15.11±0.46).

B) CD44^{high} cells:

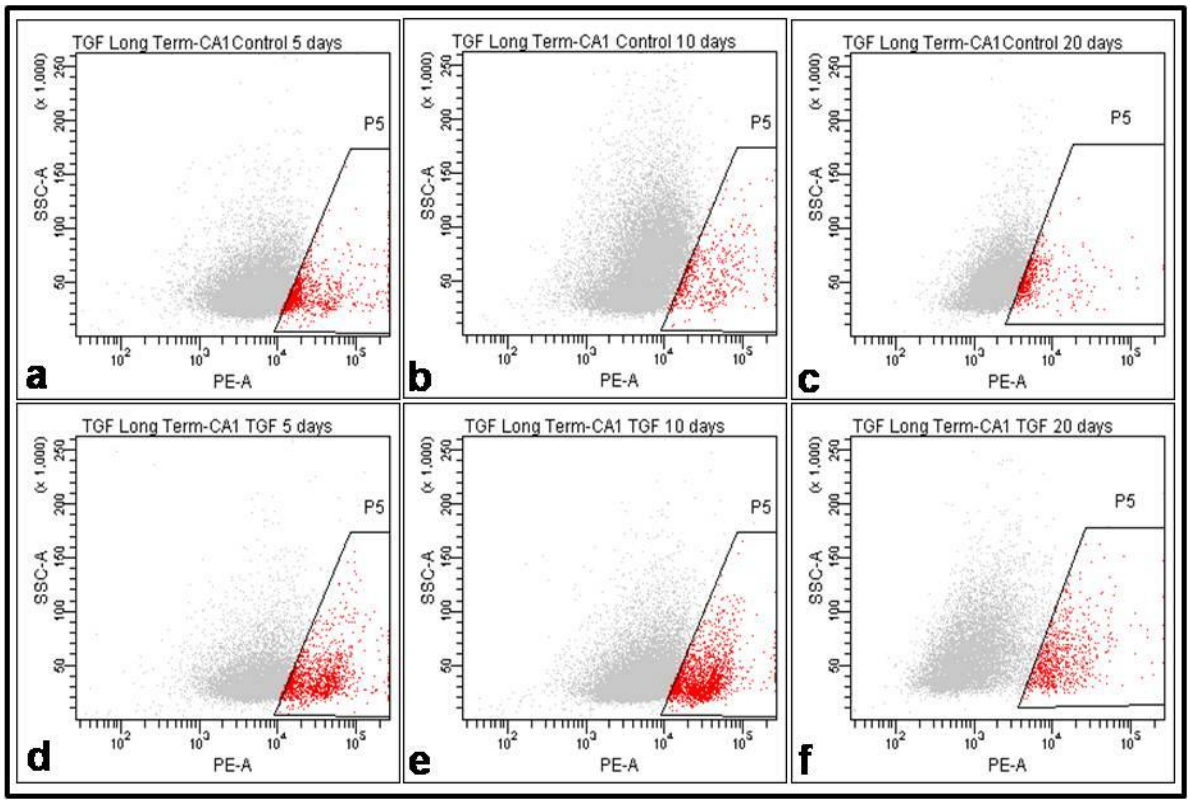

Figure 2.89: FACS analysis of CA1 cells stained with CD44 (x-axis). FACS analysis of the CD44^{high} population (red) within the CA1 cell line and the changes in this population when control cells (a-c) were compared to those treated with TGF-β for 5 days (d), for 10 days (e) and for 20 days (f). The gated cells (red) represent the CD44^{high} cells which are the putative stem cell population. The effect of the 10 and 20 day treatment is the same.

Condition	I	II	III	% CD44^{high}	SEM
5 days Control	5.17	5.30	5.37	5.28	0.10
10 days Control	3.42	3.28	3.27	3.32	0.08
20 days Control	1.93	2.06	2.45	2.15	0.27
5 days TGFβ	12.53	13.10	13.68	13.10	0.58
10 days TGFβ	14.37	13.79	14.87	14.34	0.54
20 days TGFβ	14.33	14.06	14.38	14.26	0.17

Table 2.35: The effect of long-term treatment with TGF-β on CD44^{high}CA1 cells.

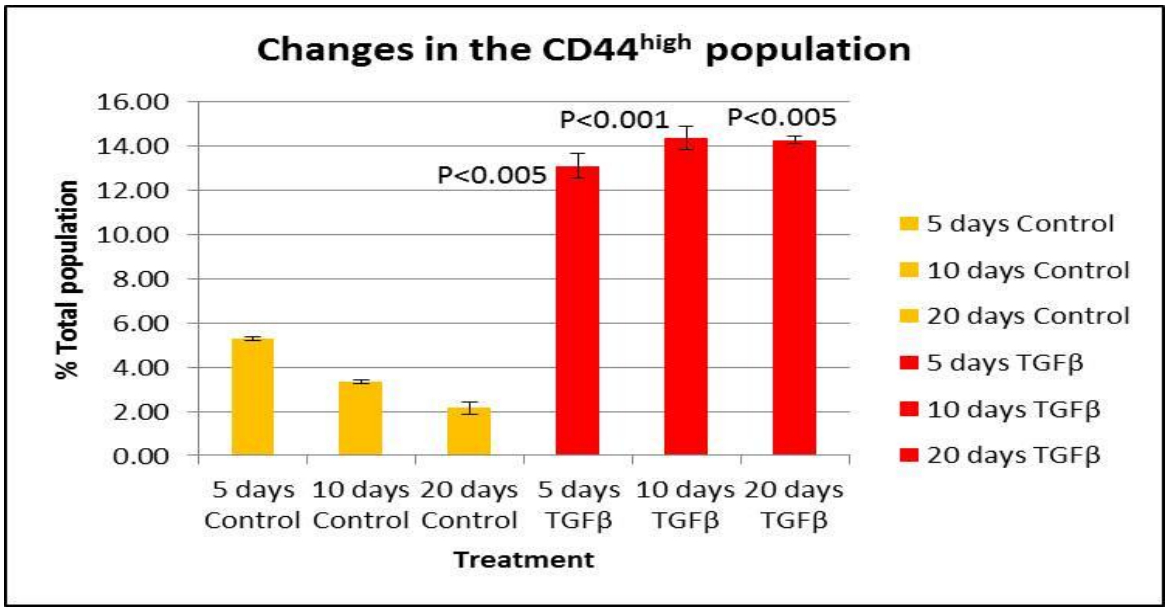

Figure 2.90: Long-term treatment with TGF-β and its effect on CD44^{high} cells. The changes in the CD44^{high} population in CA1 cells when controls were compared with cells treated with TGF-β (red) for 5, 10 and 20 days. The percentage of CD44^{high} cells was 5.28±0.10% at day 5 rose significantly with TGF-β for 5 days (13.1±0.58%), 10 days (14.34±0.54%) and 20 days (14.38±0.17%) respectively. The percentage of CD44^{high} cells increases till day 10 and then seems to remain the same at day 20. And this increase also correlates with the increase in the CD44^{high}ESA^{low} population indicating that most of the CD44 ^{high} cells were also low for ESA.

C) ESA$^{low/-}$ cells:

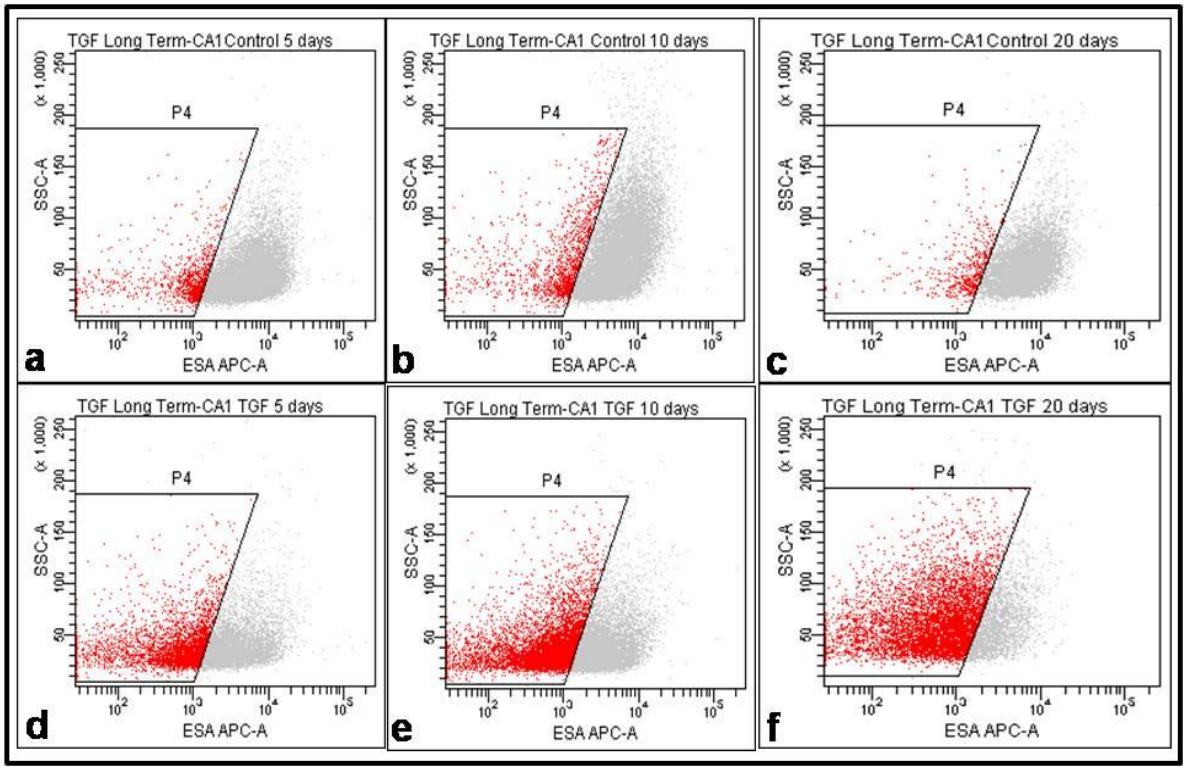

Figure 2.91: FACS analysis of CA1 cells stained with ESA (x-axis). The y-axis denotes side-scatter.FACS analysis of the ESA^{low} population (red) within the CA1 cell line and changes in the size of this population when control cells (a-c) were compared to those treated with TGF-β for 5 days (d), 10 days (e) and TGF-β for 20 days (f). The gated cells (red) represent the ESA$^{low/-}$population thatrepresents cells shedding their epithelial state and becoming more mesenchymal. The number of ESA$^{low/-}$ cells increases progressively with treatment (d-f).

Condition	I	II	III	% ESAlow	SEM
5 days Control	5.20	5.22	5.29	**5.24**	0.05
10 days Control	8.17	6.23	6.93	**7.11**	0.98
20 days Control	3.97	4.38	5.06	**4.47**	0.55
5 days TGFβ	36.70	35.89	36.66	**36.42**	0.46
10 days TGFβ	47.60	45.99	46.62	**46.74**	0.81
20 days TGFβ	69.97	67.56	66.38	**67.97**	1.83

Table 2.36: The effect of long-term treatment with TGF-β on ESA$^{low/-}$ CA1 cells

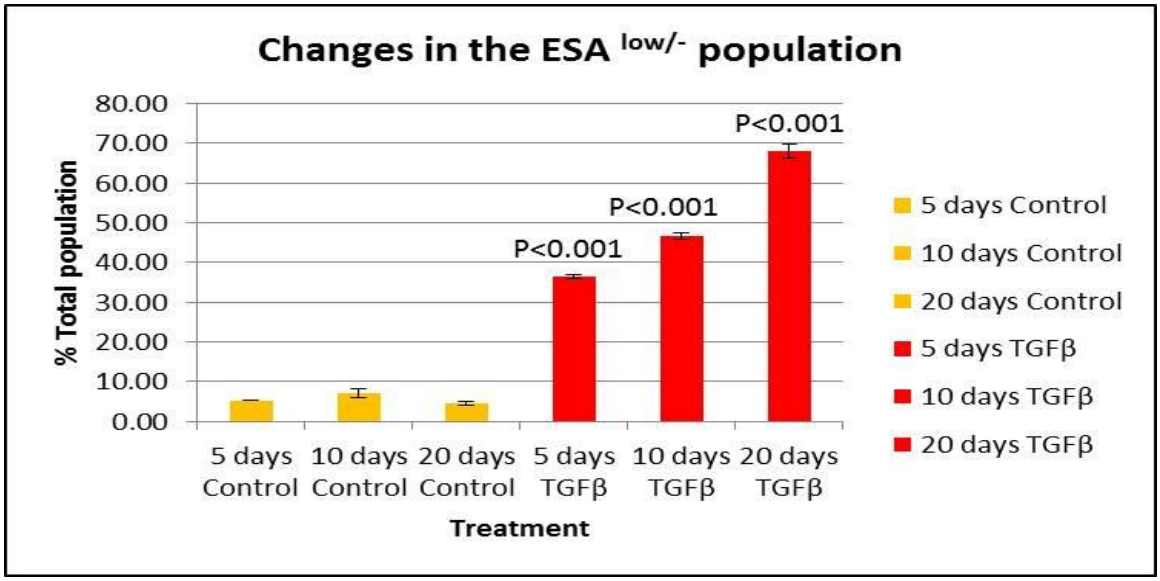

Figure 2.92: Long-term treatment with TGF-β and its effect on ESA$^{low/-}$ cells. The figure above shows the changes in the ESA$^{low/-}$ population in CA1 cells when controls were compared to cells treated with TGF-β for 5, 10 and 20 days. The percentage of ESA$^{low/-}$ cells gated in the controls was 5.24±0.05%. This rose significantly when treated with TGF-β for 5 (36.42±0.46%), 10 (46.74±0.81%) and 20 (67.97±1.83%) days. The percentage of ESA$^{low/-}$ cells increases progressively with treatments.

ii) H357 cell line

a) $CD44^{high}ESA^{low}$

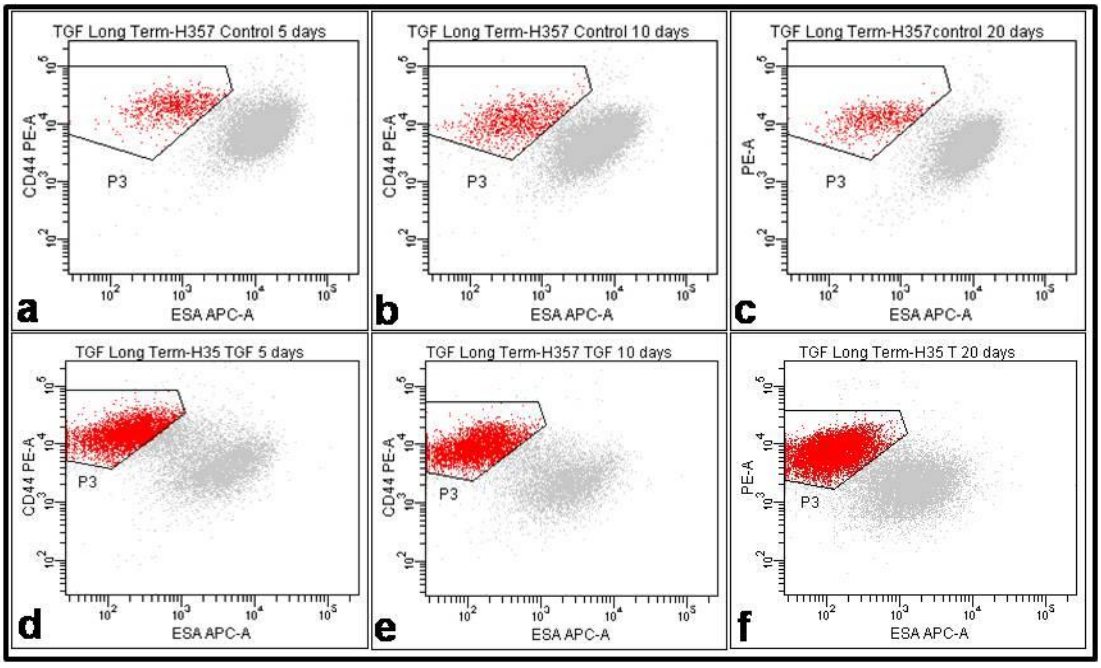

Figure 2.93: FACS analysis of H357 cells stained with CD44 (y-axis) and ESA (x-axis) PE-antibody. FACS analysis of the $CD44^{high}$ ESA^{low} population (red) within the H357 cell line and changes in the size of this population when control samples (a-c) were compared to cells treated with TGF-β for 5 days (d), 10 days (e) and 20 days (f). The gated cells (red) represent the $CD44^{high}ESA^{low}$ cells which are the EMT population. Treatment with TGF-β for 5 days results in an increase in this population as seen before. Treatment with TGF-β for 10 and 20 days causes a progressive rise in the number of $CD44^{high}ESA^{low}$ cells.

Condition	I	II	III	% $CD44^{high}ESA^{low}$	SEM
Control 5 days	4.91	5.07	5.33	**5.10**	0.21
Control 10 days	5.35	5.25	5.67	**5.42**	0.22
Control 20 days	4.63	5.17	5.33	**5.04**	0.37
TGF 5-day	26.93	27.70	26.95	**27.19**	0.44
TGF 10-day	45.00	42.79	41.03	**42.94**	1.99
TGF 20-day	48.30	50.50	53.53	**50.78**	2.63

Table 2.37: The effect of long-term treatment with TGF-β on H357 cells.

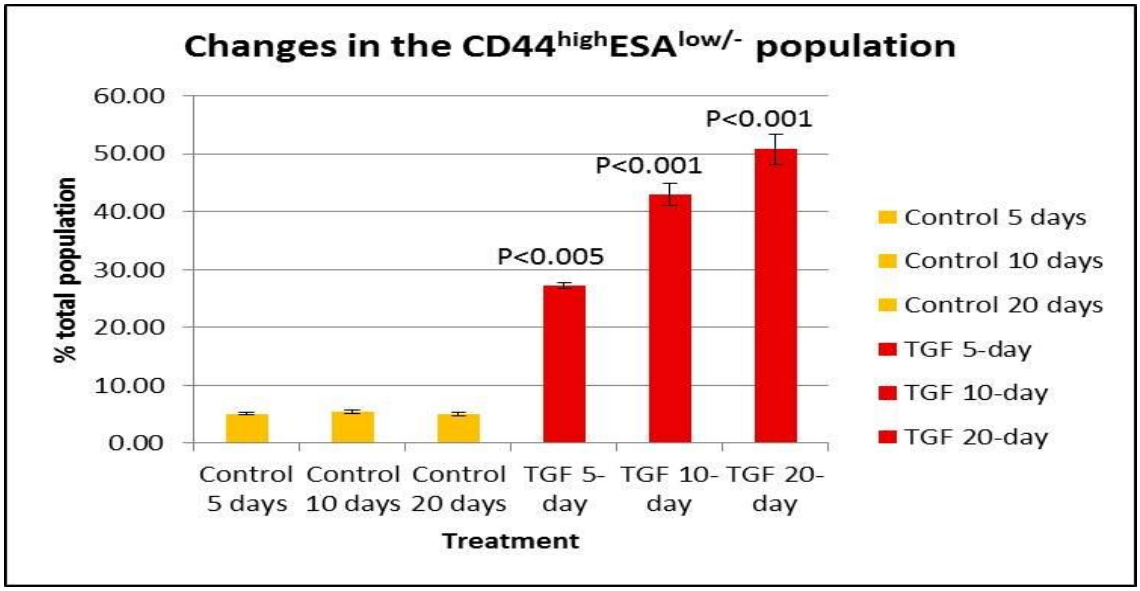

Figure 2.94: Long-term treatment with TGF-β and its effect on $CD44^{high}ESA^{low}$ cells. Changes in the $CD44^{high}ESA^{low}$ population when control cells were compared to those treated with TGF-β for 5, 10 and 20 days. The percentage of cells gated as the $CD44^{high}ESA^{low}$ population is 5.1±0.21% in control cells. This rises highly significantly after treatment with TGF-β for 5 (27.19±0.44%), 10 (42.94±1.99%) and 20 (50.78±2.63) days. Overall, there is a progressive rise in the percentage of $CD44^{high}ESA^{low}$ cells with all the treatments.

b) CD44^{high}

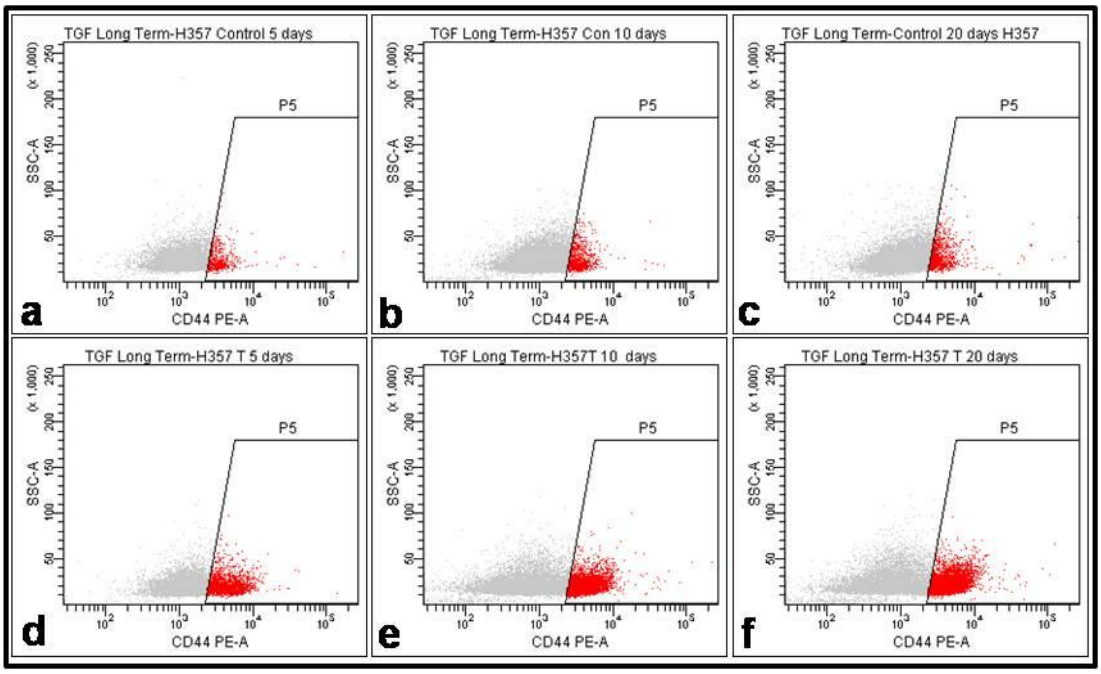

Figure 2.95: FACS analysis of H357 cells stained with CD44 (x-axis). The y-axis denotes side-scatter.FACS analysis of the CD44^{high} population (red) within the H357 cell line and changes in the size of this population when control samples (a-c) were compared to those treated with TGF-β for 5 days (d), 10 days (e) and for 20 days (f). The gated cells (red) represent the CD44^{high} cells, the putative stem cell population. Treatment with TGF-β for 5 and 10 days causes a rise in this population but the effect of treatment with 20 days is the same as that seen with 10-day treatment.

Condition	I	II	III	% CD44^{high}	SEM
5 days Control	**5.40**	5.17	5.18	**5.25**	0.13
10 days Control	5.07	4.53	5.10	**4.90**	0.32
20 days Control	4.07	3.80	3.97	**3.95**	0.14
5 days TGFβ	22.50	26.47	28.65	**25.87**	3.12
10 days TGFβ	35.28	38.33	36.83	**36.81**	1.53
20 days TGFβ	39.50	40.13	40.97	**40.20**	0.74

Table 2.38: The effect of long-term treatment with TGF-β on CD44^{high}H357 cells.

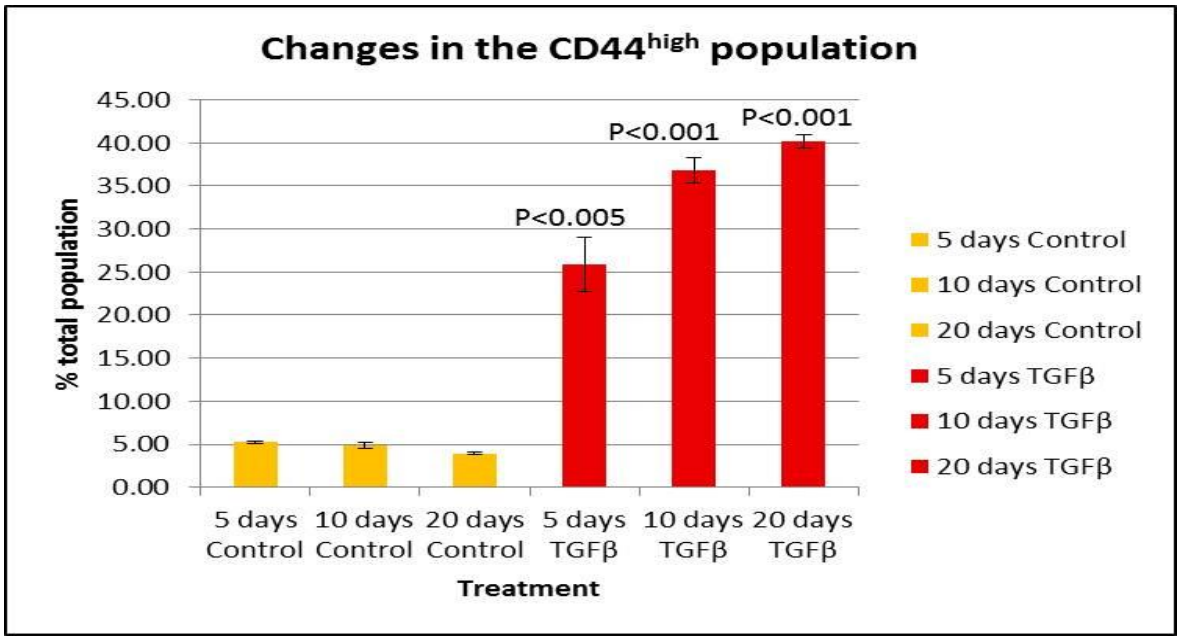

Figure 2.96: Long-term treatment with TGF-β and its effect on CD44^{high} cells. Changes in the CD44^{high} population in H357 cells when control cells were compared to those treated with TGF- β for 5, 10 and 20 days. The percentage of CD44^{high} cells gated in the controls was 5.25±0.13%, and rises significantly after treatment with TGF-β for 5 (25.87±3.12%), 10 (36.81±1.53%) and 20 (40.2±0.74%) days. This increase correlates with the increase in the CD44^{high}ESA^{low} population indicating that most of the CD44 ^{high} cells were also low for ESA.

c) ESA$^{low/-}$

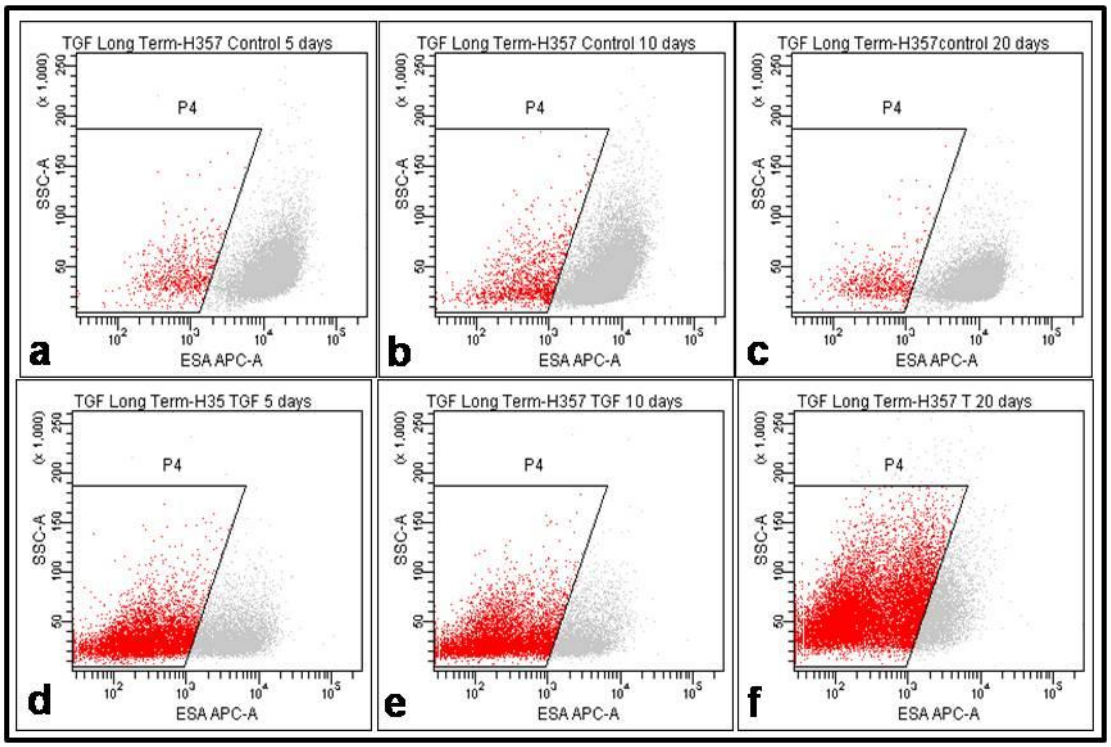

Figure 2.97: FACS analysis of H357 cells stained with ESA (x-axis). The y-axis denotes side-scatter.FACS analysis of the ESA$^{low/-}$ population (red) within the CA1 cell line and changes in the size of this population when control cells (a-c) were compared to those treated with TGF-β for 5 days (d), 10 days (e), and for 20 days (f). The gated cells (red) represent the ESA$^{low/-}$cells that are shedding their epithelial state and becoming more mesenchymal. The number of ESA$^{low/-}$ cells increases progressively with treatment (d-f).

Condition	I	II	III	% ESA$^{low/-}$	SEM
5 days Control	5.23	5.10	5.12	**5.15**	0.07
10 days Control	6.87	6.27	6.41	**6.51**	0.31
20 days Control	5.80	6.17	6.12	**6.03**	0.20
5 days TGFβ	33.00	30.00	31.02	**31.34**	1.53
10 days TGFβ	57.23	50.00	50.99	**52.74**	3.92
20 days TGFβ	70.33	68.50	70.04	**69.62**	0.98

Table 2.39: The effect of long-term treatment with TGF-β on ESA^{low} H357 cells

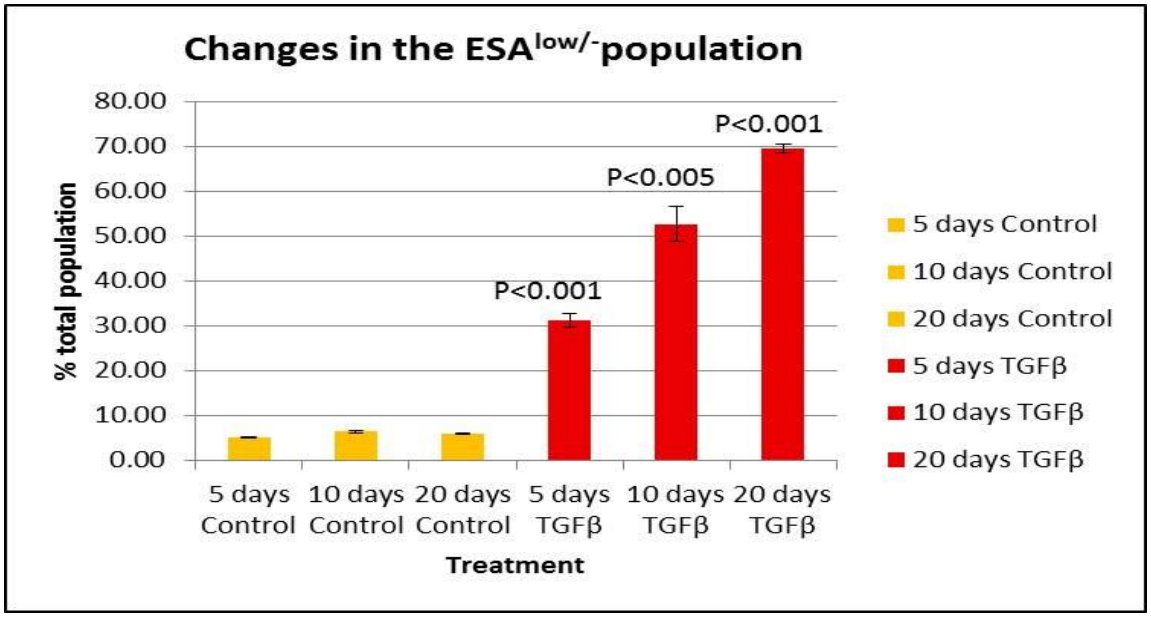

Figure 2.98: Long-term treatment with TGF-β and its effect on ESA$^{low/-}$ cells. The figure above shows the changes in the ESA$^{low/-}$ population in CA1 cells when controls were compared to cells treated with TGF-β for 5, 10 and 20 days. The percentage of ESA$^{low/-}$ cells gated in the controls was 5.15±0.07%. This rose significantly when treated with TGF-β for 5 (31.34±1.53%), 10 (52.74±3.92%) and 20 (69.62±0.98%) days. The percentage of ESA$^{low/-}$ cells increases progressively with treatments.

II) The effect of TGF-β withdrawal on OSCC cell lines

i) CA1 cell line:

(a) $CD44^{high}ESA^{low}$

Condition	I	II	III	% $CD44^{high}ESA^{low}$	STDEV
Control	1.23	1.56	2.32	**1.70**	0.56
5 days TGFβ	10.03	9.52	10.47	**10.01**	0.48
5 days TGFβ, 5 days withdrawal	8.10	8.65	9.60	**8.78**	0.76
5 days TGFβ, 15 days withdrawal	4.73	4.63	3.81	**4.39**	0.50

Table 2.40: The effect of TGF-β withdrawal on $CD44^{high}ESA^{low}$ CA1 cells

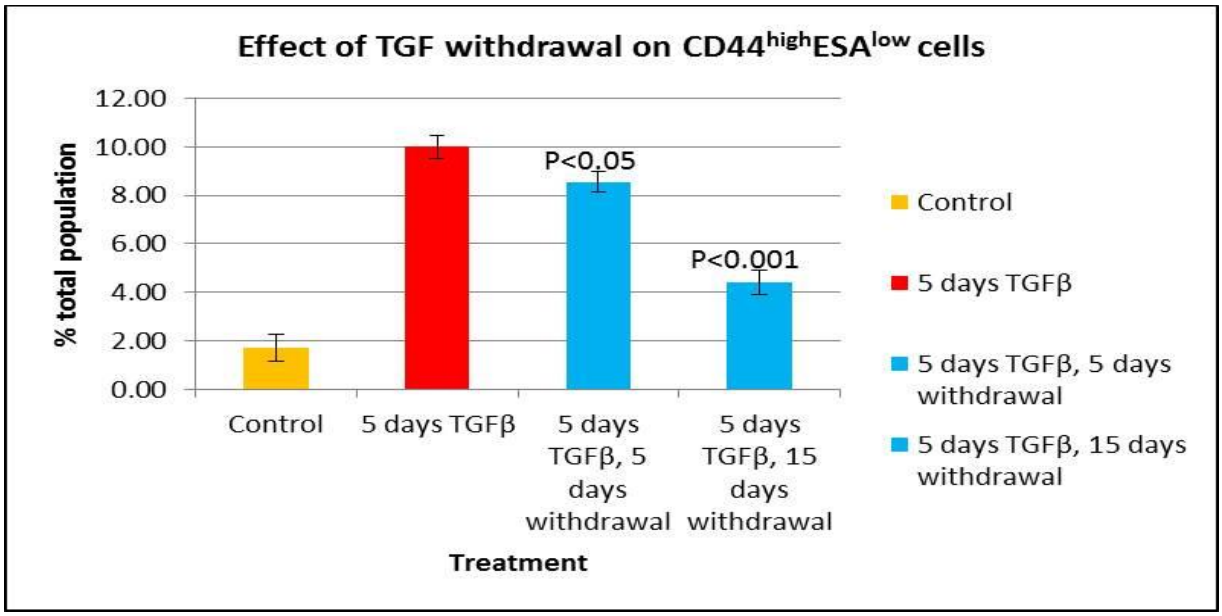

Figure 2.99: Withdrawal of TGF-β and its effect on $CD44^{high}ESA^{low}$ cells. The effect of withdrawing TGF-β treatment on the proportion of $CD44^{high}ESA^{low}$ cells within the CA1 cell line. Control samples were compared to samples treated with TGF-β for 5 days, and those that had been treated with TGF-β and further grown under control conditions for a further 5 and 15 days. Withdrawal of TGF-β causes a reduction in the percentage of **$CD44^{high}ESA^{low}$** cells and indicates that the effect of TGF treatment is reversible. However the proportion of these cells still remains higher than the controls indicating that not all cells have switched back within 15 days.

(b) CD44^{high}

Condition	I	II	III	% CD44^{high}	SEM
5 days Control	5.17	5.17	5.27	**5.20**	0.06
5 days TGFβ	12.53	12.43	11.78	**12.25**	0.41
5 days TGFβ, 5 days withdrawal	11.05	10.10	11.30	**10.82**	0.63
5 days TGFβ, 15 days withdrawal	7.13	7.43	6.63	**7.06**	0.40

Table 2.41: The effect of TGF-β withdrawal on CD44^{high} CA1 cells

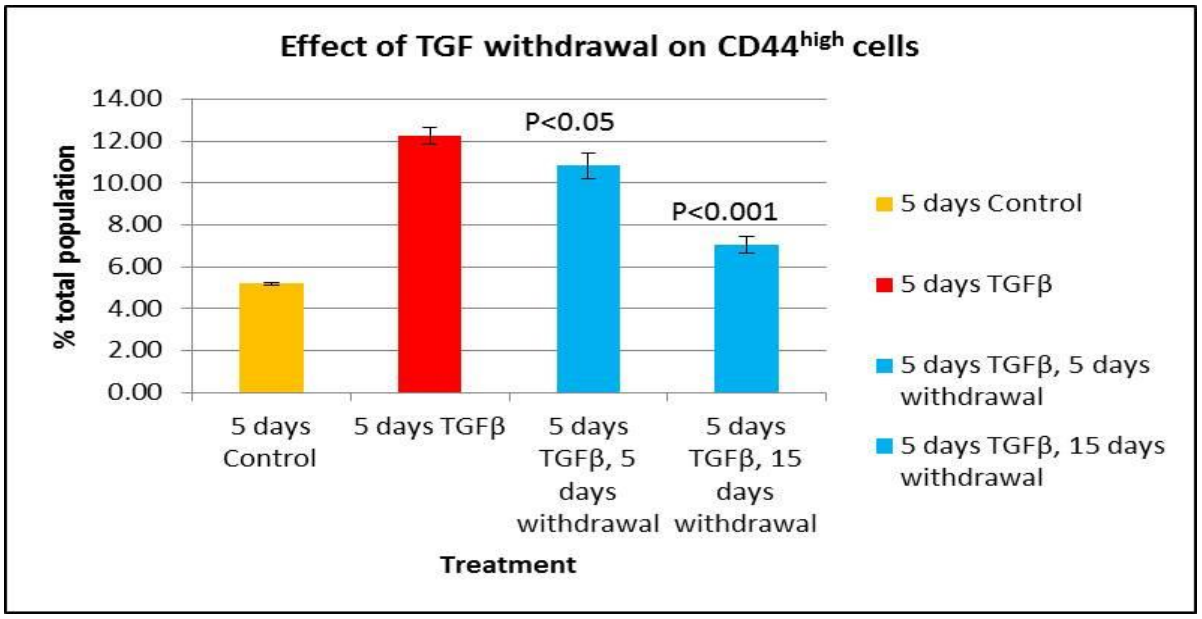

Figure 2.100: Withdrawal of TGF-β and its effect on CD44^{high} cells. The effect of withdrawing TGF treatment on the proportion of CD44^{high} cells within the CA1 cell line. Control samples were compared to those treated with TGF-β for 5 days, and those that had been treated with TGF-β and grown under control conditions for a further 5 and 15 days. Withdrawal of TGF-β causes a significant lowering in the percentage of CD44^{high} cells indicating that the effect of TGF-β treatment is reversible and by day 15 they almost resemble control samples.

(c) ESA$^{low/-}$

Condition	I	II	III	% ESA$^{low/-}$	SEM
5 days Control	5.20	5.40	5.28	**5.29**	0.10
5 days TGFβ	36.70	34.77	30.91	**34.13**	2.95
5 days TGFβ, 5 days withdrawal	36.47	33.45	29.28	**33.07**	3.61
5 days TGFβ, 15 days withdrawal	10.50	10.24	11.43	**10.72**	0.63

Table 2.42: The effect of TGF-β withdrawal on ESA^{low} CA1 cells

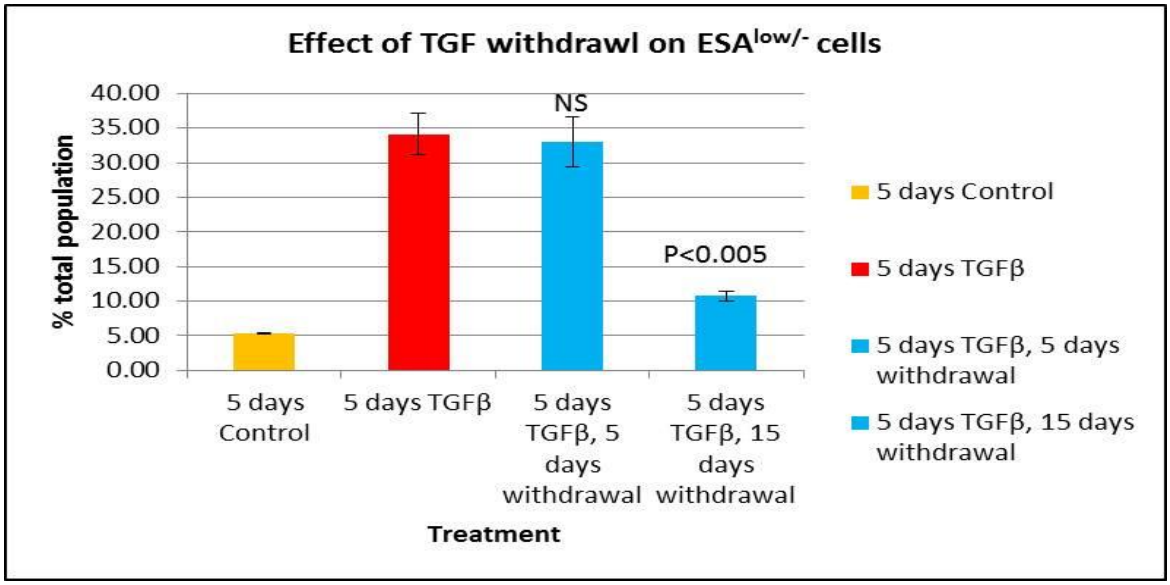

Figure 2.101: Withdrawal of TGF-β and its effect on ESA$^{low/-}$ cells. The effect of withdrawing TGF-β treatment on the proportion of ESA$^{low/-}$ cells within the CA1 cell line. Control samples were compared to samples treated with TGF-β for 5 days and those that had been treated with TGF-β and grown under control conditions for a further 5 and 15 days. Withdrawl of TGF-β for 5 days did not cause a significant reduction in the proportion of ESA$^{low/-}$ cells (33.07±3.61%). However, after 15 days of withdrawl, the percentage of ESA$^{low/-}$ cells reduced significantly (10.72±0.63%), indicating that the effect of TGF-β on ESA in OSCC lines is largely reversible.

ii) H357 cell line

(a) $CD44^{high}ESA^{low}$

Condition	I	II	III	% $CD44^{high}ESA^{low}$	SEM
Control	1.23	2.43	2.82	**2.16**	0.83
5 days TGFβ	10.03	9.93	10.30	**10.09**	0.19
5 days TGFβ, 5 days withdrawal	7.73	8.30	9.03	**8.36**	0.65
5 days TGFβ, 15 days withdrawal	4.80	5.90	6.20	**5.63**	0.74

Table 2.43: The effect of TGF-β withdrawal on $CD44^{high}ESA^{low}$ CA1 cells

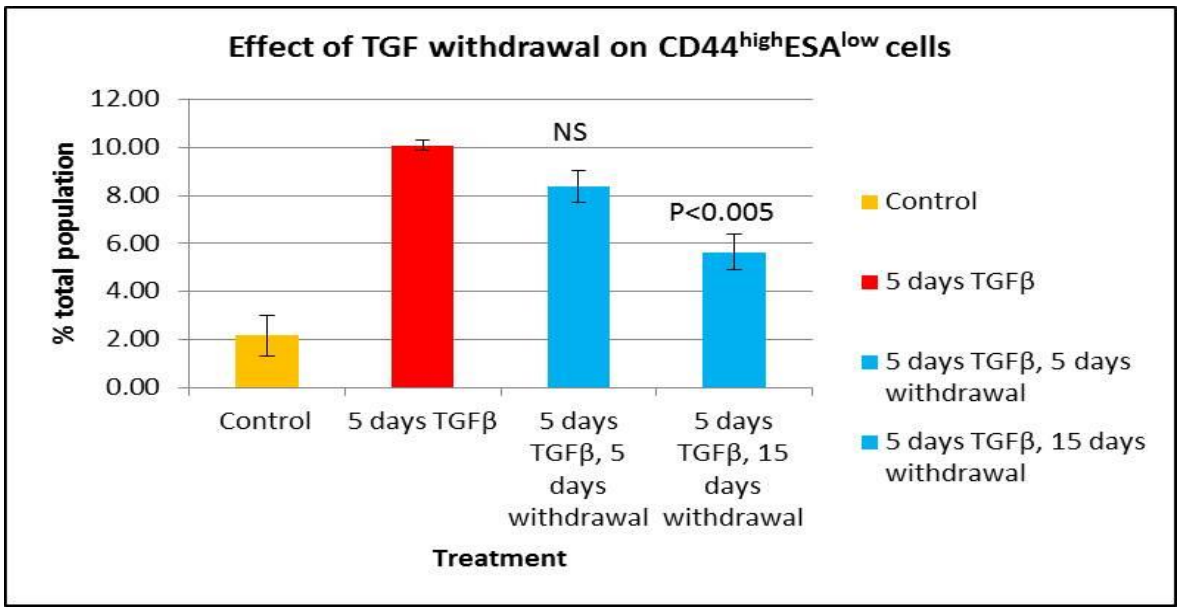

Figure 2.102: Withdrawl of TGF-β and its effect on $CD44^{high}ESA^{low}$ cells. The effect of withdrawing TGF-β treatment on the proportion of $CD44^{high}ESA^{low}$ cells within the H357 cell line. Control samples were compared to samples treated with TGF-β for 5 days, and those that had been treated with TGF-β and grown under control conditions for a further 5 and 15 days. Withdrawal of TGF-β causes a reduction in the percentage of **$CD44^{high}ESA^{low}$** cells and indicates that the effect of TGF-β treatment is reversible. However the proportion of these cells still remains higher than the controls indicating that some EMT cells have not switched back within 15 days.

(b) CD44^{high}

Condition	I	II	III	% CD44^{high}	SEM
5 days Control	5.17	5.33	5.25	5.25	0.08
5 days TGFβ	12.53	13.10	14.00	13.21	0.74
5 days TGFβ, 5 days withdrawal	9.13	11.50	12.10	10.91	1.57
5 days TGFβ, 15 days withdrawal	7.13	7.40	8.10	7.54	0.50

Table 2.44: The effect of TGF-β withdrawal on CD44^{high} H357 cells

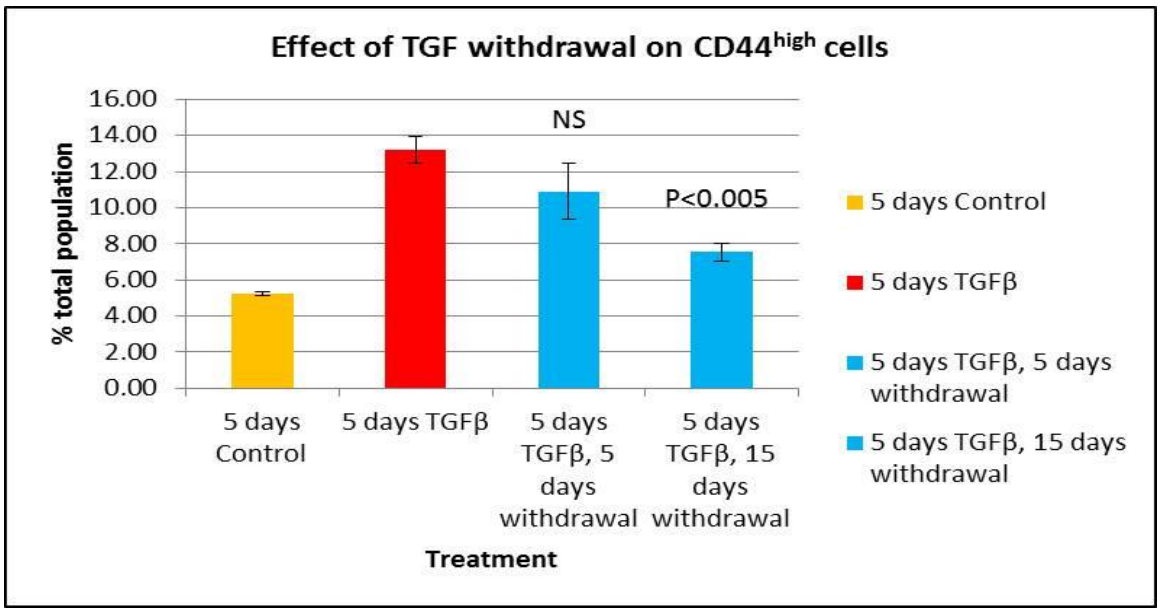

Figure 2.103: Withdrawal of TGF-β and its effect on CD44^{high} cells. The effect of withdrawing TGF treatment on the proportion of CD44^{high} cells within the H357 cell line. Control samples were compared to those treated with TGF-β for 5 days, and those that had been treated with TGF-β and grown under control conditions for a further 5 and 15 days. Withdrawal of TGF-β causes a significant lowering in the percentage of CD44^{high} cells indicating that the effect of TGF treatment is reversible and by day 15 they resemble control samples.

(c) ESA$^{low/-}$

Condition	I	II	III	% ESA$^{low/-}$	SEM
5 days Control	5.20	5.23	5.23	**5.22**	0.02
5 days TGFβ	36.70	33.00	33.00	**34.23**	2.14
5 days TGFβ, 5 days withdrawal	36.47	26.63	31.63	**31.58**	4.92
5 days TGFβ, 15 days withdrawal	14.83	19.53	19.53	**17.97**	2.71

Table 2.45: The effect of TGF-β withdrawal on ESA$^{low/-}$ H357 cells

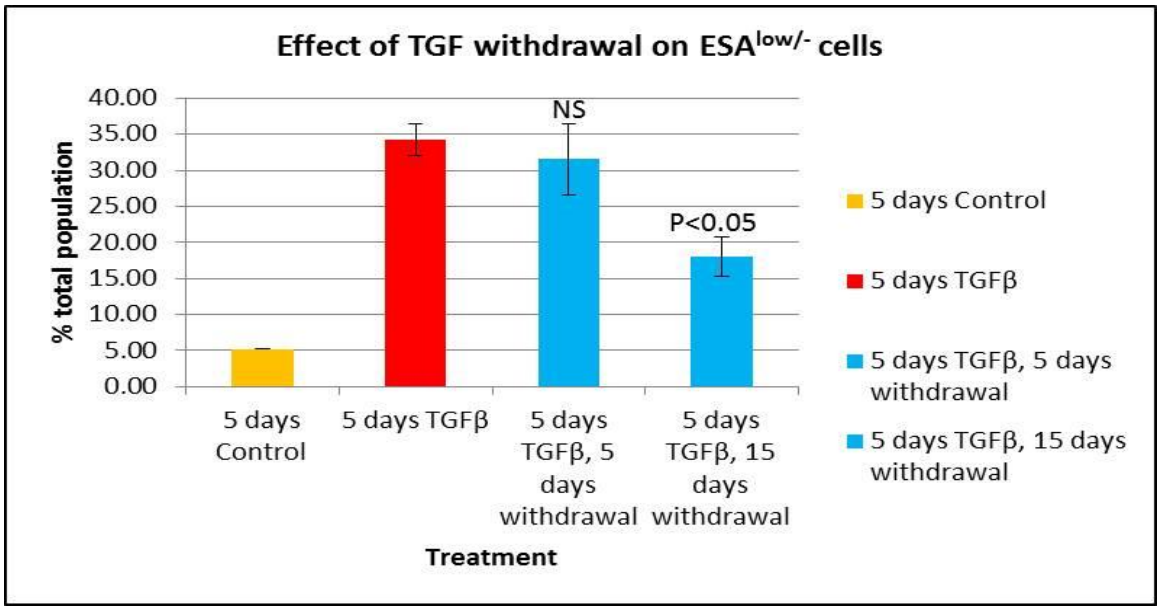

Figure 2.104: Withdrawal of TGF-β and its effect on ESA$^{low/-}$ cells. The effect of withdrawing TGF-β treatment on the behaviour of ESA$^{low/-}$ cells within the H357 cell line is demonstrated above. Control samples were compared to samples treated with TGF-β for 5 days and those that had been treated with TGF-β and grown under control conditions for a further 5 and 15 days. Withdrawl of TGF-β causes a significant reduction in the proportion of ESA$^{low/-}$ cells after withdrawl for 5 (31.58±4.92%) and 15 (17.97±2.71%) days. A large proportion of cells still remain ESA$^{low/-}$ indicating that they have not switched back from the EMT phenotype.

2.6.4 Discussion

Treatment with TGF-β for 5 days caused an increase in the relative proportion of $CD44^{high}ESA^{low}$, $CD44^{high}$ and $ESA^{low/-}$ cells within the bulk of the population. Treatment with TGF-β for longer indicated that this further increased the size of these populations. At the end of twenty days, very few cohesive cells remained. The response of the two cell lines studied varied with the H357 cells showing more susceptibility to TGF-β treatment compared to the CA1 cell line. The number of cells expressing high levels of CD44 increased in both lines examined and this correlated with the increase in the $CD44^{high}ESA^{low}$ population. TGF-β also caused a decrease in the expression of ESA and the response shown by the H357 cell line was greater than that for CA1 cells.

For both lines, withdrawing TGF-β treatment caused a decrease in the $CD44^{high}ESA^{low}$ population. By day 15, after withdrawal of TGF-β, the proportion of $CD44^{high}ESA^{low}$ cells declined in both cell lines but remained higher than the controls, suggesting that the effect of TGF-β is largely but slowly reversible. That some of the cell remained $CD44^{high}ESA^{low}$ even after 15 days of withdrawal, suggests that there may be a small proportion of $CD44^{high}ESA^{low}$ cells that does not revert back.

The next questions asked were:

Do these cells ($CD44^{high}ESA^{low}$) have the ability for self-renewal and do they possess stem potential?

Do treated cells show increased motility and migration?

2.8 The self-renewal potential of intrinsic populations within OSCC cell lines

2.8.1 Introduction

This chapter will deal with the questions raised from the previous experiments about the $CD44^{high}ESA^{low}$ population of cells within the cell lines. Mani and co-workers suggested that EMT generates cells with the properties of stem cells. As TGF-β seems to more or less exclusively affect this $CD44^{high}ESA^{low}$ population and these represents the cells that have undergone EMT, we were interested to find out whether these cells have self-renewal and clonogenic potential. Further, invasiveness and migratory tendencies are also properties possessed by stem-like cells. For this experiment, cells from both the cell lines examined previously, CA1 and H357 were sorted into three quadrants that were $CD44^{high}ESA^{low}$, $CD44^{high}ESA^{high}$ and $CD44^{low}(ESA^{high})$. It has already been shown in the previous sections that CD44 enriches for cells with the stem cell property of clonogenicity and self-renewal. In breast cancer a stem like proportion of cells was isolated which was $CD44^{high}ESA^{low}$ and $CD24^{low}$. The rationale behind this study is that if cells have stem cell ability, then they should be able to reconstitute the cellular heterogeneity or hierarchy of cells detected with FACS analysis. Hence cells from these three quadrants were sorted into collecting tubes and plated out at clonal density. They were allowed to grow/recover for five days and then detached from the dish and analyzed using the FACS Canto (BD) machine and BDFACSDiva software to check whether cellular heterogeneity had been restored.

2.8.2 Materials and Methods

The methods and rationale for FACS has been discussed in previous sections (2.3.2, 2.4.2)

2.8.3 Results

1 FACS

a) Sorting

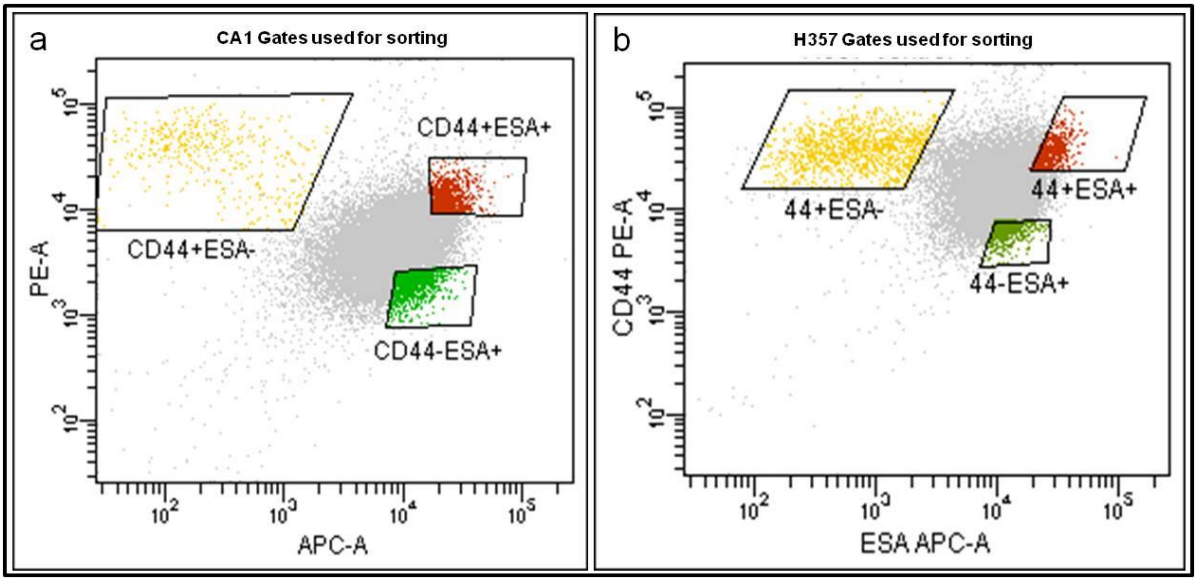

Figure 2.105: Sorting of CA1 and H357 cells. Representative FACS plots for CA1 (a) and H357 (b) cells co-stained with CD44 (y-axis) and ESA (x-axis) antibody. The gated populations are $CD44^{high}ESA^{low}$ (yellow), $CD44^{high}ESA^{high}$ (red) and $CD44^{low}ESA^{high}$ (green). Cells from the three populations were simultaneously sorted and plated at clonal density and cultured. After 5-7 days, cells were detached and analyzed for co-expression of CD44 and ESA to check whether cellular heterogeneity was restored. For controls, cell were passed through the sorter and plated out at clonal density.

(b) OSCC re-plate Analysis

(i) $CD44^{high}ESA^{high}$re-plate

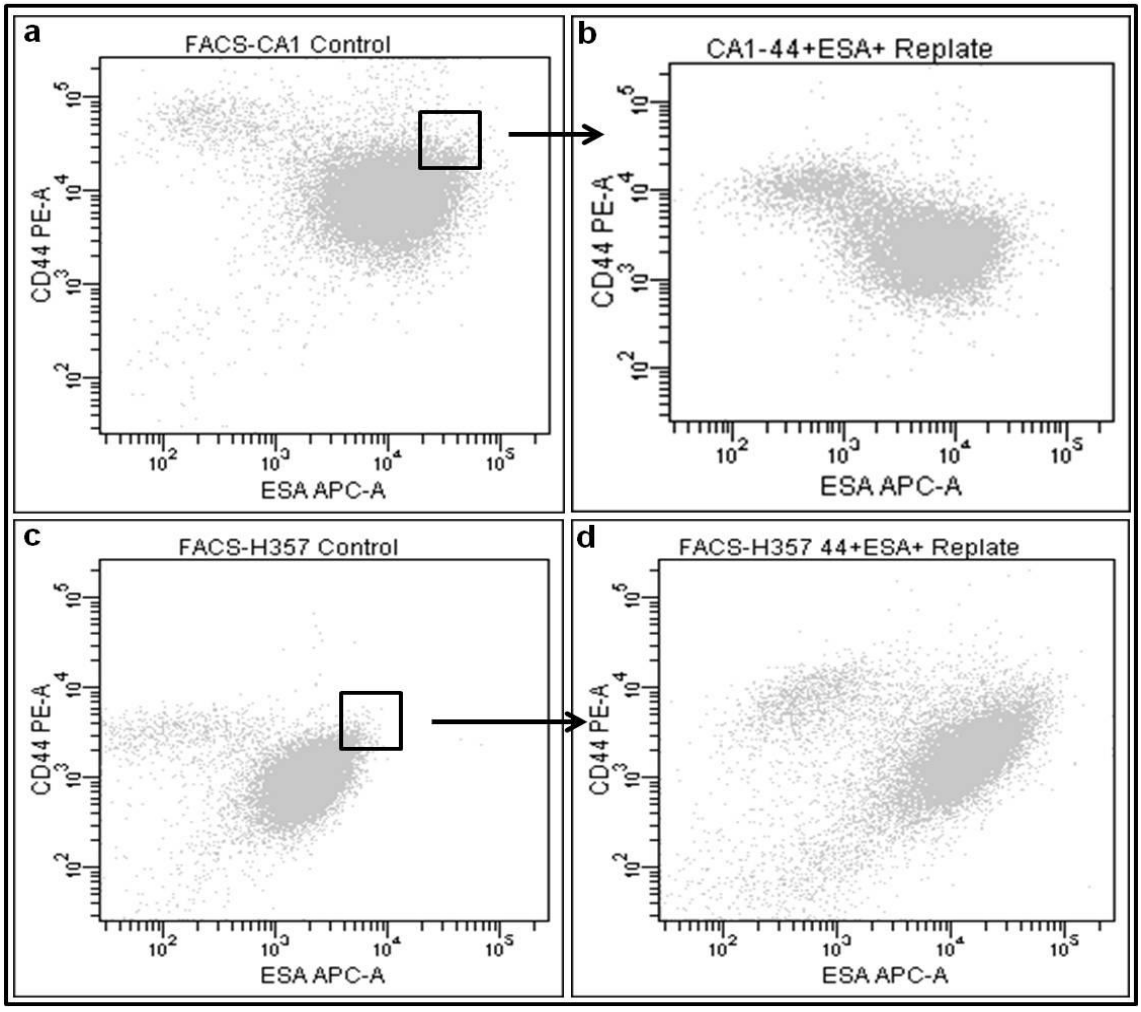

Figure 2.106: FACS analysis of sorted $CD44^{high}ESA^{high}$ OSCC cells. The FACS plots obtained for control CA1 (a) and H357 (c) cells, compared to those generated by culture of sorted $CD44^{high}ESA^{high}$ cells (b, d), stained CD44 (PE, y-axis) and ESA (APC, x-axis) antibodies.

The sorted $CD44^{high}ESA^{high}$ population seems to fully restore cellular heterogeneity of CA1 (b) and H357 (d) cells, and generate characteristic FACS plots normally seen for these cell lines. The main bulk of the cells stain high for CD44 and ESA forming the main bulk of the population and a characteristic $CD44^{high}ESA^{low}$ tail is seen to the left of this.

(ii) $CD44^{high}ESA^{low}$re-plate

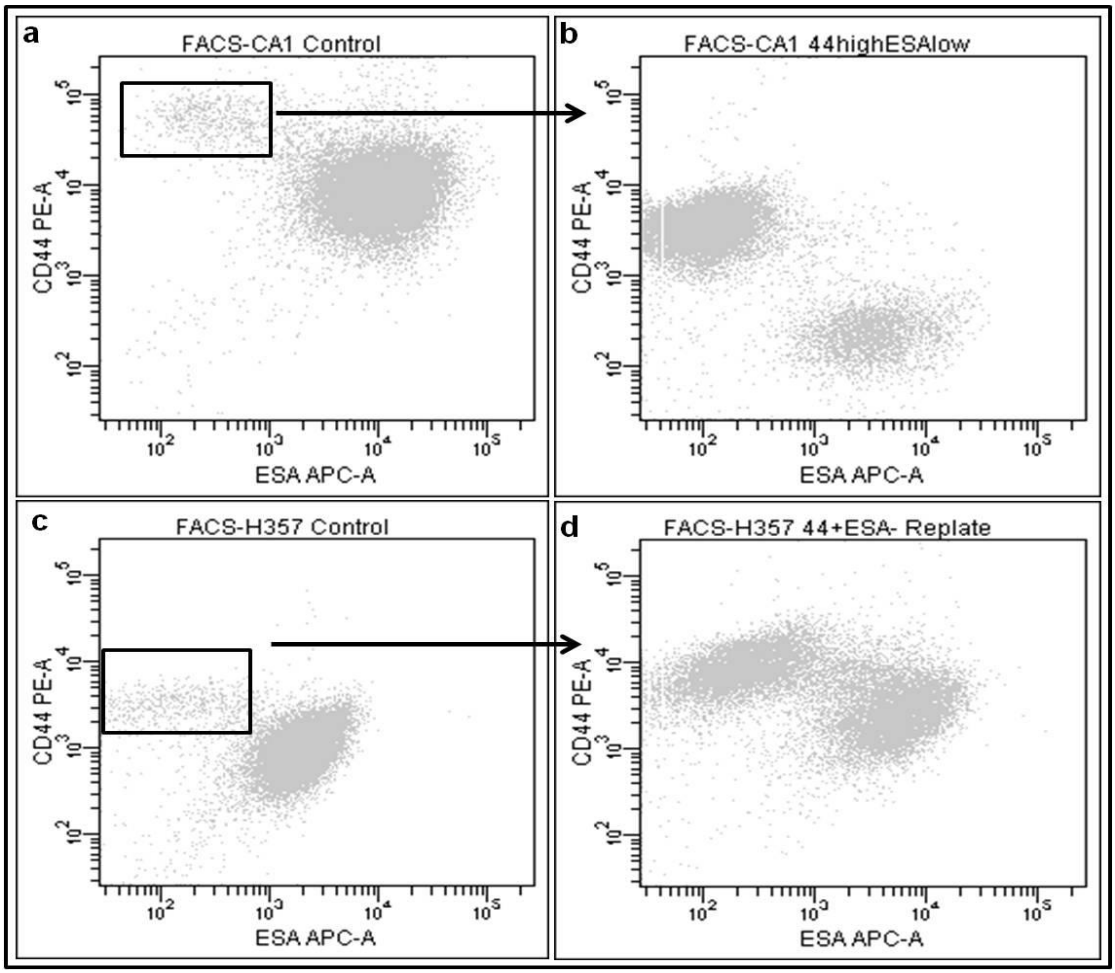

Figure 2.107: FACS analysis of sorted $CD44^{high}ESA^{low}$ OSCC cells. The FACS plots obtained for control cells CA1 (a) and H357 (c) cells, compared to those generated by culture of sorted $CD44^{high}ESA^{low}$ cells (b, c), stained with CD44 (PE, y-axis) and ESA (APC, x-axis) antibodies.

The sorted $CD44^{high}ESA^{low}$ population also restores cellular heterogeneity for CA1 (b) and H357 (d) cells generating similar FACS plots normally seen for these cell lines. For both lines examined, a higher proportion of $CD44^{high}ESA^{low}$ cells is seen compared to control plots.

(iii) CD44^{low}ESA^{high}re-plate

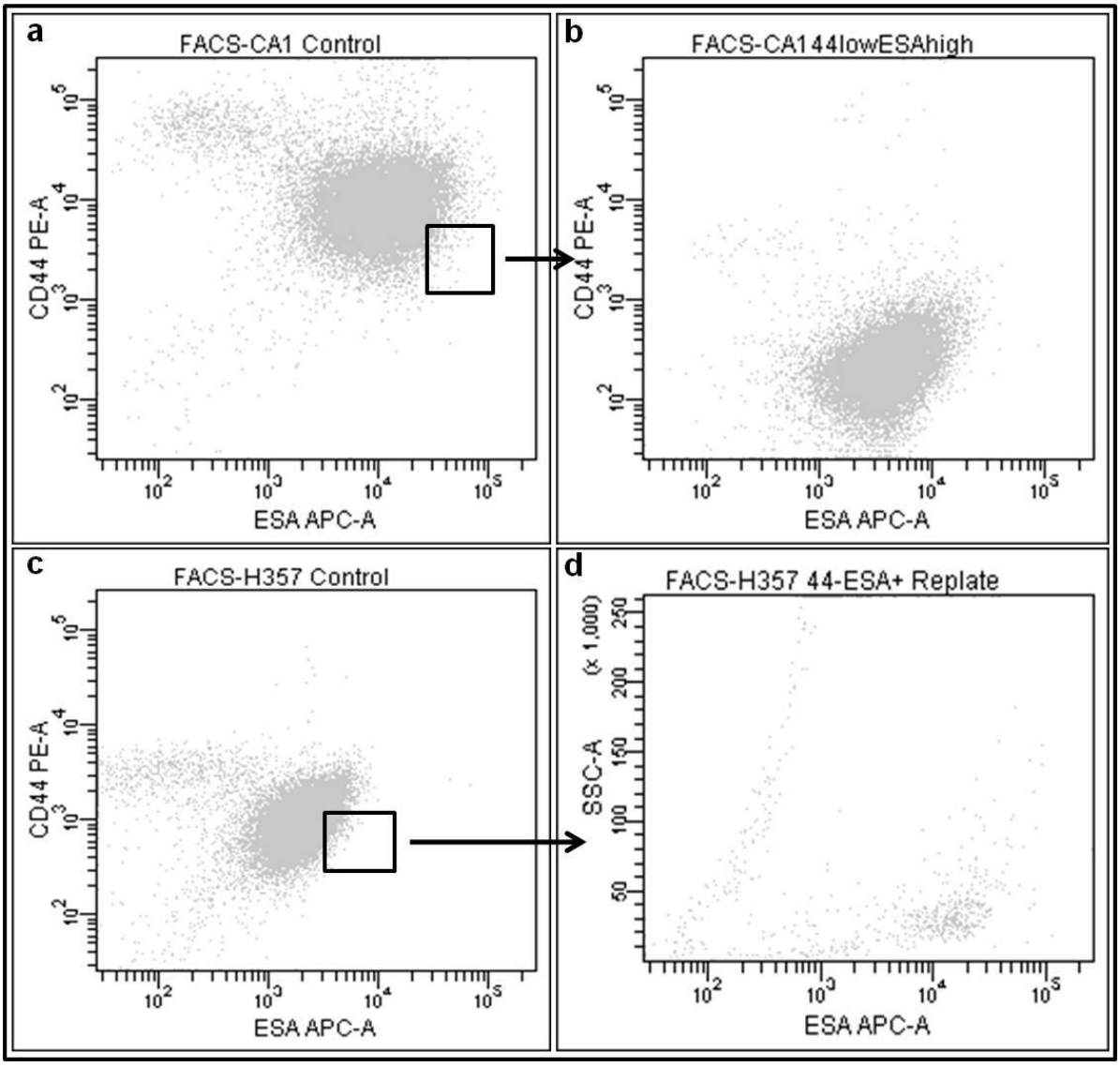

Figure 2.108: FACS analysis of sorted CD44^{low} OSCC cells. The FACS plots for control CA1 (a) and H357 (c) cells, compared to those from cultures of sorted CD44^{low}ESA^{high} cells, stained with CD44 (PE, y-axis) and ESA (APC, x-axis) antibodies. The sorted CD44^{low}ESA^{high} population does not reconstitute the characteristic facsplots seen for CA1 (b) and H357 (d) cell lines, with most of the cells being CD44^{low}, and showing poor clonogenicity when cultured.

(2) Cell morphology generated by sorted CD44^{high}ESA^{low} and CD44^{high}ESA^{high}OSCC cells

(i) CA1 cell line

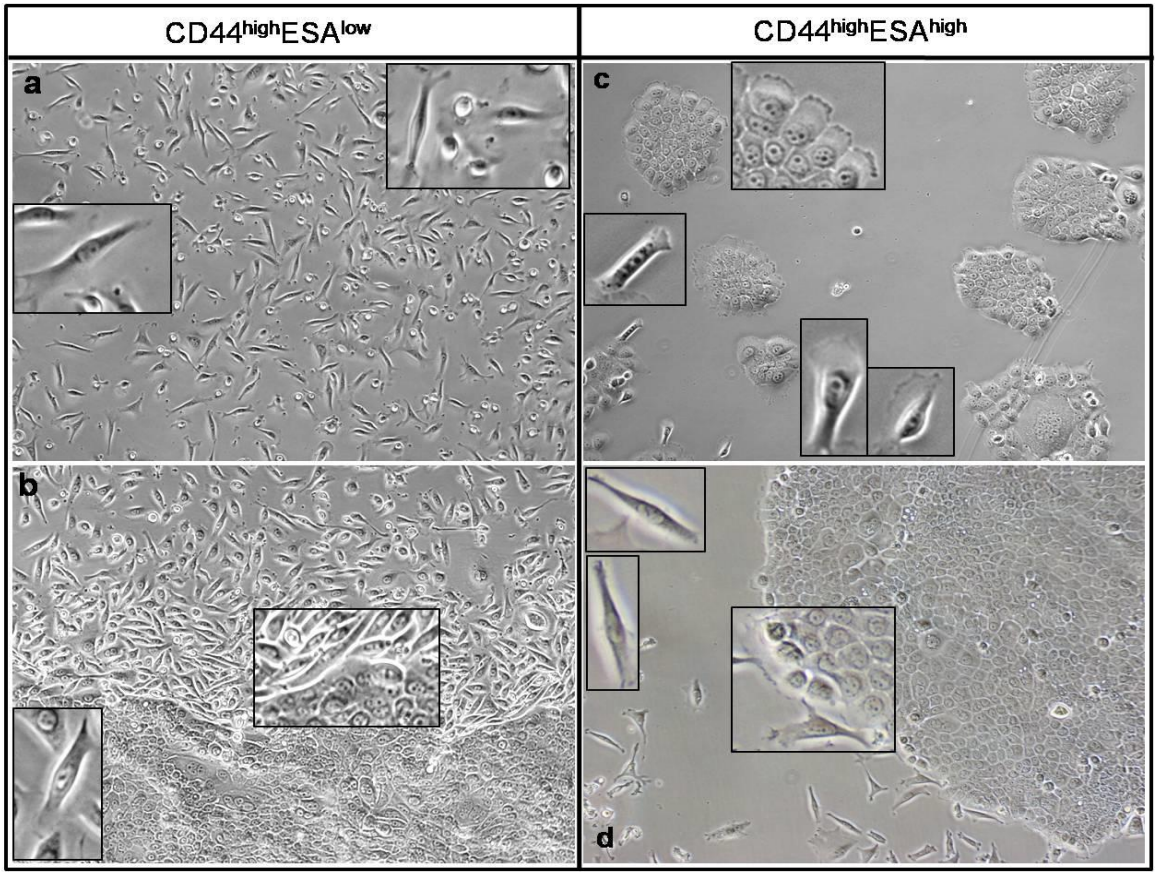

Figure 2.109: Colony morphology shown by sorted CA1 cell populations when replated. The colony morphologies generated when CD44^{high}ESA^{low} cells (a, b) and CD44^{high}ESA^{high} (c, d) cells were sorted out of the main population and replated at clonal density. CD44^{high}ESA^{low} cells give rise to two different types of cells. There were cells among these that form large scattered holoclone-like colonies (a) and show characteristic cobblestone morphology with a pronounced ring of spindle cells that look like fibroblasts and circled the colony. The other type formed clusters of elongated cells that were ovoid and spindle- like in appearance. CD44^{high}ESA^{high} cells when plated out retain their epithelial morphology and form mostly holoclones among meroclones and paraclones (c), made up of cobblestone cells. These grow up to a large size and there are also moderate numbers of spindle shaped and ovoid motile cells seen around the edges of these that resemble fibroblasts.

(ii) H357 cell line

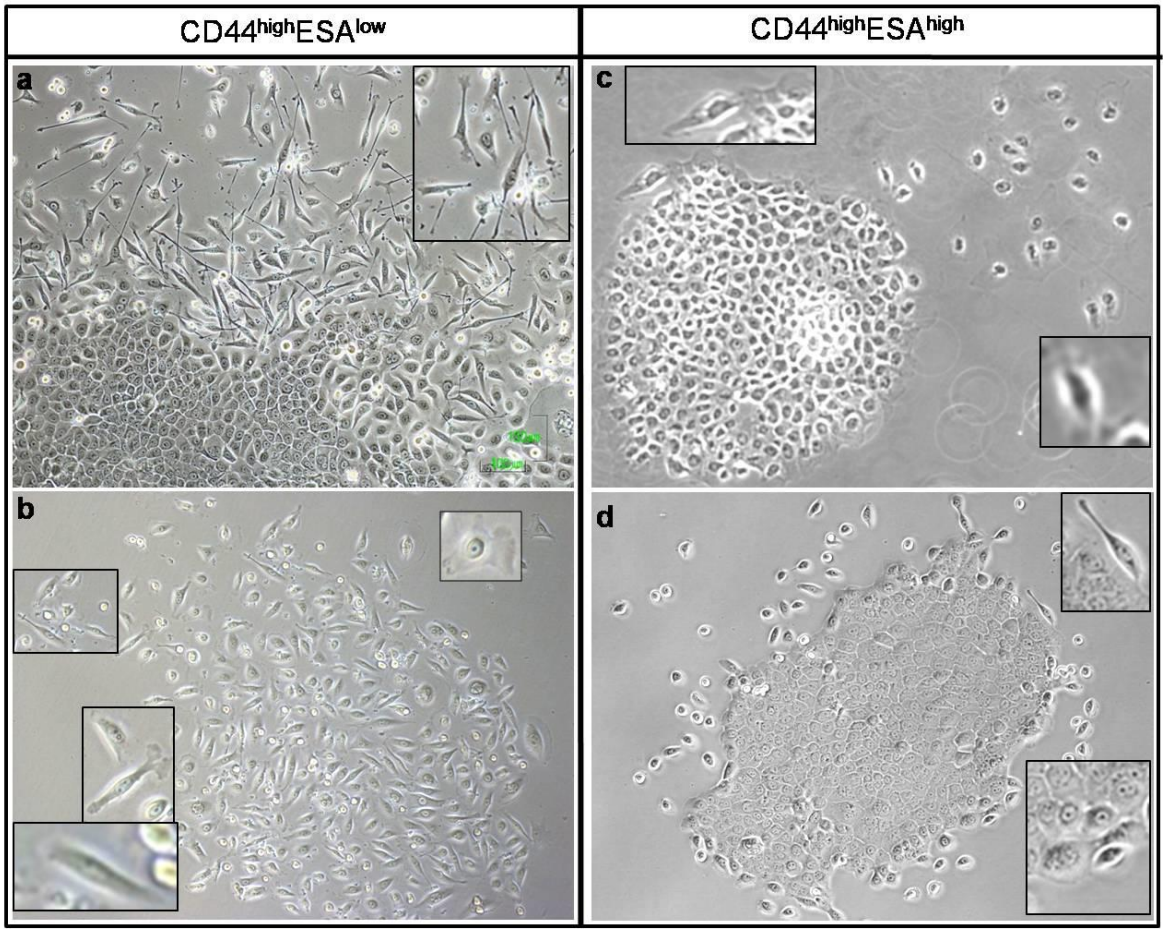

Figure 2.110: Colony morphology shown by sorted H357 cell populations when replated. The colony morphologies generated when $CD44^{high}ESA^{low}$ cells (a, b) and $CD44^{high}ESA^{high}$ (c, d) cells were sorted out of the main population and replated at clonal density. $CD44^{high}ESA^{low}$ cells give rise to two different types of cells. There were cells among these that form large holoclone-like colonies (a) and show characteristic cobblestone morphology with a pronounced ring of spindle cells that look like fibroblasts and circled the colony. The other type formed clusters of elongated cells that were ovoid and spindle- like in appearance. $CD44^{high}ESA^{high}$ cells when plated out retain their epithelial morphology and form mostly holoclones among meroclones and paraclones, made up of cobblestone cells. There are spindle shaped and ovoid motile cells seen around the edges of these that resemble fibroblasts.

2.8.4 Discussion

The aim of this experiment was to ascertain whether the EMT fraction within OSCC, the $CD44^{high}ESA^{low}$ cells, had stem cell potential and whether they could restore cellular heterogeneity seen in OSCC lines. To check this, FACS sorted $CD44^{high}ESA^{low}$ cells were compared to $CD44^{high}ESA^{high}$ cells, the known stem fraction within OSCC lines and $CD44^{low}$ cells that are thought to be differentiated cells with no stem potential. Sorted cells were grown from clonal density and then analyzed for differences in morphology and for co-expression of CD44 and ESA. $CD44^{high}ESA^{high}$ cells grew, predominantly as holoclones and showed characteristic morphology seen in OSCC lines and spindle cells could be identified at the edges of the colonies or lying outside them. In comparison to these cells, $CD44^{high}ESA^{low}$ cells grew predominantly as elongated spindle cells with few scattered holoclone colonies that grow to a large size. In contrast, $CD44^{low}$ cells showed poor growth and formed paraclones. This suggested that the $CD44^{high}ESA^{high}$ cells were the non-EMT stem cell fraction while the $CD44^{high}ESA^{low}$ cells were EMT cells that contained some cells that could switch back to the non-EMT through the process of MET and collectively show that each can regenerate the other. It has now been shown that the majority of cells in the $CD44^{high}ESA^{high}$ subpopulation are bipotent by their ability to give rise to both non-EMT and EMT fractions seen within OSCC lines (Biddle et al, 2011) when sorted cells were allowed to recover and analyzed for CD44 and ESA co-expression. Collaborative work done in the lab has also shown that the $CD44^{high}ESA^{low/+}$ (nearer to the main population) have high ALDH1 activity and represent EMT cells that have stem potential as shown by their ability to fully restore cellular heterogeneity. This shows that there are cells present within OSCC lines that could undergo EMT, become migratory, and then switch back through the process of MET, and is also in support of the migrating stem cell hypothesis proposed by Brabletz and co-workers (2005) that states that malignant stem cells acquire two phenotypes, one that favours growth and proliferation and the other that favours migration and invasion involving transient expression of mesenchymal markers by cells (EMT) that could be reversed by mesenchymal to epithelial transition (MET) and seed the growth of metastases.

2.9 The effect of TNF-α on EMT in OSCC cell lines and the combined effect of TNF-α and TGF-β on these lines.

2.9.1 Introduction

This section deals with the effect of TNF-α on OSCC cell lines and the possible involvement of TGF-β in this interaction. Recent studies on breast cancer cell lines have implicated TNF-α in augmenting or positively reinforcing TGF-β-induced EMT in these lines. Asiedu and co-workers found that TNF used in conjunction with TGF-β generated breast cancer cells with EMT characteristics that showed lowered surface expression of E-Cadherin and increased expression of Vimentin. They were also able to show that these cells showed high self-renewal and clonogenicity judged by their ability to form spheres in culture. These cells also readily initiated tumours in mice and reconstituted tumour heterogeneity. Further the cells generated by treatment were also more resistant to anti-cancer drugs such as paclitaxel (Asiedu et al, 2011). Results discussed in the previous sections suggest that TGF-β causes EMT in OSCC cell lines and we were interested to see whether this effect could be enhanced by using both TNF-α and TGF-β together. The CA1 and H357 cell lines were again used for this as they express a readily identifiable population of EMT cells which stand out from other cells by being $CD44^{high}ESA^{low}$.

2.9.2 Materials and methods

The methods for FACS analysis have been previously discussed. (2.3.2, 2.4.2). TNF-α (R&D Systems) was resuspended in PBS and used at a concentration of 10ng/ml and added once to the culture medium every 24 hours.

2.9.3 Results

1) CA1 cells:

A) Cell Morphology

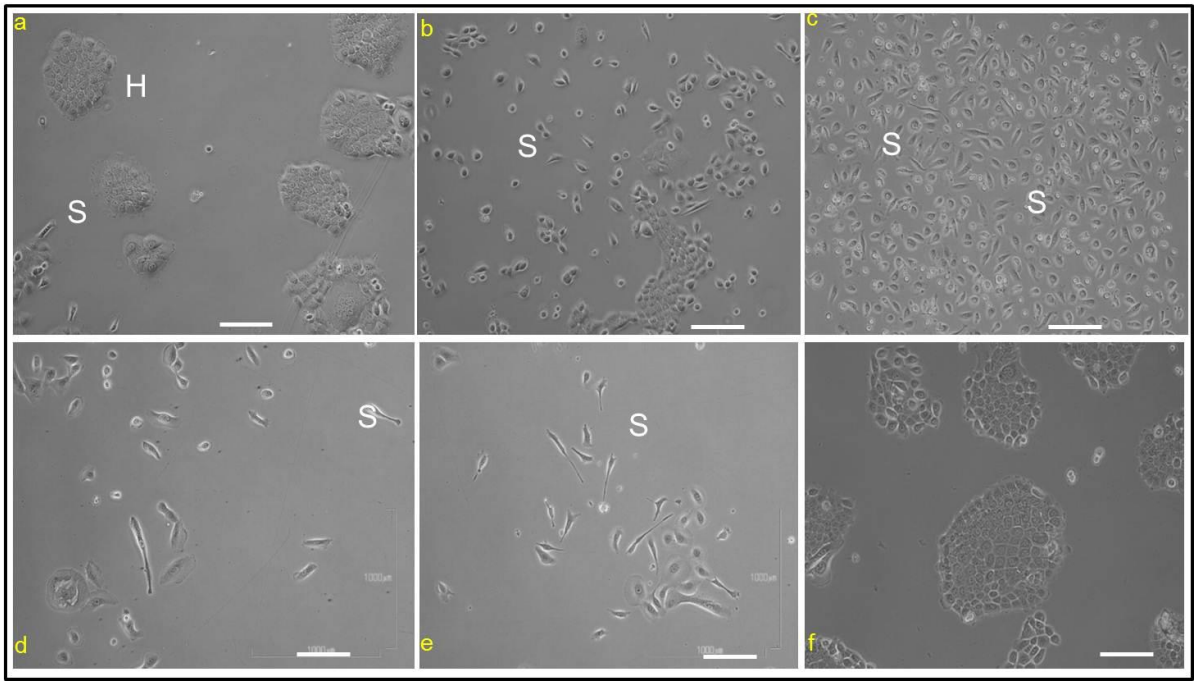

Figure 2.111: The effect of TNF-α on growth of CA1 cells. Cultures of CA1 cells grown under control conditions (a), with TGF-β (b), TNF-α and TGF-β (c), TNF-α (d), TNF-α + inhibitor (e), TGF-β + inhibitor. Control cells (a) show normal colony morphology and form holoclones (H), meroclones (M) and paraclones (P). Cells treated with TGF-β form spindle shaped cells with decreased colony formation. Cells with both TGF-β and TNF-α formed only elongated spindle cells resembling fibroblasts without any colony formation (c). Cells treated with TNF-β alone and TNF-α + inhibitor also displayed spindle morpholody with reduced colony formation (d, e).

B) FACS Analysis

a) $CD44^{high}ESA^{low}$

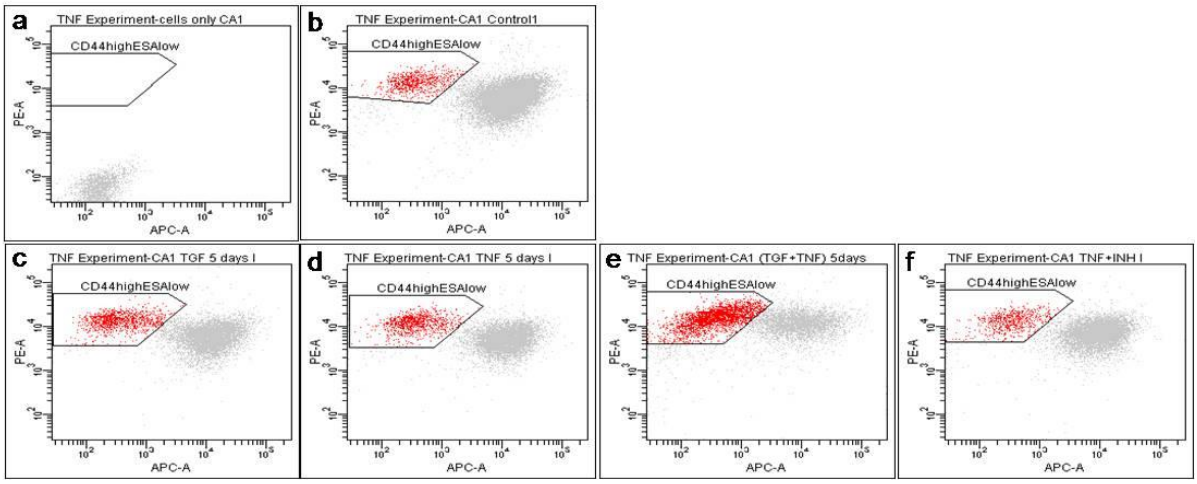

Figure 2.112: FACS analysis of CA1 cells stained with CD44 (y-axis) and ESA (x-axis) fluorescent antibodies

The FACS plots obtained when CA1 cells were stained with CD44 and ESA antibodies and analyzed for the effect of treatment with TGF-β and TNF-α on specifically the $CD44^{high}ESA^{low}$ population (gated, red). Panel (a) shows the analysis without any added antibody to adjust for background noise. Cells were analyzed as controls (b), cell treated with TGF-β (c), TNF-α (d), both TGF-β and TNF-α (e) and TNF-α added together with SB431542 (f).

Treatment with TGF-β and TNF-α alone causes the percentage of $CD44^{high}ESA^{low}$ cells to rise when they are added separately and both individually cause about the same increase. When both TGF-β and TNF-α are added together the percentage of $CD44^{high}ESA^{low}$ cells rises much more significantly as when they are added alone and the whole epithelial population shifts into the 44/ESA gate. When TNF-α and SB431542 are added together the gated population stays the same as controls.

$CD44^{high}ESA^{low}$	1	2	3	Average	SEM
Control	3.83	3.67	3.93	**3.81**	0.13
TGF	11.00	9.40	9.47	**9.96**	0.91
TNF	9.73	11.00	9.80	**10.18**	0.71
TGF+TNF	35.00	33.83	34.73	**34.52**	0.61
TNF+SB	8.27	7.73	6.47	**7.49**	0.92

Table 2.46: Change in the percentage of $CD44^{high}ESA^{low}$ cells with treatment.

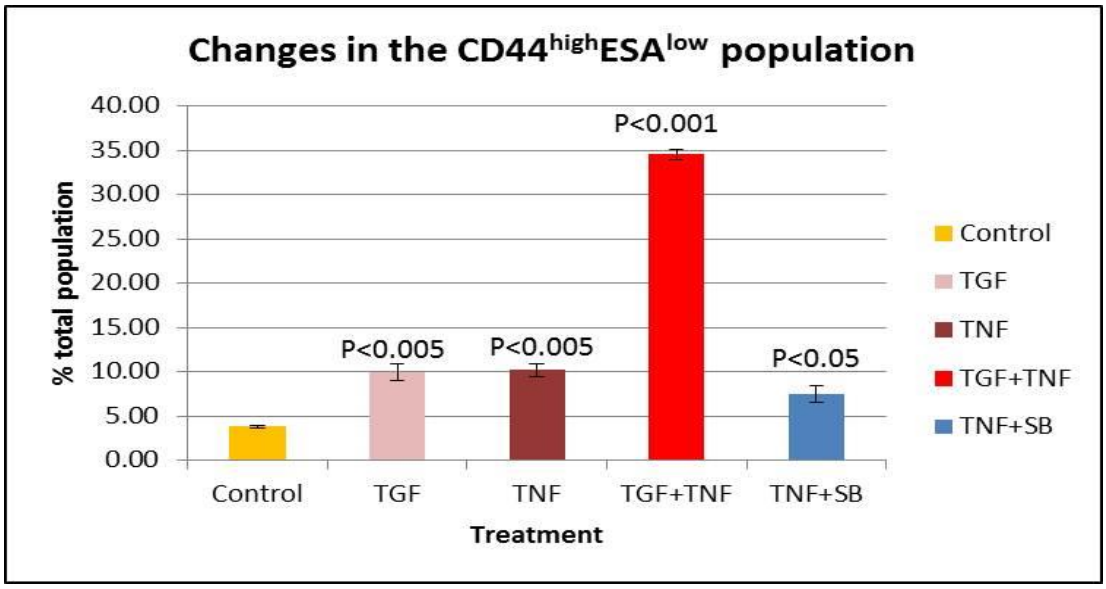

Figure 2.113: Changes in the $CD44^{high}ESA^{low}$ population in the CA1 cell line with TNF-α.

The figure above shows the changes in the $CD44^{high}ESA^{low}$ subpopulation of cells detected as a separate population when Ca1 cells were grown under control conditions, with TGF-β (20ng/ml), TNF-α (10ng/ml), both TGF-β and TNF-α, and TNF-α with SB431542 which is an inhibitor of TGF-β discussed earlier. Cells treated only with TGF-β showed a higher percentage of cells which were $CD44^{high}ESA^{low/-}$ compared to controls. The same effect was achieved when cells were treated with TNF-α alone. When both TGF-β and TNF-α were added together, it caused a major rise in this population and 34.52±0.61% of the cells were $CD44^{high}ESA^{low/-}$ showing that both work synergistically. Inhibition with SB431542 caused a decrease in TNF-α activity but did not completely block it.

b) CD44^{high}

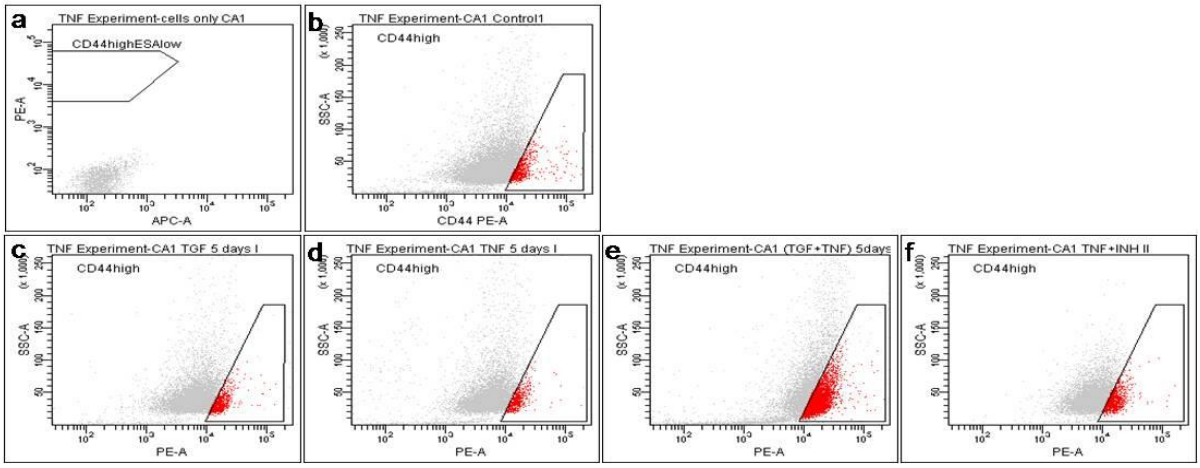

Figure 2.114: FACS analysis of CA1 cells stained with CD44 (x-axis) antibody and the effect of treatment on the CD44^{high} cell population within the cell line. The figure above shows the facsplots obtained when CA1 cells (a) were stained with CD44 antibody (b-e) and analyzed to detect changes in the population of CD44^{high} (gated, red). Cells were grown under control conditions (b), with TGF-β (c), with TNF-α (d), TGF-β and TNF-α together (e) and TNF-α with SB431542 (f). The top 5% of the cells expressing the highest levels of CD44 were selected as CD44^{high} and gated. The effects of the treatments were analyzed by keeping the gates unchanged between experimental samples. The highest increase in this population was seen when TGF-β and TNF-α were added together. TNF-α on its own did increase the percentage of cells that were CD44^{high} but this increase was insignificant compared to controls. TGF-β caused CD44^{high} cells to increase but this was insignificant as to the increase detected when the two were added together.

CD44^{high}	1	2	3	Average	SEM
Control	4.80	5.23	5.47	**5.17**	0.34
TGF	9.63	8.90	10.43	**9.66**	0.77
TNF	6.90	8.20	7.33	**7.48**	0.66
TGF+TNF	37.43	37.50	37.10	**37.34**	0.21
TNF+SB	8.00	6.00	5.87	**6.62**	1.20

Table 2.47: Changes in the percentage of CD44^{high} cells with TNF-α.

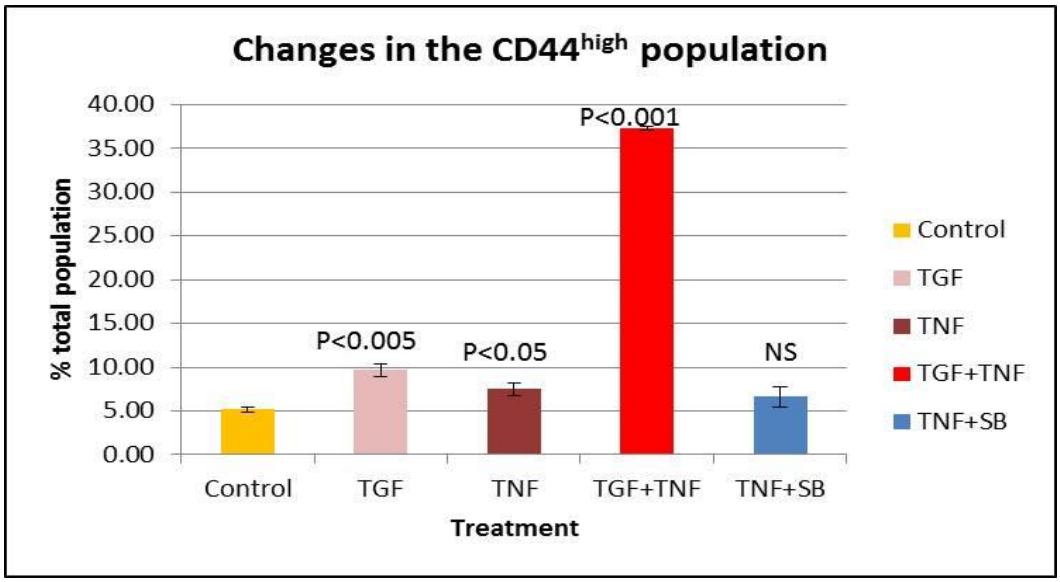

Figure 2.115: Changes in the CD44high population with treatment. The figure above shows the changes in the CD44^{high} subpopulation when the CA1 cell line were grown under control conditions, with TGF-β (20ng/ml), TNF-α (10ng/ml), both TGF and TNF, and TNF with SB431542 which is an inhibitor of TGF-β discussed earlier. Cells treated only with TGF-β showed a higher percentage of cells which were CD44^{high} (9.66±0.77%) compared to controls. The same effect was achieved when cells were treated with TNF-α (7.48±0.66%) alone although this was insignificant. When both TGF-β and TNF-α were added together, it caused a major rise in this population and 37.34±0.21% of the cells were CD44^{high} showing that both work synergistically. This also correlated with the increase in the CD44^{high}ESA^{low} cells. Inhibition with SB431542 caused a decrease in TNF-α activity but did not completely block it as there is a significant rise in the number of CD44^{high} cells.

c) ESA$^{low/-}$

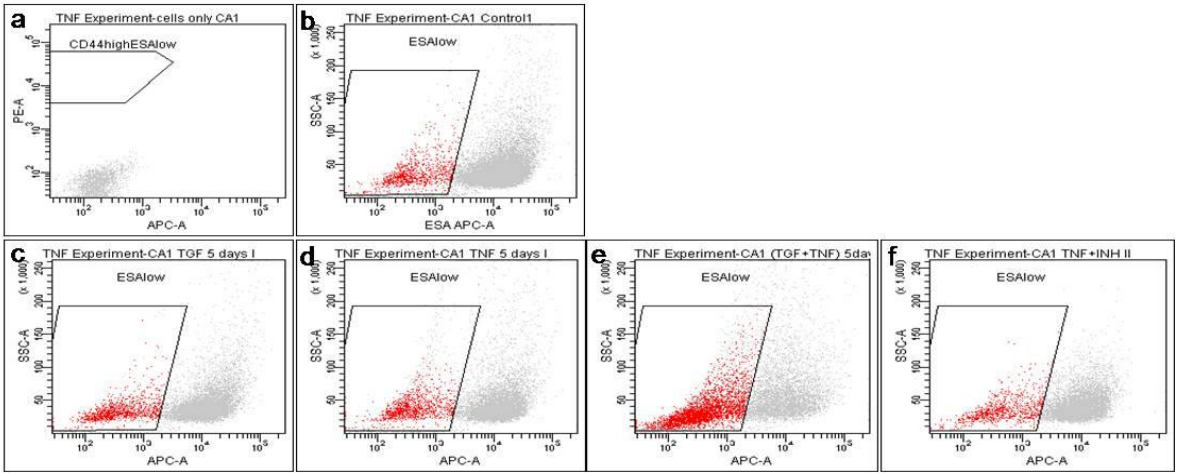

Figure 2.116: FACS analysis of CA1 cells stained with ESA(apc) antibody (x-axis) and the effect of treatment on the ESA$^{low/-}$ cell population within the cell line. The figure above shows the FACSPLOTS obtained when CA1 cells (a) were stained with ESA antibody (b-e) and analyzed to detect changes in the ESA^{low} population (gated red). Cells were grown under control conditions (b), with TGF-β (c), with TNF-α (d), TGF-β and TNF-α together (e) and TNF-α with SB431542 (f). The 5% of the cells expressing the lowest levels of ESA were selected as ESA$^{low/-}$ and gated. The effects of the treatments were analyzed by keeping the gates unchanged between experimental samples. The highest increase in this population was seen when TGF-β and TNF-α were added together. TNF-α on its own did increase the percentage of cells which were CD44high but this increase was insignificant compared to controls. TGF-β caused CD44^{high} cells to increase but this was insignificant as to the increase detected when the two were added together

ESAlow	1	2	3	Average	SEM
Control	5.20	5.17	5.17	**5.18**	0.02
TGF	9.10	10.53	9.83	**9.82**	0.72
TNF	6.20	6.70	5.40	**6.10**	0.66
TGF+TNF	27.00	25.43	26.17	**26.20**	0.78
TNF+SB	6.97	5.73	5.80	**6.17**	0.69

Table 2.48: Changes in the percentage of ESA$^{low/-}$ cells with treatment.

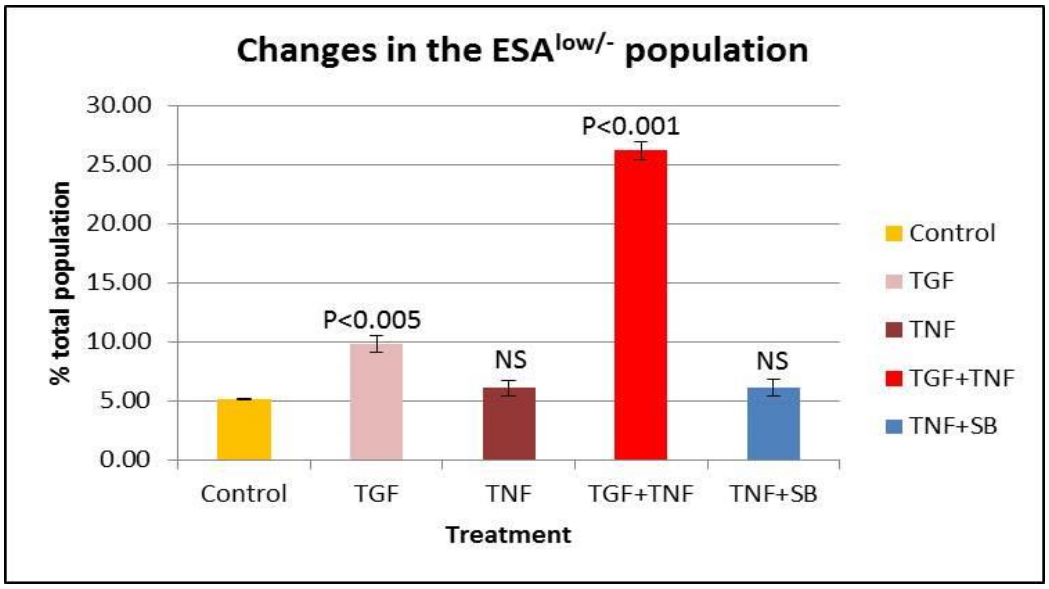

Figure 2.117: The effect of treatment on the ESA$^{low/-}$ population of CA1 cells. The changes in the ESA$^{low/-}$ subpopulation when the CA1 cell line were grown under control conditions, with TGF-β (20ng/ml), TNF-α (10ng/ml), both TGF-β and TNF-α, and TNF-α with SB431542, an inhibitor of TGF-β, discussed earlier. Cells treated with TGF-β showed a significantly higher percentage of cells that were ESA$^{low/-}$ (9.82±0.72%) compared to controls. The same effect was achieved when cells were treated with TNF-α (6.10±0.66%) alone although this was less, but still significant. When both TGF-β and TNF-α were added together, it caused a major rise in this population and 26.20±0.78% of the cells were CD44^{high} showing that both work synergistically, and this was highly significant. This also correlated with the increase in the CD44^{high}ESA^{low} cells. Inhibition with SB431542 caused a decrease in TNF-α activity but did not completely block as there was a significant rise in the proportion of ESA$^{low/-}$ cells.

2) H357 cells:

A) Cell morphology

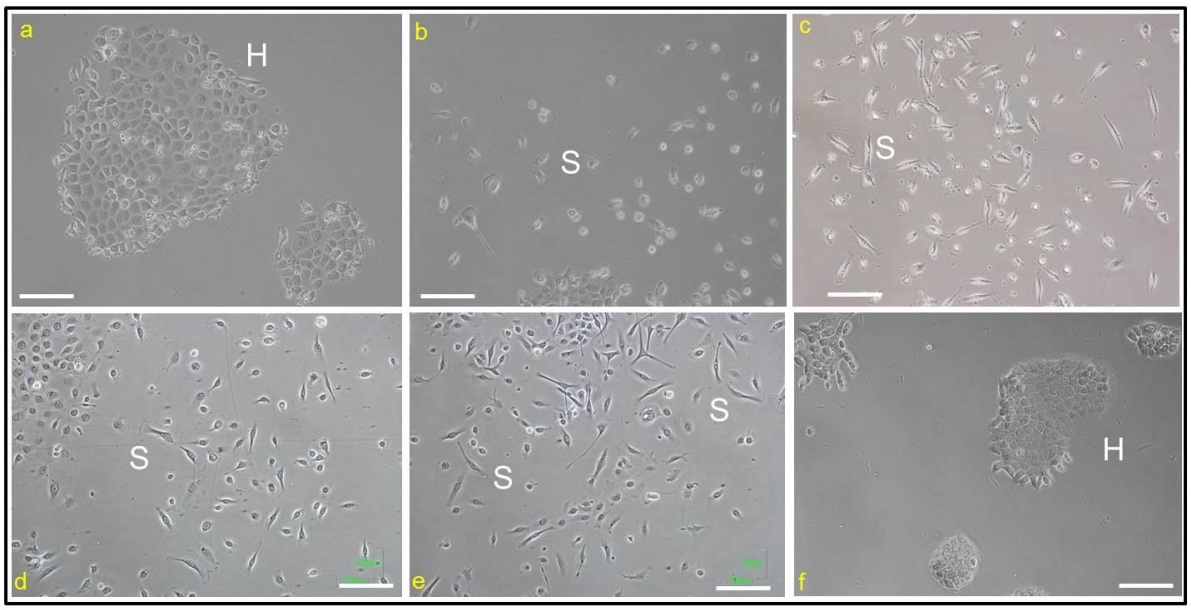

Figure 2.118: The effect of TNF-α on growth of H357 cells. Cultures of H357 cells grown under control conditions (a), with TGF-β (b), TNF-α and TGF-β (c), TNF-α (d), TNF-α + SB431542 (e), TGF-β + inhibitor. Control cells (a) show normal colony morphology and form holoclones (H), meroclones (M) and paraclones (P). Cells treated with TGF-β form spindle shaped cells with decreased colony formation. Cells with both TGF-β and TNF-α formed only elongated spindle cells resembling fibroblasts without any visibly adhesive cells. Cells treated with TNF-α alone and TNF-α + inhibitor also displayed spindle morpholody with reduced colony formation (d, e).

B) FACS Analysis

a) $CD44^{high}ESA^{low}$

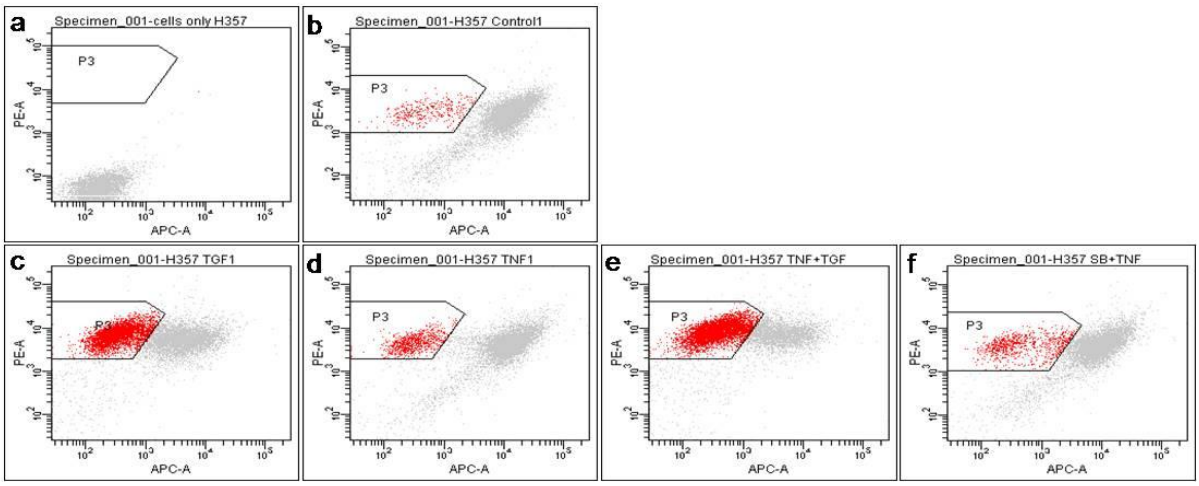

Figure 2.119: FACS analysis of H357 cells stained with CD44 (y-axis) and ESA (x-axis) fluorescent antibodies. The FACS plots obtained when H357 cells were stained with CD44 and ESA antibodies and analyzed for the effect of treatment with TGF-β and TNF-α on specifically the $CD44^{high}ESA^{low}$ population (gated, red). Panel (a) shows the analysis without any added antibody to adjust for background noise. Cells were then analyzed as controls (a), cell treated with TGF-β (c), TNF-α (d), both TGF-β and TNF-α (e) and TNF-α added together with SB431542 (f).

Treatment with TGF-β alone causes the percentage of $CD44^{high}ESA^{low}$ cells to rise more when compared to treatment with TNF alone which causes a rise in this population but this effect is less marked than with TGF-β. This is in contrast to the CA1 cell line where both TGF-β and TNF-α produce almost the same effect when they are added on their own. When both TGF-β and TNF-α are added together the percentage of $CD44^{high}ESA^{low}$cells rise to much higher levels than when TGF-β is added on its own. When TNF-α and SB431542 are added together the gated population rises slightly but this is insignificant.

CD44highESAlow	1	2	3	Average	SEM
Control	5.70	5.80	5.80	**5.77**	0.06
TGF	34.37	28.97	28.97	**30.77**	3.12
TNF	11.40	10.40	9.00	**10.27**	1.21
TGF+TNF	61.10	47.33	47.33	**51.92**	7.95
TNF+SB	7.33	5.47	5.47	**6.09**	1.08

Table 2.49: Changes in the percentage of CD44^{high}ESA^{low} cells with treatment.

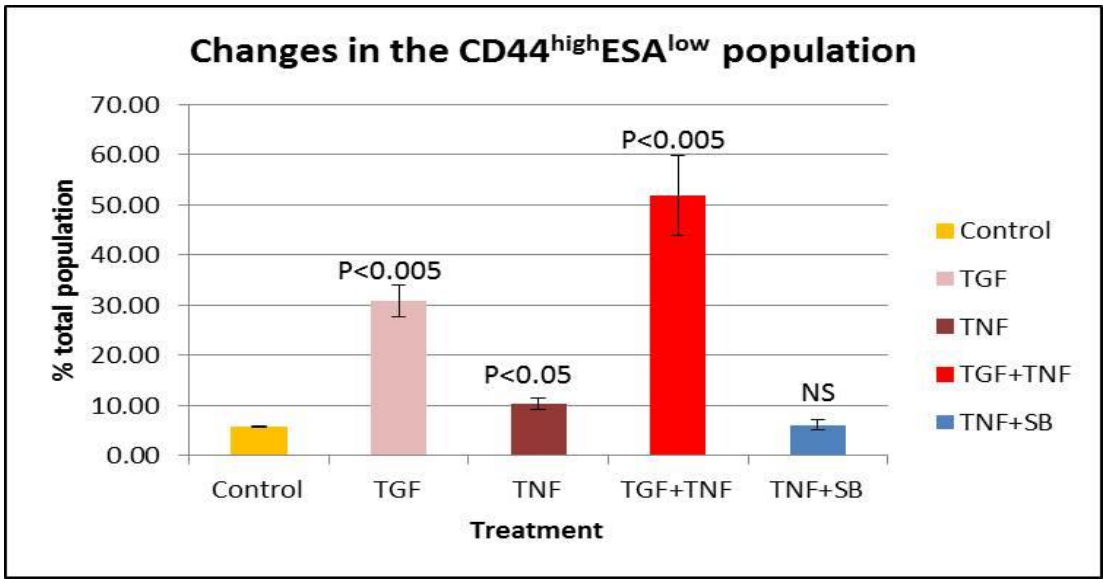

Figure 2.120: Changes in the CD44^{high}ESA^{low} population in the H357 cell line with or without treatment. The changes in the CD44^{high}ESA^{low} subpopulation of cells detected as a separate population when H357 cells were grown under control conditions, with TGF-β (20ng/ml), TNF-α (10ng/ml), both TGF-β and TNF-α, and TNF-α with SB431542 which is an inhibitor of TGF-β discussed earlier. Cells treated only with TGF-β showed a higher percentage of cells which were CD44^{high}ESA$^{low/-}$ compared to controls. The same effect was achieved when cells were treated with TNF-α alone. When both TGF-β and TNF-α were added together, it caused a major rise in this population and 51.92% of the cells were CD44^{high}ESA$^{low/-}$ showing that both work synergistically. Inhibition with SB431542 caused a decrease in TNF-α activity but did not completely block it.

b) CD44^{high}

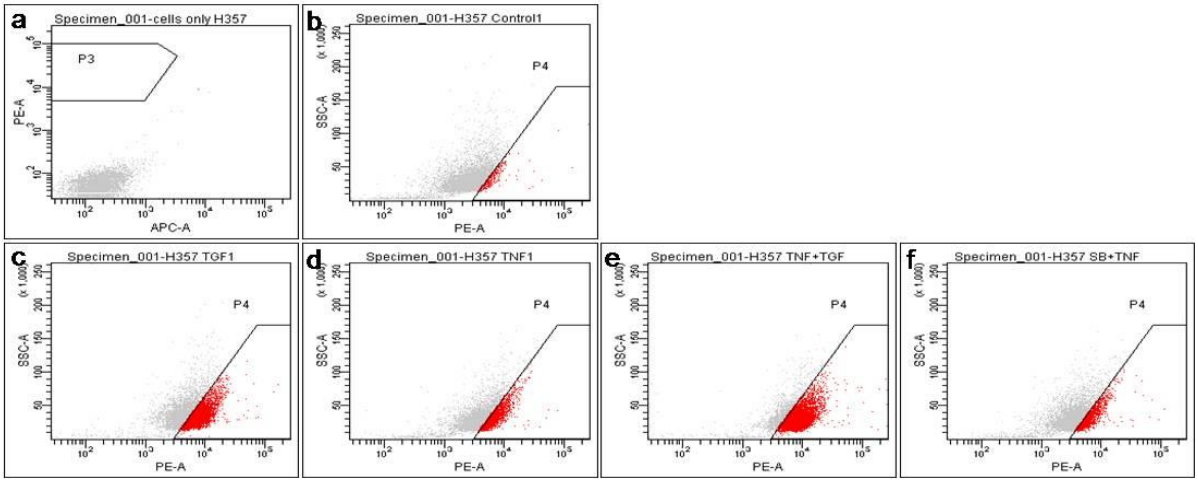

Figure 2.121: FACS analysis of H357 cells stained with CD44 (x-axis) antibody and the effect of treatment on the CD44^{high} cell population within the cell line. The FACSPLOTS obtained when H357 cells (a) were stained with CD44 antibody (b-e) and analyzed to detect changes in the population of CD44^{high} (gated, red). Cells were grown under control conditions (b), with TGF-β (c), with TNF-α (d), TGF-β and TNF-α together (e) and TNF-α with SB431542 (f). The top 5% of the cells expressing the highest levels of CD44 were selected as CD44^{high} and gated. The effects of the treatments were analyzed by keeping the gates unchanged between experimental samples. The highest increase in this population was seen when TGF-β and TNF-α were added together. TNF-α on its own did increase the percentage of cells which were CD44^{high} but this increase was insignificant compared to controls. TGF-β caused CD44^{high} cells to increase but this was insignificant as to the increase detected when the two were added together.

CD44high	1	2	3	Average	SEM
Control	5.47	5.27	5.23	**5.32**	0.13
TGF	31.33	27.40	26.90	**28.54**	2.43
TNF	17.37	12.83	16.83	**15.68**	2.48
TGF+TNF	66.23	55.00	55.00	**58.74**	6.49
TNF+SB	6.87	6.00	5.20	**6.02**	0.83

Table 2.50: Changes in the percentage of CD44^{high} cells with treatment.

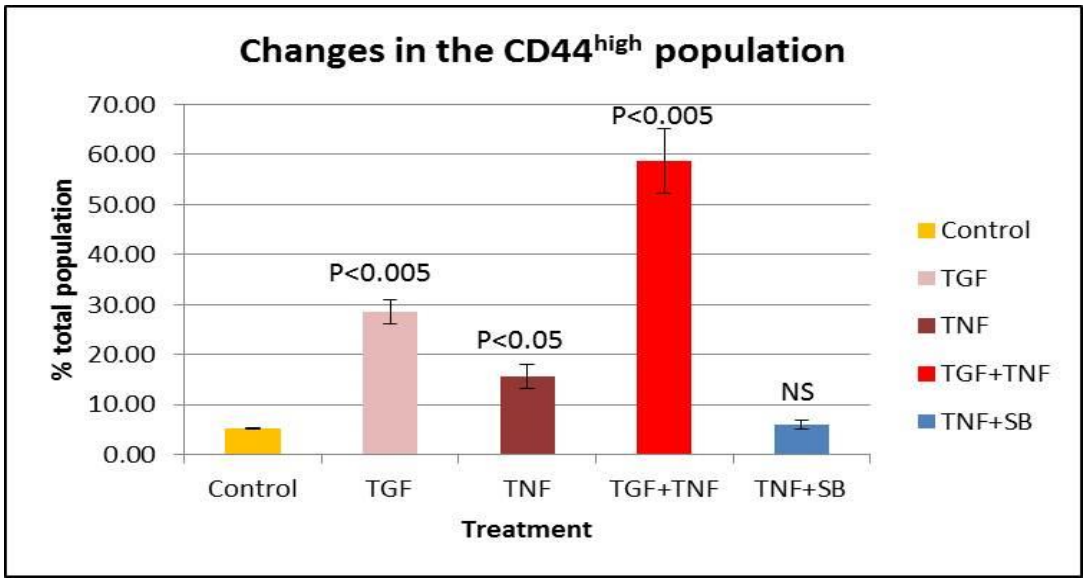

Figure 2.122: Changes in the CD44^{high} population with treatment. The changes in the size of the CD44^{high} subpopulation of cells within the H357 cell line. Cells were grown under control conditions, with TGF-β (20ng/ml), TNF-α (10ng/ml), both TGF-β and TNF-α, and TNF-α with SB431542 which is an inhibitor of TGF-β discussed earlier. Cells treated only with TGF-β showed a significantly higher percentage of cells that were CD44^{high} (28.54±2.43%) compared to controls. The same effect was achieved when cells were treated with TNF-α (15.68±2.48%) alone although to a lesser extent. When both TGF-β and TNF-α were added together, it caused a major rise in this population and 58.74±6.49% of the cells were CD44^{high} showing that both work synergistically. This also correlated with the increase in the CD44^{high}ESA^{low} cells. Inhibition with SB431542 caused a decrease in TNF-α activity but did not completely block it.

c) ESA$^{low/-}$ cells

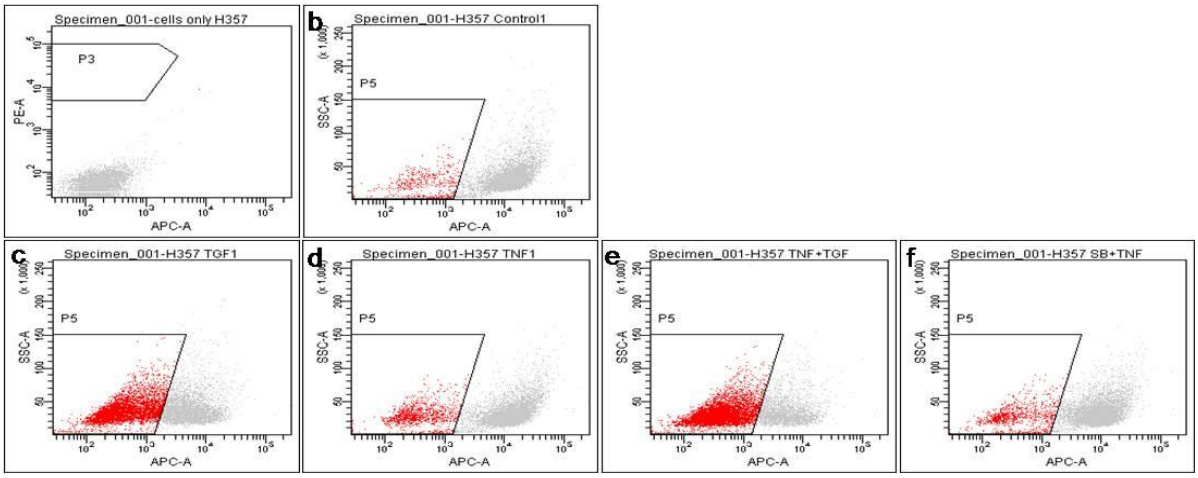

Figure 2.123: FACS analysis of H357 cells stained with ESA (APC) antibody (x-axis) and the effect of treatment on the ESA$^{low/-}$ cell population within the cell line. The facsplots obtained when H357 cells (a) were stained with ESA antibody (b-e) and analyzed to detect changes in the ESA$^{low/-}$ population (gated, red). Cells were grown under control conditions (b), with TGF-β (c), with TNF-α (d), TGF-β and TNF-α together (e) and TNF-α with SB431542 (f). The 5% of cells expressing the lowest levels of ESA were selected as ESA^{low} and gated. The effects of the treatments were analyzed by keeping the gates unchanged between experimental samples. The highest increase in this population was seen when TGF-β and TNF-α were added together. TNF-α also increases this ESA^{low} population as is evident by the increased number of cells within the gate. TGF-β also increases the percentage of cells which were ESA$^{low/-}$ as was discussed in the last chapter but this was insignificant as to the increase detected when the two were added together

ESAlow/-	1	2	3	Average	SEM
Control	5.27	5.00	5.17	**5.14**	0.13
TGF	41.40	40.13	40.62	**40.72**	0.64
TNF	12.30	7.63	9.53	**9.82**	2.35
TGF+TNF	72.10	66.70	65.60	**68.13**	3.48
TNF+SB	11.13	6.40	7.15	**8.23**	2.54

Table 2.51: Changes in the percentage of ESA$^{low/-}$ cells with TNF-α.

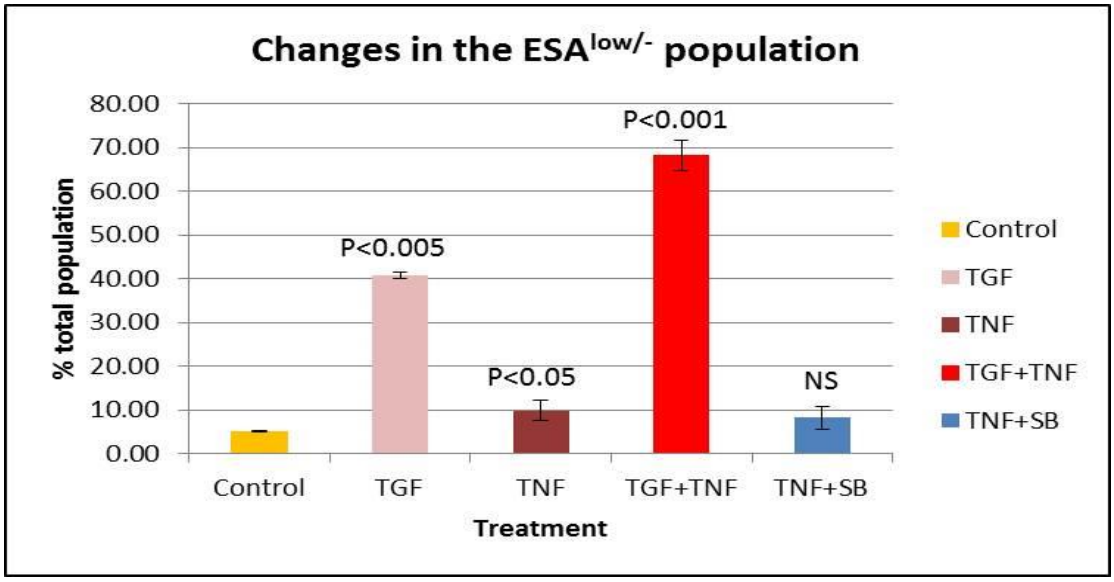

Figure 2.124: The effect of treatment on the ESA$^{low/-}$ population of H357 cells. The changes in the ESA$^{low/-}$ subpopulation when H357 cells were grown under control conditions, with TGF-β (20ng/ml), TNF-α (10ng/ml), both TGF-β and TNF-α, and TNF-α with SB431542 which is an inhibitor of TGF-β, discussed earlier. Cells treated only with TGF-β showed a higher percentage of cells which were ESA$^{low/-}$ (40.72±0.64%) compared to controls. TNF-α on its own caused a lesser effect that it did when used on the CA1 cell line. However, when both TGF-β and TNF-α were added together, it caused a major rise in this population and 68.13±3.48% of the cells were ESA$^{low/-}$ showing that both work synergistically. This also correlated with the increase in the CD44^{high}ESA^{low} cells. Inhibition with SB431542 caused a decrease in TNF-α activity but did not completely block it as there was still a significant increase in the percentage of ESA$^{low/-}$ cells.

2.9.4 Discussion

The aim of this chapter was primarily to ascertain the effect of TNF-α on OSCC cells and also the combined effect of TGF-β and TNF-α on these cell lines. FACS analysis was used to assess the changes in the size of the $CD44^{high}ESA^{low}$, $CD44^{high}$ and $ESA^{low/-}$ populations. The tumour environment has been described as a wound that never heals (Biddle and Mackenzie, 2012) and epithelial tissues are subjected to a variety of EMT-inducing stromal factors upon wounding. These include TGF-β and TNF-α, known to be secreted by immune cells (Kalluri and Weinberg, 2009) and to be enhanced by tissue inflammation at the wounding site (Wu et al, 2009). The stromal tissue surrounding the tumour to plays a vital role in promoting and maintaining tumour development as shown by the involvement of cancer associated fibroblasts (Olumi et al, 1999). Recent work with TGF-β has strengthened this observation (Kojima et al, 2010). TNF-α is a pro-inflammatory cytokine that has been associated with the progression of many cancers including osteosarcoma where it was shown to mediate the activation of pro-inflammatory genes (Cvoro et al, 2011). In breast cancer, TNF-α has been shown to interact synergistically with TGF-β to generate EMT cancer cells that also possess the hallmark $CD44^{high}CD24^{low/-}$ signature for breast cancer stem cells (Asiedu et al, 2011). Our results support this finding and show that the effect of TNF-α on OSCC cells is similar to that of TGF-β in causing an increase in the EMT population ($CD44^{high}ESA^{low}$) and an increase in the size of both the $CD44^{high}$ and $ESA^{low/-}$ populations. Further to this we found that the addition of TNF-α and TGF-β together greatly enhances the effect seen indicating that they work together synergistically to promote EMT in OSCC cells. The response of cell lines varied butwhen TGF-β and TNF-α were added together there was a significant increase in the size of the $CD44^{high}ESA^{low}$ population in both CA1 (x10) and H357 (x12) cells. Further, there was an increase in the size of both, the $CD44^{high}$ and $ESA^{low/-}$ populations. On microscopic examination, cells from both lines were seen to possess a spindle-shaped morphology and a decreased tendency to form cohesive colonies.

2.10 The effect of TGF-β, SB431542 and NS-398 on migration in OSCC cell lines.

2.9.1 Introduction

The previous chapters have primarily dealt with the effect of TGF-β on cellular morphology and the relative change in the proportion of intrinsic $CD44^{high}ESA^{low}$, the $CD44^{high}$, and $ESA^{low/-}$populations present in OSCC cell lines. To address the question of whether TGF-β directly increases cell migration (a) the effect of TGF-β on cellular migration was determine and (b) the effect on this process of other compounds potentially affecting EMT was examined.Elevated COX-2 expression has also been documented for many cancers including OSCCs (Minter et al, 2003). Nonsteroidal anti-inflammatory drugs (NSAIDS) have marked antitumour activity affected through inhibition of COX-2 regulated pathways and these have been shown to be chemopreventive in animal models of colon, bladder and breast cancers (Williams et al, 1999). Epidemiological studies indicate that NSAIDs reduce breast and oesophageal cancer mortality (Zha et al, 2004). In OSCCs, it has been shown that NS-398, a selective COX-2 inhibitor, suppressed the invasion of OSCC cells and it would found that this was dependant on the integrin $\alpha_v\beta_{6,}$ that is known to be a receptor for TGF-β (Munger et al, 1999). The role of NS-398 was this evaluated to determine its effect on the migration of OSCC cells.

2.9.2 Materials and Methods

Cells were grown to confluence in 6-well plates. A p1000 pipette tip was used to make a scratch across the center of each wellafter which the cells were washed and refreshed with complete media. Pictures were takenevery 24 hrs on an inverted microscope (Nikon) to evaluate migration across the scratch. ImageJ software (Zeiss) was used to measure the area each scratch for each of the time points examined. For each experiment, 3 fields along the scratch in each well were analyzed in triplicate for each sample. The area uncovered with cells was converted to the area covered by subtracting from the total area available for migration at time 0.

2.9.3 Results

A) CA1 cell line

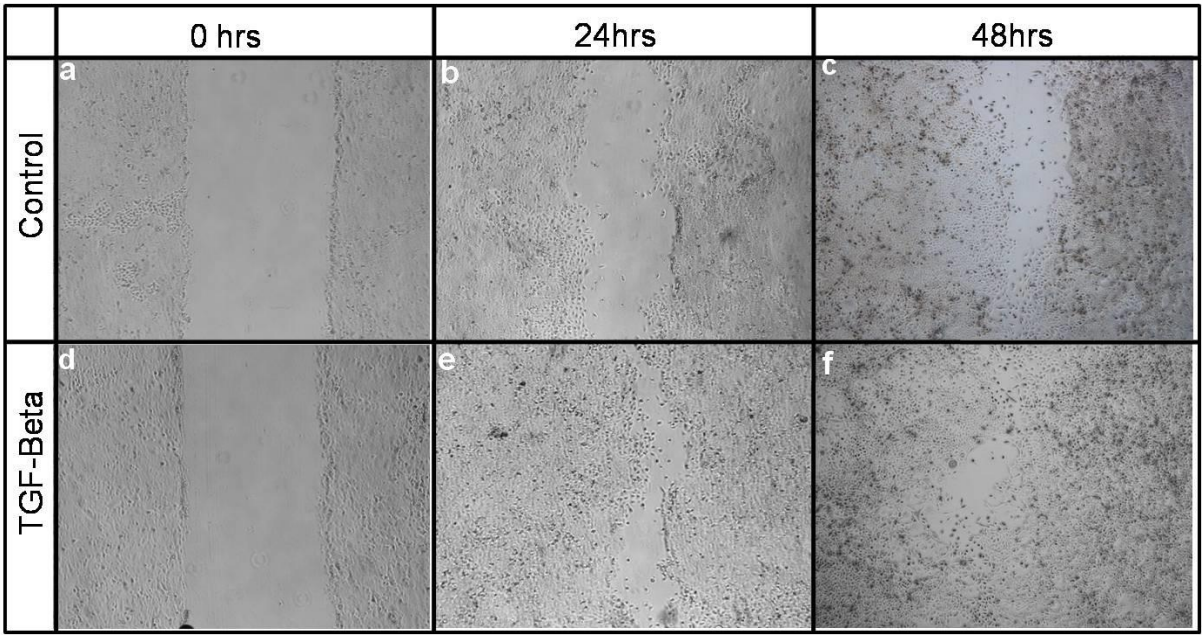

Figure 2.125: Scratch/migration assay for the CA1 cell line (part1). Cultures of control CA1 cells (top row; a-c) and those treated by TGF-β treated cells (bottom row; d-f) subjected to a scratch assay. Control cells and TGF-β treated cells were scratched and photographed at T0 (a, d) and the migration of cells across the wound was assessed at T-24hours (b, e) and T-48 hours. The relative area remaining at the end of the time periods was assessed to calculate the area covered and control cells were compared to those treated with TGF-βfor all the time points. Cells treated with TGF-β migrate across the scratch faster and within 48 hours the gap is almost covered.

CA1 cell line	% Area covered 24hrs	SD n=3	% Area covered 48hrs	SD n=3
Control	**28.70**	2.36	**74.60**	4.45
TGF-β	**84.90**	3.17	**94.93**	3.70

Table 2.52: Area that was covered by control and TGF-β treated CA1 cells.

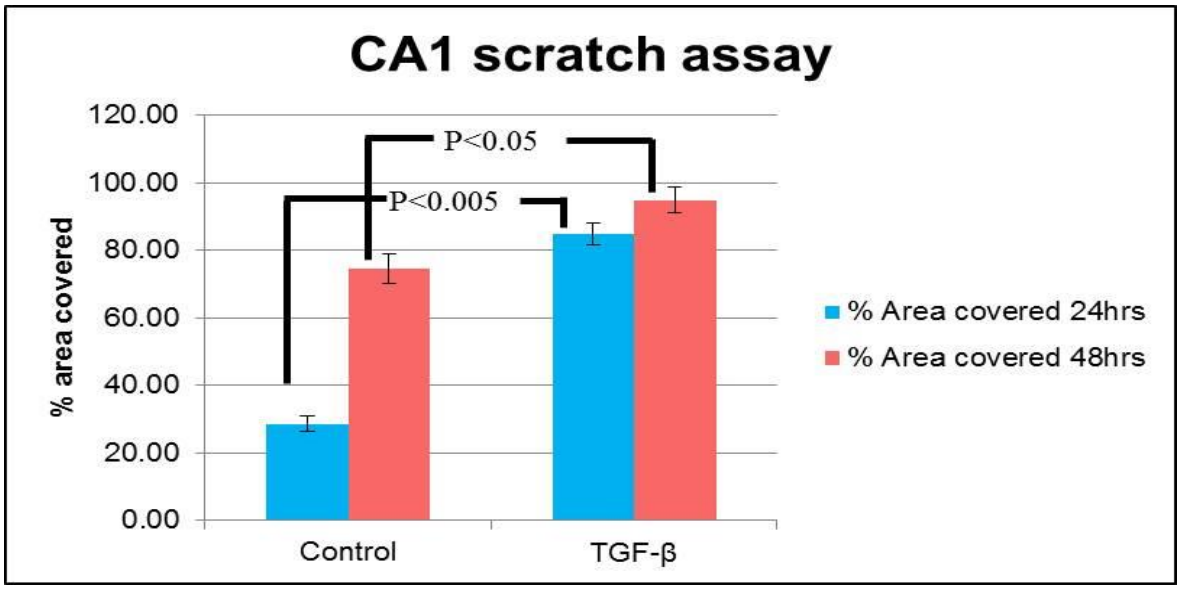

Figure 2.126: Migration of control CA1 cells compared to TGF-β treated cells. A comparison of the relative area covered in control cells compared to the area covered by TGF-β treated cells. TGF-β treated cells migrate quicker and cover 84.9±3.17% of the scratched area in 24 hours and 94.9±3.7% in 48 hours. In comparison, control cells migrate slower and cover 28.7±2.36% of the area in 24 hours and 74.6±4.45% in 48 hours.

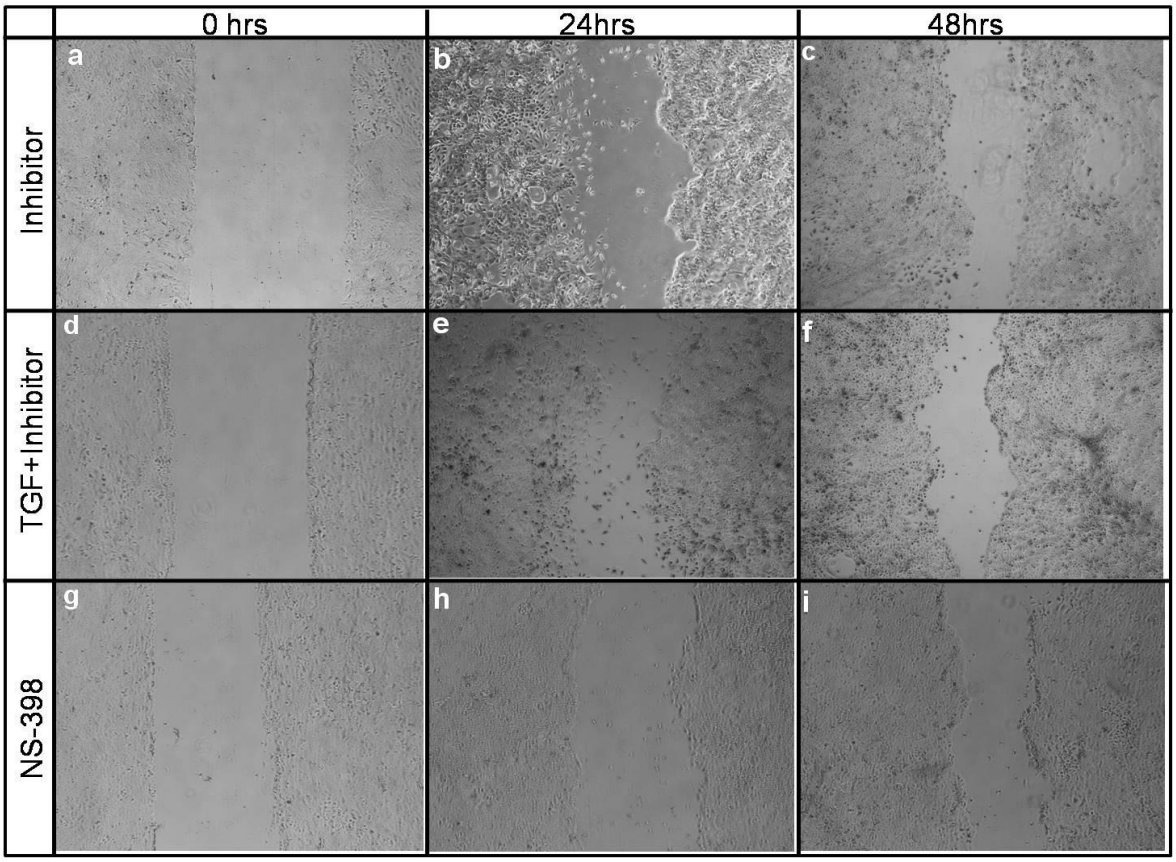

Figure 2.127: Scratch/migration assay for the CA1 cell line (part2). The results of a scratch assay of CA1 cells treated with Inhibitor of TGF-β (a-c), TGF-β and Inhibitor added together (d-f) and NS-398 (g-i). Cells for all three treatments were photographed at T0 (a, d, g), T24 hours (b, e, h) and T48 hours (c, f, i). The relative area remaining at the end of the time periods was assessed to calculate the area covered and cells were compared to controls discussed earlier (Figure 3.9b). Cells treated with inhibitor alone, and TGF-β added with the inhibitor, migrate over the same relative areas at all time periods. NS-398 slowed down the migration of cells as is evident by the uncovered area remaining at the end of 24 and 48 hours respectively.

CA1 cell line	% Area covered 24hrs	SD	% Area covered 48hrs	SD
Inhibitor	**19.71**	1.66	**65.33**	5.04
TGF-β+Inhibitor	**22.68**	3.60	**70.32**	1.98
NS-398	**15.51**	2.32	**58.88**	3.11

Table 2.53: Area covered by cells treated with SB431542 (±TGF) and NS-398

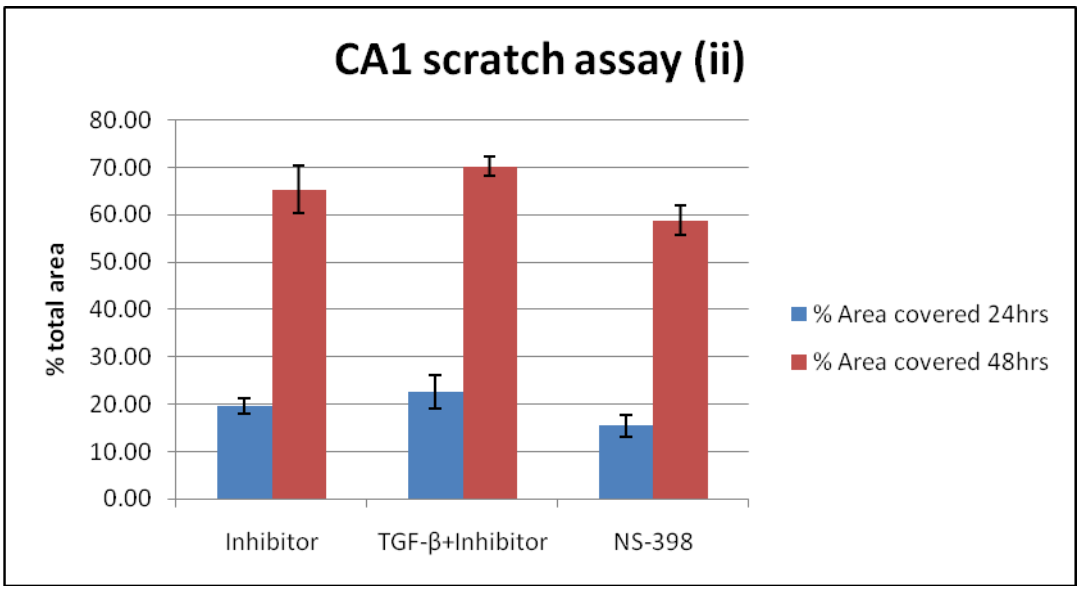

Figure 2.128: The effect of SB431542, with or without TGF-β and NS398 on migration. The effect of SB431542 (TGF-β inhibitor) alone, SB431542 together with TGF-β, and NS-398 (a COX-II inhibitor) on the migration of CA1 cells across the scratch. Cells treated with SB431542, and SB431542 added with TGF-β, showed the similar rates of migration at 24 hours (19.71±1.66%, 22.68±3.60%) and 48 hours (65.33±5.04, 70.32±1.98) to controls. Cells treated with NS-398 showed slower migration and covered less area in 24 hours (15.51±2.32) and 48 hours (58.88±3.11%) as is evident by the gaps remaining at the end of treatment. There were also fewer motile cells seen migrating across the gap.

B) Fanconi cells line

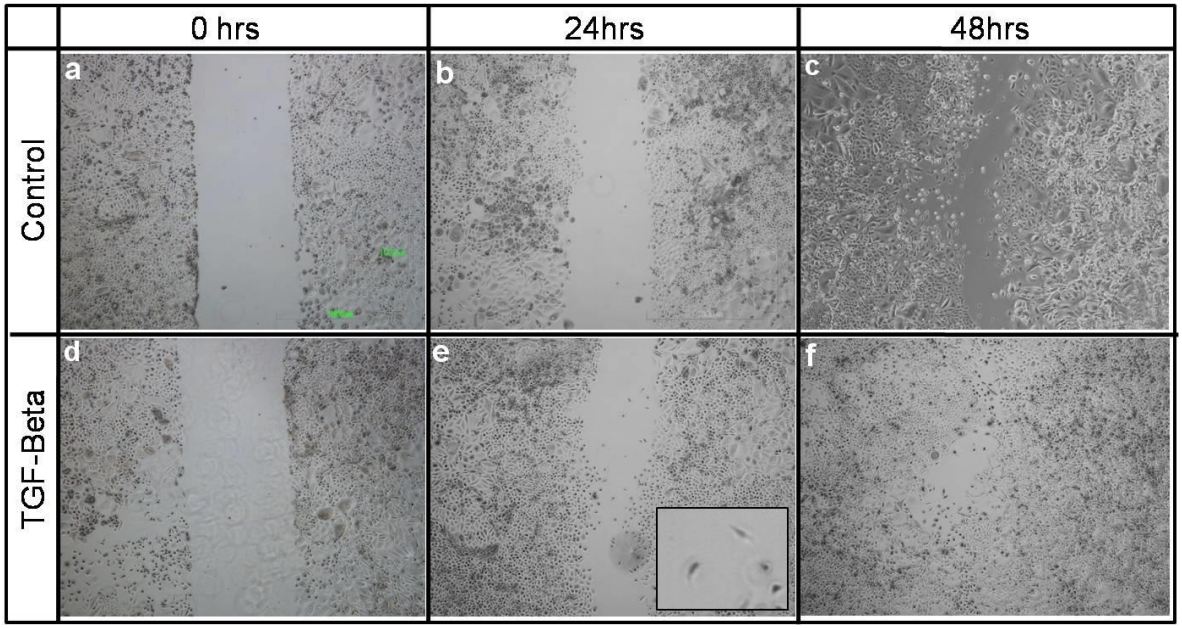

Figure 2.129: Scratch/migration assay for the OHSU Fanconi cell line (part1). The figure above shows control OHSU Fanconi cells (top row; a-c) and TGF-β treated cells (bottom row; d-f) subjected to a scratch assay. Control and TGF-β treated cells were scratched and photographed at Time 0 (a, d) and the migration of cells across the wound was assessed at 24 hours (b, e) and 48 hours. Cells treated with TGF-β migrated across the scratch the faster and within 48 hours the gap is almost covered. As discussed later, spindle shaped cells resembling fibroblasts are seen within the gap.

OHSU cell line	% Area covered 24hrs	SD n=3	% Area covered 48hrs	SD n=3
Control	**27.71**	3.84	**61.27**	2.56
TGF-β	**64.45**	4.60	**87.41**	2.18

Table 2.54: Area that was covered by control and TGF-β treated OHSU cells.

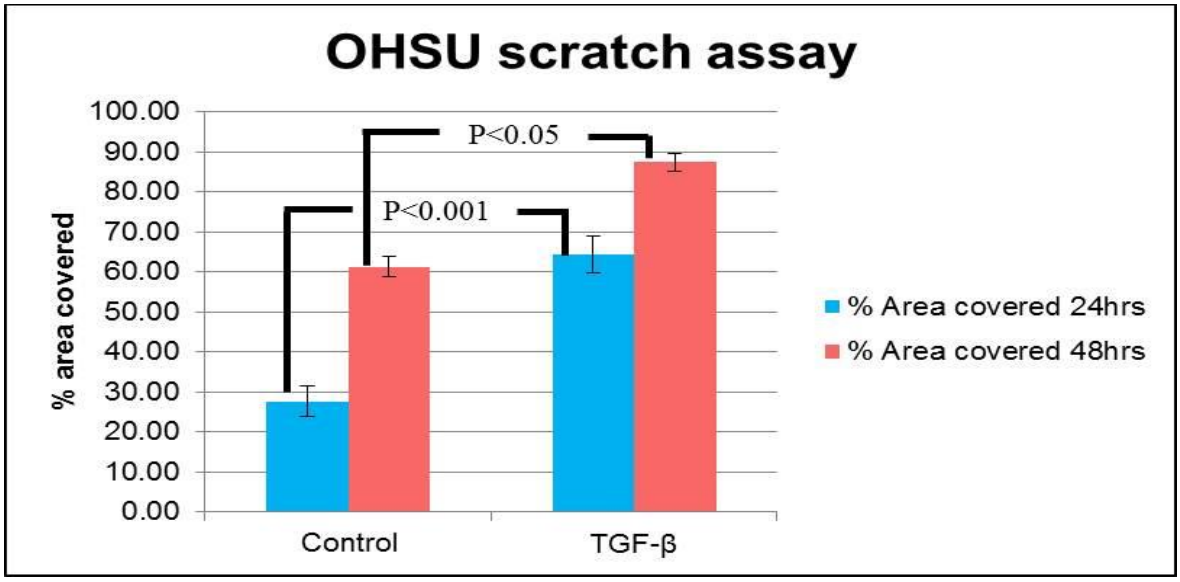

Figure 2.130: Migration of control OHSU cells compared to TGF-β treated cells. The figure above compares the relative area covered by control cells compared to the area covered by TGF-β treated cells. Again, TGF-β treated cells close the gap quicker and cover 66.45±4.6% of the scratched area in 24 hours and 87.41±2.18% in 48 hours. Control cells migrate slower and cover 27.71±3.84% of the area in 24 hours and 61.27±2.56% in 48 hours.

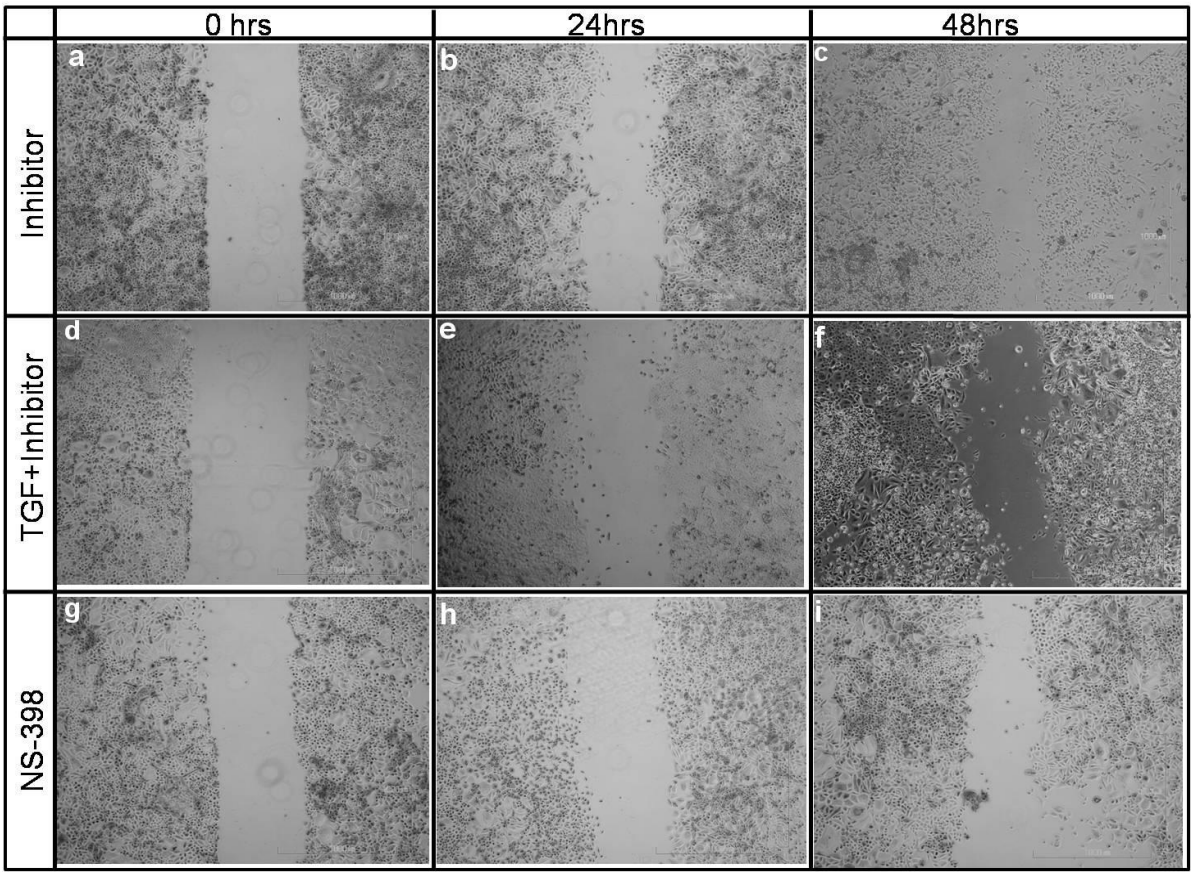

Figure 2.131: Scratch/migration assay for the OHSU cell line (part2). The figure above shows the results of a scratch assay CA1 cells treated with Inhibitor of TGF-β (a-c), TGF-β and Inhibitor added together (d-f) and NS-398 (g-i). Cells for all three treatments were photographed at T0 (a, d, g), T24 hours (b, e, h) and T48 hours (c, f, i). Cells treated with Inhibitor alone and TGF-β added with the inhibitor, migrate over similar relative areas each time period. NS-398 seems to slow down the migration of cells as is evident by the uncovered area remaining at the end of 24 and 48 hours respectively.

OHSU cell line	% Area covered 24hrs	SD	% Area covered 48hrs	SD
Inhibitor	**19.90**	1.75	**52.70**	3.10
TGF-β+Inhibitor	**25.39**	1.60	**43.25**	3.23
NS-398	**28.67**	2.70	**46.83**	1.81

Table 2.55: Area covered by cells treated with SB431542 (±TGF) and NS-398

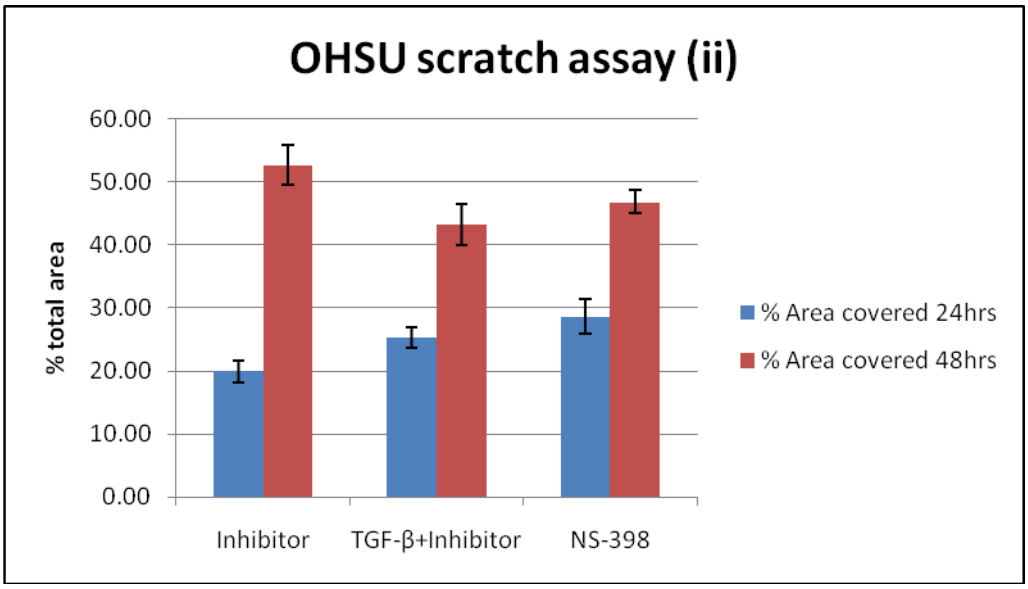

Figure 2.132: The effect of SB431542 with or without TGF-β and NS398 on migration. The figure above shows the effect of SB431542 (inhibitor) added alone, with TGF-β and NS-398 (COX-II inhibitor) on the migration of OHSU Fanconi cells across the scratch. Cells treated with SB431542 and SB431542 added with TGF-β showed roughly the same rates of migration in 24 hours (19.90±1.75%, 25.39±1.60%). In 48 hours cells with both the inhibitor and TGF added together had covered slightly less area (43.25±3.23%) compared to those with inhibitor alone (52.70±3.10%). Cells treated with NS-398 showed slower migration and covered less area in 24 hours (28.67±2.70) and 48 hours (46.83±1.81%) as is evident by the gaps remaining at the end of treatment. There were also fewer motile cells seen migrating across the gap.

2.9.4 Discussion

The aim if this experiment was to determine the effect of TGF-β and its inhibitor (SB431542) on the migration of OSCC cells. The secondary aim was to see the effect of a known COX-II inhibitor (NS-398) on these lines as it has been shown to inhibit invasion in OSCC cells through interactionswith the integrin $\alpha^{v}\beta^{6}$,also a receptor for TGF-β.It was found that TGF-β enhances cell migration and this effect was seen with boththe CA1 and Fanconi cell lines. Treated cells migrate faster than controls and covered 94% and 84% (CA1, OHSU) of the scratch area by 48 hours with control cells covering only 74% and 61% respectively. Photographedunder high magnification, the scratch area shows cells resembling fibroblasts migrating across the scratch. The cells at the edge of the scratch also seemed to have undergone EMT as is apparent by their spindly morphology. The figure below shows Ca1 cells photographed at 24 (a) and 48 hours (b) with regions withininsets further magnified to show the elongated cells.

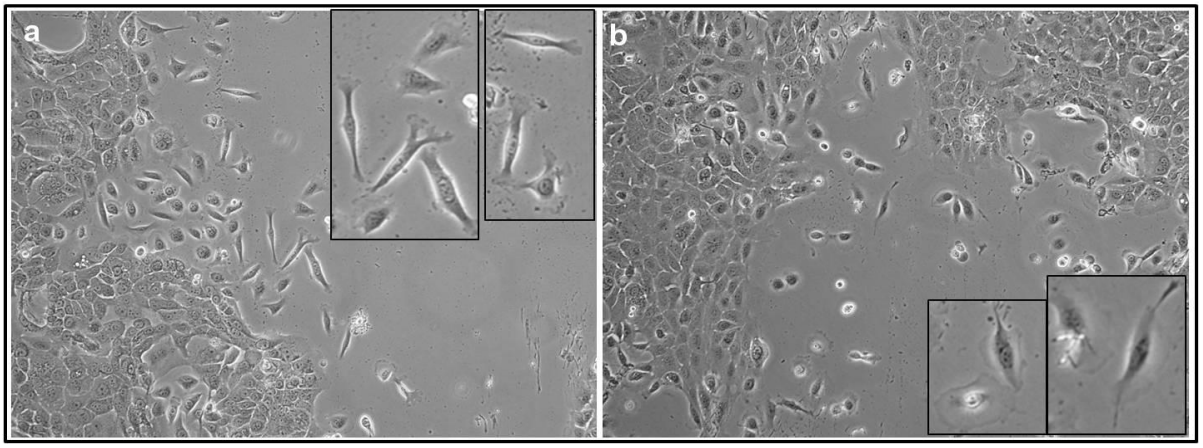

Figure 2.133: CA1 cells migrating across the scratch. The migration of CA1 cells across the scratch at 24 hours (a) and 48 hours (b) shown in phase contrast. Cells at the edge of the scratch have a spindle morphology and detach from the edge to migrate across (insets).

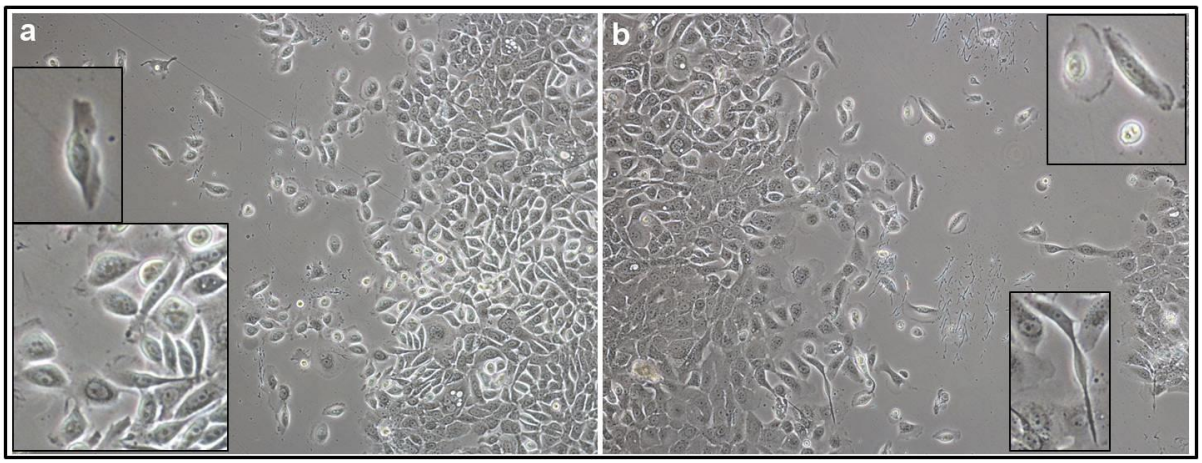

Figure 2.134: OHSU cells at 24 (a) and 48 (b) hours migrating across the scratch. The migration of OHSU cells across the scratch at 24 hours (a) and 48 hours (b) shown in phase contrast. Cells at the edge of the scratch have a spindle morphology, are elongated and detach from the edge to migrate across (insets).

2.10 Main Discussion and Summary

At the start of this PhD, the main focus was to try to find reliable markers for stem cells that could be used for consistent identification and isolation of these cells from cell lines generated from OSCCs. The previous view that all cells in cancer tissue have equal growth potential was becoming replaced by the view that, like self-renewing adult tissues, cancers are maintained by special cells,stem cells, capable of sustained growth and replication. As previously discussed, normal keratinocytes, when cultured, consistently give rise to 3 main colony morphologies; holoclones, meroclones and paraclones. Holoclones are round colonies formed by cells tightly packed together and they show robust growth, can be extensively passaged, and hence are thought to contain stem cells (Barrandon, 1987). Meroclones are formed of larger cells, show less growth potential, and are thought to be formed from amplifying cells that are lower in the clonogenic hierarchy and are committed to differentiation. Paraclones consist of cells that show very little growth, cannot be cultured extensively, and are made up of cellsfurther down the differentiation pathway. Firm evidence that cancers have a hierarchical stem cell structure was first demonstrated in haematological malignancies by Bonnet and Dick (1997). They showed that patterns of cell surface protein expression can be used to predict cell behaviour and that only $CD38^{+}/CD34^{-}$cells are able to regenerate leukemia in mice. Subsequently, tumour initiating cells, corresponding to stem cells, have been demonstrated in most solid tumours including breast, prostate, gut, head and neck, and oral cancers (Al Hajj et al, 2003; Tang et al, 2007; Li and Tang, 2011; Todaro et al, 2010; Prince et al, 2007; Mackenzie et al, 2005; Gammon et al, 2011).

Work by Locke and co-workers (2004), through microarray analysis of oral cancer cell lines, showed a number of markers that are expressed by holoclone cells but not by paraclone cells. From amongst these markers a list of most likely candidates was chosen for *in situ* hybridization to determine whether they could be used to isolate stem cell zones in oral cancers. The strategy was to use*insitu* hybridization to look for stem cell zones or “hot spots” in wax embedded sections of a variety of control tissues including lung, heart musculature, and adult skin. Foetal skin was also chosen as usually it generally expresses high levels of most markers. It was hoped that similar examination of sections of oral cancers would identify zones with high expression of putative stem cell markers. Probes for *insitu* hybridization were designed for 13 markers andspecificity of the markers to regions in the tissue where they would normally be expressed was demonstrated. However, although the technique appeared to work well, areas corresponding to stem cell zones failed to be localized. Three of the markers examined,

Vimentin, notch and Dkk3 seemed to show slightly higher generalized expression in oral cancer compared to normal tissues but results were largely inconclusive.

The next series of studies assessed whether a range of cell lines that had been generated from OSCC can provide *in vitro* models for theexamination of cancer stem cells. OSCC cell lines were confirmed to show heterogeneity similar to that of cultures of normal epithelial cells and to form holoclone, meroclone and paraclone colonies. Holoclones were found to stain brighter for putative stem cell markers than meroclones and paraclones (Mackenzie et al, 2006). Initially monoclonal antibodies against CD44, β-catenin and E-cadherin were obtained to stain cell lines in the lab and to analyze the expression patterns they generate. CD44 localized to the membrane of colony forming cells with little or no expression in the cytoplasm. Expression was higher in holoclones than paraclones for all of the cell lines studied. Interestingly, expression was stronger in the central cells of the colony than at the edge. Some cells at the edge of colonies also showed nuclear staining for CD44, butat that time it was unclear what this signified. E-cadherin was similarly localized almost exclusively to the cell membrane of adherent cells and the pattern of high expression in the center of the colony and weaker expression in the edge was again seen. β-catenin showed a similar pattern of staining found moststrongly in the membrane region of cells in the center of the colonies but cells at the edge showing staining either around the nucleus in a peri-nuclear pattern or within the nucleus (Fodde and Brabletz, 2007).These patterns were further demonstrated in cell lines established from HNSCC in Fanconi anemia patients (Gammon et al, 2011).

Locke and colleagues (2005) demonstrated that holoclones contain highly clonogenic cells that can be grown indefinitely and are able to restore cellular heterogeneity. Cells FACS sorted on the basis of CD44 expression, which is high in holoclones, showed differential growth patterns with the $CD44^{high}$ cells a) forming more holoclones than meroclones and paraclones, b) forming more colonies overall and c) ability to restore all three colony types with cellular heterogeneity. $CD44^{low}$ cells showed poor growth and formed only abortive paraclone colonies. These results generally support the hypothesis of a role for CD44 as a molecule more strongly expressed on cells with stem cell properties that can act as a stem cell marker. However, although sorting for CD44 isolated stem cell enriched fractions, the specificity of CD44 alone was limited. Subsequent experiments demonstrated that stem cells could be more efficiently isolated using a combination of markers, a technique that had been used to enrich successfully for tumorigenic breast cancer cells by Al-Hajj and colleagues (2003). When OSCC cells were stained for CD44

and CD24 and cells sorted into four quadrants and used for clonogenicity assays, $CD44^{high}CD24^{high}$ cells were found to be the most clonogenic and consistently formed more holoclones than cells from other quadrants. They could also be passaged with greater efficiency. These findings were interesting and showed an increase in purification. However, they still indicated that the overall enrichment efficiencies were relatively low and that, although cells with differential growth patterns and morphologies could be isolated, better markers are required if stem cell populations are to be isolated to greater purity.

Early in the thesis work, it was observed that when populations of cells are plated at low densities, individual cells behave in very different ways.Time-lapse videos showed that some cells tend to be stationary and divide to form cohesive holoclone colonies, whereas other cells are highly motile, move around the dish and, although they were seen to divide, remained spaced and did not form cohesive colonies. If a cell went on to form a holoclone, all cells of the first few divisions initially remained tightly packed. Later, although the cells in the center remained tightly packed, the cells at the edge tended to become slightly larger and to spread out away from the colony. A few of these edge cells tended to show an elongated spindle-like morphology and appeared to be trying to move away from the colony.In videos, some cells were seen to detach and move away from the main colony. Sometimes they then returned and adhered to the colony again but some cells wandered away out of the field of vision. This suggested that cells at the colony edge were undergoing a process similar to EMT, in which they lost their characteristic cobblestone appearance, become more spindle-like, resembled fibroblasts,and became motile.

If a holoclone colony is taken as a miniature equivalent of a tumour, the cells in the central region can be considered representative of the main bulk of the tumour, with the cells at the colony edge perhaps corresponding in some ways to cells at the invasive tumour front. Altered behaviour of cells at the invasive front of tumours has recently generated a lot of interest and there is increasing evidence for EMT occurring in this region (Bankfalvi and Piffko, 2000; Finger and Giaccia, 2010). If the cells at the colony margin undergo EMT, they possibly share some features of the cells that are present at the invasive front of the tumour-host interface and are responsible for causing tumour recurrence. Studies were therefore undertaken to examine how the *in vitro* properties and behaviour of these cells corresponded to known patterns of behaviour of cells undergoingEMT in other circumstances. TGF-βis a strong inducer of EMT for many cell types (Thiery et al, 2009; Zavadil and Bottinger, 2005) and dysregulated TGFβ activity has been linked to tumour progression and invasiveness in cancers (Moustakas and

Heldin, 2007). Hence TGF-β was selected for use on OSCC cell lines and was seen to induce EMT and to generate more cells with spindle morphologies at the edges of colonies. Activated fibroblasts, or myofibroblasts, present in the tumour microenvironment have been shown to play an important role in tumour invasion in pancreatic, breast, ovarian and bladder cancers (Bretnall et al, 2012; Micke and Ostman, 2004; Chaffer et al, 2007). To ascertain whether stromal factors present at the tumour-host interface could similarly bring about changes in OSCC cells, they were treated with medium conditioned by the growth of fibroblasts (FIBSCM) generated from specimens of oral cancers. Treatment with FIBSCM caused obvious morphological changes of OSCC cells, greater motility and a decreased tendency to form cohesive colonies. Instead of the characteristic cobblestone appearance normally displayed by epithelial cells, treated cells showed elongated spindle-like morphology. Time-lapse videos of these cells showed that they were highly motile and scattered actively about the culture. Immunocytochemistry indicated that FIBSCM treatment produced a marked loss of the normal cell surface expression of E-cadherin and β-catenin, with the latter seen to translocate to the nucleus.

Downregulation of ESA (Epcam) has been associated with the EMT process (Hollieret al, 2009) and various reports indicate that nuclear signalling by this molecule is associated with "stemness" and the progression of colon tumours (O'Brian et al, 2007; Went et al, 2006). Gires and colleagues (2009) have shown that increased nuclear signalling by ESA facilitates the translocation of β-catenin to the nucleus. Compared to control cells, cells from OSCC cell lines treated with either TGF-β or FIBSCM showed a marked reduction in the cell surface expression of ESA and also its translocation to the nucleus.

CD44 was shown to be expressed strongly by holoclone cellsand to locate mainly to the cell surface. Although CD44 expression by the central cells of holoclones was typically stronger than for cells at the colony edges, occasional cells at the colony edge were high for CD44. The scattered spindle-shaped cells around holoclones showed a range of CD44 expression levels. Some showed high levels of localization to the cell surface but others clearly showed expression of CD44 within the nucleus. Nuclear localization of CD44 to the nucleus has been associated with the acquisition of increased invasiveness by colon carcinoma cells (Ying-Jhen Su, 2011) and it is required for the clonal formation *invitro* and tumorigenicity *invivo* (Bourguignon, 2008). Lee and co-workers (2009) found that translocation of CD44 to the nucleus modulates the cadherin-catenin pathways and also modulates members of the SMAD family proteins that are closely involved with cellular growth. This suggests a possible link

with TGF-β as it functions in close association with the SMAD family of proteins. Interestingly, as can be seen in many of the illustrations, cells that are dividing (D) apparently show very high levels of staining for CD44. This was also seen for other markers examinedas shown in the figure below.

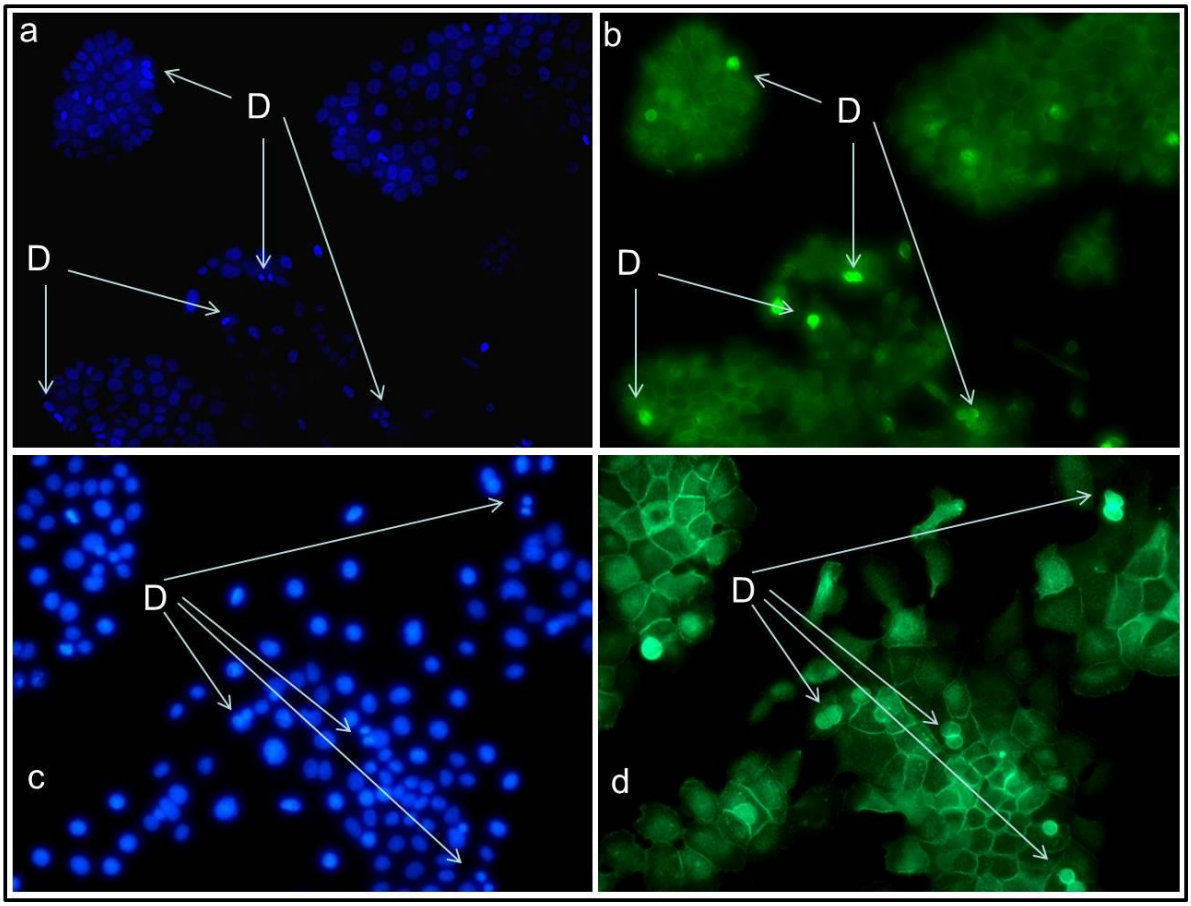

Figure 2.135: High surface expression of markers in dividing cells. CA1 cells are shown stained with DAPI nuclear stain (a, c) and anti-e-cadherin antibody (b) and anti-CD44 antibody (d). Cells that are dividing are designated 'D'.

Cell rounding-up and shrinkage during the division process might possibly result in an increased concentration of CD44 at the surface butit appears that this effect is largely an artefactas a similar pattern is seen with most antibodies and is perhaps associated with altered cell density resulting in non-specific binding of antibody.

Sphere formation is mainly a property associated with cells that have undergone EMT (Biddle 2011) and both TGF-β and FIBSCM increased the proportion of cells forming tumour spheres in suspension cultures, with the highest number of spheres formed by cells treated with conditioned medium. Reintroduction of spheres into adherent culture conditions indicated that

they readily attached and formed colonies of cells that expanded away from the adherent sphere, with a large proportion of these cells being motile elongated cells. Sphere assays have previously been used to isolate stem cells from breast cancers that have undergone EMT (Mani et al, 2008) and the ability of cells in spheres to revert back to form adherent colonies suggested that there are cells present in spheres that possess the phenotypic plasticity to switch between the epithelial and mesenchymal states, i.e. undergo EMT and MET (mesenchymal to epithelial transition). This also supports the notion that there may be two types of stem cells present within OSCC lines. Collaborative work done in the Mackenzie lab (Biddle et al, 2011) has recently confirmed the presence of two types of cells in OSCC lines, those that are proliferative and retain epithelial characteristics and those that are migratory and show an elongated spindle appearance and were the $CD44^{high}ESA^{high}$ and $CD44^{high}ESA^{low}$ populations discussed earlier. In the lab, these cells have also been demonstrated in cultures of cells from lines generated from OSCCs of Fanconi anaemia patients (Gammon et al, 2011). Studies of these sub-populations, using FACS, showed that the $CD44^{high}ESA^{high}$ cells represented the stem cell fraction within OSCC lines as they formed the most holoclones after isolation and culture. $CD44^{high}ESA^{low}$ cellspredominantly formed clusters of spindle-shaped cells with few holoclones, and showed characteristics of EMT cells. It was also seen that the $CD44^{high}ESA^{low}$ cells formed 10 times more spheres than the $CD44^{high}ESA^{high}$ cells, suggesting that a portion of $CD44^{high}ESA^{low}$ cells are clonogenic as this property has previously been associated with stem cells (Dontu et al, 2003). Analysis of gene expression patterns in these two subpopulations within OSCC liens showed that $CD44^{high}ESA^{low}$ cells expressed higher levels of Vimentin, Twist and Snail, all markers of EMT, and lower expression of E-cadherin, which is also a signature of EMT cells. To assay whether this EMT population exists in OSCC tumours *in vivo*, populations of cells were generated from fresh specimens of tumours and FACS sorted on the basis of CD44 and ESA expression and it was seen that this population also existed in cells extracted from OSCC specimens. It was further revealed that the size of the EMT $CD44^{high}ESA^{low}$ population correlated with the progressive stage of the tumour. Cell lines from dysplastic skin did not contain a detectable $C44^{high}ESA^{low}$ population but cells derived from primary and metastatic tumours showed high proportions of these cells (Biddle et al, 2011).*In vivo* tumorigenicity assays showed that both $CD44^{high}ESA^{high}$ and $CD44^{high}ESA^{low}$ cells formed tumours within mice, but it was only the tumours generated from $CD44^{high}ESA^{low}$ cells that showed evidence of lymphatic spread and contain cells that may have invasive potential. The fact that both populations of cells can form holoclone colonies suggested that there are cells present within the EMT ($CD44^{high}ESA^{low}$) population that have the ability to revert back to

form the non-EMT fraction within OSCC lines and vice versa. To verify this, single cells from both populations were plated and it was seen that the majority of $CD44^{high}ESA^{high}$ cells generated both EMT and non-EMT cell populations, but only a few $CD44^{high}ESA^{low}$ cells demonstrated this property. This suggested that not all of the $CD44^{high}ESA^{low}$ cells were bipotent and suggested that differences in the levels of ESA expression within the EMT fraction might distinguish bipotent cells from unipotent EMT cells.This link was further studied using ALDH1 and it was seen that $CD44^{high}ESA^{low/+}$ cells that are present nearer to the main population on FACS possessed the property of bipotency and also showed increased activity of ALDH1, whereas $CD44^{high}ESA^{low/-}$ cells represented differentiated EMT cells that could not revert back and did not reconstitute cellular heterogeneity.

FACS analysis of OSCC lines was used to examine further thebehaviour of the cell sub-populations identifiable in growing cultures. FACS consistently identified a population of cells with high expression of CD44 and low expression of ESA. These$CD44^{high}ESA^{low}$ cells localised as a distinct population, typically separated from the bulk of the cells which occupied the $CD44^{high}ESA^{high}$ and $CD44^{low}$ region of the plots. The $CD44^{high}ESA^{low}$ population primarily represents the EMT component present within OSCC cell lines and formed tumour spheres (Biddle et al, 2011). Although whenplated out at clonal density,they initially form scattered cells with spindle-shaped fibroblast-like morphologies, with time they begin to generate holoclone-like colonies. The reverse is seen with $CD44^{high}ESA^{high}$ cells which, when plated out at clonal density, initially give rise predominantly to epithelial-like holoclone colonies but with time also generate an EMT-like population. These observations support the concept that cells that can switch between the epithelial $CD44^{high}ESA^{high}$ phenotype and the spindle-shaped $CD44^{high}ESA^{low}$ EMT phenotype and also indicate that both populations of cells can self-renew. Division of both cell types was observed in videos and there is now experimental data (Biddle et al, 2011) and showing that certain cells within each population have the ability to restore the population heterogeneity.

The percentage of cells within OSCC lines that are $CD44^{high}ESA^{low}$ varies from cell line to cell line. For example, in the Ca1 cell line, 1-3% of the cells show the $CD44^{high}ESA^{low}$ phenotype while in the H357 cell line, the fraction is usual higher, being about 5-6%. Some other cell lines recently isolated by co-workers in the Mackenzie lab have shown very high levels of EMT (data not shown, Mackenzie lab).The susceptibility of cell lines to the effects of TGF-β also varies.For example, when exposed to TGF-β for 5 days, this population in CA1 cells increases to 8-9% and but forH357 cells increases to 25%.

When examined separately, the percentage of each of the $CD44^{high}$ and of $ESA^{low/-}$ cell populations was also seen to increase with short term treatment with TGF-β. The increase in the percentage of $ESA^{low/-}$ cells was greater than the overall increase in the $CD44^{high}ESA^{low}$ population, indicating that not all the cells that reduced their ESA levels were high for CD44. To assess whether TGF-β is responsible for the presence of the apparently innate population of $CD44^{high}ESA^{low}$ cells within cell lines, they were treated with an inhibitor of TGF that has been shown successfully to block TGF-β activity in various cellular systems. This inhibitor successfully abolished the effect seen with the addition of TGF-β,but failed to eradicate or reduce the inherentpopulation of $CD44^{high}ESA^{low}$ cells routinely seen on FACS analysis of OSCC lines that suggested that the EMT process in OSCC lines occurs in a TGF-β independent manner.It is thought that this EMT may be bought about by EGF present in the RM+ medium as switching cells to basal media results in the loss of these cells in OSCC lines in the lab. Further experiments are needed to confirm this hypothesis. Experiments were also undertaken to assess the interaction of TGF-β with other mediators of inflammatory processes as inflammatory cytokines have been shown to play a role in the aggressiveness of tumours. TNF-α when added on its ownfor 5 days produced changes similar to those caused by TGF-β in that cells took on a spindle-like morphology and increased the proportion of $CD44^{high}ESA^{low}$ cells. However, TNF-α worked synergistically with TGF-β to greatly enhancethe effect seen compared to that seen with either cytokine alone, with the levels of EMT rising to 35% for Ca1 cells and 60% for H357 cells.

Cells were also stained with an anti-Vimentin antibody as Vimentin is known to be a signature protein acquired during EMT. Vimentin expression has been linked to the invasiveness of breast cancer cells (Kokkinos et al, 2011) and has been shown to regulate the EMT process through interaction with the slug and AXL family of proteins (Vuoriluoto et al, 2007). Holoclone cells generally show no expression of vimentin but there werescattered elongated cells that showed strong expression of vimentin with some cells at the edges of holoclones also being Vimentin positive. Cells treated with TGF-β showed very high expression of vimentin in almost all the cells.

$CD44^{high}ESA^{high}$, $CD44^{high}ESA^{low}$ and $CD44^{low}ESA^{high}$ cells were also sorted and cultured from clonal density for 5-6 days. Following this, these cells were detached from the dish, again stained with anti-CD44 and anti-ESA antibodies and analyzed using FACS. It was found that both $CD44^{high}ESA^{low}$ and $CD44^{high}ESA^{high}$ cells reconstitute the native FACS plots generated and restore cellular heterogeneity seen in OSCC lines. This means that both population contain

self-renewing cells that are able to maintain themselves within the total population and also supports the concept of the mobile cancer stem cell.

Experimental data also show that TGF-β enhances the motility and migration of OSCC cells. To check the effect of TGF-β on the migration and motility of cells, scratch assays were conducted and migration of treated cells was compared to controls over a period of 48 hours. It was found that TGF-β treated cells migrate across the gap the fastest and cover more than 80% of the scratched area within 24 hours whereas control cells cover about 50-60% of the scratch area. Further the effect of NS-398 which is a COX-II inhibitor was also checked and it was found that it slowed the migration of cells across the gap. We had previously analyzed the effect of NS-398 using FACS and were able to show that it does not completely eradicate the innate EMT population present within OSCC lines but does decrease it, although this decrease is not significant.

Summary and Conclusions

2.1 Analysis of the distribution of putative stem-cell-related molecules in wax-embedded sections of OSCC using in situ hybridization.

1. Control tissues indicated that both the probe and the vector functioned well to give a good signal in both the cancer blocks and the control tissues.

2. Out of nine probes examined, only CEBP-α, Notch3 and Vimentin showed a good differential hybridization signal in cancer sections compared to normal adult skin, and although the probes for these molecules showed a higher signal in cancer blocks, they failed to localize stem cell zones/hot spots.

3. The rest of the probes examined, namely Hurpin, Pirin, RDHL and Erb-b3, were similarly selected on the basis of their differential expression in holoclones and paraclones (Locke et al, 2005) and suggestions in the literature of their potential differential expression in stem cells. However these probes failed to elicit any interesting patterns of probe localization. Thus, although it was hoped that patterns of stem cell localization within oral mucosa and oral tumours might be revealed with these probes, the observed distribution of label did not provide such information.

4. *Insitu* hybridization was also performed on cells cultured from OSCC cell lines, but they were either lost owing to technical failure, or showed poor specificity.

2.2 Identification and isolation of stem/stem-like cells in OSCC cell lines

a) Cell culture

1. The cell lines examined, consistently showed the generation of three types of colony morphologies, classified as holoclones meroclones and paraclones after cells were plated at clonal densities.

2. It also appeared that the cells forming holoclones are heterogeneous. The center of the holoclone is made up of tightly packed cobblestone shaped cells and slightly larger cells at the edge that are arranged loosely.

b) Immunocytochemistry

1. When stained for CD44, holoclones show the brightest staining, with meroclones being the next in intensity and the weakest signal being detected in paraclones. The CD44 in holoclones seems to be predominantly present in the cell surface in all the cell lines examined.

There was also nuclear localization of CD44 seen, present in mostly all the cells making up the meroclones and paraclones and only weak nuclear staining of CD44 could be detected within the central cells of the holoclone and it seems to be more pronounced in the cells making up the edge.

Also seen consistently was the pattern of strong CD44 expression in the central cells of the holoclones and weak expression in cells making up the edges of these colonies.

2. E-cadherin was shown to be expressed at the protein level in all the cell lines examined. In holoclone colonies E-cadherin was shown to be present at the cell periphery with little or no expression in the cytoplasm. Central cells of the holoclone were shown to express higher levels than those making up the edge of the colonies. The scattered fibroblast-like cells showed reduced expression in the membrane and very weak levels within cytoplasm. A few cells also showed nuclear accumulation of the protein.

3. β-Catenin was expressed in all three cell lines examined however the patterns observed differed. CA1 and H357 cells showed strong expression of the protein almost exclusively at the cell periphery with very little being present in the cytoplasm. Cells at the edge showed reduced levels. In the Fanconi 1131 cell line, β-catenin was expressed in the cell membrane and in the nucleus of all the cells in the colonies but nuclear accumulation was more marked in cells present at the edge.

c) Time Lapse Video

1. On video it can be seen that when holoclones form, 2 types of cells exist, the ones forming the central zone and the other the colony periphery. The central cells appear relatively stationary and adhere tightly to other cells and have characteristic cobblestone morphology. These cells are also seen to divide to maintain the central region of the holoclone. Cells at the edge of colonies are spindle-shaped in appearance and appear to break away from the colony. There are also spindle-shaped cells lying outside the edges of the colonies that are highly motile and make contact with other cells and they appear to be generated from the colony itself.

2.3 Detection of CD44 at protein level using Fluorescent Activated Cell Sorting (FACS)

1. Cells were sorted on the basis of CD44 expression and the 4-6% of the highest and lowest expressing cells wereselected as $CD44^{high}$ or $CD44^{low}$. When plated out at clonal density, the $CD44^{high}$ population consistently produced more holoclones and meroclones and also formed a higher total number of colonies in comparison to the $CD44^{low}$ cells. This trend was also demonstrated in each of the three cell lines examined namely H357, Ca1 and UK1.

2.4 Detection of CD44 and CD24 at protein level using Fluorescent Activated Cell Sorting (FACS)

1. **$CD44^{high}CD24^{high}$** (Q2) cells from both cell lines formed significantly higher proportions of holoclones ($p<0.05$).The number of holoclones formed by these cells remained significantly higher when cells were plated immediately after sorting and also after the first passage.

2. The total colony counts for **$CD44^{high}CD24^{high}$** were also higher than those obtained for **$CD44^{high}CD24^{low}$**, **$CD44^{low}CD24^{low}$** and **$CD44^{low}CD24^{high}$** but this difference was not statistically significant ($p>0.05$). These resultswere consistent for all the cell lines examined,suggesting that these proteins are similarlyexpressed in both cell lines.

3. **$CD44^{low}CD24^{low}$** cells significantly formed the highest number of paraclones. They also formed the least amount of holoclones, 32.5±3.54 for CA1 and 26±5.66 for 5PT. The number of colonies generated by these cells were also more than the other populations, but this difference was not only insignificant ($p>0.05$), but it could also be argued that paraclones divide more frequently than holoclones which is why they give rise to a much larger colony number.

4. These results suggest that the use of CD44 and CD24 together does give greater enrichment for stem cells as opposed to CD44 alone, and suggest that CD44 and CD24 are both expressed on stem cells in oral cell lines.

5. These results also demonstrate heterogeneous patterns of cell surface expression of markers, and indicate that they are related to the heterogeneous behavioural properties of cell sub-populations present in cell lines.

2.5 Induction of EMT in cancer cell lines and the role of TGF-β and external factors that may influence the extent of this process

a) Cell culture:

1. Control cells formed characteristic colonies in the form of holoclones, meroclones, and paraclones and populations of spindle shaped cells, resembling fibroblasts were seen at the edges of colonies or lying outside the colonies in both cell lines. Cells treated with TGF-β tended not to form colonies but formed scattered cells that had elongated spindle morphology and looked similar to the cells formed at the edges of colonies.

2. Time-lapse video showed that cells treated with TGF-β and FIBSCM show a high level of motility and scattering, and take on elongated spindle morphologies. The cells also showed decreased cohesiveness and did not form colonies as under control conditions (2.2.1.3 E). Thus both treatments enhanced the phenomenon occurring around the edges of colonies that resulted in the formation of elongated spindle cells just described.

b) Immunocytochemistry

1. Cells grown under control conditions showed good expression of ESA at the cell surface with central cells within colonies expressing higher levels of ESA than those at the edges. Elongated spindle cells at the edge also displayed loss of membranous ESA and some of these cells showed accumulation of ESA around the nucleus. Treated cells also showed nuclear expression of ESA and this was associated with loss of the epithelial phenotype and the acquisition of a more mesenchymal, characterized by the elongated spindle cells.

2. In both cell lines, E-cadherin expression was seen at the surface of cells in the center of colonies and was lower in the cells around the edge. Treatment with TGF-β also resulted in loss of membranous E-cadherin. Strong expression of E-cadherin was seen in the nuclei of both types of treated cells but TGF-β caused a greater effect than the fibroblast conditioned medium.

3. CD44 was expressed in both cell lines examined. There was strong cell surface CD44 expression within central colony cells with little evidence of nuclear accumulation. The motile cells differed in their CD44 expression patterns, with some staining brightly for CD44 in the cytoplasm, while others showed nuclear accumulation and moderate membrane expression. Treated cells showed decreased CD44 at the cell surface with increased accumulation evident within the nucleus of spindle cells.

c) FACS analysis:

1. FACS analysis using CD44 and ESA antibodies consistently identified a subpopulation of cells that was $CD44^{high}ESA^{low}$.

2. This population increased significantly when cells were treated with TGF-β in both cell lines, with the H357 showing the greater response to treatment.

3. Both treatments caused an increase in the number of cells that were $CD44^{high}$ and this was statistically significant with TGF-β.

4. Both treatments also resulted in an increase in the number of cells that were $ESA^{low/-}$ and this was statistically significant with TGF-β.

d) Sphere Assay

1. Our studies show that OSCC cell lines contain a population of cells which have the ability to form spheres (CA1=8.4%; H357=12%) under control conditions.

2. Treatment with TGF-β caused a significant increase in the number of spheres formed and interestingly, treatment with fibroblast conditioned medium produced an even greater increase in the number of spheres formed.

3. When control spheres were reintroduced into adherent conditions, cells from the spheres attached and spread out to form epithelial looking cells and formed large colonies resembling holoclones. These colonies had a prominent halo of spindly motile cells around the edge.

4. Once these cells were again plated into a sphere assay, they formed more spheres per 1000 cells than they had before.

2.6 The effect of short-term treatment with TGF-β and its inhibitor (SB431542) on subpopulations of cells within OSCC cell lines and their effects of these on the expression of vimentin.

a) Cell culture

1. Cells from both cell lines displayed an elongated spindle-like morphology and showed increased migratory capacity as seen on time lapse videos. Cells from both lines also showed a decreased propensity to form adherent colonies. Treatment with the inhibitor had no adverse effects on the growth of these cells and SB431542 was seen to effectively block TGF-β activity as when cells were grown with both the inhibitor and TGF-β added together, they resembled control cells.

b) FACS analysis

1. FACS analysis for CD44 and ESA showed an increase in the size of the $CD44^{high}ESA^{low}$ and $CD44^{high}$ and the $ESA^{low/-}$ populations with TGF-β treatment in both cell lines but it was the H357 cell line that was found to be more susceptible to TGF-β as seen by the greater responses to treatment.

c) Immunocytochemistry:

1. The expression of Vimentin was assessed in OSCC cell lines and was seen to be high in spindle-shaped lying outside colonies (CA1) or in some cells at the edge (H357). Other cells in the colonies showed no expression. Treated cells showed strong cytoplasmic expression of vimentin. These staining patterns support the suggestion that $CD44^{high}ESA^{low}$ cells have undergone EMT

2.7 The effect of long-term treatment with TGF-□ and treatment withdrawl on OSCC cells

1. Treatment with TGF-β for 5 days caused an increase in the relative proportion of $CD44^{high}ESA^{low}$, $CD44^{high}$ and $ESA^{low/-}$ cells within the bulk of the population.

2. Treatment with TGF-β for longer indicated that this further increased the size of these populations. At the end of twenty days, very few cohesive cells remained. The response of the two cell lines studied varied with the H357 cells showing more susceptibility to TGF-β treatment compared to the CA1 cell line. The number of cells expressing high levels of CD44

increased in both lines examined and this correlated with the increase in the $CD44^{high}ESA^{low}$ population. TGF-β also caused a decrease in the expression of ESA and the response shown by the H357 cell line was greater than that for CA1 cells.

3. Withdrawing TGF-β treatment caused a decrease in the $CD44^{high}ESA^{low}$ population in both cell lines and by day 15, after withdrawal of TGF-β, the proportion of $CD44^{high}ESA^{low}$ cells declined in both cell lines. but remained higher than the controls, suggesting that the effect of TGF-β is largely reversible.

4. Some of the cell remained $CD44^{high}ESA^{low}$ even after 15 days of withdrawal, suggests that there may be a small proportion of $CD44^{high}ESA^{low}$ cells that does not revert back.

2.8 The self-renewal potential of intrinsic populations within OSCC cell lines

1. $CD44^{high}ESA^{high}$ cells grew, predominantly as holoclones and showed characteristic morphology seen in OSCC lines and spindle cells could be identified at the edges of the colonies or lying outside them.

2. In comparison to these cells, $CD44^{high}ESA^{low}$ cells grew as elongated spindle cells with few scattered holoclone colonies that grow to a large size.

3. In contrast, $CD44^{low}$ cells showed poor growth and formed paraclones.

4. This suggested that the $CD44^{high}ESA^{high}$ cells were the non-EMT stem cell fraction while the $CD44^{high}ESA^{low}$ cells were EMT cells and both populations contain cells with regenerative potential that can switch back and forth from the epithelial phenotype to the mesenchymal phenotype through EMT and MET.

2.9 The effect of TNF-α on EMT in OSCC cell lines and the combined effect of TNF-α and TGF-β on these lines.

1. Our results show that the effect of TNF-α on OSCC cells is similar to that of TGF-β in causing an increase in the EMT population ($CD44^{high}ESA^{low}$) and an increase in the size of both the $CD44^{high}$ and $ESA^{low/-}$ populations.

2. Further to this we found that the addition of TNF-α and TGF-β together greatly enhances the effect seen indicating that they work together synergistically to promote EMT in OSCC cells. The response of cell lines varied butwhen TGF-β and TNF-α were added together there was a significant increase in the size of the $CD44^{high}ESA^{low}$ population in both CA1 (x10) and H357 (x12) cells.

3. Further, there was an increase in the size of both, the $CD44^{high}$ and $ESA^{low/-}$ populations.

4. On microscopic examination, cells from both lines were seen to possess a spindle-shaped morphology and a decreased tendency to form cohesive colonies.

2.10 The effect of TGF-β, SB431542 and NS-398 on migration in OSCC cell lines.

1. It was found that TGF-β enhances cell migration and this effect was seen with boththe CA1 and Fanconi cell lines. Treated cells migrate faster than controls and covered 94% and 84% (CA1, OHSU) of the scratch area by 48 hours with control cells covering only 74% and 61% respectively.

2. High magnification pictures of the scratch area show cells resembling fibroblasts migrating across the scratch. The cells at the edge of the scratch also seemed to have undergone EMT as is apparent by their spindly morphology.

References

1-230

1 Aigner, S. *et al.* CD24 mediates rolling of breast carcinoma cells on P-selectin. *Faseb J***12**, 1241-1251 (1998).

2 Al-Hajj, M., Becker, M. W., Wicha, M., Weissman, I. & Clarke, M. F. Therapeutic implications of cancer stem cells. *Curr Opin Genet Dev***14**, 43-47 (2004).

3 Al-Hajj, M. & Clarke, M. F. Self-renewal and solid tumor stem cells. *Oncogene***23**, 7274-7282 (2004).

4 Al-Hajj, M., Wicha, M. S., Benito-Hernandez, A., Morrison, S. J. & Clarke, M. F. Prospective identification of tumorigenic breast cancer cells. *Proc Natl Acad Sci U S A***100**, 3983-3988 (2003).

5 Alison, M. R., Poulsom, R., Forbes, S. & Wright, N. A. An introduction to stem cells. *J Pathol***197**, 419-423 (2002).

6 Alonso, L. & Fuchs, E. Stem cells of the skin epithelium. *Proc Natl Acad Sci U S A***100 Suppl 1**, 11830-11835 (2003).

7 Alonso, L. & Fuchs, E. The hair cycle. *J Cell Sci***119**, 391-393 (2006).

8 Anneroth, G., Batsakis, J. G. & Luna, M. Malignancy grading of squamous cell carcinoma in the floor of the mouth related to clinical evaluation. *Scand J Dent Res***94**, 347-356 (1986).

9 Armstrong, L. *et al.* Phenotypic characterization of murine primitive hematopoietic progenitor cells isolated on basis of aldehyde dehydrogenase activity. *Stem Cells***22**, 1142-1151 (2004).

10 Asiedu, M. K., Ingle, J. N., Behrens, M. D., Radisky, D. C. & Knutson, K. L. TGFbeta/TNF(alpha)-mediated epithelial-mesenchymal transition generates breast cancer stem cells with a claudin-low phenotype. *Cancer Res***71**, 4707-4719 (2011).

11 Bakin, A. V., Tomlinson, A. K., Bhowmick, N. A., Moses, H. L. & Arteaga, C. L. Phosphatidylinositol 3-kinase function is required for transforming growth factor beta-mediated epithelial to mesenchymal transition and cell migration. *J Biol Chem***275**, 36803-36810 (2000).

12 Bankfalvi, A. *et al.* Gains and losses of adhesion molecules (CD44, E-cadherin, and beta-catenin) during oral carcinogenesis and tumour progression. *J Pathol***198**, 343-351 (2002).

13 Bankfalvi, A. & Piffko, J. Prognostic and predictive factors in oral cancer: the role of the invasive tumour front. *J Oral Pathol Med***29**, 291-298 (2000).

14 Barrandon, Y. & Green, H. Three clonal types of keratinocyte with different capacities for multiplication. *Proc Natl Acad Sci U S A***84**, 2302-2306 (1987).

15 Barrandon, Y., Morgan, J. R., Mulligan, R. C. & Green, H. Restoration of growth potential in paraclones of human keratinocytes by a viral oncogene. *Proc Natl Acad Sci U S A***86**, 4102-4106 (1989).

16 Bates, R. C. & Mercurio, A. M. The epithelial-mesenchymal transition (EMT) and colorectal cancer progression. *Cancer Biol Ther***4**, 365-370 (2005).

17 Berndt, A., Borsi, L., Hyckel, P. & Kosmehl, H. Fibrillary co-deposition of laminin-5 and large unspliced tenascin-C in the invasive front of oral squamous cell carcinoma in vivo and in vitro. *J Cancer Res Clin Oncol***127**, 286-292 (2001).

18 Berndt, A., Hyckel, P., Konneker, A., Katenkamp, D. & Kosmehl, H. Oral squamous cell carcinoma invasion is associated with a laminin-5 matrix re-organization but independent of basement membrane and hemidesmosome formation. clues from an in vitro invasion model. *Invasion Metastasis***17**, 251-258 (1997).

19 Bickenbach, J. R. Identification and behavior of label-retaining cells in oral mucosa and skin. *J Dent Res***60 Spec No C**, 1611-1620 (1981).
20 Biddle, A. *et al.* Cancer stem cells in squamous cell carcinoma switch between two distinct phenotypes that are preferentially migratory or proliferative. *Cancer Res***71**, 5317-5326 (2011).
21 Biddle, A. & Mackenzie, I. C. Cancer stem cells and EMT in carcinoma. *Cancer Metastasis Rev* (2012).
22 Blanpain, C. & Fuchs, E. Epidermal homeostasis: a balancing act of stem cells in the skin. *Nat Rev Mol Cell Biol***10**, 207-217 (2009).
23 Bonner-Weir, S. & Sharma, A. Pancreatic stem cells. *J Pathol***197**, 519-526 (2002).
24 Bonnet, D. & Dick, J. E. Human acute myeloid leukemia is organized as a hierarchy that originates from a primitive hematopoietic cell. *Nat Med***3**, 730-737 (1997).
25 Bortolomai, I. *et al.* Tumor initiating cells: development and critical characterization of a model derived from the A431 carcinoma cell line forming spheres in suspension. *Cell Cycle***9**, 1194-1206 (2010).
26 Bouquot, J. E. & Ephros, H. Erythroplakia: the dangerous red mucosa. *Pract Periodontics Aesthet Dent***7**, 59-67; quiz 68 (1995).
27 Brabletz, T. *et al.* Invasion and metastasis in colorectal cancer: epithelial-mesenchymal transition, mesenchymal-epithelial transition, stem cells and beta-catenin. *Cells Tissues Organs***179**, 56-65 (2005).
28 Brabletz, T., Jung, A., Spaderna, S., Hlubek, F. & Kirchner, T. Opinion: migrating cancer stem cells - an integrated concept of malignant tumour progression. *Nat Rev Cancer***5**, 744-749 (2005).
29 Bryne, M. *et al.* The invasive front of carcinomas. The most important area for tumour prognosis? *Anticancer Res***18**, 4757-4764 (1998).
30 Burkert, J., Wright, N. A. & Alison, M. R. Stem cells and cancer: an intimate relationship. *J Pathol***209**, 287-297 (2006).
31 Byun, T. *et al.* Expression of secreted Wnt antagonists in gastrointestinal tissues: potential role in stem cell homeostasis. *J Clin Pathol***58**, 515-519 (2005).
32 Cairns, J. Cancer and the immortal strand hypothesis. *Genetics***174**, 1069-1072 (2006).
33 Cano, E. R. *et al.* Management of squamous cell carcinoma of the base of tongue with chemoradiation and brachytherapy. *Head Neck***31**, 1431-1438 (2009).
34 Cantz, T., Manns, M. P. & Ott, M. Stem cells in liver regeneration and therapy. *Cell Tissue Res***331**, 271-282 (2008).
35 Chaffer, C. L. *et al.* Mesenchymal-to-epithelial transition facilitates bladder cancer metastasis: role of fibroblast growth factor receptor-2. *Cancer Res***66**, 11271-11278 (2006).
36 Chaffer, C. L., Dopheide, B., Savagner, P., Thompson, E. W. & Williams, E. D. Aberrant fibroblast growth factor receptor signaling in bladder and other cancers. *Differentiation***75**, 831-842 (2007).
37 Chambers, S. M. & Studer, L. Cell fate plug and play: direct reprogramming and induced pluripotency. *Cell***145**, 827-830 (2011).
38 Chaubal, S., Wollenberg, B., Kastenbauer, E. & Zeidler, R. Ep-CAM--a marker for the detection of disseminated tumor cells in patients suffering from SCCHN. *Anticancer Res***19**, 2237-2242 (1999).
39 Chen, M. S. *et al.* Wnt/beta-catenin mediates radiation resistance of Sca1+ progenitors in an immortalized mammary gland cell line. *J Cell Sci***120**, 468-477 (2007).
40 Cheng, H. & Leblond, C. P. Origin, differentiation and renewal of the four main epithelial cell types in the mouse small intestine. III. Entero-endocrine cells. *Am J Anat***141**, 503-519 (1974).

41 Chetty, R. & Serra, S. Nuclear E-cadherin immunoexpression: from biology to potential applications in diagnostic pathology. *Adv Anat Pathol***15**, 234-240 (2008).
42 Clarke, M. F. *et al.* Cancer stem cells--perspectives on current status and future directions: AACR Workshop on cancer stem cells. *Cancer Res***66**, 9339-9344 (2006).
43 Clay, M. R. *et al.* Single-marker identification of head and neck squamous cell carcinoma cancer stem cells with aldehyde dehydrogenase. *Head Neck***32**, 1195-1201 (2010).
44 Clevers, H. Stem cells, asymmetric division and cancer. *Nat Genet***37**, 1027-1028 (2005).
45 Compton, C. C. *et al.* Cultured human sole-derived keratinocyte grafts re-express site-specific differentiation after transplantation. *Differentiation***64**, 45-53 (1998).
46 Costea, D. E., Gammon, L., Kitajima, K., Harper, L. & Mackenzie, I. C. Epithelial stem cells and malignancy. *J Anat***213**, 45-51 (2008).
47 Costea, D. E., Tsinkalovsky, O., Vintermyr, O. K., Johannessen, A. C. & Mackenzie, I. C. Cancer stem cells - new and potentially important targets for the therapy of oral squamous cell carcinoma. *Oral Dis***12**, 443-454 (2006).
48 Cotsarelis, G., Kaur, P., Dhouailly, D., Hengge, U. & Bickenbach, J. Epithelial stem cells in the skin: definition, markers, localization and functions. *Exp Dermatol***8**, 80-88 (1999).
49 Coussens, L. M. & Werb, Z. Inflammation and cancer. *Nature***420**, 860-867 (2002).
50 Cvoro, A. *et al.* Cross talk between glucocorticoid and estrogen receptors occurs at a subset of proinflammatory genes. *J Immunol***186**, 4354-4360 (2011).
51 Davis, S. J. *et al.* Metastatic potential of cancer stem cells in head and neck squamous cell carcinoma. *Arch Otolaryngol Head Neck Surg***136**, 1260-1266 (2010).
52 De Luca, L. M., Adamo, S. & Kato, S. Retinoids and cell adhesion. *Methods Enzymol***190**, 81-91 (1990).
53 Debies, M. T. *et al.* Tumor escape in a Wnt1-dependent mouse breast cancer model is enabled by p19Arf/p53 pathway lesions but not p16 Ink4a loss. *J Clin Invest***118**, 51-63 (2008).
54 Dontu, G. & Wicha, M. S. Survival of mammary stem cells in suspension culture: implications for stem cell biology and neoplasia. *J Mammary Gland Biol Neoplasia***10**, 75-86 (2005).
55 Duband, J. L., Monier, F., Delannet, M. & Newgreen, D. Epithelium-mesenchyme transition during neural crest development. *Acta Anat (Basel)***154**, 63-78 (1995).
56 Eastham, A. M. *et al.* Epithelial-mesenchymal transition events during human embryonic stem cell differentiation. *Cancer Res***67**, 11254-11262 (2007).
57 Eger, A. *et al.* beta-Catenin and TGFbeta signalling cooperate to maintain a mesenchymal phenotype after FosER-induced epithelial to mesenchymal transition. *Oncogene***23**, 2672-2680 (2004).
58 El-Bahrawy, M. A., Talbot, I. C., Poulsom, R., Jeffery, R. & Alison, M. R. The expression of E-cadherin and catenins in colorectal tumours from familial adenomatous polyposis patients. *J Pathol***198**, 69-76 (2002).
59 Fillmore, C. M. & Kuperwasser, C. Human breast cancer cell lines contain stem-like cells that self-renew, give rise to phenotypically diverse progeny and survive chemotherapy. *Breast Cancer Res***10**, R25 (2008).
60 Finger, E. C. & Giaccia, A. J. Hypoxia, inflammation, and the tumor microenvironment in metastatic disease. *Cancer Metastasis Rev***29**, 285-293 (2010).

61 Franz, M. *et al.* Expression of Snail is associated with myofibroblast phenotype development in oral squamous cell carcinoma. *Histochem Cell Biol***131**, 651-660 (2009).
62 Gammon, L., Biddle, A., Fazil, B., Harper, L. & Mackenzie, I. C. Stem cell characteristics of cell sub-populations in cell lines derived from head and neck cancers of Fanconi anemia patients. *J Oral Pathol Med***40**, 143-152 (2011).
63 Ginestier, C. *et al.* ALDH1 is a marker of normal and malignant human mammary stem cells and a predictor of poor clinical outcome. *Cell Stem Cell***1**, 555-567 (2007).
64 Gjorevski, N., Boghaert, E. & Nelson, C. M. Regulation of Epithelial-Mesenchymal Transition by Transmission of Mechanical Stress through Epithelial Tissues. *Cancer Microenviron* (2011).
65 Goodall, A. R., Walker, J. H. & Vaughan, P. F. Translocation of the PKC isoforms present in the human neuroblastoma, SH-SY5Y, following short-term treatment with the phorbol ester, TPA. *Biochem Soc Trans***24**, 427S (1996).
66 Gotte, M. & Yip, G. W. Heparanase, hyaluronan, and CD44 in cancers: a breast carcinoma perspective. *Cancer Res***66**, 10233-10237 (2006).
67 Graziano, A. *et al.* The stem cell hypothesis in head and neck cancer. *J Cell Biochem***103**, 408-412 (2008).
68 Griffin, J. D. & Lowenberg, B. Clonogenic cells in acute myeloblastic leukemia. *Blood***68**, 1185-1195 (1986).
69 Grunert, S., Jechlinger, M. & Beug, H. Diverse cellular and molecular mechanisms contribute to epithelial plasticity and metastasis. *Nat Rev Mol Cell Biol***4**, 657-665 (2003).
70 Gunthert, U. *et al.* Functional involvement of CD44, a family of cell adhesion molecules, in immune responses, tumour progression and haematopoiesis. *Adv Exp Med Biol***451**, 43-49 (1998).
71 Gupta, P. B. *et al.* Identification of selective inhibitors of cancer stem cells by high-throughput screening. *Cell***138**, 645-659 (2009).
72 Gurdon, J. B. The developmental capacity of nuclei taken from differentiating endoderm cells of Xenopus laevis. *J Embryol Exp Morphol***8**, 505-526 (1960).
73 Hanahan, D. & Weinberg, R. A. The hallmarks of cancer. *Cell***100**, 57-70 (2000).
74 Harper, L. J. *et al.* Normal and malignant epithelial cells with stem-like properties have an extended G2 cell cycle phase that is associated with apoptotic resistance. *BMC Cancer***10**, 166 (2010).
75 Harper, L. J., Piper, K., Common, J., Fortune, F. & Mackenzie, I. C. Stem cell patterns in cell lines derived from head and neck squamous cell carcinoma. *J Oral Pathol Med***36**, 594-603 (2007).
76 Harrison, H. *et al.* Regulation of breast cancer stem cell activity by signaling through the Notch4 receptor. *Cancer Res***70**, 709-718.
77 Heinzelmann-Schwarz, V. A. *et al.* Overexpression of the cell adhesion molecules DDR1, Claudin 3, and Ep-CAM in metaplastic ovarian epithelium and ovarian cancer. *Clin Cancer Res***10**, 4427-4436 (2004).
78 Herold-Mende, C. *et al.* Expression of CD44 splice variants in squamous epithelia and squamous cell carcinomas of the head and neck. *J Pathol***179**, 66-73 (1996).
79 Hill, C. S. The Smads. *Int J Biochem Cell Biol***31**, 1249-1254 (1999).
80 Hirschmann-Jax, C. *et al.* A distinct "side population" of cells with high drug efflux capacity in human tumor cells. *Proc Natl Acad Sci U S A***101**, 14228-14233 (2004).
81 Hollier, B. G., Evans, K. & Mani, S. A. The epithelial-to-mesenchymal transition and cancer stem cells: a coalition against cancer therapies. *J Mammary Gland Biol Neoplasia***14**, 29-43 (2009).

82 Huang, E. H. *et al.* Aldehyde dehydrogenase 1 is a marker for normal and malignant human colonic stem cells (SC) and tracks SC overpopulation during colon tumorigenesis. *Cancer Res***69**, 3382-3389 (2009).
83 Huhn, A. & Nairn, R. C. A nuclear staining artefact in immunofluorescence. *Clin Exp Immunol***2**, 697-700 (1967).
84 Inman, G. J. *et al.* SB-431542 is a potent and specific inhibitor of transforming growth factor-beta superfamily type I activin receptor-like kinase (ALK) receptors ALK4, ALK5, and ALK7. *Mol Pharmacol***62**, 65-74 (2002).
85 Janes, S. M., Lowell, S. & Hutter, C. Epidermal stem cells. *J Pathol***197**, 479-491 (2002).
86 Javle, M. M. *et al.* Epithelial-mesenchymal transition (EMT) and activated extracellular signal-regulated kinase (p-Erk) in surgically resected pancreatic cancer. *Ann Surg Oncol***14**, 3527-3533 (2007).
87 Jones, P. A. & Baylin, S. B. The epigenomics of cancer. *Cell***128**, 683-692 (2007).
88 Jones, P. H. Stem cell fate in proliferating tissues: equal odds in a game of chance. *Dev Cell***19**, 489-490 (2010).
89 Joo, Y. E. *et al.* Changes in the E-cadherin-catenin complex expression in early and advanced gastric cancers. *Digestion***64**, 111-119 (2001).
90 Joshua, B. *et al.* Frequency of cells expressing CD44, a head and neck cancer stem cell marker: correlation with tumor aggressiveness. *Head Neck***34**, 42-49.
91 Kainz, C. *et al.* Prognostic value of CD44 splice variants in human stage III cervical cancer. *Eur J Cancer***31A**, 1706-1709 (1995).
92 Kalluri, R. & Neilson, E. G. Epithelial-mesenchymal transition and its implications for fibrosis. *J Clin Invest***112**, 1776-1784 (2003).
93 Kalluri, R. & Weinberg, R. A. The basics of epithelial-mesenchymal transition. *J Clin Invest***119**, 1420-1428 (2009).
94 Kaplan, R. N., Psaila, B. & Lyden, D. Niche-to-niche migration of bone-marrow-derived cells. *Trends Mol Med***13**, 72-81 (2007).
95 Kasai, H., Allen, J. T., Mason, R. M., Kamimura, T. & Zhang, Z. TGF-beta1 induces human alveolar epithelial to mesenchymal cell transition (EMT). *Respir Res***6**, 56 (2005).
96 Kearsley, J. H., Furlong, K. L., Cooke, R. A. & Waters, M. J. An immunohistochemical assessment of cellular proliferation markers in head and neck squamous cell cancers. *Br J Cancer***61**, 821-827 (1990).
97 Keller, P. J. *et al.* Mapping the cellular and molecular heterogeneity of normal and malignant breast tissues and cultured cell lines. *Breast Cancer Res***12**, R87.
98 Kim, C. F. *et al.* Identification of bronchioalveolar stem cells in normal lung and lung cancer. *Cell***121**, 823-835 (2005).
99 Kim, K. & Hay, E. D. New evidence that nuclear import of endogenous beta-catenin is LEF-1 dependent, while LEF-1 independent import of exogenous beta-catenin leads to nuclear abnormalities. *Cell Biol Int***25**, 1149-1161 (2001).
100 Klein, A. M., Nikolaidou-Neokosmidou, V., Doupe, D. P., Jones, P. H. & Simons, B. D. Patterning as a signature of human epidermal stem cell regulation. *J R Soc Interface***8**, 1815-1824 (2011).
101 Klein, A. M. & Simons, B. D. Universal patterns of stem cell fate in cycling adult tissues. *Development***138**, 3103-3111.
102 Knoblich, J. A. Mechanisms of asymmetric stem cell division. *Cell***132**, 583-597 (2008).

103 Kojima, Y. *et al.* Autocrine TGF-beta and stromal cell-derived factor-1 (SDF-1) signaling drives the evolution of tumor-promoting mammary stromal myofibroblasts. *Proc Natl Acad Sci U S A***107**, 20009-20014.
104 Koopman, G. *et al.* Activated human lymphocytes and aggressive non-Hodgkin's lymphomas express a homologue of the rat metastasis-associated variant of CD44. *J Exp Med***177**, 897-904 (1993).
105 Krantz, S. B., Shields, M. A., Dangi-Garimella, S., Munshi, H. G. & Bentrem, D. J. Contribution of Epithelial-to-Mesenchymal Transition and Cancer Stem Cells to Pancreatic Cancer Progression. *J Surg Res***173**, 105-112.
106 Kristensen, G. B., Abeler, V. M., Risberg, B., Trop, C. & Bryne, M. Tumor size, depth of invasion, and grading of the invasive tumor front are the main prognostic factors in early squamous cell cervical carcinoma. *Gynecol Oncol***74**, 245-251 (1999).
107 Lavker, R. M. & Sun, T. T. Epidermal stem cells: properties, markers, and location. *Proc Natl Acad Sci U S A***97**, 13473-13475 (2000).
108 Lechler, T. & Fuchs, E. Asymmetric cell divisions promote stratification and differentiation of mammalian skin. *Nature***437**, 275-280 (2005).
109 Lee, J. & Moon, C. Current status of experimental therapeutics for head and neck cancer. *Exp Biol Med (Maywood)***236**, 375-389 (2011).
110 Li, L. & Xie, T. Stem cell niche: structure and function. *Annu Rev Cell Dev Biol***21**, 605-631 (2005).
111 Liang, L. & Bickenbach, J. R. Somatic epidermal stem cells can produce multiple cell lineages during development. *Stem Cells***20**, 21-31 (2002).
112 Lin, H., Shabbir, A., Molnar, M. & Lee, T. Stem cell regulatory function mediated by expression of a novel mouse Oct4 pseudogene. *Biochem Biophys Res Commun***355**, 111-116 (2007).
113 Locke, M., Heywood, M., Fawell, S. & Mackenzie, I. C. Retention of intrinsic stem cell hierarchies in carcinoma-derived cell lines. *Cancer Res***65**, 8944-8950 (2005).
114 Maas-Szabowski, N. & Fusenig, N. E. Interleukin-1-induced growth factor expression in postmitotic and resting fibroblasts. *J Invest Dermatol***107**, 849-855 (1996).
115 Maas-Szabowski, N. *et al.* Organotypic cocultures with genetically modified mouse fibroblasts as a tool to dissect molecular mechanisms regulating keratinocyte growth and differentiation. *J Invest Dermatol***116**, 816-820 (2001).
116 Mack, B. & Gires, O. CD44s and CD44v6 expression in head and neck epithelia. *PLoS One***3**, e3360 (2008).
117 Mackenzie, I. C. Retroviral transduction of murine epidermal stem cells demonstrates clonal units of epidermal structure. *J Invest Dermatol***109**, 377-383 (1997).
118 Mackenzie, I. C. Growth of malignant oral epithelial stem cells after seeding into organotypical cultures of normal mucosa. *J Oral Pathol Med***33**, 71-78 (2004).
119 Mackenzie, I. C. Retention of stem cell patterns in malignant cell lines. *Cell Prolif***38**, 347-355 (2005).
120 Mackenzie, I. C. Stem cell properties and epithelial malignancies. *Eur J Cancer***42**, 1204-1212 (2006).
121 Mackenzie, I. C. & Bickenbach, J. R. Label-retaining keratinocytes and Langerhans cells in mouse epithelia. *Cell Tissue Res***242**, 551-556 (1985).
122 Mackenzie, I. C. & Fusenig, N. E. Regeneration of organized epithelial structure. *J Invest Dermatol***81**, 189s-194s (1983).
123 Maetzel, D. *et al.* Nuclear signalling by tumour-associated antigen EpCAM. *Nat Cell Biol***11**, 162-171 (2009).
124 Mani, S. A. *et al.* The epithelial-mesenchymal transition generates cells with properties of stem cells. *Cell***133**, 704-715 (2008).

125 Marhaba, R., Bourouba, M. & Zoller, M. CD44v7 interferes with activation-induced cell death by up-regulation of anti-apoptotic gene expression. *J Leukoc Biol***74**, 135-148 (2003).
126 Marques-Pereira, J. P. & Leblond, C. P. Mitosis and Differentiation in the Stratified Squamous Epithelium of the Rat Esophagus. *Am J Anat***117**, 73-87 (1965).
127 Marsh, D. *et al.* Stromal features are predictive of disease mortality in oral cancer patients. *J Pathol***223**, 470-481.
128 Massague, J. TGFbeta in Cancer. *Cell***134**, 215-230 (2008).
129 Massague, J. & Chen, Y. G. Controlling TGF-beta signaling. *Genes Dev***14**, 627-644 (2000).
130 Matin, M. M. *et al.* Specific knockdown of Oct4 and beta2-microglobulin expression by RNA interference in human embryonic stem cells and embryonic carcinoma cells. *Stem Cells***22**, 659-668 (2004).
131 Matsumura, Y. *et al.* Unusual retention of introns in CD44 gene transcripts in bladder cancer provides new diagnostic and clinical oncological opportunities. *J Pathol***177**, 11-20 (1995).
132 Mehanna, H., Paleri, V., West, C. M. & Nutting, C. Head and neck cancer-part 1: epidemiology, presentation, and preservation. *Clin Otolaryngol***36**, 65-68 (2011).
133 Mehanna, H., West, C. M., Nutting, C. & Paleri, V. Head and neck cancer--Part 2: Treatment and prognostic factors. *Bmj***341**, c4690 (2010).
134 Meyer, M. J. *et al.* Dynamic regulation of CD24 and the invasive, CD44posCD24neg phenotype in breast cancer cell lines. *Breast Cancer Res***11**, R82 (2009).
135 Molofsky, A. V., Pardal, R. & Morrison, S. J. Diverse mechanisms regulate stem cell self-renewal. *Curr Opin Cell Biol***16**, 700-707 (2004).
136 Morel, A. P. *et al.* Generation of breast cancer stem cells through epithelial-mesenchymal transition. *PLoS One***3**, e2888 (2008).
137 Morrison, S. J., Uchida, N. & Weissman, I. L. The biology of hematopoietic stem cells. *Annu Rev Cell Dev Biol***11**, 35-71 (1995).
138 Moserle, L., Ghisi, M., Amadori, A. & Indraccolo, S. Side population and cancer stem cells: therapeutic implications. *Cancer Lett***288**, 1-9 (2009).
139 Mueller, B. U. & Pabst, T. C/EBPalpha and the pathophysiology of acute myeloid leukemia. *Curr Opin Hematol***13**, 7-14 (2006).
140 Murata, M., Takayama, K., Choi, B. C. & Pak, A. W. A nested case-control study on alcohol drinking, tobacco smoking, and cancer. *Cancer Detect Prev***20**, 557-565 (1996).
141 Neumuller, R. A. & Knoblich, J. A. Dividing cellular asymmetry: asymmetric cell division and its implications for stem cells and cancer. *Genes Dev***23**, 2675-2699 (2009).
142 Nicholls, J. *et al.* Comparative analysis of the expression of the Epstein-Barr virus (EBV) anti-apoptotic gene BHRF1 in nasopharyngeal carcinoma and EBV-related lymphoid diseases. *J Med Virol***65**, 105-113 (2001).
143 Niwa, H., Miyazaki, J. & Smith, A. G. Quantitative expression of Oct-3/4 defines differentiation, dedifferentiation or self-renewal of ES cells. *Nat Genet***24**, 372-376 (2000).
144 Oliveira, D. T. & Odell, E. W. Expression of CD44 variant exons by normal oral epithelia. *Oral Oncol***33**, 260-262 (1997).
145 Olumi, A. F. *et al.* Carcinoma-associated fibroblasts direct tumor progression of initiated human prostatic epithelium. *Cancer Res***59**, 5002-5011 (1999).
146 Orian-Rousseau, V. CD44, a therapeutic target for metastasising tumours. *Eur J Cancer***46**, 1271-1277 (2010).
147 Owens, D. M. & Watt, F. M. Contribution of stem cells and differentiated cells to epidermal tumours. *Nat Rev Cancer***3**, 444-451 (2003).

148 Ozdamar, B. *et al.* Regulation of the polarity protein Par6 by TGFbeta receptors controls epithelial cell plasticity. *Science***307**, 1603-1609 (2005).
149 Palmer, T. D., Willhoite, A. R. & Gage, F. H. Vascular niche for adult hippocampal neurogenesis. *J Comp Neurol***425**, 479-494 (2000).
150 Papadimitrakopoulou, V. A. *et al.* Biologic correlates of a biochemoprevention trial in advanced upper aerodigestive tract premalignant lesions. *Cancer Epidemiol Biomarkers Prev***11**, 1605-1610 (2002).
151 Pardal, R., Clarke, M. F. & Morrison, S. J. Applying the principles of stem-cell biology to cancer. *Nat Rev Cancer***3**, 895-902 (2003).
152 Parenteau, N. L., Bilbo, P., Nolte, C. J., Mason, V. S. & Rosenberg, M. The organotypic culture of human skin keratinocytes and fibroblasts to achieve form and function. *Cytotechnology***9**, 163-171 (1992).
153 Pearce, D. J. *et al.* Characterization of cells with a high aldehyde dehydrogenase activity from cord blood and acute myeloid leukemia samples. *Stem Cells***23**, 752-760 (2005).
154 Pellegrini, G. *et al.* p63 identifies keratinocyte stem cells. *Proc Natl Acad Sci U S A***98**, 3156-3161 (2001).
155 Pellegrini, G. *et al.* Location and clonal analysis of stem cells and their differentiated progeny in the human ocular surface. *J Cell Biol***145**, 769-782 (1999).
156 Perez-Plasencia, C. *et al.* Genome wide expression analysis in HPV16 cervical cancer: identification of altered metabolic pathways. *Infect Agent Cancer***2**, 16 (2007).
157 Piffko, J. *et al.* Unaltered strong immunohistochemical expression of CD44-v6 and -v5 isoforms during development and progression of oral squamous cell carcinomas. *J Oral Pathol Med***25**, 502-506 (1996).
158 Pine, S. R., Ryan, B. M., Varticovski, L., Robles, A. I. & Harris, C. C. Microenvironmental modulation of asymmetric cell division in human lung cancer cells. *Proc Natl Acad Sci U S A***107**, 2195-2200 (2010).
159 Pisani, P., Bray, F. & Parkin, D. M. Estimates of the world-wide prevalence of cancer for 25 sites in the adult population. *Int J Cancer***97**, 72-81 (2002).
160 Piscaglia, A. C., Shupe, T. D., Petersen, B. E. & Gasbarrini, A. Stem cells, cancer, liver, and liver cancer stem cells: finding a way out of the labyrinth. *Curr Cancer Drug Targets***7**, 582-590 (2007).
161 Potten, C. S. Apoptosis in oral mucosa: lessons from the crypt. A commentary. *Oral Dis***7**, 81-85 (2001).
162 Potten, C. S. Keratinocyte stem cells, label-retaining cells and possible genome protection mechanisms. *J Investig Dermatol Symp Proc***9**, 183-195 (2004).
163 Potten, C. S. & Grant, H. K. The relationship between ionizing radiation-induced apoptosis and stem cells in the small and large intestine. *Br J Cancer***78**, 993-1003 (1998).
164 Potten, C. S., Hume, W. J., Reid, P. & Cairns, J. The segregation of DNA in epithelial stem cells. *Cell***15**, 899-906 (1978).
165 Potten, C. S. & Loeffler, M. Stem cells: attributes, cycles, spirals, pitfalls and uncertainties. Lessons for and from the crypt. *Development***110**, 1001-1020 (1990).
166 Priddle, H., Jones, D. R., Burridge, P. W. & Patient, R. Hematopoiesis from human embryonic stem cells: overcoming the immune barrier in stem cell therapies. *Stem Cells***24**, 815-824 (2006).
167 Prime, S. S. *et al.* The behaviour of human oral squamous cell carcinoma in cell culture. *J Pathol***160**, 259-269 (1990).
168 Prince, M. E. & Ailles, L. E. Cancer stem cells in head and neck squamous cell cancer. *J Clin Oncol***26**, 2871-2875 (2008).

169 Prince, M. E. *et al.* Identification of a subpopulation of cells with cancer stem cell properties in head and neck squamous cell carcinoma. *Proc Natl Acad Sci U S A***104**, 973-978 (2007).
170 Quesenberry, P. J. & Becker, P. S. Stem cell homing: rolling, crawling, and nesting. *Proc Natl Acad Sci U S A***95**, 15155-15157 (1998).
171 Reya, T. Regulation of hematopoietic stem cell self-renewal. *Recent Prog Horm Res***58**, 283-295 (2003).
172 Reya, T., Morrison, S. J., Clarke, M. F. & Weissman, I. L. Stem cells, cancer, and cancer stem cells. *Nature***414**, 105-111 (2001).
173 Reynolds, B. A., Tetzlaff, W. & Weiss, S. A multipotent EGF-responsive striatal embryonic progenitor cell produces neurons and astrocytes. *J Neurosci***12**, 4565-4574 (1992).
174 Richter, P. *et al.* EGF/TGFbeta1 co-stimulation of oral squamous cell carcinoma cells causes an epithelial-mesenchymal transition cell phenotype expressing laminin 332. *J Oral Pathol Med***40**, 46-54.
175 Roberts, A. B. & Sporn, M. B. Physiological actions and clinical applications of transforming growth factor-beta (TGF-beta). *Growth Factors***8**, 1-9 (1993).
176 Rochat, A., Kobayashi, K. & Barrandon, Y. Location of stem cells of human hair follicles by clonal analysis. *Cell***76**, 1063-1073 (1994).
177 Rogers, S. N. Quality of life perspectives in patients with oral cancer. *Oral Oncol***46**, 445-447 (2010).
178 Ruan, W. & Lai, M. Actin, a reliable marker of internal control? *Clin Chim Acta***385**, 1-5 (2007).
179 Sahai, E. & Marshall, C. J. Differing modes of tumour cell invasion have distinct requirements for Rho/ROCK signalling and extracellular proteolysis. *Nat Cell Biol***5**, 711-719 (2003).
180 Salahshor, S. *et al.* Frequent accumulation of nuclear E-cadherin and alterations in the Wnt signaling pathway in esophageal squamous cell carcinomas. *Mod Pathol***21**, 271-281 (2008).
181 Scheel, C. *et al.* Paracrine and autocrine signals induce and maintain mesenchymal and stem cell states in the breast. *Cell***145**, 926-940.
182 Schmalhofer, O., Brabletz, S. & Brabletz, T. E-cadherin, beta-catenin, and ZEB1 in malignant progression of cancer. *Cancer Metastasis Rev***28**, 151-166 (2009).
183 Schofield, R. The relationship between the spleen colony-forming cell and the haemopoietic stem cell. *Blood Cells***4**, 7-25 (1978).
184 Seery, J. P. & Watt, F. M. Asymmetric stem-cell divisions define the architecture of human oesophageal epithelium. *Curr Biol***10**, 1447-1450 (2000).
185 Shah, A. N. *et al.* Development and characterization of gemcitabine-resistant pancreatic tumor cells. *Ann Surg Oncol***14**, 3629-3637 (2007).
186 Shah, N. M., Groves, A. K. & Anderson, D. J. Alternative neural crest cell fates are instructively promoted by TGFbeta superfamily members. *Cell***85**, 331-343 (1996).
187 Sherr, C. J. The Pezcoller lecture: cancer cell cycles revisited. *Cancer Res***60**, 3689-3695 (2000).
188 Shi, Y. & Massague, J. Mechanisms of TGF-beta signaling from cell membrane to the nucleus. *Cell***113**, 685-700 (2003).
189 Shinto, E. *et al.* Prognostic implication of laminin-5 gamma 2 chain expression in the invasive front of colorectal cancers, disclosed by area-specific four-point tissue microarrays. *Lab Invest***85**, 257-266 (2005).

190 Shorning, B. Y., Griffiths, D. & Clarke, A. R. Lkb1 and Pten synergise to suppress mTOR-mediated tumorigenesis and epithelial-mesenchymal transition in the mouse bladder. *PLoS One***6**, e16209 (2011).
191 Singh, A. & Settleman, J. EMT, cancer stem cells and drug resistance: an emerging axis of evil in the war on cancer. *Oncogene***29**, 4741-4751.
192 Smith, A. G. Embryo-derived stem cells: of mice and men. *Annu Rev Cell Dev Biol***17**, 435-462 (2001).
193 Sneddon, J. B. & Werb, Z. Location, location, location: the cancer stem cell niche. *Cell Stem Cell***1**, 607-611 (2007).
194 Song, X., Call, G. B., Kirilly, D. & Xie, T. Notch signaling controls germline stem cell niche formation in the Drosophila ovary. *Development***134**, 1071-1080 (2007).
195 Spizzo, G. *et al.* EpCAM expression in primary tumour tissues and metastases: an immunohistochemical analysis. *J Clin Pathol***64**, 415-420.
196 Spizzo, G. *et al.* High Ep-CAM expression is associated with poor prognosis in node-positive breast cancer. *Breast Cancer Res Treat***86**, 207-213 (2004).
197 St John, M. A. *et al.* Proinflammatory mediators upregulate snail in head and neck squamous cell carcinoma. *Clin Cancer Res***15**, 6018-6027 (2009).
198 Stadtfeld, M. & Hochedlinger, K. Induced pluripotency: history, mechanisms, and applications. *Genes Dev***24**, 2239-2263.
199 Stadtfeld, M. & Hochedlinger, K. Induced pluripotency: history, mechanisms, and applications. *Genes Dev***24**, 2239-2263 (2010).
200 Stingl, J. Detection and analysis of mammary gland stem cells. *J Pathol***217**, 229-241 (2009).
201 Su, Y. J., Lai, H. M., Chang, Y. W., Chen, G. Y. & Lee, J. L. Direct reprogramming of stem cell properties in colon cancer cells by CD44. *Embo J***30**, 3186-3199.
202 Sumi, T., Tsuneyoshi, N., Nakatsuji, N. & Suemori, H. Apoptosis and differentiation of human embryonic stem cells induced by sustained activation of c-Myc. *Oncogene***26**, 5564-5576 (2007).
203 Takahashi, K. & Yamanaka, S. Induction of pluripotent stem cells from mouse embryonic and adult fibroblast cultures by defined factors. *Cell***126**, 663-676 (2006).
204 Tamiolakis, D. *et al.* Gains and losses of glycoprotein CD44 and secretory component expression in endometrial hyperplasia and neoplasia. *Eur J Gynaecol Oncol***23**, 453-456 (2002).
205 Terskikh, A. V., Bryant, P. J. & Schwartz, P. H. Mammalian stem cells. *Pediatr Res***59**, 13R-20R (2006).
206 Thiery, J. P. Epithelial-mesenchymal transitions in tumour progression. *Nat Rev Cancer***2**, 442-454 (2002).
207 Thiery, J. P., Acloque, H., Huang, R. Y. & Nieto, M. A. Epithelial-mesenchymal transitions in development and disease. *Cell***139**, 871-890 (2009).
208 Tian, Z. *et al.* Prognostic significance of tumor grading and staging in mammary carcinomas with neuroendocrine differentiation. *Hum Pathol***42**, 1169-1177.
209 Tudor, D., Chaudry, F., Harper, L. & Mackenzie, I. C. The in vitro behaviour and patterns of colony formation of murine epithelial stem cells. *Cell Prolif***40**, 706-720 (2007).
210 Tudor, D., Locke, M., Owen-Jones, E. & Mackenzie, I. C. Intrinsic patterns of behavior of epithelial stem cells. *J Investig Dermatol Symp Proc***9**, 208-214 (2004).
211 van Zeeburg, H. J. *et al.* Generation and molecular characterization of head and neck squamous cell lines of fanconi anemia patients. *Cancer Res***65**, 1271-1276 (2005).
212 Veeck, J. & Dahl, E. Targeting the Wnt pathway in cancer: The emerging role of Dickkopf-3. *Biochim Biophys Acta***1825**, 18-28.

213 Vesely, P. *et al.* Confocal microscopy reveals Myzitiras and Vthela morphotypes as new signatures of malignancy progression. *Scanning***31**, 102-106 (2009).
214 Vonderhaar, B. K. & Smith, G. H. Stem cells and breast cancer. Introduction. *Breast Dis***29**, 1 (2008).
215 Voog, J. & Jones, D. L. Stem cells and the niche: a dynamic duo. *Cell Stem Cell***6**, 103-115 (2010).
216 Walton, J. D. *et al.* Characteristics of stem cells from human neuroblastoma cell lines and in tumors. *Neoplasia***6**, 838-845 (2004).
217 Wang, X. D. *et al.* Notch signaling is required for normal prostatic epithelial cell proliferation and differentiation. *Dev Biol***290**, 66-80 (2006).
218 Wang, Z. X. *et al.* Oct4 and Sox2 directly regulate expression of another pluripotency transcription factor, Zfp206, in embryonic stem cells. *J Biol Chem***282**, 12822-12830 (2007).
219 Watt, F. M. & Hogan, B. L. Out of Eden: stem cells and their niches. *Science***287**, 1427-1430 (2000).
220 Wei, C., Guomin, W., Yujun, L. & Ruizhe, Q. Cancer Stem-like Cells in Human Prostate Carcinoma Cells DU145: The Seeds of the Cell Line? *Cancer Biol Ther***6** (2007).
221 Weintraub, H. *et al.* Activation of muscle-specific genes in pigment, nerve, fat, liver, and fibroblast cell lines by forced expression of MyoD. *Proc Natl Acad Sci U S A***86**, 5434-5438 (1989).
222 Weissman, I. L., Anderson, D. J. & Gage, F. Stem and progenitor cells: origins, phenotypes, lineage commitments, and transdifferentiations. *Annu Rev Cell Dev Biol***17**, 387-403 (2001).
223 Wu, Y. *et al.* Stabilization of snail by NF-kappaB is required for inflammation-induced cell migration and invasion. *Cancer Cell***15**, 416-428 (2009).
224 Wu, Y. & Zhou, B. P. New insights of epithelial-mesenchymal transition in cancer metastasis. *Acta Biochim Biophys Sin (Shanghai)***40**, 643-650 (2008).
225 Xie, Z. *et al.* Inhibition of CD44 expression in hepatocellular carcinoma cells enhances apoptosis, chemosensitivity, and reduces tumorigenesis and invasion. *Cancer Chemother Pharmacol***62**, 949-957 (2008).
226 Xu, Z., Jiang, Y., Steed, H., Davidge, S. & Fu, Y. TGFbeta and EGF synergistically induce a more invasive phenotype of epithelial ovarian cancer cells. *Biochem Biophys Res Commun***401**, 376-381.
227 Zavadil, J. & Bottinger, E. P. TGF-beta and epithelial-to-mesenchymal transitions. *Oncogene***24**, 5764-5774 (2005).
228 Zhang, L. *et al.* Tumorspheres derived from prostate cancer cells possess chemoresistant and cancer stem cell properties. *J Cancer Res Clin Oncol* (2012).
229 Zhu, A. J. & Watt, F. M. beta-catenin signalling modulates proliferative potential of human epidermal keratinocytes independently of intercellular adhesion. *Development***126**, 2285-2298 (1999).
230 Zoller, M. CD44: can a cancer-initiating cell profit from an abundantly expressed molecule? *Nat Rev Cancer***11**, 254-267 (2011).